

République Algérienne Démocratique et Populaire
Ministère de l'Enseignement Supérieur et de la Recherche Scientifique
École Nationale Polytechnique d'Alger



Department of Automatic Control

Thesis

Presented by **Yassine SOUKKOU**

For the degree of **Doctor of Sciences** in

Electrical Engineering

Option: **Automatic Control**

Theme

CONTRIBUTION TO ADAPTIVE CONTROL OF TRIANGULAR NONLINEAR SYSTEMS WITH APPLICATION

Discussed on: 28/09/2020 in front of the jury:

| | | |
|---------------------------|---|---|
| Hachemi Chekireb | Prof. National Polytechnic School of Algiers (ENP) | President |
| Mohamed Tadjine | Prof. National Polytechnic School of Algiers (ENP) | Director of thesis |
| Salim Labiod | Prof. University of Jijel | Co-Director of thesis |
| Mokhtar Nibouche | Dr. University of the West of England (UWE), Bristol, UK | Co-Director of thesis abroad |
| Khelifa Benmansour | Prof. Higher School of the Territory Air Defense (ESDAT) | Examinator |
| Abdelkrim Nemra | Dr. Polytechnic Military School (EMP) | Examinator |
| Ahsene Boubakir | Dr. University of Jijel | Examinator |
| Rachid Illoul | Dr. National Polytechnic School of Algiers (ENP) | Examinator |

ENP 2020

This thesis was prepared within the Process Control Laboratory (LCP) of the National Polytechnic School of Algiers (ENP),
10, Avenue of the Oudek Brothers, Hassen Badi, BP.182, 16200, El-Harrach, Algiers, Algeria
www.enp.edu.dz

République Algérienne Démocratique et Populaire
Ministère de l'Enseignement Supérieur et de la Recherche Scientifique
École Nationale Polytechnique d'Alger



Department of Automatic Control

Thesis

Presented by **Yassine SOUKKOU**

For the degree of **Doctor of Sciences** in

Electrical Engineering

Option: **Automatic Control**

Theme

CONTRIBUTION TO ADAPTIVE CONTROL OF TRIANGULAR NONLINEAR SYSTEMS WITH APPLICATION

Discussed on: 28/09/2020 in front of the jury:

| | | |
|---------------------------|---|---|
| Hachemi Chekireb | Prof. National Polytechnic School of Algiers (ENP) | President |
| Mohamed Tadjine | Prof. National Polytechnic School of Algiers (ENP) | Director of thesis |
| Salim Labiod | Prof. University of Jijel | Co-Director of thesis |
| Mokhtar Nibouche | Dr. University of the West of England (UWE), Bristol, UK | Co-Director of thesis abroad |
| Khelifa Benmansour | Prof. Higher School of the Territory Air Defense (ESDAT) | Examinator |
| Abdelkrim Nemra | Dr. Polytechnic Military School (EMP) | Examinator |
| Ahsene Boubakir | Dr. University of Jijel | Examinator |
| Rachid Illoul | Dr. National Polytechnic School of Algiers (ENP) | Examinator |

ENP 2020

This thesis was prepared within the Process Control Laboratory (LCP) of the National Polytechnic School of Algiers (ENP),
10, Avenue of the Oudek Brothers, Hassen Badi, BP.182, 16200, El-Harrach, Algiers, Algeria
www.enp.edu.dz

République Algérienne Démocratique et Populaire
Ministère de l'Enseignement Supérieur et de la Recherche Scientifique
École Nationale Polytechnique d'Alger



Département d'Automatique

Thèse

Présentée par **Yassine SOUKKOU**

Pour l'obtention du diplôme de **Docteur en Sciences en**

Génie Électrique

Option: **Automatique**

Thème

CONTRIBUTION À LA COMMANDE ADAPTATIVE DES SYSTÈMES NON LINÉAIRES TRIANGULAIRES AVEC APPLICATION

Soutenue le: 28/09/2020 devant le jury:

| | | |
|---------------------------|--|--|
| Hachemi Chekireb | Prof. École Nationale Polytechnique d'Alger (ENP) | Président |
| Mohamed Tadjine | Prof. École Nationale Polytechnique d'Alger (ENP) | Directeur de la thèse |
| Salim Labiod | Prof. Université de Jijel | Co-Directeur de la thèse |
| Mokhtar Nibouche | Dr. Université de l'Ouest de l'Angleterre (UWE), Bristol, UK | Co-Directeur de la thèse à l'étranger |
| Khelifa Benmansour | Prof. École Supérieure de la Défense Aérienne du Territoire (ESDAT) | Examineur |
| Abdelkrim Nemra | Dr. École Militaire Polytechnique (EMP) | Examineur |
| Ahsene Boubakir | Dr. Université de Jijel | Examineur |
| Rachid Illoul | Dr. École Nationale Polytechnique d'Alger (ENP) | Examineur |

ENP 2020

ملخص:

في هذه الأطروحة، قمنا بدراسة وتطوير إستراتيجيات التحكم التكيفي المركبة لفئة من الأنظمة اللاخطية الغير مؤكدة في شكل مثلثي سفلي. يعاني مخطط التحكم التكيفي الرجعي مع دوال الضبط المركب من مشكلة إنفجار التعقيد بسبب الإستقاقات المتكررة لمدخلات التحكم الإفتراضية. بإستخدام طرق التحكم التكيفي و التحكم التكيفي المتين بواسطة التحكم في السطح الديناميكي المركبين، و الإنغماس و الثبات على أساس التحكم التكيفي الرجعي المرشح المركب، يتم القضاء على مشكلة إنفجار التعقيد. تم إستخدام القوانين التكيفية المركبة إستنادا إلى التدرج و أقل المربعات مع نوع المجموع، الإسقاط و σ -تعديل. تم تحليل إستقرار مخططات التحكم التكيفي المركبة المقترحة بإستخدام نظرية الإستقرار ليابونوف لضمان أن تكون جميع الإشارات في نظام الحلقة المغلقة محدودة. تم عرض نتائج المحاكاة لنظام كهروميكانيكي لإظهار فعالية تقنيات التحكم التكيفي المركبة المقترحة.

كلمات مفتاحية: التحكم التكيفي، التحكم المتين، دوال الضبط، التحكم في السطح الديناميكي، الإنغماس و الثبات، التحكم الرجعي المرشح، أنظمة لاخطية غير مؤكدة، نظرية الإستقرار ليابونوف، قوانين التكيف المركبة، نظام كهروميكانيكي.

Résumé:

Dans cette thèse, on s'est intéressé à l'étude et le développement de stratégies de la commande adaptative composite pour une classe des systèmes non linéaires incertains en forme triangulaire inférieure. Le schéma de commande adaptative par backstepping avec fonctions de réglage composite souffre du problème de l'explosion de la complexité causée par les dérivations répétées des entrées de commande virtuelles. Par l'utilisation des méthodes de commande adaptative et adaptative robuste par la commande de surface dynamique composites, et immersion et invariance basée sur la commande filtrée adaptative par backstepping composite, le problème de l'explosion de la complexité est éliminé. Lois adaptatives composites de type somme, projection et σ -modification basées sur le gradient et les moindres carrés sont utilisées. L'analyse de la stabilité des schémas de commande adaptative composite proposés est effectuée par la théorie de la stabilité de Lyapunov pour garantir la bornitude de tous les signaux du système en boucle fermée. Les résultats de simulation d'un système électromécanique sont présentés pour montrer l'efficacité des techniques de commande adaptative composite proposées.

Mots-clés: Commande adaptative, commande robuste, fonctions de réglage, commande de surface dynamique, immersion et invariance, commande filtrée par backstepping, systèmes non linéaires incertains, théorie de la stabilité de Lyapunov, lois adaptatives composites, système électromécanique.

Abstract:

In this thesis, we are interested in the study and development of composite adaptive control strategies for uncertain nonlinear systems in lower triangular form. Composite tuning functions based adaptive backstepping control scheme suffers from the problem of explosion of complexity caused by the repeated derivations of virtual control inputs. By using the composite adaptive and robust adaptive dynamic surface control, and composite immersion and invariance based adaptive command filtered backstepping control methods, the problem of explosion of complexity is eliminated. Composite sum, projection and σ -modification based gradient and least squares adaptive laws are used. Stability analysis of the proposed composite adaptive control schemes is performed by using the Lyapunov stability theory to guarantee that all signals in the closed-loop system are bounded. Simulation results of an electromechanical system are presented to show the effectiveness of the proposed composite adaptive control techniques.

Key words: Adaptive control, robust control, tuning functions, dynamic surface control, immersion and invariance, command filtered backstepping control, uncertain nonlinear systems, Lyapunov stability theory, composite adaptive laws, electromechanical system.

Acknowledgements

This thesis was carried out at the National Polytechnic School of Algiers (ENP), within the Process Control Laboratory (LCP), the University of Jijel, within the Automatic Laboratory of Jijel (LAJ), the Research Center in Industrial Technologies (CRTI) and the Power Systems and Electronics Research Laboratory, University of the West of England (UWE), Bristol, UK.

Above all, I thank the Almighty GOD (ALLAH) for his generosity to give me health, willingness and patience throughout this research work.

I would like to thank Prof. **Mohamed Tadjine** and Prof. **Salim Labiod** for their supervision, advices, help, invaluable guidance and the confidence that they have shown me throughout this thesis.

In addition, I would like to thank my supervisory team in UK; Dr. **Mokhtar Nibouche** and Prof. **Quan Min Zhu** for their supervision during my stay at UWE and for allowing me to use the research facilities in the Power Systems and Electronics Research Laboratory.

My gratitude goes to Prof. **Hachemi Chekireb** for doing me the honor of being the jury president.

I am very thankful to the jury members, Prof. **Khelifa Benmansour**, Dr. **Abdelkrim Nemra**, Dr. **Ahsene Boubakir** and Dr. **Rachid Illoul** for discussing this thesis.

I would like also to take this opportunity to thank all those who have contributed from near or far to the success of this research work.

Dedications

I dedicate this thesis

- To my mother and father
 - To my brothers and sisters
 - To my wife
 - To my friends and colleagues
 - To my professors
-

Table of contents

List of figures

| | |
|-----------------------------|----|
| General introduction | 13 |
|-----------------------------|----|

Chapter 1: State of the art and basic notions

| | | |
|-------|--------------------------------|----|
| 1.1 | Introduction | 18 |
| 1.2 | Lyapunov stability | 19 |
| 1.2.1 | Stability definitions | 19 |
| 1.2.2 | Lyapunov's direct method | 20 |
| 1.2.3 | Control Lyapunov functions | 22 |
| 1.2.4 | Some useful lemmas | 23 |
| 1.3 | Design of backstepping control | 23 |
| 1.4 | Adaptive control techniques | 25 |
| 1.5 | Conclusion | 27 |

Chapter 2: Composite tuning functions based adaptive backstepping control

| | | |
|---------|---|----|
| 2.1 | Introduction | 29 |
| 2.2 | Direct tuning functions based adaptive backstepping control | 30 |
| 2.3 | Indirect adaptive control | 36 |
| 2.3.1 | Identification based x-swapping filters | 36 |
| 2.3.2 | Choice of adaptive laws | 37 |
| 2.3.3 | Proof of stability | 38 |
| 2.3.3.1 | Gradient adaptive law | 38 |
| 2.3.3.2 | Least squares adaptive law | 39 |
| 2.4 | Composite tuning functions based adaptive backstepping control | 40 |
| 2.4.1 | Composite sum based gradient adaptive law | 40 |
| 2.4.2 | Composite σ -modification based gradient and least squares adaptive laws | 42 |
| 2.5 | Dynamic model of the electromechanical system | 44 |
| 2.6 | Simulation results | 45 |
| 2.6.1 | Composite sum based gradient adaptive laws | 46 |
| 2.6.2 | Composite σ -modification based gradient adaptive laws | 48 |
| 2.6.3 | Composite σ -modification based least squares adaptive laws | 50 |
| 2.7 | Conclusion | 52 |

Chapter 3: Composite adaptive dynamic surface control

| | | |
|-------|---|----|
| 3.1 | Introduction | 54 |
| 3.2 | Direct adaptive dynamic surface control | 55 |
| 3.2.1 | Stability analysis | 57 |
| 3.3 | Indirect adaptive control | 59 |

| | | |
|---------|---|----|
| 3.3.1 | Identification based x-swapping filters | 60 |
| 3.3.2 | Choice of adaptive laws | 60 |
| 3.3.3 | Proof of stability | 61 |
| 3.3.3.1 | Gradient adaptive laws | 61 |
| 3.3.3.2 | Least squares adaptive laws | 62 |
| 3.4 | Composite adaptive dynamic surface control | 63 |
| 3.4.1 | Composite projection based gradient adaptive laws | 64 |
| 3.4.2 | Composite projection based least squares adaptive laws | 65 |
| 3.4.3 | Composite σ -modification based gradient and least squares adaptive laws | 67 |
| 3.5 | Simulation results | 70 |
| 3.5.1 | Composite projection based gradient adaptive laws | 70 |
| 3.5.2 | Composite projection based least squares adaptive laws | 72 |
| 3.5.3 | Composite σ -modification based gradient adaptive laws | 74 |
| 3.5.4 | Composite σ -modification based least squares adaptive laws | 76 |
| 3.6 | Conclusion | 78 |

Chapter 4: Composite robust adaptive dynamic surface control

| | | |
|---------|---|-----|
| 4.1 | Introduction | 81 |
| 4.2 | Direct robust adaptive dynamic surface control | 82 |
| 4.2.1 | Stability analysis | 85 |
| 4.3 | Indirect robust adaptive control | 88 |
| 4.3.1 | Identification based modified x-swapping filters | 89 |
| 4.3.2 | Choice of adaptive laws | 90 |
| 4.3.3 | Proof of stability | 90 |
| 4.3.3.1 | Gradient adaptive laws | 90 |
| 4.3.3.2 | Least squares adaptive laws | 92 |
| 4.4 | Composite robust adaptive dynamic surface control | 93 |
| 4.4.1 | Composite projection based gradient adaptive laws | 94 |
| 4.4.2 | Composite projection based least squares adaptive laws | 96 |
| 4.4.3 | Composite σ -modification based gradient and least squares adaptive laws | 99 |
| 4.5 | Simulation results | 102 |
| 4.5.1 | Composite projection based gradient adaptive laws | 103 |
| 4.5.2 | Composite projection based least squares adaptive laws | 105 |
| 4.5.3 | Composite σ -modification based gradient adaptive laws | 107 |
| 4.5.4 | Composite σ -modification based least squares adaptive laws | 109 |
| 4.6 | Conclusion | 111 |

Chapter 5: Composite immersion and invariance based adaptive command filtered backstepping control

| | | |
|-------|---|-----|
| 5.1 | Introduction | 113 |
| 5.2 | Immersion and invariance based adaptive command filtered backstepping control | 114 |
| 5.2.1 | Estimator design | 115 |
| 5.2.2 | Controller design | 117 |
| 5.3 | Indirect adaptive control | 119 |
| 5.3.1 | Identification based x-swapping filters | 120 |

| | | |
|---------|---|------------|
| 5.3.2 | Choice of modified adaptive laws | 120 |
| 5.3.3 | Proof of stability | 121 |
| 5.3.3.1 | Modified gradient adaptive laws | 121 |
| 5.3.3.2 | Modified least squares adaptive laws | 122 |
| 5.4 | Composite immersion and invariance based adaptive command filtered backstepping control | 123 |
| 5.4.1 | Composite projection based gradient adaptive laws | 124 |
| 5.4.2 | Composite σ -modification based gradient and least squares adaptive laws | 125 |
| 5.5 | Simulation results | 128 |
| 5.5.1 | Composite projection based gradient adaptive laws | 129 |
| 5.5.2 | Composite σ -modification based gradient adaptive laws | 131 |
| 5.5.3 | Composite σ -modification based least squares adaptive laws | 133 |
| 5.6 | Conclusion | 135 |
| | General conclusion and future works | 136 |
| | Bibliographical references | 139 |

List of figures

| | | |
|--------------------|---|----|
| Figure 2.1 | <i>Angular position: desired x_{1d} ("") and actual x_1 ("--").</i> | 46 |
| Figure 2.2 | <i>Angular velocity: desired x_{2d} ("") and actual x_2 ("--").</i> | 46 |
| Figure 2.3 | <i>Motor armature current: desired x_{3d} ("") and actual x_3 ("--").</i> | 47 |
| Figure 2.4 | <i>Angular position tracking error: e_1.</i> | 47 |
| Figure 2.5 | <i>Angular velocity tracking error: e_2.</i> | 47 |
| Figure 2.6 | <i>Motor armature current tracking error: e_3.</i> | 47 |
| Figure 2.7 | <i>Parameter estimate: actual θ_2 ("") and estimate $\hat{\theta}_2$ ("--").</i> | 47 |
| Figure 2.8 | <i>Parameter estimate: actual θ_3 ("") and estimate $\hat{\theta}_3$ ("--").</i> | 47 |
| Figure 2.9 | <i>Control input: u.</i> | 47 |
| Figure 2.10 | <i>Angular position: desired x_{1d} ("") and actual x_1 ("--").</i> | 48 |
| Figure 2.11 | <i>Angular velocity: desired x_{2d} ("") and actual x_2 ("--").</i> | 48 |
| Figure 2.12 | <i>Motor armature current: desired x_{3d} ("") and actual x_3 ("--").</i> | 49 |
| Figure 2.13 | <i>Angular position tracking error: e_1.</i> | 49 |
| Figure 2.14 | <i>Angular velocity tracking error: e_2.</i> | 49 |
| Figure 2.15 | <i>Motor armature current tracking error: e_3.</i> | 49 |
| Figure 2.16 | <i>Parameter estimate: actual θ_2 ("") and estimate $\hat{\theta}_2$ ("--").</i> | 49 |
| Figure 2.17 | <i>Parameter estimate: actual θ_3 ("") and estimate $\hat{\theta}_3$ ("--").</i> | 49 |
| Figure 2.18 | <i>Control input: u.</i> | 49 |
| Figure 2.19 | <i>Angular position: desired x_{1d} ("") and actual x_1 ("--").</i> | 50 |
| Figure 2.20 | <i>Angular velocity: desired x_{2d} ("") and actual x_2 ("--").</i> | 50 |
| Figure 2.21 | <i>Motor armature current: desired x_{3d} ("") and actual x_3 ("--").</i> | 51 |
| Figure 2.22 | <i>Angular position tracking error: e_1.</i> | 51 |
| Figure 2.23 | <i>Angular velocity tracking error: e_2.</i> | 51 |
| Figure 2.24 | <i>Motor armature current tracking error: e_3.</i> | 51 |
| Figure 2.25 | <i>Parameter estimate: actual θ_2 ("") and estimate $\hat{\theta}_2$ ("--").</i> | 51 |
| Figure 2.26 | <i>Parameter estimate: actual θ_3 ("") and estimate $\hat{\theta}_3$ ("--").</i> | 51 |
| Figure 2.27 | <i>Control input: u.</i> | 51 |
| Figure 3.1 | <i>Angular position: desired x_{1d} ("") and actual x_1 ("--").</i> | 71 |
| Figure 3.2 | <i>Angular velocity: desired x_{2d} ("") and actual x_2 ("--").</i> | 71 |
| Figure 3.3 | <i>Motor armature current: desired x_{3d} ("") and actual x_3 ("--").</i> | 71 |
| Figure 3.4 | <i>Angular position surface error: S_1.</i> | 71 |
| Figure 3.5 | <i>Angular velocity surface error: S_2.</i> | 71 |
| Figure 3.6 | <i>Motor armature current surface error: S_3.</i> | 71 |
| Figure 3.7 | <i>Parameter estimate: actual θ_2 ("") and estimate $\hat{\theta}_2$ ("--").</i> | 72 |
| Figure 3.8 | <i>Parameter estimate: actual θ_3 ("") and estimate $\hat{\theta}_3$ ("--").</i> | 72 |
| Figure 3.9 | <i>Control input: u.</i> | 72 |
| Figure 3.10 | <i>Angular position: desired x_{1d} ("") and actual x_1 ("--").</i> | 73 |
| Figure 3.11 | <i>Angular velocity: desired x_{2d} ("") and actual x_2 ("--").</i> | 73 |
| Figure 3.12 | <i>Motor armature current: desired x_{3d} ("") and actual x_3 ("--").</i> | 73 |
| Figure 3.13 | <i>Angular position surface error: S_1.</i> | 73 |

| | | |
|--------------------|---|-----|
| Figure 3.14 | <i>Angular velocity surface error: S_2.</i> | 73 |
| Figure 3.15 | <i>Motor armature current surface error: S_3.</i> | 73 |
| Figure 3.16 | <i>Parameter estimate: actual θ_2 ("") and estimate $\hat{\theta}_2$ ("--").</i> | 74 |
| Figure 3.17 | <i>Parameter estimate: actual θ_3 ("") and estimate $\hat{\theta}_3$ ("--").</i> | 74 |
| Figure 3.18 | <i>Control input: u.</i> | 74 |
| Figure 3.19 | <i>Angular position: desired x_{1d} ("") and actual x_1 ("--").</i> | 75 |
| Figure 3.20 | <i>Angular velocity: desired x_{2d} ("") and actual x_2 ("--").</i> | 75 |
| Figure 3.21 | <i>Motor armature current: desired x_{3d} ("") and actual x_3 ("--").</i> | 75 |
| Figure 3.22 | <i>Angular position surface error: S_1.</i> | 75 |
| Figure 3.23 | <i>Angular velocity surface error: S_2.</i> | 75 |
| Figure 3.24 | <i>Motor armature current surface error: S_3.</i> | 75 |
| Figure 3.25 | <i>Parameter estimate: actual θ_2 ("") and estimate $\hat{\theta}_2$ ("--").</i> | 76 |
| Figure 3.26 | <i>Parameter estimate: actual θ_3 ("") and estimate $\hat{\theta}_3$ ("--").</i> | 76 |
| Figure 3.27 | <i>Control input: u.</i> | 76 |
| Figure 3.28 | <i>Angular position: desired x_{1d} ("") and actual x_1 ("--").</i> | 77 |
| Figure 3.29 | <i>Angular velocity: desired x_{2d} ("") and actual x_2 ("--").</i> | 77 |
| Figure 3.30 | <i>Motor armature current: desired x_{3d} ("") and actual x_3 ("--").</i> | 77 |
| Figure 3.31 | <i>Angular position surface error: S_1.</i> | 77 |
| Figure 3.32 | <i>Angular velocity surface error: S_2.</i> | 77 |
| Figure 3.33 | <i>Motor armature current surface error: S_3.</i> | 77 |
| Figure 3.34 | <i>Parameter estimate: actual θ_2 ("") and estimate $\hat{\theta}_2$ ("--").</i> | 78 |
| Figure 3.35 | <i>Parameter estimate: actual θ_3 ("") and estimate $\hat{\theta}_3$ ("--").</i> | 78 |
| Figure 3.36 | <i>Control input: u.</i> | 78 |
| | | |
| Figure 4.1 | <i>Angular position: desired x_{1d} ("") and actual x_1 ("--").</i> | 104 |
| Figure 4.2 | <i>Angular velocity: desired x_{2d} ("") and actual x_2 ("--").</i> | 104 |
| Figure 4.3 | <i>Motor armature current: desired x_{3d} ("") and actual x_3 ("--").</i> | 104 |
| Figure 4.4 | <i>Angular position surface error: S_1.</i> | 104 |
| Figure 4.5 | <i>Angular velocity surface error: S_2.</i> | 104 |
| Figure 4.6 | <i>Motor armature current surface error: S_3.</i> | 104 |
| Figure 4.7 | <i>Parameter estimate: actual θ_2 ("") and estimate $\hat{\theta}_2$ ("--").</i> | 104 |
| Figure 4.8 | <i>Parameter estimate: actual θ_3 ("") and estimate $\hat{\theta}_3$ ("--").</i> | 104 |
| Figure 4.9 | <i>Parameter estimate: $\hat{\delta}_2$.</i> | 105 |
| Figure 4.10 | <i>Control input: u.</i> | 105 |
| Figure 4.11 | <i>Angular position: desired x_{1d} ("") and actual x_1 ("--").</i> | 106 |
| Figure 4.12 | <i>Angular velocity: desired x_{2d} ("") and actual x_2 ("--").</i> | 106 |
| Figure 4.13 | <i>Motor armature current: desired x_{3d} ("") and actual x_3 ("--").</i> | 106 |
| Figure 4.14 | <i>Angular position surface error: S_1.</i> | 106 |
| Figure 4.15 | <i>Angular velocity surface error: S_2.</i> | 106 |
| Figure 4.16 | <i>Motor armature current surface error: S_3.</i> | 106 |
| Figure 4.17 | <i>Parameter estimate: actual θ_2 ("") and estimate $\hat{\theta}_2$ ("--").</i> | 106 |
| Figure 4.18 | <i>Parameter estimate: actual θ_3 ("") and estimate $\hat{\theta}_3$ ("--").</i> | 106 |
| Figure 4.19 | <i>Parameter estimate: $\hat{\delta}_2$.</i> | 107 |
| Figure 4.20 | <i>Control input: u.</i> | 107 |
| Figure 4.21 | <i>Angular position: desired x_{1d} ("") and actual x_1 ("--").</i> | 108 |
| Figure 4.22 | <i>Angular velocity: desired x_{2d} ("") and actual x_2 ("--").</i> | 108 |

| | | |
|--------------------|---|-----|
| Figure 4.23 | <i>Motor armature current: desired x_{3d} ("") and actual x_3 ("--").</i> | 108 |
| Figure 4.24 | <i>Angular position surface error: S_1.</i> | 108 |
| Figure 4.25 | <i>Angular velocity surface error: S_2.</i> | 108 |
| Figure 4.26 | <i>Motor armature current surface error: S_3.</i> | 108 |
| Figure 4.27 | <i>Parameter estimate: actual θ_2 ("") and estimate $\hat{\theta}_2$ ("--").</i> | 108 |
| Figure 4.28 | <i>Parameter estimate: actual θ_3 ("") and estimate $\hat{\theta}_3$ ("--").</i> | 108 |
| Figure 4.29 | <i>Parameter estimate: $\hat{\delta}_2$.</i> | 109 |
| Figure 4.30 | <i>Control input: u.</i> | 109 |
| Figure 4.31 | <i>Angular position: desired x_{1d} ("") and actual x_1 ("--").</i> | 110 |
| Figure 4.32 | <i>Angular velocity: desired x_{2d} ("") and actual x_2 ("--").</i> | 110 |
| Figure 4.33 | <i>Motor armature current: desired x_{3d} ("") and actual x_3 ("--").</i> | 110 |
| Figure 4.34 | <i>Angular position surface error: S_1.</i> | 110 |
| Figure 4.35 | <i>Angular velocity surface error: S_2.</i> | 110 |
| Figure 4.36 | <i>Motor armature current surface error: S_3.</i> | 110 |
| Figure 4.37 | <i>Parameter estimate: actual θ_2 ("") and estimate $\hat{\theta}_2$ ("--").</i> | 110 |
| Figure 4.38 | <i>Parameter estimate: actual θ_3 ("") and estimate $\hat{\theta}_3$ ("--").</i> | 110 |
| Figure 4.39 | <i>Parameter estimate: $\hat{\delta}_2$.</i> | 111 |
| Figure 4.40 | <i>Control input: u.</i> | 111 |
| | | |
| Figure 5.1 | <i>Angular position: desired x_{1d} ("") and actual x_1 ("--").</i> | 130 |
| Figure 5.2 | <i>Angular velocity: signal x_{2c} ("") and actual x_2 ("--").</i> | 130 |
| Figure 5.3 | <i>Motor armature current: signal x_{3c} ("") and actual x_3 ("--").</i> | 130 |
| Figure 5.4 | <i>Angular position tracking error: e_1.</i> | 130 |
| Figure 5.5 | <i>Angular velocity tracking error: e_2.</i> | 130 |
| Figure 5.6 | <i>Motor armature current tracking error: e_3.</i> | 130 |
| Figure 5.7 | <i>Parameter estimate: actual θ_2 ("") and estimate $\hat{\theta}_2$ ("--").</i> | 130 |
| Figure 5.8 | <i>Parameter estimate: actual θ_3 ("") and estimate $\hat{\theta}_3$ ("--").</i> | 130 |
| Figure 5.9 | <i>Control input: u.</i> | 131 |
| Figure 5.10 | <i>Angular position: desired x_{1d} ("") and actual x_1 ("--").</i> | 132 |
| Figure 5.11 | <i>Angular velocity: signal x_{2c} ("") and actual x_2 ("--").</i> | 132 |
| Figure 5.12 | <i>Motor armature current: signal x_{3c} ("") and actual x_3 ("--").</i> | 132 |
| Figure 5.13 | <i>Angular position tracking error: e_1.</i> | 132 |
| Figure 5.14 | <i>Angular velocity tracking error: e_2.</i> | 132 |
| Figure 5.15 | <i>Motor armature current tracking error: e_3.</i> | 132 |
| Figure 5.16 | <i>Parameter estimate: actual θ_2 ("") and estimate $\hat{\theta}_2$ ("--").</i> | 132 |
| Figure 5.17 | <i>Parameter estimate: actual θ_3 ("") and estimate $\hat{\theta}_3$ ("--").</i> | 132 |
| Figure 5.18 | <i>Control input: u.</i> | 133 |
| Figure 5.19 | <i>Angular position: desired x_{1d} ("") and actual x_1 ("--").</i> | 134 |
| Figure 5.20 | <i>Angular velocity: signal x_{2c} ("") and actual x_2 ("--").</i> | 134 |
| Figure 5.21 | <i>Motor armature current: signal x_{3c} ("") and actual x_3 ("--").</i> | 134 |
| Figure 5.22 | <i>Angular position tracking error: e_1.</i> | 134 |
| Figure 5.23 | <i>Angular velocity tracking error: e_2.</i> | 134 |
| Figure 5.24 | <i>Motor armature current tracking error: e_3.</i> | 134 |
| Figure 5.25 | <i>Parameter estimate: actual θ_2 ("") and estimate $\hat{\theta}_2$ ("--").</i> | 134 |
| Figure 5.26 | <i>Parameter estimate: actual θ_3 ("") and estimate $\hat{\theta}_3$ ("--").</i> | 134 |
| Figure 5.27 | <i>Control input: u.</i> | 135 |

General introduction

In recent years, the control design of nonlinear systems has attracted considerable attention from both theoretical interests and practical applications, and many effective control schemes have been proposed. Over the past decades, adaptive control of uncertain nonlinear systems has obtained many significant results where numerous approaches have been proposed for the design of nonlinear control systems. Among these adaptive control strategies, as an efficient design methodology, adaptive backstepping control has been studied for a class of uncertain nonlinear systems in lower triangular form (strict feedback form) with overparameterization [Kan91]. The overparameterization problem inherent in the conventional adaptive backstepping control has been eliminated by introducing tuning functions [Krs92]. The book of Krstic et al. [Krs95a] introduced a comprehensive methodology for adaptive backstepping control and tuning functions based adaptive backstepping control designs to deal with large classes of uncertain nonlinear systems. In recent years, tuning functions based adaptive backstepping control approach has been widely designed to control a class of uncertain nonlinear systems [Cil07, Wan16, Zho08]. Nevertheless, the conventional backstepping control approach suffers from the problem of explosion of complexity, which is caused by repeated differentiations of the virtual controllers at each step, as pointed out in [Hed00, Swa00, Swa97]. As a result, the computational complexity of backstepping controller grows drastically as the order of the system increases. To overcome the problem of explosion of complexity, the dynamic surface control (DSC) approach was proposed for a class of nonlinear systems in [Hed00, Swa00, Swa97] by introducing a first-order low-pass filter at each step of the conventional backstepping control method. Consequently, the dynamic surface control technique was suggested for designing adaptive controllers of uncertain nonlinear systems [Hed00, Yip98]. Several adaptive dynamic surface control schemes have been developed for a class of uncertain nonlinear systems [Khe15, Liu18a, Yu15b]. Besides dynamic surface control, the command filtered backstepping control was also proposed to solve the problem of explosion of complexity inherent in the conventional backstepping control approach [Far09, Far08]. In [Don12, Don10], the command filtered backstepping control method has extended to adaptive control. Several adaptive command filtered backstepping control

approaches have been introduced to control a class of uncertain nonlinear systems [Pan18, Yu18b, Yu15a].

Recently, immersion and invariance (I&I) based adaptive control of nonlinear systems was proposed by Astolfi and Ortega [Ast03]. It has been established for controlling many uncertain nonlinear systems in lower triangular form [Ast08a, Ast08b, Kar08, Sou21]. The design procedures of immersion and invariance based adaptive control consisted of a general two steps, while the first step is to design an estimator and the second step is to design a control law. Recently, immersion and invariance based adaptive command filtered backstepping control method has been designed for uncertain nonlinear systems [Son10a, Son10b]. Moreover, immersion and invariance based adaptive dynamic surface control technique has been also proposed [Fuj12, Sou21].

In adaptive control, the way of parameter estimation gives rise to two different schemes, direct and indirect techniques, a direct scheme that utilizes tracking errors and an indirect scheme that utilizes estimation errors. Composite adaptive control method is an integrated direct and indirect adaptive control schemes which aim to achieve better tracking and parameter convergence through faster and smoother parameter adaptation [Slo89]. The types of adaptive law modifications have been presented such as sum, σ -modification, ϵ -modification and projection [Che10, Far06, Ioa07, Ioa96, Pol96, Sou21, Sou19, Sou18, Sou17, Sou15, Yao97]. In [Cil07], a composite tuning functions based adaptive backstepping control method has been utilized for a class of single-input and single-output (SISO) uncertain nonlinear systems in lower triangular form to avoid the overparametrization problem. A composite adaptive dynamic surface control technique has been introduced for a class of SISO uncertain nonlinear systems in lower triangular form to overcome the problem of explosion of complexity [Sou18]. In [Pan16b], a composite adaptive command filtered backstepping control approach has been also proposed for a class of SISO uncertain nonlinear systems in lower triangular form to solve the problem of explosion of complexity.

Besides adaptive control, robust adaptive control scheme that combine robust control and adaptive control for uncertain nonlinear systems with external disturbances has also received a great attention in recent years and has been extensively used to control a large class of nonlinear systems. In [Zha15b], robust tuning functions based adaptive backstepping control approach has been presented for a class of uncertain nonlinear systems with external disturbances to avoid the overparametrization problem. In [Hou11, Zha18a, Zha18b, Zha17], robust adaptive dynamic surface control technique has been

proposed for a class of uncertain nonlinear systems with external disturbances to overcome the problem of explosion of complexity. Furthermore, composite robust adaptive dynamic surface control method of uncertain nonlinear system has been also designed in [Che10].

This thesis proposes the study of the composite adaptive control for a class of uncertain nonlinear systems in lower triangular form. This is to synthesize stable adaptive control laws with composite adaptive laws. The complexity of these control laws should be kept reasonable by the introduction of a filtering at the level of the virtual controllers. The combination aims to combine the direct adaptive laws (from a Lyapunov function) and the indirect adaptive laws (gradient or least squares) by considering sum, projection and σ -modification based adaptive laws.

This thesis presents a new approaches that combines adaptive laws for the adaptive control schemes of SISO uncertain nonlinear systems in lower triangular form. In these schemes, by utilizing the adaptive control designs and the gradient and least squares identifier with x-swapping filters of the indirect adaptive control designs, a novel composite mechanisms of adaptive laws with sum, projection and σ -modification techniques are developed while both tracking (surface) errors and estimation errors are combined to obtain better trajectory tracking performances, parameter estimates and control convergence. Composite tuning functions based adaptive backstepping control design is proposed to avoid the overparametrization problem. Composite adaptive dynamic surface control and composite robust adaptive dynamic surface control approaches are presented to overcome the problem of explosion of complexity. Composite immersion and invariance based adaptive command filtered backstepping control design is also developed to solve the problem of explosion of complexity. The boundedness of all signals in the closed-loop system is guaranteed based on the Lyapunov stability analysis theory. Simulation results for an electromechanical system (one-link manipulator actuated by a brush DC motor system) are provided to demonstrate the effectiveness of the proposed composite adaptive control techniques.

The thesis is organized as follows.

- The first chapter gives some basic definitions and tools on Lyapunov stability. These important tools are utilized to introduce the backstepping control design procedure. Then, the state of the art on the adaptive control techniques is discussed.
- In the second chapter, the composite tuning functions based adaptive backstepping control technique for a class of SISO uncertain nonlinear systems in lower triangular form is applied to remove the overparametrization problem in the conventional adaptive

backstepping control design. Stability analysis using Lyapunov stability theory is performed to guarantee that all signals in the closed-loop system are bounded. A comparative simulation results for the control of an electromechanical system are implemented to demonstrate the validity of the proposed composite adaptive control method.

- The third chapter discusses a novel design of composite adaptive dynamic surface control technique for a class of SISO uncertain nonlinear systems in lower triangular form in order to avoid the problem of explosion of complexity inherent in the conventional adaptive backstepping control and the composite tuning functions based adaptive backstepping control schemes. By introducing the Lyapunov stability theory, the proposed composite adaptive control method guarantees the boundedness of all signals in the closed-loop system. Simulation results for the control of an electromechanical system are provided to show the performance of the proposed composite adaptive control scheme in comparison with direct and indirect adaptive control designs.
- In the fourth chapter, the results of third chapter are extended to robust adaptive nonlinear control. The composite robust adaptive dynamic surface control approach for a class of SISO uncertain nonlinear systems in lower triangular form with unknown external disturbances is proposed to overcome also the problem of explosion of complexity. The proposed composite robust adaptive control technique guarantees that all signals in the closed-loop system are bounded by using the Lyapunov stability theory. A comparison for the control of an electromechanical system with direct and indirect robust adaptive control designs is made to illustrate the efficiency and robustness of the proposed composite robust adaptive control method.
- The last chapter introduces the composite immersion and invariance based adaptive command filtered backstepping control method for a class of SISO uncertain nonlinear systems in lower triangular form to overcome also the problem of explosion of complexity. The boundedness of all signals in the closed-loop system is guaranteed by introducing the Lyapunov stability theory. A comparative study for the control of an electromechanical system is tested to verify the effectiveness of the proposed composite adaptive control approach.

Finally, general conclusion and future research works are formulated to finish the thesis.

CHAPTER 1

State of the art and basic notions

Chapter 1

State of the art and basic notions

1.1 Introduction

The Lyapunov stability theory is a very important tool for the control of nonlinear systems. It is used to analyse the stability of the closed-loop system. The backstepping control method is one of the nonlinear control techniques. It has been widely adopted in the control of so many nonlinear systems, and has been also introduced in adaptive control methods. Then, the adaptive control techniques have also received a lot of attention from the control research community in recent years.

In this chapter, the important definitions and basic tools on Lyapunov stability are presented. These important tools are then utilized to introduce the backstepping control design procedure for SISO nonlinear systems in lower triangular form. Then, several adaptive control techniques are introduced to handle a large class of uncertain nonlinear systems.

The rest of this chapter is structured as follows. The Lyapunov stability concepts are presented in Section 1.2. In Section 1.3, the backstepping control method is designed. The state of the art on adaptive control techniques is discussed in Section 1.4. Conclusions are given in Section 1.5.

The following notations are adopted throughout this thesis. \mathbb{R} , \mathbb{R}^+ and \mathbb{R}^n denote the set of all real numbers, the positive real numbers and the real n -dimensional vectors space, respectively. $|\bullet|$ and $\|\bullet\|$ denote the absolute value and the Euclidean norm. L_2 and L_∞ denote the spaces of square integrable and bounded signals. $\text{sign}(\bullet)$ and $\tanh(\bullet)$ are the standard sign function and hyperbolic tangent function, respectively. $\min(\bullet)$ and $\max(\bullet)$ denote the functions of minimum and maximum. $\text{tr}(\bullet)$ denotes the trace operation. $(\hat{\bullet})$ denotes the estimate of (\bullet) and $(\tilde{\bullet})$ denotes the parameter estimation error of (\bullet) .

1.2 Lyapunov stability

In this section, we present some definitions and basic tools on stability [Far06, Ioa96, Kha02, Kha96, Krs95a, Slo91, Son10a].

1.2.1 Stability definitions

We consider the following system described by ordinary differential equation of the form:

$$\dot{x} = f(t, x), \quad x(t_0) = x_0 \quad (1.1)$$

where, $x \in \mathbb{R}^n$, and $f: \mathbb{R}^n \times \mathbb{R}^+ \rightarrow \mathbb{R}^n$ is a piecewise continuous function in t and locally Lipschitz in x . The following definitions of stability (stability in the sense of Lyapunov) are presented [Far06, Kha96].

Definition 1.2.1: A function $f(t, x)$ satisfies a Lipschitz condition on \mathcal{D} if $\|f(t, x) - f(t, y)\| \leq \gamma \|x - y\|$, with Lipschitz constant γ for all points (t, x) and (t, y) in \mathcal{D} , where $\mathcal{D} \subset \mathbb{R}^n$ is a domain that contains the origin $x = 0$.

Definition 1.2.2: Any point $x_e \in \mathbb{R}^n$ such that $f(t, x_e) = 0$, for all $t \geq t_0$ is an equilibrium point of the system described by (1.1). It can be assumed, without loss of generality, that the system described by (1.1) has an equilibrium point $x_e = 0$.

The following definitions 1.2.3 to 1.2.8 give the stability of this equilibrium point.

Definition 1.2.3: The equilibrium point $x_e = 0$ of the system described by (1.1) is stable (stability in the sense of Lyapunov) if for each $\epsilon > 0$ and any $t_0 > 0$, there exists a $\delta(\epsilon, t_0) > 0$ such that $\|x(t_0)\| < \delta(\epsilon, t_0)$ implies that $\|x(t)\| < \epsilon$ for all $t \geq t_0$.

Definition 1.2.4: The equilibrium point $x_e = 0$ of the system described by (1.1) is uniformly stable if for each $\epsilon > 0$ and any $t_0 > 0$, there exists a $\delta(\epsilon) > 0$ such that $\|x(t_0)\| < \delta(\epsilon)$ implies that $\|x(t)\| < \epsilon$ for all $t \geq t_0$.

Definition 1.2.5: The equilibrium point $x_e = 0$ of the system described by (1.1) is unstable if it is not stable.

Definition 1.2.6: The equilibrium point $x_e = 0$ of the system described by (1.1) is asymptotically stable if it is stable, and for any $t_0 \geq 0$, there exists a $\eta(t_0) > 0$ such that $\|x(t_0)\| < \eta(t_0)$ implies that $\lim_{t \rightarrow \infty} \|x(t)\| = 0$.

Definition 1.2.7: The equilibrium point $x_e = 0$ of the system described by (1.1) is uniformly asymptotically stable if it is uniformly stable, and there exists a $\delta > 0$ independent of t such that for all $\epsilon > 0$, there exists a $T(\epsilon) > 0$ such that $\|x(t_0)\| < \delta$ implies that $\|x(t)\| < \epsilon$ for all $t \geq t_0 + T(\epsilon)$.

Definition 1.2.8: The equilibrium point $x_e = 0$ of the system described by (1.1) is exponentially stable if for any $\epsilon > 0$ there exists a $\delta(\epsilon) > 0$ such that $\|x(t_0)\| < \delta$ implies that $\|x(t)\| < \epsilon e^{-\alpha(t-t_0)}$ for all $t \geq t_0 \geq 0$ for some $\alpha > 0$.

In some cases, it may not be possible to prove stability of x_e . In such cases concepts related to boundedness are important [Far06, Kha96].

Definition 1.2.9: The equilibrium point $x_e = 0$ of the system described by (1.1) is uniformly ultimately bounded if there exist positive constants R , $T(R)$ and b such that $\|x(t_0)\| \leq R$ implies that $\|x(t)\| < b$ for all $t > t_0 + T$.

Definition 1.2.10: The equilibrium point $x_e = 0$ of the system described by (1.1) is globally uniformly ultimately bounded if $R = \infty$.

The constant b is referred to as the ultimate bound.

1.2.2 Lyapunov's direct method

The stability properties of the equilibrium point or solution of (1.1) can be studied by using the so-called Lyapunov's direct method (or Lyapunov's second method). The ideas of Lyapunov's direct method are rigorously summarized by the Theorem 1.2.1 [Far06, Kha96]. Before presenting that theorem, the following definitions are introduced [Far06, Kha96]. $\mathcal{B}(r)$ denotes an open set containing the origin.

Definition 1.2.11: A continuous function $V(x)$ is positive definite on $\mathcal{B}(r)$ if $V(0) = 0$ and $V(x) > 0$ for all $x \in \mathcal{B}(r)$ such that $x \neq 0$.

Definition 1.2.12: A continuous function $V(x)$ is positive semi-definite on $\mathcal{B}(r)$ if $V(0) = 0$ and $V(x) \geq 0$ for all $x \in \mathcal{B}(r)$ such that $x \neq 0$.

Definition 1.2.13: A continuous function $V(x)$ is negative (semi-)definite on $\mathcal{B}(r)$ if $-V(x)$ is positive (semi-)definite.

Definition 1.2.14: A continuous function $V(x)$ is radially unbounded if $V(0)=0$, $V > 0$ on $\mathbb{R}^n - \{0\}$ and $V(x) \rightarrow \infty$ as $\|x\| \rightarrow \infty$.

Definition 1.2.15: A continuous function $V(t, x)$ is positive definite on $\mathbb{R} \times \mathcal{B}(r)$ if there exists a positive definite function $\omega(x)$ on $\mathcal{B}(r)$ such that $V(t, 0)=0$ for all $t \geq 0$, and $V(t, x) \geq \omega(x)$ for all $t \geq 0$ and for all $x \in \mathcal{B}(r)$.

Definition 1.2.16: A continuous function $V(t, x)$ is radially unbounded if there exists a radially unbounded function $\omega(x)$ such that $V(t, 0)=0$ for all $t \geq 0$, and $V(t, x) \geq \omega(x)$ for all $t \geq 0$ and for all $x \in \mathbb{R}^n$.

Definition 1.2.17: A continuous function $V(t, x)$ is decrescent on $\mathbb{R} \times \mathcal{B}(r)$ if there exists a positive definite function $\omega(x)$ on $\mathcal{B}(r)$ such that $V(t, x) \leq \omega(x)$ for all $t \geq 0$ and for all $x \in \mathcal{B}(r)$.

Let us assume (without loss of generality) that $x_e = 0$ is an equilibrium point of the system described by (1.1) and define \dot{V} to be the time derivative of the function $V(t, x)$ along the solution of the system described by (1.1), i.e.,

$$\dot{V} = \frac{\partial V}{\partial t} + \frac{\partial V}{\partial x} f(t, x) \quad (1.2)$$

The Lyapunov's direct method is summarized by the following theorem.

Theorem 1.2.1: Let $V(t, x): \mathbb{R}^+ \times \mathcal{D} \rightarrow \mathbb{R}$ be a continuously differentiable and positive definite function, where \mathcal{D} is an open region containing the origin. Then, the following statements are true:

- (i) If $\dot{V} \leq 0$ (negative semi-definite) for $x \in \mathcal{D}$, then the equilibrium point $x_e = 0$ is stable.
- (ii) If V is decrescent and $\dot{V} \leq 0$ for $x \in \mathcal{D}$, then the equilibrium point $x_e = 0$ is uniformly stable.
- (iii) If $\dot{V} < 0$ (negative definite) for $x \in \mathcal{D}$, then the equilibrium point $x_e = 0$ is asymptotically stable.
- (iv) If V is decrescent and $\dot{V} < 0$ for $x \in \mathcal{D}$, then the equilibrium point $x_e = 0$ is uniformly asymptotically stable.

(v) If there exist three positive constants c_1 , c_2 and c_3 such that

$$c_1 \|x\|^2 \leq V(t, x) \leq c_2 \|x\|^2 \text{ and } \dot{V}(t, x) \leq -c_3 \|x\|^2 \text{ for all } t \geq 0 \text{ and for all } x \in \mathcal{D},$$

then the equilibrium point $x_e = 0$ is exponentially stable.

1.2.3 Control Lyapunov functions

The control Lyapunov function (CLF) is an extension of the Lyapunov function concept to control design. Consider the following system [Krs95a]:

$$\dot{x} = f(x, u), \quad f(0, 0) = 0 \quad (1.3)$$

where, $x \in \mathbb{R}^n$ is the system state and $u \in \mathbb{R}$ is the control input. The control objective is to design a feedback control law $\alpha(x)$ for the control input u such that the equilibrium $x=0$ of the closed-loop system $\dot{x} = f(x, \alpha(x))$ is globally asymptotically stable. To prove stability, we can choose a function $V(x)$ as a Lyapunov candidate, and require that its derivative along the solutions of $\dot{x} = f(x, \alpha(x))$ satisfies $\dot{V}(x) \leq -W(x)$, where $W(x)$ is a positive definite function. Therefore, we need to find $\alpha(x)$ to ensure that for all $x \in \mathbb{R}^n$:

$$\frac{\partial V}{\partial x}(x) f(x, \alpha(x)) \leq -W(x) \quad (1.4)$$

A stabilizing control law for the system described by (1.3) may exist but we may fail to satisfy (1.4) due to a poor choice of $V(x)$ and $W(x)$. A system for which a good choice of $V(x)$ and $W(x)$ exists is said to possess a CLF. More precisely, the definition of a CLF is given below.

Definition 1.2.18 (CLF) [Krs95a]: A smooth positive definite and radially unbounded function $V : \mathbb{R}^n \times \mathbb{R}^+ \rightarrow \mathbb{R}^+$ is called a CLF for the system described by (1.3) if:

$$\inf_{u \in \mathbb{R}} \left\{ \frac{\partial V}{\partial x}(x) f(x, u) \right\} < 0, \quad \forall x \neq 0 \quad (1.5)$$

The existence of a CLF is equivalent to global asymptotic stabilizability.

For systems affine in the control [Krs95a]:

$$\dot{x} = f(x) + g(x)u \quad (1.6)$$

The CLF inequality described by (1.4) becomes:

$$\frac{\partial V}{\partial x} f(x) + \frac{\partial V}{\partial x} g(x) \alpha(x) \leq -W(x) \quad (1.7)$$

The main deficiency of the CLF concept as a design tool is that for most nonlinear systems a CLF is not known and the task of finding one may be as complex as that of designing a stabilizing feedback law. Backstepping control design procedure was introduced to solve these two tasks simultaneously for several important classes of nonlinear systems.

1.2.4 Some useful lemmas

The following useful lemmas are introduced for the convenience of the subsequent synthesis and analysis.

Lemma 1.2.1 (Barbalat lemma) [Far06]: Let $\phi(t): \mathbb{R}^+ \rightarrow \mathbb{R}$ be uniformly continuous function on $[0, \infty)$. If $\lim_{t \rightarrow \infty} \int_0^t \phi(\tau) d\tau = M < \infty$ (exists and finite), then $\lim_{t \rightarrow \infty} \phi(t) = 0$.

Remark 1.2.1: Combining this lemma with Lyapunov's direct method leads to the powerful theorem by LaSalle and Yoshizawa [Krs95a].

Lemma 1.2.2 [Far06]: Suppose $V(t) \geq 0$ satisfies the following inequality:

$$\dot{V}(t) \leq -cV(t) + \lambda \quad (1.8)$$

where, c and λ are positive constants. Then, $V(t)$ satisfies:

$$V(t) \leq \frac{\lambda}{c} + \left(V(0) - \frac{\lambda}{c} \right) e^{-ct} \quad (1.9)$$

Lemma 1.2.3 (Young's inequality) [Krs95a]: The following inequality holds for any $(x, y) \in \mathbb{R}^2$:

$$xy \leq \frac{\varepsilon^p}{p} \|x\|^p + \frac{1}{q\varepsilon^q} \|y\|^q \quad (1.10)$$

where, $\varepsilon > 0$ is a positive constant, $p > 1$ and $q > 1$ are constants which satisfy $(p-1)(q-1) = 1$.

1.3 Design of backstepping control

The control of nonlinear systems has attracted a great attention from the research community. Backstepping control design is one of these nonlinear control methods [Kha02, Krs95a]. Over the past few decades, Backstepping control method is one of the most popular and effective control approaches to deal with nonlinear systems in lower

triangular form. Nevertheless, the backstepping control technique suffers from the problem of explosion of complexity resulting from repeated derivations of virtual controllers at each recursive step. The problem of explosion of complexity has been solved by dynamic surface control [Hed00, Swa00, Swa97], and command filtered backstepping control [Far09, Far08]. Consider the following SISO nonlinear system in lower triangular form:

$$\begin{aligned}\dot{x}_1 &= f_1(x_1) + g_1(x_1)x_2 \\ \dot{x}_i &= f_i(\bar{x}_i) + g_i(\bar{x}_i)x_{i+1}, i = 2, \dots, n-1 \\ \dot{x}_n &= f_n(x) + g_n(x)u\end{aligned}\quad (1.11)$$

where, $x = [x_1 \ x_2 \ \dots \ x_n]^T \in \mathbb{R}^n$ is the system state vector with $\bar{x}_i = [x_1 \ x_2 \ \dots \ x_i]^T$ and $x = \bar{x}_n$, and $u \in \mathbb{R}$ is the control input. The nonlinear functions f_i and $g_i \neq 0$ are assumed to be known and continuous. The control objective of this approach is to construct a backstepping controller u such that the system output x_1 tracks the desired trajectory x_{1d} , where x_{1d} and its derivatives $\dot{x}_{1d}, \dots, x_{1d}^{(n-1)}$ and $x_{1d}^{(n)}$ are assumed to be known, continuous and bounded.

The main procedures of the backstepping control design are summarized as follows.

Define the tracking errors as $e_1 = x_1 - x_{1d}$ and $e_i = x_i - \alpha_{i-1}$ for $i = 2, \dots, n$, where α_{i-1} are virtual controllers. Construct the virtual controllers α_i and the actual control law u as:

$$\alpha_1 = \frac{1}{g_1}(-k_1 e_1 - f_1 + \dot{x}_{1d}) \quad (1.12)$$

$$\alpha_i = \frac{1}{g_i}(-k_i e_i - f_i + \dot{\alpha}_{i-1} - g_{i-1} e_{i-1}), i = 2, \dots, n-1 \quad (1.13)$$

$$u = \frac{1}{g_n}(-k_n e_n - f_n + \dot{\alpha}_{n-1} - g_{n-1} e_{n-1}) \quad (1.14)$$

where, $k_i > 0$ are positive constants, and $\dot{\alpha}_{i-1}$ with $i = 2, \dots, n$, are obtained by:

$$\dot{\alpha}_{i-1} = \sum_{k=1}^{i-1} \frac{\partial \alpha_{i-1}}{\partial x_k} (f_k + g_k x_{k+1}) + \sum_{k=1}^i \frac{\partial \alpha_{i-1}}{\partial x_{1d}^{(k-1)}} x_{1d}^{(k)} \quad (1.15)$$

The closed-loop tracking error dynamics are given by:

$$\dot{e}_1 = -k_1 e_1 + g_1 e_2 \quad (1.16)$$

$$\dot{e}_i = -k_i e_i + g_i e_{i+1} - g_{i-1} e_{i-1}, i = 2, \dots, n-1 \quad (1.17)$$

$$\dot{e}_n = -k_n e_n - g_{n-1} e_{n-1} \quad (1.18)$$

By choosing the Lyapunov function as:

$$V = \frac{1}{2} \sum_{i=1}^n e_i^2 \quad (1.19)$$

and taking its time derivative, further analysis shows that:

$$\dot{V} = -\sum_{k=1}^n k_k e_k^2 \leq -\alpha V \quad (1.20)$$

where, $\alpha = \min(2k_k) > 0$. This implies the exponential converge of the tracking errors to zero. Then, the controller guarantees that the closed-loop tracking error dynamics is globally exponentially stable.

1.4 Adaptive control techniques

The adaptive control techniques have been widely designed to control a large class of uncertain nonlinear systems in recent decades due to great demands from the industrial applications. In the literature, several significant types of adaptive control for uncertain nonlinear systems have been proposed including adaptive backstepping control [Kan91, Krs95a], adaptive feedback linearization [Isi89, Sas89], immersion and invariance based adaptive control [Ast08a] and adaptive sliding mode control [Utk92]. By introducing tuning functions, the overparametrization problem inherent in the conventional adaptive backstepping control has been eliminated [Krs95a, Krs92]. In [Lee12], adaptive backstepping control of uncertain nonlinear systems using fuzzy neural networks has been proposed. In [Din15, She17a, She17b, Wei16, Wei15], adaptive backstepping control for a class of nonlinear fractional order systems has been also proposed. In addition, adaptive backstepping control for a class of nonlinear chaotic systems has been introduced in [Ge04, Ge00a, Ge00b, Wan01].

Recently, adaptive dynamic surface control technique has been proposed to solve the problem of explosion of complexity arose from the repeated differentiations of virtual control functions for adaptive backstepping control and composite tuning functions based adaptive backstepping control approaches [Hed00, Yip98]. Several fuzzy or neural adaptive dynamic surface control approaches have been developed [Wan05, Yoo07, Zha16, Zha08]. In [Li12a, Liu11], adaptive dynamic surface control for a class of nonlinear chaotic systems has been also studied. For uncertain nonaffine nonlinear systems, an adaptive dynamic surface approach has been presented by using the modified linear filters [Liu17a]. In this way, adaptive command filtered backstepping control method has been also proposed to overcome the problem of explosion of complexity

[Don12, Don10], and has been widely utilized to control a particular class of uncertain nonlinear systems [Pan18, Sou19, Yu18b, Yu15a, Zou20].

The immersion and invariance based adaptive control has been also a great attention in the few recent years, which has been widely used to the control of a class of uncertain nonlinear systems [Han19, Han18, Liu14, Son10a, Zha12b, Zha11]. Many significant different types of nonlinear control approaches have been devised in the literature including, adaptive command filtered backstepping control [Son10a], adaptive backstepping control [Kar08, Zha12b, Zha11], adaptive sliding mode control [Han15] and adaptive dynamic surface control [Fuj12, Sou21].

To deal with the uncertain nonlinear systems with unmeasured states, two useful observers have been proposed. An Observer based adaptive backstepping control with tuning functions method has been proposed in [Krs95a, She17b, Wei16, Zha12a, Zho07]. In [Li12a, Liu12, Liu11, Zha15a, Zha13, Wan12], observer based adaptive dynamic surface control method has been presented.

During the last years, to improve parameter estimation and obtain better control performance than conventional adaptive control techniques, the composite adaptive control method that utilized both the tracking errors and the estimation errors for parameter adaptive laws has been proposed for uncertain nonlinear systems. The performance improvements of composite adaptive control schemes which integrate direct and indirect adaptive laws have been implemented in several control techniques [Cil09, Hu10, Li10b, Moh11, Pan17, Pan13, Pat10, Slo89, Wei13, Yao03]. A composite tuning functions based adaptive backstepping control technique has been proposed to avoid the overparametrization problem [Cil07, Sou15]. In [Sou18, Sou17], a composite adaptive dynamic surface control approach has been developed to eliminate the problem of explosion of complexity. In [Pan16a, Pan16b, Pan16c], a composite adaptive command filtered backstepping control method has been further developed to overcome the problem of explosion of complexity.

In particular, a robust tuning functions based adaptive backstepping control scheme has been applied to eliminate the overparametrization problem [Zha15b]. A robust adaptive dynamic surface control method has been proposed to avoid the problem of explosion of complexity [Elm19, Gan15, He16, Hou11, Liu18b, Li12b, Li10a, Li10b, She17c, Zha18a, Zha18b, Zha17]. In [Che10], a robust composite adaptive dynamic surface control approach has been also developed.

1.5 Conclusion

This chapter presents some basic definitions and lemmas on the system stability, which play important roles in the controller design and the stability analysis. The backstepping control design with stability analysis is studied for SISO nonlinear systems in lower triangular form. The state of the art on adaptive control methods of uncertain nonlinear systems is discussed. Next works will focus on designing of composite adaptive control techniques.

CHAPTER 2

Composite tuning functions based adaptive backstepping control

Chapter 2

Composite tuning functions based adaptive backstepping control

2.1 Introduction

Backstepping control technique is a systematic nonlinear control approach based on the Lyapunov stability theory. It provides a systematic and a recursive formulation for nonlinear control systems [Kha02]. Backstepping control design has been widely used in many nonlinear control systems, and has been also introduced in adaptive control methods. Adaptive backstepping control design is one of nonlinear adaptive control approaches, which has received much attention [Krs95a]. The first adaptive backstepping design has been developed and proposed by Kanellakopoulos et al. [Kan91] to achieve global stabilization in the presence of unknown parameters. It has been established for controlling of many uncertain nonlinear systems [Ben00, Kan91, Krs95a, van11, Wan17, Zho08]. However, the main drawback in this approach is the overparametrization problem. This problem has been removed by using tuning functions design [Krs95a, Krs92], in which the number of parameter estimates is reduced to be minimal, that is, exactly equal to the number of unknown constant parameters. Tuning functions based adaptive backstepping control has been also a great attention in the few recent years, which has been widely used to the control of a class of uncertain nonlinear systems [Cil07, Cob19, Sou15, Wan16, Zha15b, Zho08]. Composite adaptive control has also received a great attention in recent years and has been extensively used to control a particular class of nonlinear systems [Cil09, Hu10, Moh11, Pan17, Pan13, Pat10, Slo89, Wei13, Yao03]. In the recent years, composite tuning functions based adaptive backstepping control has been utilized for a class of SISO uncertain nonlinear systems [Cil07, Sou15].

This chapter presents a new approach that combines direct and indirect adaptive laws for composite tuning functions based adaptive backstepping control for a class of SISO uncertain nonlinear systems in lower triangular form. In this method, by applying of direct

tuning functions based adaptive backstepping control and the x-swapping filters with gradient and least squares adaptive laws of indirect adaptive control, a novel composite mechanism of adaptation is proposed. The composite sum based gradient adaptive law and the composite σ -modification based gradient and least squares adaptive laws are introduced in order to achieve better parameter estimation and, hence, better trajectory tracking performances. Tuning functions are introduced to avoid the overparametrization problem inherent in the conventional adaptive backstepping control. The boundedness of all signals in the closed-loop system is performed by using the Lyapunov stability analysis theory. In order to demonstrate the effectiveness of the proposed composite adaptive control approach, simulation results for an electromechanical system are provided. Moreover, direct and indirect adaptive control designs are also studied and simulated for comparison purposes with the proposed composite adaptive control scheme.

The remaining of the chapter is organized as follows. The direct tuning functions based adaptive backstepping control is presented in Section 2.2. Section 2.3 is devoted to the indirect adaptive control. The composite tuning functions based adaptive backstepping control is proposed in Section 2.4. Section 2.5 is discussed the description of the dynamic model of an electromechanical system. Section 2.6 is concerned with the simulation results and discussions of the proposed adaptive controller designs. Conclusions are given in Section 2.7.

2.2 Direct tuning functions based adaptive backstepping control

In this section, we will consider the following SISO uncertain nonlinear system in lower triangular form:

$$\begin{aligned}\dot{x}_1 &= g_1(x_1)x_2 + \varphi_1^T(x_1)\theta + \psi_1(x_1) \\ \dot{x}_i &= g_i(\bar{x}_i)x_{i+1} + \varphi_i^T(\bar{x}_i)\theta + \psi_i(\bar{x}_i), i = 2, \dots, n-1 \\ \dot{x}_n &= g_n(x)u + \varphi_n^T(x)\theta + \psi_n(x)\end{aligned}\quad (2.1)$$

where, $x = [x_1 \ x_2 \ \dots \ x_n]^T \in \mathbb{R}^n$ and $u \in \mathbb{R}$ are system states and the control input, respectively. $\theta \in \mathbb{R}^P$ is unknown constant parameter vector, $\bar{x}_i = [x_1 \ x_2 \ \dots \ x_i]^T$ and $x = \bar{x}_n$. The nonlinear functions φ_i^T , ψ_i and $g_i \neq 0$ are known and continuous. The control objective of this approach is to construct a direct tuning functions based adaptive backstepping controller u such that the system output x_1 tracks the desired trajectory x_{1d} and to ensure that all signals in the closed-loop system are bounded. Throughout this

chapter, to achieve the control objective, the following standard assumptions of the system (2.1) are required.

Assumption 2.2.1: There is a positive constant g_0 where, $|g_i(\bar{x}_i)| \geq g_0$, $i = 1, \dots, n$.

Assumption 2.2.2: The desired trajectory x_{1d} and its derivatives $\dot{x}_{1d}, \dots, x_{1d}^{(n-1)}$ and $x_{1d}^{(n)}$ are known, continuous and bounded.

Remark 2.2.1: Assumption 2.2.1 is employed to guarantee the controllability of system (2.1). Assumption 2.2.2 is required to ensure the boundedness of the time derivatives of virtual controllers during the stability analysis.

The detailed procedures of the direct tuning functions based adaptive backstepping control design for system (2.1) with stability analysis using Lyapunov stability theory are given as follows.

Step 1: Define the first tracking error as $e_1 = x_1 - x_{1d}$, then, the time derivative of e_1 is obtained as:

$$\dot{e}_1 = g_1 x_2 + \varphi_1^T \theta + \psi_1 - \dot{x}_{1d} = g_1 e_2 + g_1 \alpha_1 + \varphi_1^T \theta + \psi_1 - \dot{x}_{1d} \quad (2.2)$$

The corresponding Lyapunov function candidate V_1 is defined as:

$$V_1 = \frac{1}{2} e_1^2 + \frac{1}{2} \tilde{\theta}^T \Gamma^{-1} \tilde{\theta} \quad (2.3)$$

where, $\Gamma = \Gamma^T > 0$ is a positive definite constant matrix and $\tilde{\theta} = \theta - \hat{\theta}$ is the parametric estimation error. The time derivative of V_1 is given by:

$$\dot{V}_1 = e_1 (g_1 e_2 + g_1 \alpha_1 + \varphi_1^T \hat{\theta} + \psi_1 - \dot{x}_{1d}) - \tilde{\theta}^T \Gamma^{-1} (\dot{\hat{\theta}} - \Gamma \varphi_1 e_1) \quad (2.4)$$

The tuning function τ_1 is defined as:

$$\tau_1 = \Gamma \varphi_1 e_1 \quad (2.5)$$

We choose the virtual control α_1 as:

$$\alpha_1 = \frac{1}{g_1} (-k_1 e_1 - \varphi_1^T \hat{\theta} - \psi_1 + \dot{x}_{1d}) \quad (2.6)$$

where, $k_1 > 0$ is a positive design constant. Substituting (2.6) into (2.4), the derivative of the Lyapunov function \dot{V}_1 becomes:

$$\dot{V}_1 = -k_1 e_1^2 + g_1 e_1 e_2 - \tilde{\theta}^T \Gamma^{-1} (\dot{\hat{\theta}} - \tau_1) \quad (2.7)$$

Step 2: Define the second tracking error as $e_2 = x_2 - \alpha_1$, then, the time derivative of e_2 is obtained as:

$$\dot{e}_2 = g_2 e_3 + g_2 \alpha_2 + \varphi_2^T \theta + \psi_2 - \frac{\partial \alpha_1}{\partial x_1} (g_1 x_2 + \varphi_1^T \theta + \psi_1) - \frac{\partial \alpha_1}{\partial \hat{\theta}} \dot{\hat{\theta}} - \sum_{k=1}^2 \frac{\partial \alpha_1}{\partial x_{1d}^{(k-1)}} x_{1d}^{(k)} \quad (2.8)$$

The corresponding Lyapunov function candidate V_2 is defined as:

$$V_2 = V_1 + \frac{1}{2} e_2^2 \quad (2.9)$$

The time derivative of V_2 is given by:

$$\begin{aligned} \dot{V}_2 = & -k_1 e_1^2 + e_2 \left(g_1 e_1 + g_2 e_3 + g_2 \alpha_2 + \varphi_2^T \hat{\theta} + \psi_2 - \frac{\partial \alpha_1}{\partial x_1} (g_1 x_2 + \varphi_1^T \hat{\theta} + \psi_1) \right. \\ & \left. - \frac{\partial \alpha_1}{\partial \hat{\theta}} \dot{\hat{\theta}} - \sum_{k=1}^2 \frac{\partial \alpha_1}{\partial x_{1d}^{(k-1)}} x_{1d}^{(k)} \right) - \tilde{\theta}^T \Gamma^{-1} \left(\dot{\hat{\theta}} - \tau_1 + \Gamma \left(-\varphi_2 + \frac{\partial \alpha_1}{\partial x_1} \varphi_1 \right) e_2 \right) \end{aligned} \quad (2.10)$$

The tuning function τ_2 is defined as:

$$\tau_2 = \tau_1 - \Gamma \left(-\varphi_2 + \frac{\partial \alpha_1}{\partial x_1} \varphi_1 \right) e_2 \quad (2.11)$$

We choose the virtual control α_2 as:

$$\alpha_2 = \frac{1}{g_2} \left(-k_2 e_2 - g_1 e_1 - \varphi_2^T \hat{\theta} - \psi_2 + \frac{\partial \alpha_1}{\partial x_1} (g_1 x_2 + \varphi_1^T \hat{\theta} + \psi_1) + \frac{\partial \alpha_1}{\partial \hat{\theta}} \tau_2 + \sum_{k=1}^2 \frac{\partial \alpha_1}{\partial x_{1d}^{(k-1)}} x_{1d}^{(k)} \right) \quad (2.12)$$

where, $k_2 > 0$ is a positive design constant. Substituting (2.12) into (2.10), the derivative of the Lyapunov function \dot{V}_2 becomes:

$$\dot{V}_2 = -k_1 e_1^2 - k_2 e_2^2 + g_2 e_2 e_3 - e_2 \frac{\partial \alpha_1}{\partial \hat{\theta}} \left(\dot{\hat{\theta}} - \tau_2 \right) - \tilde{\theta}^T \Gamma^{-1} \left(\dot{\hat{\theta}} - \tau_2 \right) \quad (2.13)$$

Step 3: Define the third tracking error as $e_3 = x_3 - \alpha_2$, then, the time derivative of e_3 is obtained as:

$$\begin{aligned} \dot{e}_3 = & g_3 e_4 + g_3 \alpha_3 + \varphi_3^T \theta + \psi_3 - \frac{\partial \alpha_2}{\partial x_1} (g_1 x_2 + \varphi_1^T \theta + \psi_1) \\ & - \frac{\partial \alpha_2}{\partial x_2} (g_2 x_3 + \varphi_2^T \theta + \psi_2) - \frac{\partial \alpha_2}{\partial \hat{\theta}} \dot{\hat{\theta}} - \sum_{k=1}^3 \frac{\partial \alpha_2}{\partial x_{1d}^{(k-1)}} x_{1d}^{(k)} \end{aligned} \quad (2.14)$$

The corresponding Lyapunov function candidate V_3 is defined as:

$$V_3 = V_2 + \frac{1}{2} e_3^2 \quad (2.15)$$

The time derivative of V_3 is given by:

$$\begin{aligned} \dot{V}_3 = & -k_1 e_1^2 - k_2 e_2^2 + e_3 \left(g_2 e_2 + g_3 e_4 + g_3 \alpha_3 + \varphi_3^T \hat{\theta} + \psi_3 - \frac{\partial \alpha_2}{\partial x_1} (g_1 x_2 + \varphi_1^T \hat{\theta} + \psi_1) \right. \\ & - \frac{\partial \alpha_2}{\partial x_2} (g_2 x_3 + \varphi_2^T \hat{\theta} + \psi_2) - \frac{\partial \alpha_2}{\partial \hat{\theta}} \dot{\hat{\theta}} - \sum_{k=1}^3 \frac{\partial \alpha_2}{\partial x_{1d}^{(k-1)}} x_{1d}^{(k)} \left. \right) - e_2 \frac{\partial \alpha_1}{\partial \hat{\theta}} (\dot{\hat{\theta}} - \tau_2) \\ & - \tilde{\theta}^T \Gamma^{-1} \left(\dot{\hat{\theta}} - \tau_2 + \Gamma \left(-\varphi_3 + \frac{\partial \alpha_2}{\partial x_1} \varphi_1 + \frac{\partial \alpha_2}{\partial x_2} \varphi_2 \right) e_3 \right) \end{aligned} \quad (2.16)$$

The tuning function τ_3 is defined as:

$$\tau_3 = \tau_2 - \Gamma \left(-\varphi_3 + \frac{\partial \alpha_2}{\partial x_1} \varphi_1 + \frac{\partial \alpha_2}{\partial x_2} \varphi_2 \right) e_3 \quad (2.17)$$

We choose the virtual control α_3 as:

$$\begin{aligned} \alpha_3 = & \frac{1}{g_3} \left(-k_3 e_3 - g_2 e_2 - \varphi_3^T \hat{\theta} - \psi_3 + \frac{\partial \alpha_2}{\partial x_1} (g_1 x_2 + \varphi_1^T \hat{\theta} + \psi_1) \right. \\ & \left. + \frac{\partial \alpha_2}{\partial x_2} (g_2 x_3 + \varphi_2^T \hat{\theta} + \psi_2) + \frac{\partial \alpha_2}{\partial \hat{\theta}} \tau_3 + \sum_{k=1}^3 \frac{\partial \alpha_2}{\partial x_{1d}^{(k-1)}} x_{1d}^{(k)} - v_3 \right) \end{aligned} \quad (2.18)$$

where, $v_3 = e_2 \frac{\partial \alpha_1}{\partial \hat{\theta}} \Gamma \left(-\varphi_3 + \frac{\partial \alpha_2}{\partial x_1} \varphi_1 + \frac{\partial \alpha_2}{\partial x_2} \varphi_2 \right)$ and $k_3 > 0$ is a positive design constant.

Substituting (2.18) into (2.16), the derivative of the Lyapunov function \dot{V}_3 becomes:

$$\dot{V}_3 = -k_1 e_1^2 - k_2 e_2^2 - k_3 e_3^2 + g_3 e_3 e_4 - e_3 \frac{\partial \alpha_2}{\partial \hat{\theta}} (\dot{\hat{\theta}} - \tau_3) - e_2 \frac{\partial \alpha_1}{\partial \hat{\theta}} (\dot{\hat{\theta}} - \tau_2) - \tilde{\theta}^T \Gamma^{-1} (\dot{\hat{\theta}} - \tau_3) - e_3 v_3 \quad (2.19)$$

one has,

$$\dot{\hat{\theta}} - \tau_2 = \dot{\hat{\theta}} - \tau_3 - \Gamma \left(-\varphi_3 + \frac{\partial \alpha_2}{\partial x_1} \varphi_1 + \frac{\partial \alpha_2}{\partial x_2} \varphi_2 \right) e_3 \quad (2.20)$$

Substituting (2.20) into (2.19), we obtain:

$$\dot{V}_3 = -k_1 e_1^2 - k_2 e_2^2 - k_3 e_3^2 + g_3 e_3 e_4 - \left(e_3 \frac{\partial \alpha_2}{\partial \hat{\theta}} + e_2 \frac{\partial \alpha_1}{\partial \hat{\theta}} \right) (\dot{\hat{\theta}} - \tau_3) - \tilde{\theta}^T \Gamma^{-1} (\dot{\hat{\theta}} - \tau_3) \quad (2.21)$$

Step i ($i=4, \dots, n-1$): Define the i^{th} tracking error as $e_i = x_i - \alpha_{i-1}$, then, the time derivative of e_i is obtained as:

$$\dot{e}_i = g_i e_{i+1} + g_i \alpha_i + \varphi_i^T \theta + \psi_i - \sum_{k=1}^{i-1} \frac{\partial \alpha_{i-1}}{\partial x_k} (g_k x_{k+1} + \varphi_k^T \theta + \psi_k) - \frac{\partial \alpha_{i-1}}{\partial \hat{\theta}} \dot{\hat{\theta}} - \sum_{k=1}^i \frac{\partial \alpha_{i-1}}{\partial x_{1d}^{(k-1)}} x_{1d}^{(k)} \quad (2.22)$$

The corresponding Lyapunov function candidate V_i is defined as:

$$V_i = V_{i-1} + \frac{1}{2}e_i^2 \quad (2.23)$$

The time derivative of V_i is given by:

$$\begin{aligned} \dot{V}_i = & -\sum_{k=1}^{i-1} k_k e_k^2 + e_i \left(g_{i-1} e_{i-1} + g_i e_{i+1} + g_i \alpha_i + \varphi_i^T \hat{\theta} + \psi_i - \sum_{k=1}^{i-1} \frac{\partial \alpha_{i-1}}{\partial x_k} (g_k x_{k+1} + \varphi_k^T \hat{\theta} + \psi_k) - \frac{\partial \alpha_{i-1}}{\partial \hat{\theta}} \dot{\hat{\theta}} \right. \\ & \left. - \sum_{k=1}^i \frac{\partial \alpha_{i-1}}{\partial x_{1d}^{(k-1)}} x_{1d}^{(k)} \right) - \sum_{k=1}^{i-2} e_{k+1} \frac{\partial \alpha_k}{\partial \hat{\theta}} (\dot{\hat{\theta}} - \tau_{i-1}) - \tilde{\theta}^T \Gamma^{-1} \left(\dot{\hat{\theta}} - \tau_{i-1} + \Gamma \left(-\varphi_i + \sum_{k=1}^{i-1} \frac{\partial \alpha_{i-1}}{\partial x_k} \varphi_k \right) e_i \right) \end{aligned} \quad (2.24)$$

The tuning functions τ_i are defined as:

$$\tau_i = \tau_{i-1} - \Gamma \left(-\varphi_i + \sum_{k=1}^{i-1} \frac{\partial \alpha_{i-1}}{\partial x_k} \varphi_k \right) e_i \quad (2.25)$$

We choose the virtual controllers α_i as:

$$\begin{aligned} \alpha_i = & \frac{1}{g_i} \left(-k_i e_i - g_{i-1} e_{i-1} - \varphi_i^T \hat{\theta} - \psi_i + \sum_{k=1}^{i-1} \frac{\partial \alpha_{i-1}}{\partial x_k} (g_k x_{k+1} + \varphi_k^T \hat{\theta} + \psi_k) \right. \\ & \left. + \frac{\partial \alpha_{i-1}}{\partial \hat{\theta}} \tau_i + \sum_{k=1}^i \frac{\partial \alpha_{i-1}}{\partial x_{1d}^{(k-1)}} x_{1d}^{(k)} - v_i \right) \end{aligned} \quad (2.26)$$

where, $v_i = \sum_{k=1}^{i-2} e_{k+1} \frac{\partial \alpha_k}{\partial \hat{\theta}} \Gamma \left(-\varphi_i + \sum_{k=1}^{i-1} \frac{\partial \alpha_{i-1}}{\partial x_k} \varphi_k \right)$ and $k_i > 0$ is a positive design constants.

Substituting (2.26) into (2.24), the derivative of the Lyapunov function \dot{V}_i becomes:

$$\dot{V}_i = -\sum_{k=1}^i k_k e_k^2 + g_i e_i e_{i+1} - e_i \frac{\partial \alpha_{i-1}}{\partial \hat{\theta}} (\dot{\hat{\theta}} - \tau_i) - \sum_{k=1}^{i-2} e_{k+1} \frac{\partial \alpha_k}{\partial \hat{\theta}} (\dot{\hat{\theta}} - \tau_{i-1}) - \tilde{\theta}^T \Gamma^{-1} (\dot{\hat{\theta}} - \tau_i) - e_i v_i \quad (2.27)$$

one has,

$$\dot{\hat{\theta}} - \tau_{i-1} = \dot{\hat{\theta}} - \tau_i - \Gamma \left(-\varphi_i + \sum_{k=1}^{i-1} \frac{\partial \alpha_{i-1}}{\partial x_k} \varphi_k \right) e_i \quad (2.28)$$

Substituting (2.28) into (2.27), we obtain:

$$\dot{V}_i = -\sum_{k=1}^i k_k e_k^2 + g_i e_i e_{i+1} - \sum_{k=1}^{i-1} e_{k+1} \frac{\partial \alpha_k}{\partial \hat{\theta}} (\dot{\hat{\theta}} - \tau_i) - \tilde{\theta}^T \Gamma^{-1} (\dot{\hat{\theta}} - \tau_i) \quad (2.29)$$

Step n : Define the n^{th} tracking error as $e_n = x_n - \alpha_{n-1}$, then, the time derivative of e_n is obtained as:

$$\dot{e}_n = g_n u + \varphi_n^T \theta + \psi_n - \sum_{k=1}^{n-1} \frac{\partial \alpha_{n-1}}{\partial x_k} (g_k x_{k+1} + \varphi_k^T \theta + \psi_k) - \frac{\partial \alpha_{n-1}}{\partial \hat{\theta}} \dot{\hat{\theta}} - \sum_{k=1}^n \frac{\partial \alpha_{n-1}}{\partial x_{1d}^{(k-1)}} x_{1d}^{(k)} \quad (2.30)$$

The corresponding Lyapunov function candidate $V = V_n$ is defined as:

$$V = V_{n-1} + \frac{1}{2}e_n^2 \quad (2.31)$$

The time derivative of V is given by:

$$\begin{aligned} \dot{V} = & -\sum_{k=1}^{n-1} k_k e_k^2 + e_n \left(g_{n-1} e_{n-1} + g_n u + \varphi_n^T \hat{\theta} + \psi_n - \sum_{k=1}^{n-1} \frac{\partial \alpha_{n-1}}{\partial x_k} (g_k x_{k+1} + \varphi_k^T \hat{\theta} + \psi_k) - \frac{\partial \alpha_{n-1}}{\partial \hat{\theta}} \dot{\hat{\theta}} \right. \\ & \left. - \sum_{k=1}^n \frac{\partial \alpha_{n-1}}{\partial x_{1d}^{(k-1)}} x_{1d}^{(k)} \right) - \sum_{k=1}^{n-2} e_{k+1} \frac{\partial \alpha_k}{\partial \hat{\theta}} (\dot{\hat{\theta}} - \tau_{n-1}) - \tilde{\theta}^T \Gamma^{-1} \left(\dot{\hat{\theta}} - \tau_{n-1} + \Gamma \left(-\varphi_n + \sum_{k=1}^{n-1} \frac{\partial \alpha_{n-1}}{\partial x_k} \varphi_k \right) e_n \right) \end{aligned} \quad (2.32)$$

The tuning function τ_n is defined as:

$$\tau_n = \tau_{n-1} - \Gamma \left(-\varphi_n + \sum_{k=1}^{n-1} \frac{\partial \alpha_{n-1}}{\partial x_k} \varphi_k \right) e_n \quad (2.33)$$

We choose the actual control input u as:

$$\begin{aligned} u = & \frac{1}{g_n} \left(-k_n e_n - g_{n-1} e_{n-1} - \varphi_n^T \hat{\theta} - \psi_n + \sum_{k=1}^{n-1} \frac{\partial \alpha_{n-1}}{\partial x_k} (g_k x_{k+1} + \varphi_k^T \hat{\theta} + \psi_k) \right. \\ & \left. + \frac{\partial \alpha_{n-1}}{\partial \hat{\theta}} \tau_n + \sum_{k=1}^n \frac{\partial \alpha_{n-1}}{\partial x_{1d}^{(k-1)}} x_{1d}^{(k)} - v_n \right) \end{aligned} \quad (2.34)$$

where, $v_n = \sum_{k=1}^{n-2} e_{k+1} \frac{\partial \alpha_k}{\partial \hat{\theta}} \Gamma \left(-\varphi_n + \sum_{k=1}^{n-1} \frac{\partial \alpha_{n-1}}{\partial x_k} \varphi_k \right)$ and $k_n > 0$ is a positive design constant.

Substituting (2.34) into (2.32), the derivative of the Lyapunov function \dot{V} becomes:

$$\dot{V} = -\sum_{k=1}^n k_k e_k^2 - e_n \frac{\partial \alpha_{n-1}}{\partial \hat{\theta}} (\dot{\hat{\theta}} - \tau_n) - \sum_{k=1}^{n-2} e_{k+1} \frac{\partial \alpha_k}{\partial \hat{\theta}} (\dot{\hat{\theta}} - \tau_{n-1}) - \tilde{\theta}^T \Gamma^{-1} (\dot{\hat{\theta}} - \tau_n) - e_n v_n \quad (2.35)$$

The direct adaptive law is given by:

$$\dot{\hat{\theta}} = \tau_n \quad (2.36)$$

Substituting (2.36) into (2.35), we obtain:

$$\dot{V} = -\sum_{k=1}^n k_k e_k^2 - \sum_{k=1}^{n-2} e_{k+1} \frac{\partial \alpha_k}{\partial \hat{\theta}} (\dot{\hat{\theta}} - \tau_{n-1}) - e_n v_n \quad (2.37)$$

one has,

$$\dot{\hat{\theta}} - \tau_{n-1} = \tau_n - \tau_{n-1} = -\Gamma \left(-\varphi_n + \sum_{k=1}^{n-1} \frac{\partial \alpha_{n-1}}{\partial x_k} \varphi_k \right) e_n \quad (2.38)$$

Substituting (2.38) into (2.37), we obtain:

$$\dot{V} = -\sum_{k=1}^n k_k e_k^2 \leq 0 \quad (2.39)$$

From (2.39), it is clearly that \dot{V} is negative semi-definite and $V \in L_\infty$ (bounded).

From (2.39), we establish that V is non-increasing. Hence, e_k , $k=1, \dots, n$ and $\tilde{\theta}$ are bounded. Furthermore, all signals in the closed-loop system, i.e., x_{1d} , $\dot{x}_{1d}, \dots, x_{1d}^{(n-1)}$, $x_{1d}^{(n)}$, α_i , u and $\hat{\theta}$ are also bounded.

By integrating of inequality (2.39) over $[0, \infty]$, we obtain:

$$\int_0^{\infty} \sum_{k=1}^n k_k e_k^2 d\tau \leq V(0) - V(\infty) < \infty \quad (2.40)$$

It means that, $e_k \in L_2$, $k=1, \dots, n$ (square integrable). Therefore, $e_k \in L_2 \cap L_\infty$, $k=1, \dots, n$. By applying Barbala's lemma [Slo91], we get $\lim_{t \rightarrow \infty} e_k = 0$, $k=1, \dots, n$, which implies the asymptotic convergence of tracking errors to zero.

2.3 Indirect adaptive control

In this section, the x-swapping filters with gradient and least squares adaptive laws are designed for the indirect adaptive control design. The indirect adaptive law based on x-swapping filters as described in this section is used to estimate the unknown parameters. In the following, the detailed procedures for the indirect adaptive control design with stability analysis are established.

2.3.1 Identification based x-swapping filters

The swapping filters are used as an analytical device that uses regressor filtering to account for the time-varying nature of the parameter estimates. The idea of a swapping filter is to use nonlinear regressor filtering to convert the dynamic parametric system into a static form in such a way that a standard parameter estimation algorithm can be used. Two different types of swapping schemes are presented, one using z-swapping based identifier derived from the tracking error model, and the other using x-swapping based identifier derived from the state dynamics [Krs95a, Krs95b, Krs93, Son09, Sou18, Sou17, Sou15, van11, van10, Wu18]. Each of these two swapping based identifiers allows application of gradient and least squares adaptive laws. The uncertain nonlinear system in lower triangular form (2.1) can be rewritten under the following nonlinear system in parametric x-model form as:

$$\dot{x} = f(x, u) + \varphi^T(x)\theta \quad (2.41)$$

where,

$$f(x, u) = \begin{bmatrix} g_1 x_2 + \psi_1 \\ \vdots \\ g_{n-1} x_n + \psi_{n-1} \\ g_n u + \psi_n \end{bmatrix} \quad (2.42)$$

We introduce the following x-swapping filters as [Krs95a]:

$$\dot{\Omega}_0 = A(\Omega_0 + x) - f(x, u), \Omega_0 \in \mathbb{R}^n \quad (2.43)$$

$$\dot{\Omega}^T = A\Omega^T + \varphi^T(x), \Omega \in \mathbb{R}^{p \times n} \quad (2.44)$$

where, $A < 0$ is a negative definite matrix for each x continuous in t . We define the estimation error vector as:

$$\epsilon = x + \Omega_0 - \Omega^T \hat{\theta}, \epsilon \in \mathbb{R}^n \quad (2.45)$$

with, $\hat{\theta}$ the estimate of θ and let:

$$\tilde{\epsilon} = x + \Omega_0 - \Omega^T \theta, \tilde{\epsilon} \in \mathbb{R}^n \quad (2.46)$$

We obtain:

$$\epsilon = \Omega^T \tilde{\theta} + \tilde{\epsilon} \quad (2.47)$$

The dynamics of $\tilde{\epsilon}$ is governed by:

$$\dot{\tilde{\epsilon}} = \dot{x} + \dot{\Omega}_0 - \dot{\Omega}^T \theta = A\tilde{\epsilon} \quad (2.48)$$

To guarantee the boundedness of Ω when $\varphi(x)$ grows unbounded, a particular choice of A is made:

$$A = A_0 - \lambda \varphi^T(x) \varphi(x) P \quad (2.49)$$

where, $\lambda > 0$ and A_0 is an arbitrary constant matrix satisfying:

$$PA_0 + A_0^T P = -I, P = P^T > 0 \quad (2.50)$$

2.3.2 Choice of adaptive laws

The gradient adaptive law is given by:

$$\dot{\hat{\theta}} = \Gamma \frac{\Omega \epsilon}{1 + \nu \text{tr}\{\Omega^T \Omega\}}, \Gamma = \Gamma^T > 0, \nu \geq 0 \quad (2.51)$$

The least squares adaptive law is given by:

$$\dot{\hat{\theta}} = \Gamma \frac{\Omega \epsilon}{1 + \nu \text{tr}\{\Omega^T \Gamma \Omega\}} \quad (2.52)$$

where, Γ is defined as:

$$\dot{\Gamma} = -\Gamma \frac{\Omega \Omega^T}{1 + \nu \text{tr}\{\Omega^T \Gamma \Omega\}} \Gamma, \Gamma(0) = \Gamma^T(0) > 0, \nu \geq 0 \quad (2.53)$$

2.3.3 Proof of stability

Lemma 2.3.1: To establish the identifier properties, let $[0, t_f)$, the maximal interval of existence of solutions of (2.41), the x-swapping filters (2.43) and (2.44), and the gradient adaptive law (2.51) or the least squares adaptive law (2.52) and (2.53). Then for $\nu \geq 0$, the following properties hold [Krs95a]:

$$\tilde{\theta} \in L_\infty \quad (2.54)$$

$$\epsilon \in L_2 \cap L_\infty \quad (2.55)$$

$$\dot{\tilde{\theta}} \in L_2 \cap L_\infty \quad (2.56)$$

2.3.3.1 Gradient adaptive law

We consider the following Lyapunov function as:

$$V = \frac{1}{2} \tilde{\theta}^T \Gamma^{-1} \tilde{\theta} + \tilde{\epsilon}^T P \tilde{\epsilon} \quad (2.57)$$

Along the dynamic equations (2.48) and (2.51), the derivative of the Lyapunov function \dot{V} becomes:

$$\dot{V} = \tilde{\theta}^T \Gamma^{-1} \dot{\tilde{\theta}} + \dot{\tilde{\epsilon}}^T P \tilde{\epsilon} + \tilde{\epsilon}^T P \dot{\tilde{\epsilon}} = \tilde{\theta}^T \Gamma^{-1} \dot{\tilde{\theta}} + \tilde{\epsilon}^T A^T P \tilde{\epsilon} + \tilde{\epsilon}^T P A \tilde{\epsilon} \quad (2.58)$$

Applying of the following inequality [Krs95b]:

$$P A + A^T P = -I - 2\lambda P \varphi^T(x) \varphi(x) P \leq -I \quad (2.59)$$

We obtain:

$$\begin{aligned} \dot{V} &\leq -\tilde{\theta}^T \Gamma^{-1} \dot{\tilde{\theta}} - \tilde{\epsilon}^T \tilde{\epsilon} = -\frac{\tilde{\theta}^T \Omega \epsilon}{1 + \nu \text{tr}\{\Omega^T \Omega\}} - \tilde{\epsilon}^T \tilde{\epsilon} \\ &= -\frac{\epsilon^T \epsilon}{1 + \nu \text{tr}\{\Omega^T \Omega\}} + \frac{\epsilon^T}{1 + \nu \text{tr}\{\Omega^T \Omega\}} \tilde{\epsilon} - \tilde{\epsilon}^T \tilde{\epsilon} \\ &\leq -\frac{3}{4} \frac{\epsilon^T \epsilon}{1 + \nu \text{tr}\{\Omega^T \Omega\}} - \frac{1}{4} \frac{\epsilon^T \epsilon}{(1 + \nu \text{tr}\{\Omega^T \Omega\})^2} + \frac{\epsilon^T}{1 + \nu \text{tr}\{\Omega^T \Omega\}} \tilde{\epsilon} - \tilde{\epsilon}^T \tilde{\epsilon} \\ &= -\frac{3}{4} \frac{\epsilon^T \epsilon}{1 + \nu \text{tr}\{\Omega^T \Omega\}} - \left(\frac{\epsilon}{2(1 + \nu \text{tr}\{\Omega^T \Omega\})} - \tilde{\epsilon} \right)^T \left(\frac{\epsilon}{2(1 + \nu \text{tr}\{\Omega^T \Omega\})} - \tilde{\epsilon} \right) \\ &\leq -\frac{3}{4} \frac{\epsilon^T \epsilon}{1 + \nu \text{tr}\{\Omega^T \Omega\}} \end{aligned} \quad (2.60)$$

The nonpositivity of \dot{V} proves that, $\tilde{\theta} \in L_\infty$ (bounded). Due to $\epsilon = \Omega^T \tilde{\theta} + \tilde{\epsilon}$ and the boundedness of Ω , it follows that $\epsilon \in L_\infty$, which, in turn proves that $\dot{\hat{\theta}} \in L_\infty$.

By integrating of inequality (2.60) over $[0, \infty]$, we obtain:

$$\int_0^\infty \frac{\epsilon^T \epsilon}{1 + \nu \text{tr}\{\Omega^T \Omega\}} d\tau \leq \frac{4}{3} (V(0) - V(\infty)) < \infty \quad (2.61)$$

This means that, $\frac{\epsilon}{\sqrt{1 + \nu \text{tr}\{\Omega^T \Omega\}}} \in L_2$. Since Ω is bounded, then $\epsilon \in L_2$. The boundedness

of Ω and the square integrability of ϵ prove that $\dot{\hat{\theta}} \in L_2$.

2.3.3.2 Least squares adaptive law

From (2.52) and (2.53), we have the following identity:

$$\frac{d}{dt}(\Gamma^{-1}) = -\Gamma^{-1} \dot{\Gamma} \Gamma^{-1} = \frac{\Omega \Omega^T}{1 + \nu \text{tr}\{\Omega^T \Gamma \Omega\}} \geq 0 \quad (2.62)$$

We consider the following Lyapunov function as:

$$V = \tilde{\theta}^T \Gamma^{-1}(t) \tilde{\theta} + \tilde{\epsilon}^T P \tilde{\epsilon} \quad (2.63)$$

Along the dynamic equations (2.48), (2.52) and (2.53), and by applying of inequality (2.59), the derivative of the Lyapunov function \dot{V} becomes:

$$\begin{aligned} \dot{V} &= \dot{\tilde{\theta}}^T \Gamma^{-1} \tilde{\theta} + \tilde{\theta}^T \frac{d}{dt}(\Gamma^{-1} \tilde{\theta}) + \dot{\tilde{\epsilon}}^T P \tilde{\epsilon} + \tilde{\epsilon}^T P \dot{\tilde{\epsilon}} \\ &= \dot{\tilde{\theta}}^T \Gamma^{-1} \tilde{\theta} - \tilde{\theta}^T \Gamma^{-1} \dot{\Gamma} \Gamma^{-1} \tilde{\theta} - \tilde{\theta}^T \Gamma^{-1} \dot{\hat{\theta}} + \tilde{\epsilon}^T A^T P \tilde{\epsilon} + \tilde{\epsilon}^T P A \tilde{\epsilon} \\ &\leq -\dot{\tilde{\theta}}^T \Gamma^{-1} \tilde{\theta} - \tilde{\theta}^T \Gamma^{-1} \dot{\Gamma} \Gamma^{-1} \tilde{\theta} - \tilde{\theta}^T \Gamma^{-1} \dot{\hat{\theta}} - \tilde{\epsilon}^T \tilde{\epsilon} \\ &= -\frac{\epsilon^T \Omega^T \tilde{\theta}}{1 + \nu \text{tr}\{\Omega^T \Gamma \Omega\}} + \frac{\tilde{\theta}^T \Omega \Omega^T \tilde{\theta}}{1 + \nu \text{tr}\{\Omega^T \Gamma \Omega\}} - \frac{\tilde{\theta}^T \Omega \epsilon}{1 + \nu \text{tr}\{\Omega^T \Gamma \Omega\}} - \tilde{\epsilon}^T \tilde{\epsilon} \\ &\leq -\frac{\epsilon^T \Omega^T \tilde{\theta}}{1 + \nu \text{tr}\{\Omega^T \Gamma \Omega\}} - \frac{\tilde{\theta}^T \Omega \tilde{\epsilon}}{1 + \nu \text{tr}\{\Omega^T \Gamma \Omega\}} - \tilde{\epsilon}^T \tilde{\epsilon} \\ &= -\frac{\epsilon^T \epsilon}{1 + \nu \text{tr}\{\Omega^T \Gamma \Omega\}} + \frac{\tilde{\epsilon}^T \tilde{\epsilon}}{1 + \nu \text{tr}\{\Omega^T \Gamma \Omega\}} - \tilde{\epsilon}^T \tilde{\epsilon} \\ &\leq -\frac{\epsilon^T \epsilon}{1 + \nu \text{tr}\{\Omega^T \Gamma \Omega\}} \end{aligned} \quad (2.64)$$

Which, due to the positive definiteness of $\Gamma^{-1}(t)$, proves that, $\tilde{\theta} \in L_\infty$ (bounded).

By integrating of inequality (2.64) over $[0, \infty]$, we obtain:

$$\int_0^{\infty} \frac{\epsilon^T \epsilon}{1 + \nu \text{tr}\{\Omega^T \Gamma \Omega\}} d\tau \leq V(0) - V(\infty) < \infty \quad (2.65)$$

This means that, $\frac{\epsilon}{\sqrt{1 + \nu \text{tr}\{\Omega^T \Gamma \Omega\}}} \in L_2$. Using the boundedness of Γ and Ω , following the same line of argument as for the gradient adaptive law, we prove that $\epsilon \in L_2 \cap L_\infty$ and $\dot{\hat{\theta}} \in L_2 \cap L_\infty$.

2.4 Composite tuning functions based adaptive backstepping control

In this section, the proposed composite tuning functions based adaptive backstepping control is based on the combination of both tracking error based parameter adaptive law of the direct tuning functions based adaptive backstepping control described by (2.36) with the estimation error based parameter adaptive law of the indirect adaptive control described by (2.51) and (2.52). The control objective of this approach is to design a composite tuning functions based adaptive backstepping controller u such that the system output x_1 tracks the desired trajectory x_{1d} and to ensure the boundedness of all signals in the closed-loop system. The main procedures for designing the composite tuning functions based adaptive backstepping control method for system (2.1) with stability analysis are given as follows.

2.4.1 Composite sum based gradient adaptive law

We use the same steps as that in the direct tuning functions based adaptive backstepping control described by (2.2)-(2.33).

Then, we choose the actual control input u as:

$$u = \frac{1}{g_n} \left(-k_n e_n - g_{n-1} e_{n-1} - \varphi_n^T \hat{\theta} - \psi_n + \sum_{k=1}^{n-1} \frac{\partial \alpha_{n-1}}{\partial x_k} (g_k x_{k+1} + \varphi_k^T \hat{\theta} + \psi_k) + \frac{\partial \alpha_{n-1}}{\partial \hat{\theta}} \tau_n \right. \\ \left. + \sum_{k=1}^n \frac{\partial \alpha_{n-1}}{\partial x_{1d}^{(k-1)}} x_{1d}^{(k)} - v_n + \left(\frac{\partial \alpha_{n-1}}{\partial \hat{\theta}} + \frac{e_n}{\zeta_0 + e_n^2} \sum_{k=1}^{n-2} e_{k+1} \frac{\partial \alpha_k}{\partial \hat{\theta}} \right) \left(\Gamma \frac{\Omega \epsilon}{1 + \nu \text{tr}\{\Omega^T \Omega\}} \right) \right) \quad (2.66)$$

where, $v_n = \sum_{k=1}^{n-2} e_{k+1} \frac{\partial \alpha_k}{\partial \hat{\theta}} \Gamma \left(-\varphi_n + \sum_{k=1}^{n-1} \frac{\partial \alpha_{n-1}}{\partial x_k} \varphi_k \right)$ and $k_n > 0$ is a positive design constant.

Substituting (2.66) into (2.32), the derivative of the Lyapunov function \dot{V} becomes:

$$\begin{aligned} \dot{V} = & -\sum_{k=1}^n k_k e_k^2 - e_n \frac{\partial \alpha_{n-1}}{\partial \hat{\theta}} (\dot{\hat{\theta}} - \tau_n) - \sum_{k=1}^{n-2} e_{k+1} \frac{\partial \alpha_k}{\partial \hat{\theta}} (\dot{\hat{\theta}} - \tau_n) - \tilde{\theta}^T \Gamma^{-1} (\dot{\hat{\theta}} - \tau_n) \\ & + e_n \left(\frac{\partial \alpha_{n-1}}{\partial \hat{\theta}} + \frac{e_n}{\zeta_0 + e_n^2} \sum_{k=1}^{n-2} e_{k+1} \frac{\partial \alpha_k}{\partial \hat{\theta}} \right) \left(\Gamma \frac{\Omega \epsilon}{1 + \nu \text{tr} \{ \Omega^T \Omega \}} \right) \end{aligned} \quad (2.67)$$

The composite sum based gradient adaptive law is defined as:

$$\dot{\hat{\theta}} = \tau_n + \Gamma \frac{\Omega \epsilon}{1 + \nu \text{tr} \{ \Omega^T \Omega \}} \quad (2.68)$$

where, $\epsilon = x + \Omega_0 - \Omega^T \hat{\theta}$. We assume that, $\frac{e_n^2}{\zeta_0 + e_n^2} \sum_{k=1}^{n-2} e_{k+1} \approx \sum_{k=1}^{n-2} e_{k+1}$ for sufficiently small ζ_0 , then,

$$\dot{V} = -\sum_{k=1}^n k_k e_k^2 - \frac{\tilde{\theta}^T \Omega \epsilon}{1 + \nu \text{tr} \{ \Omega^T \Omega \}} \quad (2.69)$$

Theorem 2.4.1: Consider the SISO uncertain nonlinear system in lower triangular form composed of the plant described by state space form (2.1). Suppose that assumptions 2.2.1 and 2.2.2 are satisfied. Then, the virtual controllers (2.6), (2.12), (2.18) and (2.26), the actual control input (2.66) and the composite sum based gradient adaptive law (2.68) guarantee that all signals in the closed-loop system are bounded.

Proof: We consider the following Lyapunov function as:

$$V = \frac{1}{2} \sum_{i=1}^n e_i^2 + \frac{1}{2} \tilde{\theta}^T \Gamma^{-1} \tilde{\theta} + \tilde{\epsilon}^T P \tilde{\epsilon} \quad (2.70)$$

The derivative of the Lyapunov function \dot{V} becomes:

$$\begin{aligned} \dot{V} = & -\sum_{k=1}^n k_k e_k^2 - \frac{\tilde{\theta}^T \Omega \epsilon}{1 + \nu \text{tr} \{ \Omega^T \Omega \}} + \dot{\tilde{\epsilon}}^T P \tilde{\epsilon} + \tilde{\epsilon}^T P \dot{\tilde{\epsilon}} \\ = & -\sum_{k=1}^n k_k e_k^2 - \frac{\tilde{\theta}^T \Omega \epsilon}{1 + \nu \text{tr} \{ \Omega^T \Omega \}} + \tilde{\epsilon}^T A^T P \tilde{\epsilon} + \tilde{\epsilon}^T P A \tilde{\epsilon} \end{aligned} \quad (2.71)$$

Applying of inequality (2.59), we obtain:

$$\begin{aligned} \dot{V} \leq & -\sum_{k=1}^n k_k e_k^2 - \frac{\tilde{\theta}^T \Omega \epsilon}{1 + \nu \text{tr} \{ \Omega^T \Omega \}} - \tilde{\epsilon}^T \tilde{\epsilon} \\ \leq & -\sum_{k=1}^n k_k e_k^2 - \frac{3}{4} \frac{\epsilon^T \epsilon}{1 + \nu \text{tr} \{ \Omega^T \Omega \}} \end{aligned} \quad (2.72)$$

Therefore, we can conclude that, V , e_k , $k = 1, \dots, n$, $\tilde{\theta}$ and ϵ are bounded.

Furthermore, all signals in the closed-loop system, i.e., x_{1d} , $\dot{x}_{1d}, \dots, x_{1d}^{(n-1)}$, $x_{1d}^{(n)}$, α_i , u and $\hat{\theta}$ are also bounded.

2.4.2 Composite σ -modification based gradient and least squares adaptive laws

In order to robustify the adaptive law, we introduce a σ -modification term into the adaptive law (2.36). Then, we use the same steps as that in the direct tuning functions based adaptive backstepping control described by (2.2)-(2.33).

The actual control input u is defined as:

$$u = \frac{1}{g_n} \left(-k_n e_n - g_{n-1} e_{n-1} - \varphi_n^T \hat{\theta} - \psi_n + \sum_{k=1}^{n-1} \frac{\partial \alpha_{n-1}}{\partial x_k} (g_k x_{k+1} + \varphi_k^T \hat{\theta} + \psi_k) + \frac{\partial \alpha_{n-1}}{\partial \hat{\theta}} \tau_n \right. \\ \left. + \sum_{k=1}^n \frac{\partial \alpha_{n-1}}{\partial x_{1d}^{(k-1)}} x_{1d}^{(k)} - v_n - \left(\frac{\partial \alpha_{n-1}}{\partial \hat{\theta}} + \frac{e_n}{\zeta_0 + e_n^2} \sum_{k=1}^{n-2} e_{k+1} \frac{\partial \alpha_k}{\partial \hat{\theta}} \right) \Gamma \sigma_\theta (\hat{\theta} - \bar{\theta}) \right) \quad (2.73)$$

where, $v_n = \sum_{k=1}^{n-2} e_{k+1} \frac{\partial \alpha_k}{\partial \hat{\theta}} \Gamma \left(-\varphi_n + \sum_{k=1}^{n-1} \frac{\partial \alpha_{n-1}}{\partial x_k} \varphi_k \right)$ and $k_n > 0$ is a positive design constant.

Substituting (2.73) into (2.32), the derivative of the Lyapunov function \dot{V} becomes:

$$\dot{V} = -\sum_{k=1}^n k_k e_k^2 - e_n \frac{\partial \alpha_{n-1}}{\partial \hat{\theta}} (\dot{\hat{\theta}} - \tau_n) - \sum_{k=1}^{n-2} e_{k+1} \frac{\partial \alpha_k}{\partial \hat{\theta}} (\dot{\hat{\theta}} - \tau_n) - \tilde{\theta}^T \Gamma^{-1} (\dot{\hat{\theta}} - \tau_n) \\ - e_n \left(\frac{\partial \alpha_{n-1}}{\partial \hat{\theta}} + \frac{e_n}{\zeta_0 + e_n^2} \sum_{k=1}^{n-2} e_{k+1} \frac{\partial \alpha_k}{\partial \hat{\theta}} \right) \Gamma \sigma_\theta (\hat{\theta} - \bar{\theta}) \quad (2.74)$$

The composite σ -modification based gradient and least squares adaptive laws are given by:

$$\dot{\hat{\theta}} = \tau_n - \Gamma \sigma_\theta (\hat{\theta} - \bar{\theta}) \quad (2.75)$$

We assume that, $\frac{e_n^2}{\zeta_0 + e_n^2} \sum_{k=1}^{n-2} e_{k+1} \approx \sum_{k=1}^{n-2} e_{k+1}$ for sufficiently small ζ_0 , then,

$$\dot{V} = -\sum_{k=1}^n k_k e_k^2 + \sigma_\theta \tilde{\theta}^T (\hat{\theta} - \bar{\theta}) \quad (2.76)$$

where, σ_θ is small design constant to introduce the σ -modification for the closed-loop system and $\bar{\theta}$ is computed with the gradient method as follows:

$$\dot{\bar{\theta}} = \bar{\Gamma} \frac{\Omega \epsilon}{1 + \nu \text{tr} \{ \Omega^T \Omega \}}, \bar{\Gamma} = \bar{\Gamma}^T > 0 \quad (2.77)$$

or with the least squares method as follows:

$$\dot{\bar{\theta}} = \bar{\Gamma} \frac{\Omega \epsilon}{1 + \nu \text{tr} \{ \Omega^T \bar{\Gamma} \Omega \}} \quad (2.78)$$

where, $\bar{\Gamma}$ is given by:

$$\dot{\bar{\Gamma}} = -\bar{\Gamma} \frac{\Omega\Omega^T}{1 + \nu \text{tr}\{\Omega^T \bar{\Gamma} \Omega\}} \bar{\Gamma}, \bar{\Gamma}(0) = \bar{\Gamma}^T(0) > 0, \nu \geq 0 \quad (2.79)$$

with, $\epsilon = x + \Omega_0 - \Omega^T \bar{\theta}$.

Theorem 2.4.2: Consider the SISO uncertain nonlinear system in lower triangular form composed of the plant described by state space form (2.1). Suppose that assumptions 2.2.1 and 2.2.2 are satisfied. Then, the virtual controllers (2.6), (2.12), (2.18) and (2.26), the actual control input (2.73) and the composite σ -modification based gradient and least squares adaptive laws (2.75) guarantee that all signals in the closed-loop system are uniformly ultimately bounded (UUB) and the tracking errors converge to a sufficiently small neighborhood of the origin by appropriately adjusting the design parameters.

Proof: We consider the following Lyapunov function as:

$$V = \frac{1}{2} \sum_{i=1}^n e_i^2 + \frac{1}{2} \tilde{\theta}^T \Gamma^{-1} \tilde{\theta} \quad (2.80)$$

We assume that, $\theta - \bar{\theta}$ is bounded, thus, $e_\theta = \theta - \bar{\theta}$ is bounded, $\bar{\theta} = \theta - e_\theta$ and $\tilde{\theta} = \theta - \hat{\theta}$.

The derivative of the Lyapunov function \dot{V} becomes:

$$\begin{aligned} \dot{V} &= -\sum_{k=1}^n k_k e_k^2 + \sigma_\theta \tilde{\theta}^T (\hat{\theta} - \theta + e_\theta) \\ &= -\sum_{k=1}^n k_k e_k^2 - \sigma_\theta \tilde{\theta}^T \tilde{\theta} + \sigma_\theta \tilde{\theta}^T e_\theta \end{aligned} \quad (2.81)$$

Applying of the following inequality:

$$\tilde{\theta}^T e_\theta \leq \frac{\tilde{\theta}^T \tilde{\theta}}{2} + \frac{e_\theta^2}{2} \quad (2.82)$$

We obtain:

$$\begin{aligned} \dot{V} &\leq -\sum_{k=1}^n k_k e_k^2 - \frac{\sigma_\theta}{2} \tilde{\theta}^T \tilde{\theta} + \frac{\sigma_\theta}{2} e_\theta^2 \\ &\leq -\sum_{k=1}^n k_k e_k^2 - \frac{\sigma_\theta}{2} \tilde{\theta}^T \tilde{\theta} + \mu \end{aligned} \quad (2.83)$$

Based on the above discussions, we can get the following inequality:

$$\dot{V} \leq -\pi V + \mu \quad (2.84)$$

where, $\pi = \min\{2k_k, \Gamma\sigma_\theta\}$ and $\mu = \frac{\sigma_\theta}{2} e_\theta^2$. From the inequality (2.84), if $V = p$ and $\pi > \frac{\mu}{p}$,

then $\dot{V} \leq 0$. It implies that $V(t) \leq p$ for all $t \geq 0$ for $V(0) \leq p$.

Multiplying both sides in (2.84) by $e^{\pi t}$ yields:

$$\frac{d}{dt}(V(t)e^{\pi t}) \leq \mu e^{\pi t} \quad (2.85)$$

Moreover, by integrating (2.85) over $[0, t]$, we have:

$$0 \leq V(t) \leq \frac{\mu}{\pi} + \left(V(0) - \frac{\mu}{\pi} \right) e^{-\pi t} \quad (2.86)$$

Since $\frac{\mu}{\pi} > 0$, it can be obtained that:

$$0 \leq V(t) \leq V(0)e^{-\pi t} + \frac{\mu}{\pi} \quad (2.87)$$

Therefore, we know that, e_k , $k = 1, \dots, n$, $\tilde{\theta}$ and ϵ are UUB. Furthermore, all signals in the closed-loop system, i.e., x_i , x_{1d} , $\dot{x}_{1d}, \dots, x_{1d}^{(n-1)}$, $x_{1d}^{(n)}$, α_i , u and $\hat{\theta}$ are also UUB. In

addition, from (2.80) and (2.87), it follows that: $\|e\| = \sqrt{\sum_{k=1}^n e_k^2} \leq \sqrt{2V(0)}e^{-0.5\pi t} + \sqrt{2\mu/\pi}$.

Accordingly, when $t \rightarrow \infty$, it is easy to show that: $\|e\| \leq \sqrt{2\mu/\pi}$. This completes the proof.

2.5 Dynamic model of the electromechanical system

This section describes the dynamic model of the electromechanical system (one-link manipulator actuated by a brush DC motor) [Bec13, Car95, Daw94, Li10a, Pan15, Sou21, Sun13, Yu18a, Yu15a, Zha18a, Zha18b, Zha17]. The dynamic model of the electromechanical system can be described by following equations as in [Bec13, Li10a, Zha18a, Zha18b, Zha17]:

$$\begin{aligned} D\ddot{q} + B\dot{q} + N \sin(q) &= I + \Delta_I(t) \\ M\dot{I} + HI + K_m\dot{q} &= V \end{aligned} \quad (2.88)$$

where, q , \dot{q} and \ddot{q} denote the link angular position, the angular velocity, and the acceleration, respectively. I is the motor armature current. V is the input control voltage. M is the armature inductance. H is the armature resistance. K_m is the back-emf coefficient. D , B and N are constants. $\Delta_I(t)$ is the external disturbance.

Let's then define the state variables as follows: $x_1 = q$, $x_2 = \dot{q}$ and $x_3 = I$. We obtain then the dynamic model of the electromechanical system, described in the following state space form as:

$$\begin{aligned}
\dot{x}_1 &= x_2 \\
\dot{x}_2 &= f_2(\bar{x}_2) + b_2 x_3 + d_2(t) \\
\dot{x}_3 &= f_3(x) + b_3 u
\end{aligned} \tag{2.89}$$

where, $f_2(\bar{x}_2) = -\frac{N}{D} \sin(x_1) - \frac{B}{D} x_2$, $f_3(x) = -\frac{K_m}{M} x_2 - \frac{H}{M} x_3$, $b_2 = \frac{1}{D}$, $b_3 = \frac{1}{M}$ and $u = V$.

2.6 Simulation results

This section presents the simulation results for composite tuning functions based adaptive backstepping control method as applied to an electromechanical system mathematical model. Direct tuning functions based adaptive backstepping control, indirect adaptive control and composite tuning functions based adaptive backstepping control techniques have been simulated in order to verify the performance, validity and effectiveness of the proposed composite adaptive control approach. The simulations are performed using MATLAB/Simulink. The simulation results are obtained based on the electromechanical system parameters [Bec13, Li10a, Sun13]: $D = 1$, $B = 1$, $M = 0.05$, $H = 0.5$, $N = 10$ and $K_m = 10$. The external disturbance is chosen as [Daw94, Pan15, Sun13]: $d_2(t) = 0$.

The values of unknown constant parameters are assumed as: $\theta_2 = \frac{N}{D}$ and $\theta_3 = \frac{K_m}{M}$, where,

$\theta = [\theta_2 \ \theta_3]^T$, $\varphi_2^T = -\sin(x_1)$ and $\varphi_3^T = -x_2$. The control objective of this simulation is to design the composite tuning functions based adaptive backstepping controller u for the electromechanical system in such a way that the link angular position q tracks the desired trajectory x_{1d} and to ensure the boundedness of all signals in the closed-loop system. The desired trajectory used in the simulation test is taken from [Car95]:

$x_{1d} = \frac{\pi}{2} \sin(t) (1 - e^{-0.1t^2})$ [rad]. The virtual controllers α_1 and α_2 are defined as:

$$\alpha_1 = -k_1 e_1 + \dot{x}_{1d} \tag{2.90}$$

$$\alpha_2 = \frac{1}{b_2} \left(-k_2 e_2 - e_1 + \sin(x_1) \hat{\theta}_2 + \frac{B}{D} x_2 + \frac{\partial \alpha_1}{\partial x_1} x_2 + \sum_{k=1}^2 \frac{\partial \alpha_1}{\partial x_{1d}^{(k-1)}} x_{1d}^{(k)} \right) \tag{2.91}$$

For the swapping based identifier, we use the following x-swapping filters:

$$\dot{\Omega}_{02} = \left(-0.5 - \lambda_2 (\sin(x_1))^2 \right) (\Omega_{02} + x_2) + \frac{B}{D} x_2 - b_2 x_3 \tag{2.92}$$

$$\dot{\Omega}_2^T = \left(-0.5 - \lambda_2 (\sin(x_1))^2 \right) \Omega_2^T - \sin(x_1) \tag{2.93}$$

$$\dot{\Omega}_{03} = (-0.5 - \lambda_3 x_2^2)(\Omega_{03} + x_3) + \frac{H}{M} x_3 - b_3 u \quad (2.94)$$

$$\dot{\Omega}_3^T = (-0.5 - \lambda_3 x_2^2)\Omega_3^T - x_2 \quad (2.95)$$

2.6.1 Composite sum based gradient adaptive laws

The actual control input u is chosen as:

$$u = \frac{1}{b_3} \left(-k_3 e_3 - b_2 e_2 + x_2 \hat{\theta}_3 + \frac{H}{M} x_3 + \frac{\partial \alpha_2}{\partial x_1} x_2 + \frac{\partial \alpha_2}{\partial x_2} \left(-\sin(x_1) \hat{\theta}_2 - \frac{B}{D} x_2 + b_2 x_3 \right) \right. \\ \left. + \frac{\partial \alpha_2}{\partial \hat{\theta}_2} \left(-\Gamma_2 \sin(x_1) \left(e_2 - \frac{\partial \alpha_2}{\partial x_2} e_3 \right) \right) + \sum_{k=1}^3 \frac{\partial \alpha_2}{\partial x_{1d}^{(k-1)}} x_{1d}^{(k)} + \frac{\partial \alpha_2}{\partial \hat{\theta}_2} \left(\Gamma_2 \frac{\Omega_2 \epsilon_2}{1 + \nu_2 \text{tr}\{\Omega_2^T \Omega_2\}} \right) \right) \quad (2.96)$$

The composite sum based gradient adaptive laws are defined as:

$$\dot{\hat{\theta}}_2 = -\Gamma_2 \left(\sin(x_1) \left(e_2 - \frac{\partial \alpha_2}{\partial x_2} e_3 \right) - \frac{\Omega_2 \epsilon_2}{1 + \nu_2 \text{tr}\{\Omega_2^T \Omega_2\}} \right) \quad (2.97)$$

$$\dot{\hat{\theta}}_3 = -\Gamma_3 \left(x_2 e_3 - \frac{\Omega_3 \epsilon_3}{1 + \nu_3 \text{tr}\{\Omega_3^T \Omega_3\}} \right) \quad (2.98)$$

where, $\epsilon_i = x_i + \Omega_{0i} - \Omega_i^T \hat{\theta}_i$, $i = 2, 3$. The selected initial conditions are set as:

$x(0) = [0 \ 0 \ 0]^T$, $\hat{\theta}_2(0) = 0$, $\hat{\theta}_3(0) = 0$, $\Omega_{02}(0) = \Omega_2^T(0) = 0$ and $\Omega_{03}(0) = \Omega_3^T(0) = 0$.

The design parameters are selected as follows: $k_1 = 0.5$, $k_2 = 50$, $k_3 = 3500$, $\Gamma_2 = 1$, $\Gamma_3 = 300$, $\lambda_2 = \lambda_3 = 0.1$ and $\nu_2 = \nu_3 = 0.1$. The simulation results are shown in Figures 2.1-2.9. Figures 2.1-2.3 show the trajectories of the output variables. The trajectories of the tracking errors are illustrated in Figures 2.4-2.6. Figures 2.7 and 2.8 show the trajectories of the parameter estimates. The trajectories of the control inputs are shown in Figure 2.9.

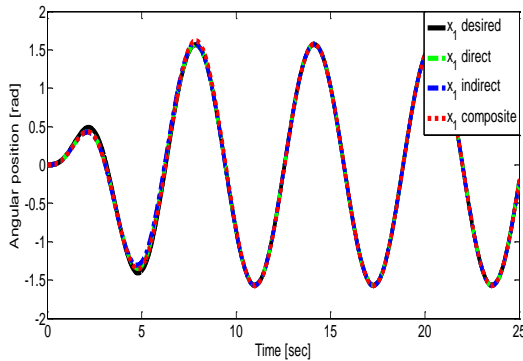


Fig. 2.1: Angular position: desired x_{1d} ("--") and actual x_1 ("--").

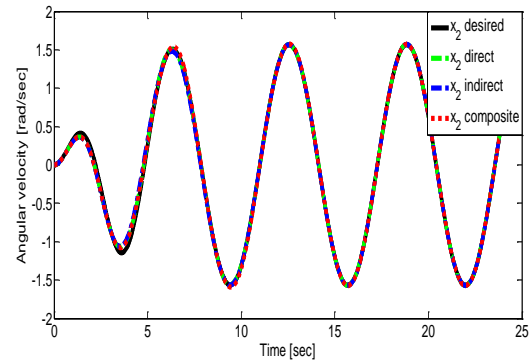


Fig. 2.2: Angular velocity: desired x_{2d} ("--") and actual x_2 ("--").

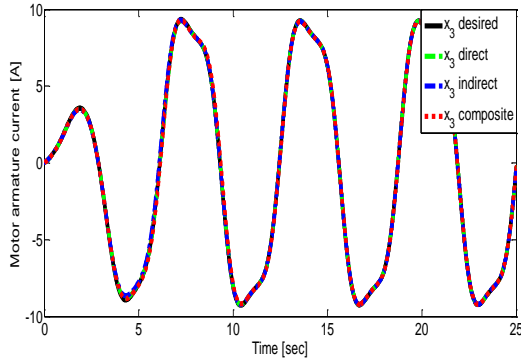


Fig. 2.3: Motor armature current: desired x_{3d} ("—") and actual x_3 ("--").

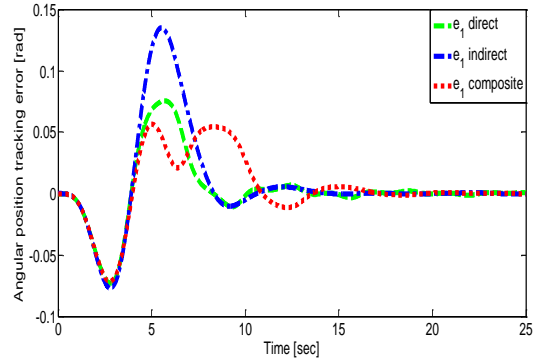


Fig. 2.4: Angular position tracking error: e_1 .

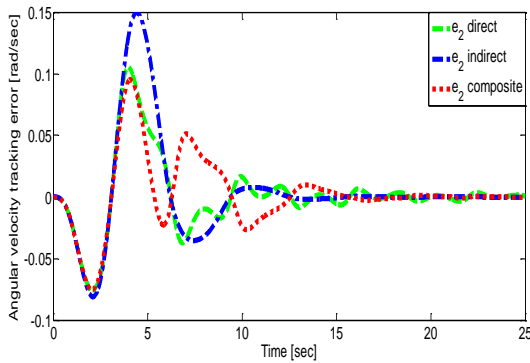


Fig. 2.5: Angular velocity tracking error: e_2 .

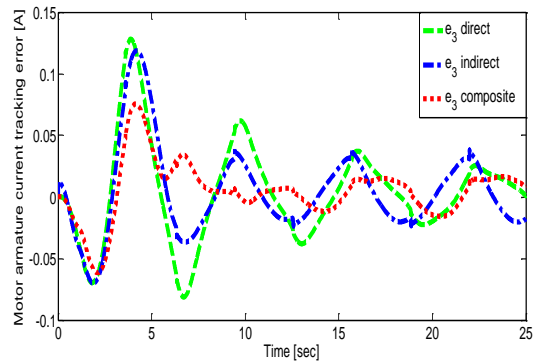


Fig. 2.6: Motor armature current tracking error: e_3 .

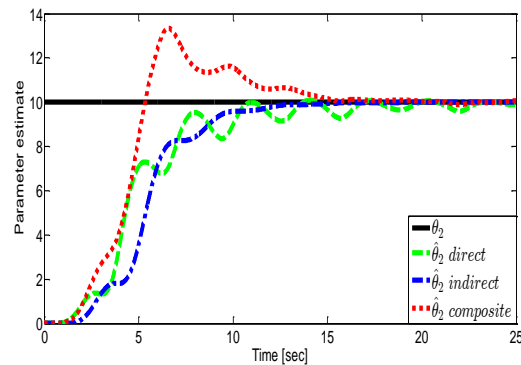


Fig. 2.7: Parameter estimate: actual θ_2 ("—") and estimate $\hat{\theta}_2$ ("--").

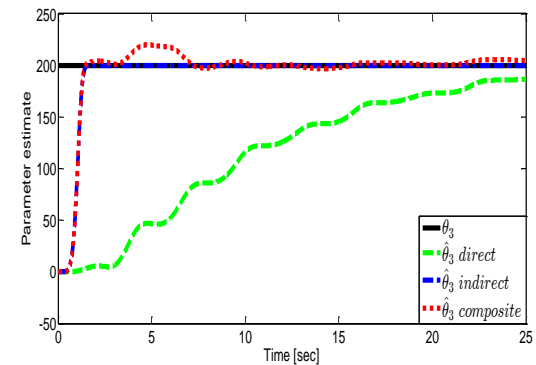


Fig. 2.8: Parameter estimate: actual θ_3 ("—") and estimate $\hat{\theta}_3$ ("--").

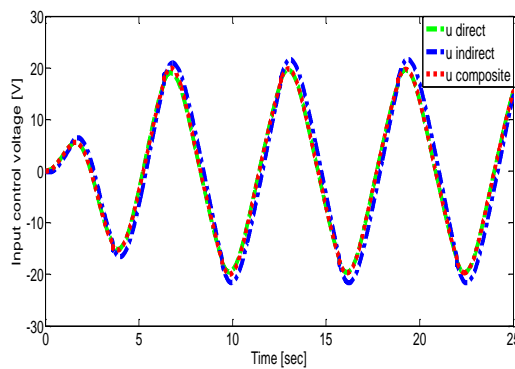


Fig. 2.9: Control input: u .

2.6.2 Composite σ -modification based gradient adaptive laws

The actual control input u is given by:

$$u = \frac{1}{b_3} \left(-k_3 e_3 - b_2 e_2 + x_2 \hat{\theta}_3 + \frac{H}{M} x_3 + \frac{\partial \alpha_2}{\partial x_1} x_2 + \frac{\partial \alpha_2}{\partial x_2} \left(-\sin(x_1) \hat{\theta}_2 - \frac{B}{D} x_2 + b_2 x_3 \right) \right. \\ \left. + \frac{\partial \alpha_2}{\partial \hat{\theta}_2} \left(-\Gamma_2 \sin(x_1) \left(e_2 - \frac{\partial \alpha_2}{\partial x_2} e_3 \right) \right) + \sum_{k=1}^3 \frac{\partial \alpha_2}{\partial x_{1d}^{(k-1)}} x_{1d}^{(k)} - \frac{\partial \alpha_2}{\partial \hat{\theta}_2} \Gamma_2 \sigma_{\theta_2} (\hat{\theta}_2 - \bar{\theta}_2) \right) \quad (2.99)$$

The composite σ -modification based gradient adaptive laws are defined as:

$$\dot{\hat{\theta}}_2 = -\Gamma_2 \left(\sin(x_1) \left(e_2 - \frac{\partial \alpha_2}{\partial x_2} e_3 \right) + \sigma_{\theta_2} (\hat{\theta}_2 - \bar{\theta}_2) \right) \quad (2.100)$$

and,

$$\dot{\hat{\theta}}_3 = -\Gamma_3 \left(x_2 e_3 + \sigma_{\theta_3} (\hat{\theta}_3 - \bar{\theta}_3) \right) \quad (2.101)$$

where, $\bar{\theta}_2$ and $\bar{\theta}_3$ are computed with the gradient method as follows:

$$\dot{\bar{\theta}}_i = \bar{\Gamma}_i \frac{\Omega_i \epsilon_i}{1 + \nu_i \text{tr} \{ \Omega_i^T \Omega_i \}} \quad (2.102)$$

where, $\epsilon_i = x_i + \Omega_{0i} - \Omega_i^T \bar{\theta}_i$, $i = 2, 3$. The selected initial conditions are set as: $x(0) = [0 \ 0 \ 0]^T$, $\hat{\theta}_2(0) = \bar{\theta}_2(0) = 0$, $\hat{\theta}_3(0) = \bar{\theta}_3(0) = 0$, $\Omega_{02}(0) = \Omega_2^T(0) = 0$ and $\Omega_{03}(0) = \Omega_3^T(0) = 0$. The design parameters are selected as follows: $k_1 = 0.5$, $k_2 = 50$, $k_3 = 3500$, $\Gamma_2 = 1$, $\bar{\Gamma}_2 = 5$, $\Gamma_3 = 300$, $\bar{\Gamma}_3 = 10$, $\sigma_{\theta_2} = \sigma_{\theta_3} = 0.1$, $\lambda_2 = \lambda_3 = 0.1$ and $\nu_2 = \nu_3 = 0.1$. The simulation results are shown in Figures 2.10-2.18. Figures 2.10-2.12 show the trajectories of the output variables. The trajectories of the tracking errors are illustrated in Figures 2.13-2.15. Figures 2.16 and 2.17 show the trajectories of the parameter estimates. The trajectories of the control inputs are shown in Figure 2.18.

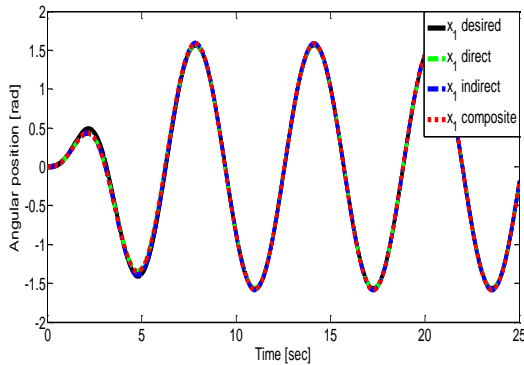


Fig. 2.10: Angular position: desired x_{1d} ("--") and actual x_1 ("--").

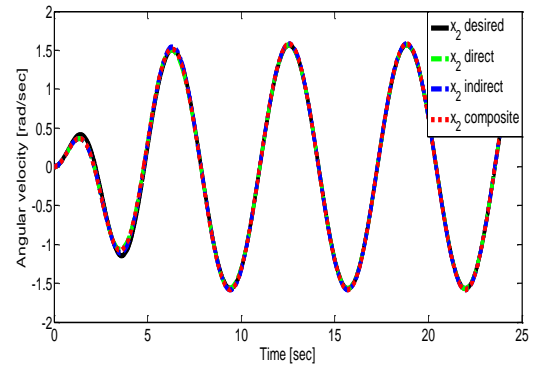


Fig. 2.11: Angular velocity: desired x_{2d} ("--") and actual x_2 ("--").

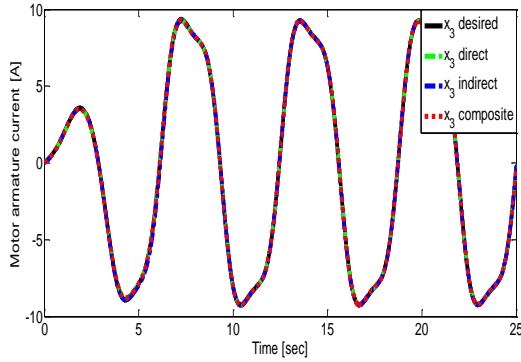


Fig. 2.12: Motor armature current: desired x_{3d} ("—") and actual x_3 ("--").

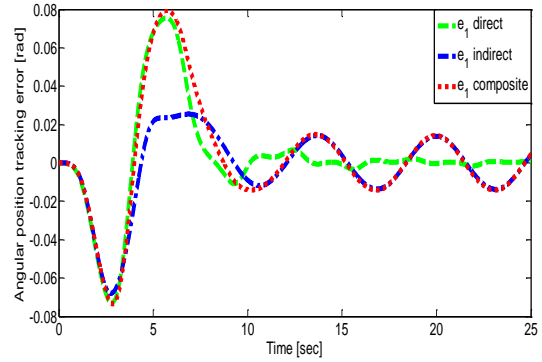


Fig. 2.13: Angular position tracking error: e_1 .

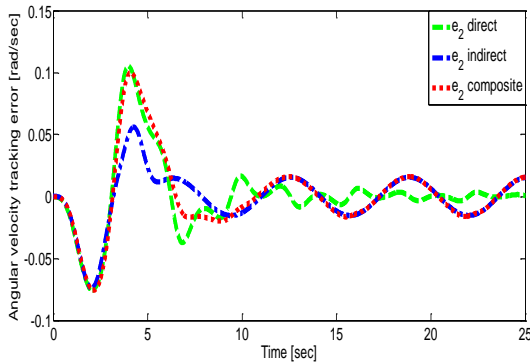


Fig. 2.14: Angular velocity tracking error: e_2 .

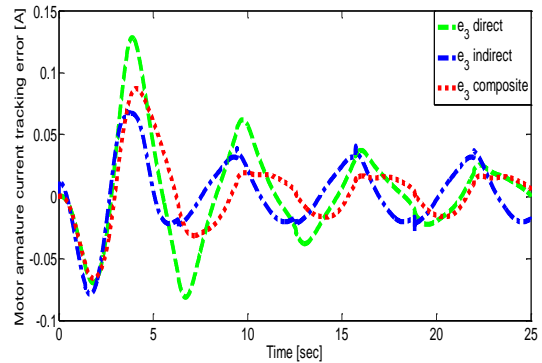


Fig. 2.15: Motor armature current tracking error: e_3 .

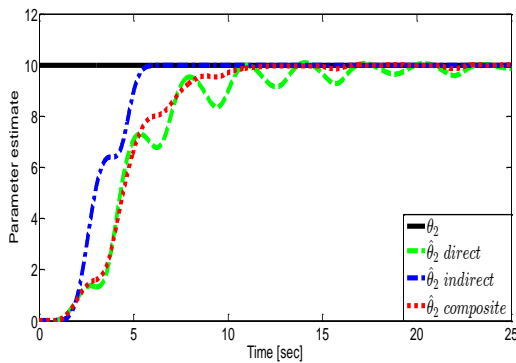


Fig. 2.16: Parameter estimate: actual θ_2 ("—") and estimate $\hat{\theta}_2$ ("--").

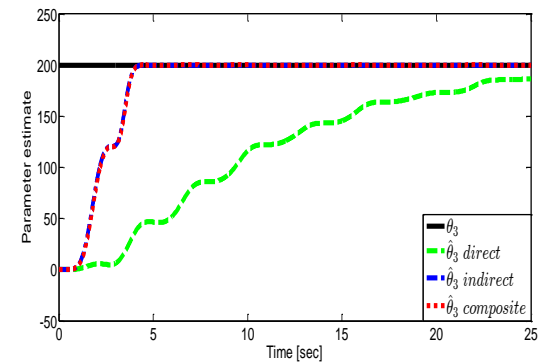


Fig. 2.17: Parameter estimate: actual θ_3 ("—") and estimate $\hat{\theta}_3$ ("--").

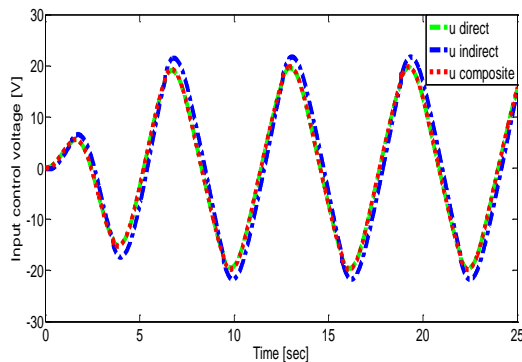


Fig. 2.18: Control input: u .

2.6.3 Composite σ -modification based least squares adaptive laws

The actual control input u and the composite σ -modification based least squares adaptive laws are the same as that in the composite σ -modification based gradient adaptive laws described by (2.99)-(2.101), respectively. $\bar{\theta}_2$ and $\bar{\theta}_3$ are computed with the least squares method as follows:

$$\dot{\bar{\theta}}_i = \bar{\Gamma}_i \frac{\Omega_i \epsilon_i}{1 + \nu_i \text{tr}\{\Omega_i^T \bar{\Gamma}_i \Omega_i\}} \quad (2.103)$$

with, $\bar{\Gamma}_i$ is given by:

$$\dot{\bar{\Gamma}}_i = -\bar{\Gamma}_i \frac{\Omega_i \Omega_i^T}{1 + \nu_i \text{tr}\{\Omega_i^T \bar{\Gamma}_i \Omega_i\}} \bar{\Gamma}_i \quad (2.104)$$

where, $\epsilon_i = x_i + \Omega_{0i} - \Omega_i^T \bar{\theta}_i$, $i = 2, 3$. The selected initial conditions are set as: $x(0) = [0 \ 0 \ 0]^T$, $\hat{\theta}_2(0) = \bar{\theta}_2(0) = 0$, $\hat{\theta}_3(0) = \bar{\theta}_3(0) = 0$, $\Omega_{02}(0) = \Omega_2^T(0) = 0$ and $\Omega_{03}(0) = \Omega_3^T(0) = 0$. The design parameters are selected as follows: $k_1 = 0.5$, $k_2 = 50$, $k_3 = 3500$, $\Gamma_2 = 1$, $\bar{\Gamma}_2(0) = 5$, $\Gamma_3 = 300$, $\bar{\Gamma}_3(0) = 10$, $\sigma_{\theta_2} = \sigma_{\theta_3} = 0.1$, $\lambda_2 = \lambda_3 = 0.1$ and $\nu_2 = \nu_3 = 0.1$.

The simulation results are shown in Figures 2.19-2.27. Figures 2.19-2.21 show the trajectories of the output variables. The trajectories of the tracking errors are illustrated in Figures 2.22-2.24. Figures 2.25 and 2.26 show the trajectories of the parameter estimates. The trajectories of the control inputs are shown in Figure 2.27.

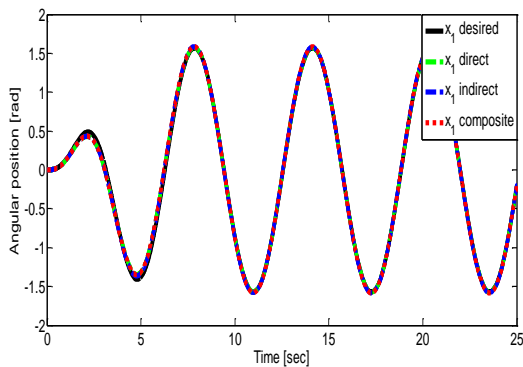


Fig. 2.19: Angular position: desired x_{1d} ("--") and actual x_1 ("--").

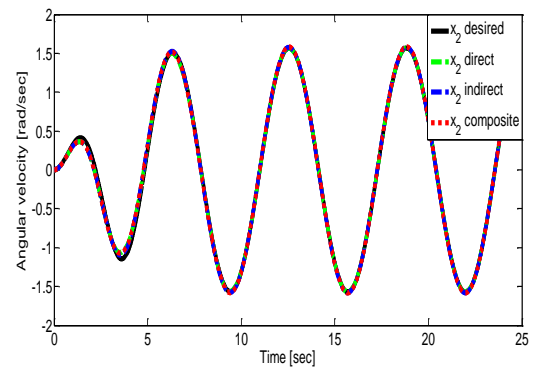


Fig. 2.20: Angular velocity: desired x_{2d} ("--") and actual x_2 ("--").

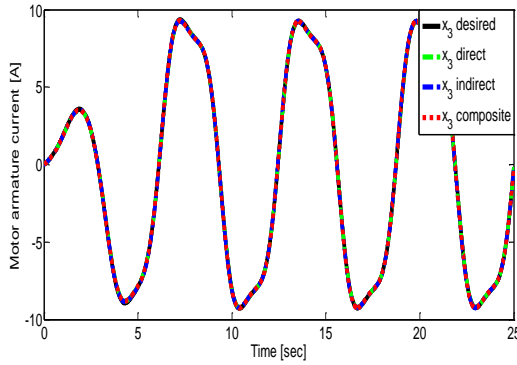


Fig. 2.21: Motor armature current: desired x_{3d} ("—") and actual x_3 ("--").

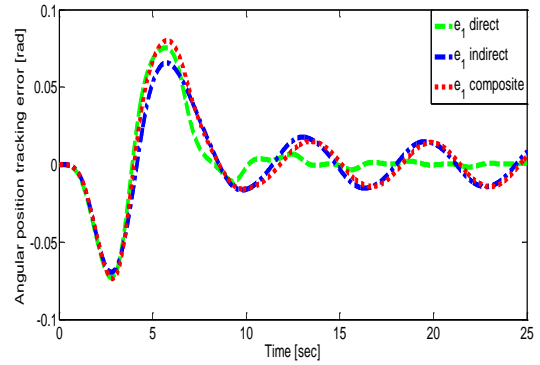


Fig. 2.22: Angular position tracking error: e_1 .

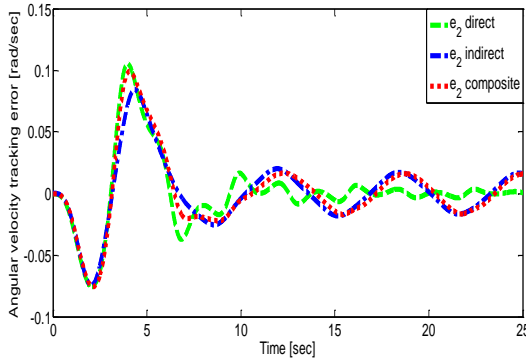


Fig. 2.23: Angular velocity tracking error: e_2 .

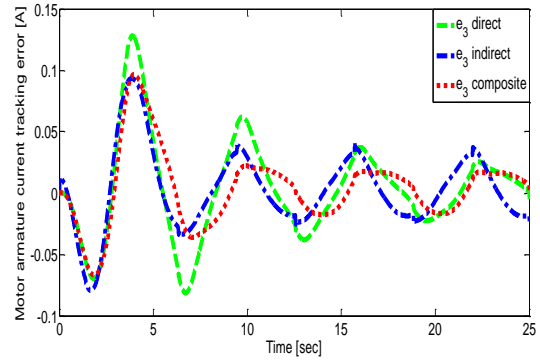


Fig. 2.24: Motor armature current tracking error: e_3 .

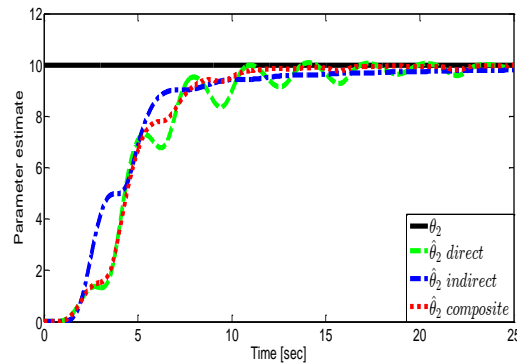


Fig. 2.25: Parameter estimate: actual θ_2 ("—") and estimate $\hat{\theta}_2$ ("--").

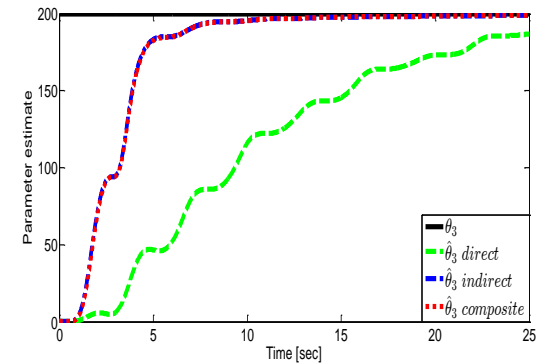


Fig. 2.26: Parameter estimate: actual θ_3 ("—") and estimate $\hat{\theta}_3$ ("--").

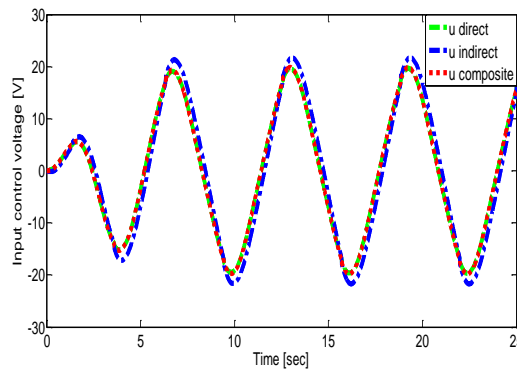


Fig. 2.27: Control input: u .

From all the results, it can be seen that all system states asymptotically converge to their desired values, that the tracking errors converge to zero and that the convergence of the parameter estimates to their true values is guaranteed. As shown in simulation results, we can conclude then that the proposed composite adaptive control scheme is effective, ensures faster convergence and achieve better parameter estimation in comparison with direct and indirect adaptive control designs.

2.7 Conclusion

In this chapter, a new composite tuning functions based adaptive backstepping control method for a class of SISO uncertain nonlinear systems in lower triangular form is proposed. The proposed composite adaptive control scheme is designed to avoid the overparametrization problem inherent in the conventional adaptive backstepping control design. The proposed composite adaptive control scheme is applied to an electromechanical system. Based on the Lyapunov stability analysis theory, it has been proven that the proposed composite adaptive control algorithm guarantees the boundedness of all signals in the closed-loop system. The performance of the proposed composite adaptive control scheme is validated through numerical simulations. The simulation results clearly show that performance, validity and effectiveness, and, improved tracking performance can be achieved with the proposed composite adaptive control scheme compared to direct and indirect adaptive control designs. In the next chapters, we will develop novel composite adaptive control methods in order to overcome the problem of explosion of complexity.

CHAPTER 3

Composite adaptive dynamic surface control

Chapter 3

Composite adaptive dynamic surface control

3.1 Introduction

Over the past few years, adaptive backstepping control and tuning functions based adaptive backstepping control methods are the most popular and effective control approaches for uncertain nonlinear systems, which has received much attention [Cil07, Kan91, Krs95a, Krs92, Wan16, Zho08]. However, adaptive backstepping control and composite tuning functions based adaptive backstepping control techniques suffer from the problem of explosion of complexity, which is caused by the repeated derivations of the virtual control inputs. In recent years, a dynamic surface control (DSC) scheme has been proposed to eliminate this problem by introducing a first-order low-pass filter at each step of the conventional backstepping control method [Hed00, Swa00, Swa97]. In [Hed00, Yip98], the dynamic surface control method has extended to adaptive control and has been widely applied for a class of uncertain nonlinear systems [Khe15, Liu18a, Liu17a, Liu17b, Yu15b]. Composite adaptive dynamic surface control has been also introduced for a class of SISO uncertain nonlinear systems in lower triangular form [Sou18, Sou17].

In this chapter, a novel composite adaptive dynamic surface control approach is proposed for a class of SISO uncertain nonlinear systems in lower triangular form. The proposed composite adaptive control technique is introduced to improve parameter estimation. By using the proposed composite adaptive control technique, the problem of explosion of complexity inherent in the conventional adaptive backstepping control and composite tuning functions based adaptive backstepping control designs is eliminated. It has been proved that all signals in the closed-loop system are bounded by using the Lyapunov stability theory. Simulation results for an electromechanical system are presented to illustrate the efficiency of the proposed composite adaptive control scheme compared to direct and indirect adaptive control designs.

The rest of this chapter is arranged as follows. The direct adaptive dynamic surface control is presented in Section 3.2. Section 3.3 is dedicated to the indirect adaptive control. The

composite adaptive dynamic surface control is proposed in Section 3.4. The simulation results are included in Section 3.5. Finally, conclusions are given in Section 3.6.

3.2 Direct adaptive dynamic surface control

In this section, we will consider the following SISO uncertain nonlinear system in lower triangular form:

$$\begin{aligned}\dot{x}_1 &= g_1(x_1)x_2 + \varphi_1^T(x_1)\theta_1 + \psi_1(x_1) \\ \dot{x}_i &= g_i(\bar{x}_i)x_{i+1} + \varphi_i^T(\bar{x}_i)\theta_i + \psi_i(\bar{x}_i), i = 2, \dots, n-1 \\ \dot{x}_n &= g_n(x)u + \varphi_n^T(x)\theta_n + \psi_n(x)\end{aligned}\quad (3.1)$$

where, $x = [x_1 \ x_2 \ \dots \ x_n]^T \in \mathbb{R}^n$ and $u \in \mathbb{R}$ are system states and the control input, respectively. $\theta_i \in \mathbb{R}^{p_i}$ are unknown constant parameter vectors, $\bar{x}_i = [x_1 \ x_2 \ \dots \ x_i]^T$ and $x = \bar{x}_n$. The nonlinear functions φ_i^T , ψ_i and $g_i \neq 0$ are known and continuous. The control objective of this approach is to construct a direct adaptive dynamic surface controller u which ensures that the system output x_1 tracks the desired trajectory x_{1d} , while all signals in the closed-loop system are bounded. Throughout this chapter, to facilitate the control design and synthesis, the following standard assumptions of the system (3.1) are exploited.

Assumption 3.2.1: There is a positive constant g_0 where, $|g_i(\bar{x}_i)| \geq g_0$, $i = 1, \dots, n$.

Assumption 3.2.2: The desired trajectory x_{1d} and both its first and second derivatives \dot{x}_{1d} and \ddot{x}_{1d} are known, continuous and bounded.

The main procedures of the direct adaptive dynamic surface control design for system (3.1) with stability analysis using Lyapunov stability theory are summarized as follows.

Step 1: Define the first surface error as $S_1 = x_1 - x_{1d}$, then, the time derivative of S_1 is obtained as:

$$\dot{S}_1 = \dot{x}_1 - \dot{x}_{1d} = g_1x_2 + \varphi_1^T\theta_1 + \psi_1 - \dot{x}_{1d}\quad (3.2)$$

We choose the virtual control \bar{x}_2 to drive S_1 towards zero with,

$$\bar{x}_2 = \frac{1}{g_1} \left(-\varphi_1^T\hat{\theta}_1 - \psi_1 + \dot{x}_{1d} - K_1S_1 \right) - g_1S_1\quad (3.3)$$

where, K_1 is a positive design parameter.

To avoid the problem of explosion of complexity in the conventional adaptive backstepping control and composite tuning functions based adaptive backstepping control,

we introduce a new variable x_{2d} and let \bar{x}_2 pass through a first order filter, with time constant τ_2 to obtain x_{2d} as:

$$\tau_2 \dot{x}_{2d} + x_{2d} = \bar{x}_2, x_{2d}(0) = \bar{x}_2(0) \quad (3.4)$$

$$\dot{x}_{2d} = \frac{1}{\tau_2} \left(-x_{2d} + \frac{1}{g_1} \left(-\varphi_1^T \hat{\theta}_1 - \psi_1 + \dot{x}_{1d} - K_1 S_1 \right) - g_1 S_1 \right) \quad (3.5)$$

Step i ($i = 2, \dots, n-1$): Define the i^{th} surface error as $S_i = x_i - x_{id}$, then, the time derivative of S_i is obtained as:

$$\dot{S}_i = \dot{x}_i - \dot{x}_{id} = g_i x_{i+1} + \varphi_i^T \theta_i + \psi_i - \dot{x}_{id} \quad (3.6)$$

We choose the virtual controllers \bar{x}_{i+1} to drive S_i towards zero with,

$$\bar{x}_{i+1} = \frac{1}{g_i} \left(-\varphi_i^T \hat{\theta}_i - \psi_i + \dot{x}_{id} - K_i S_i \right) - g_i S_i \quad (3.7)$$

where, K_i is the positive design parameters. We introduce a new variable $x_{(i+1)d}$ and let \bar{x}_{i+1} pass through a first order filter, with time constant τ_{i+1} to obtain $x_{(i+1)d}$ as:

$$\tau_{i+1} \dot{x}_{(i+1)d} + x_{(i+1)d} = \bar{x}_{i+1}, x_{(i+1)d}(0) = \bar{x}_{i+1}(0) \quad (3.8)$$

$$\dot{x}_{(i+1)d} = \frac{1}{\tau_{i+1}} \left(-x_{(i+1)d} + \frac{1}{g_i} \left(-\varphi_i^T \hat{\theta}_i - \psi_i + \dot{x}_{id} - K_i S_i \right) - g_i S_i \right) \quad (3.9)$$

Step n : Define the n^{th} surface error as $S_n = x_n - x_{nd}$, then, the time derivative of S_n is obtained as:

$$\dot{S}_n = \dot{x}_n - \dot{x}_{nd} = g_n u + \varphi_n^T \theta_n + \psi_n - \dot{x}_{nd} \quad (3.10)$$

We choose the actual control input u to drive S_n towards zero with,

$$u = \frac{1}{g_n} \left(-\varphi_n^T \hat{\theta}_n - \psi_n + \dot{x}_{nd} - K_n S_n \right) \quad (3.11)$$

where, K_n is a positive design parameter. The direct adaptive laws are given by [Yip98]:

$$\begin{aligned} \dot{\hat{\theta}}_1 &= \Gamma_1 S_1 \varphi_1 \\ \dot{\hat{\theta}}_i &= \Gamma_i S_i \varphi_i, i = 2, \dots, n-1 \\ \dot{\hat{\theta}}_n &= \Gamma_n S_n \varphi_n \end{aligned} \quad (3.12)$$

where, $\Gamma_i > 0$, $i = 1, \dots, n$ are design parameters that can be adjusted for the rate of convergence of the parameter estimates.

3.2.1 Stability analysis

Define the boundary layer errors as [Yip98]:

$$y_i = x_{id} - \bar{x}_i, i = 2, \dots, n \quad (3.13)$$

and the parameter estimation errors as:

$$\tilde{\theta}_i = \theta_i - \hat{\theta}_i, i = 1, 2, \dots, n \quad (3.14)$$

Then, the closed-loop dynamics can be expressed in terms of the surface errors S_i , the boundary layer errors y_i , and the parameter estimation errors $\tilde{\theta}_i$.

The dynamics of the surface errors are expressed, for $i = 1$, as:

$$\begin{aligned} \dot{S}_1 &= \dot{x}_1 - \dot{x}_{1d} = g_1 x_2 + \varphi_1^T \theta_1 + \psi_1 - \dot{x}_{1d} \\ &= g_1 S_2 + g_1 x_{2d} + \varphi_1^T \theta_1 + \psi_1 - \dot{x}_{1d} \\ &= g_1 S_2 + g_1 y_2 + g_1 \bar{x}_2 + \varphi_1^T \theta_1 + \psi_1 - \dot{x}_{1d} \\ &= g_1 S_2 + g_1 y_2 - K_1 S_1 + \varphi_1^T \tilde{\theta}_1 - g_1^2 S_1 \end{aligned} \quad (3.15)$$

For $i = 2, \dots, n-1$:

$$\begin{aligned} \dot{S}_i &= \dot{x}_i - \dot{x}_{id} = g_i x_{i+1} + \varphi_i^T \theta_i + \psi_i - \dot{x}_{id} \\ &= g_i S_{i+1} + g_i x_{(i+1)d} + \varphi_i^T \theta_i + \psi_i - \dot{x}_{id} \\ &= g_i S_{i+1} + g_i y_{i+1} + g_i \bar{x}_{i+1} + \varphi_i^T \theta_i + \psi_i - \dot{x}_{id} \\ &= g_i S_{i+1} + g_i y_{i+1} - K_i S_i + \varphi_i^T \tilde{\theta}_i - g_i^2 S_i \end{aligned} \quad (3.16)$$

For $i = n$:

$$\begin{aligned} \dot{S}_n &= \dot{x}_n - \dot{x}_{nd} = g_n u + \varphi_n^T \theta_n + \psi_n - \dot{x}_{nd} \\ &= -K_n S_n + \varphi_n^T \tilde{\theta}_n \end{aligned} \quad (3.17)$$

The dynamics of the boundary layer errors y_i are expressed, for $i = 2$, as:

$$\begin{aligned} \dot{y}_2 &= \dot{x}_{2d} - \dot{\bar{x}}_2 = \frac{1}{\tau_2} \left(-x_{2d} + \frac{1}{g_1} \left(-\varphi_1^T \hat{\theta}_1 - \psi_1 + \dot{x}_{1d} - K_1 S_1 \right) - g_1 S_1 \right) - \dot{\bar{x}}_2 \\ &= \frac{1}{\tau_2} (-x_{2d} + \bar{x}_2) - \dot{\bar{x}}_2 = \frac{1}{\tau_2} (-y_2 - \bar{x}_2 + \bar{x}_2) - \dot{\bar{x}}_2 = -\frac{1}{\tau_2} y_2 - \dot{\bar{x}}_2 \end{aligned} \quad (3.18)$$

For $i = 3, \dots, n$:

$$\begin{aligned} \dot{y}_i &= \dot{x}_{id} - \dot{\bar{x}}_i = \frac{1}{\tau_i} \left(-x_{id} + \frac{1}{g_{i-1}} \left(-\varphi_{i-1}^T \hat{\theta}_{i-1} - \psi_{i-1} + \dot{x}_{(i-1)d} - K_{i-1} S_{i-1} \right) - g_{i-1} S_{i-1} \right) - \dot{\bar{x}}_i \\ &= \frac{1}{\tau_i} (-x_{id} + \bar{x}_i) - \dot{\bar{x}}_i = \frac{1}{\tau_i} (-y_i - \bar{x}_i + \bar{x}_i) - \dot{\bar{x}}_i = -\frac{1}{\tau_i} y_i - \dot{\bar{x}}_i \end{aligned} \quad (3.19)$$

We consider the following Lyapunov function as:

$$V = \sum_{i=1}^n V_{is} + \sum_{i=2}^n V_{iy} + \sum_{i=1}^n V_{i\theta} \quad (3.20)$$

where,

$$V_{is} = \frac{1}{2} S_i^2, V_{iy} = \frac{1}{2} y_i^2, V_{i\theta} = \frac{1}{2} \tilde{\theta}_i^T \Gamma_i^{-1} \tilde{\theta}_i \quad (3.21)$$

Then, for $i = 1, \dots, n-1$, by some simple computations, one has,

$$\dot{V}_{is} = S_i \dot{S}_i = g_i S_i S_{i+1} + g_i S_i y_{i+1} - K_i S_i^2 + S_i \varphi_i^T \tilde{\theta}_i - g_i^2 S_i^2 \quad (3.22)$$

Applying of the following Young's inequalities:

$$g_i S_i S_{i+1} \leq \frac{1}{2} g_i^2 S_i^2 + \frac{1}{2} S_{i+1}^2 \quad (3.23)$$

$$g_i S_i y_{i+1} \leq \frac{1}{2} g_i^2 S_i^2 + \frac{1}{2} y_{i+1}^2 \quad (3.24)$$

We obtain:

$$\dot{V}_{is} \leq -K_i S_i^2 + \frac{1}{2} S_{i+1}^2 + \frac{1}{2} y_{i+1}^2 + S_i \varphi_i^T \tilde{\theta}_i \quad (3.25)$$

and, for $i = n$:

$$\dot{V}_{ns} = S_n \dot{S}_n = -K_n S_n^2 + S_n \varphi_n^T \tilde{\theta}_n \quad (3.26)$$

one has, $\dot{x}_1 = \dot{S}_1 + \dot{x}_{1d}$ and $\dot{x}_i = \dot{S}_i + \dot{y}_i + \dot{x}_i^*$, then from,

$$\dot{x}_2 = \frac{1}{g_1} \left(- \left(\frac{\partial \varphi_1^T}{\partial x_1} \dot{x}_1 \right) \hat{\theta}_1 - \varphi_1^T \dot{\hat{\theta}}_1 - \frac{\partial \psi_1}{\partial x_1} \dot{x}_1 + \ddot{x}_{1d} - K_1 \dot{S}_1 \right) - g_1 \dot{S}_1 - \left(\frac{\partial g_1}{\partial x_1} \dot{x}_1 \right) S_1 \quad (3.27)$$

and, by induction, it is easy from:

$$\dot{x}_i = \frac{1}{g_{i-1}} \left(- \left(\sum_{j=1}^{i-1} \frac{\partial \varphi_{i-1}^T}{\partial x_j} \dot{x}_j \right) \hat{\theta}_{i-1} - \varphi_{i-1}^T \dot{\hat{\theta}}_{i-1} - \sum_{j=1}^{i-1} \frac{\partial \psi_{i-1}}{\partial x_j} \dot{x}_j + \ddot{x}_{(i-1)d} - K_{i-1} \dot{S}_{i-1} \right) - g_{i-1} \dot{S}_{i-1} - \left(\sum_{j=1}^{i-1} \frac{\partial g_{i-1}}{\partial x_j} \dot{x}_j \right) S_{i-1} \quad (3.28)$$

one has,

$$\dot{y}_2 = -\frac{1}{\tau_2} y_2 - \frac{1}{g_1} \left(- \left(\frac{\partial \varphi_1^T}{\partial x_1} \dot{x}_1 \right) \hat{\theta}_1 - \varphi_1^T \dot{\hat{\theta}}_1 - \frac{\partial \psi_1}{\partial x_1} \dot{x}_1 + \ddot{x}_{1d} - K_1 \dot{S}_1 \right) + g_1 \dot{S}_1 + \left(\frac{\partial g_1}{\partial x_1} \dot{x}_1 \right) S_1 \quad (3.29)$$

Since all terms in (3.29) can be dominated by some continuous functions, it follows that:

$$\dot{y}_2 + \frac{1}{\tau_2} y_2 \leq \left| \dot{y}_2 + \frac{1}{\tau_2} y_2 \right| \leq B_2 \left(S_1, S_2, y_2, \hat{\theta}_1, x_{1d}, \dot{x}_{1d}, \ddot{x}_{1d} \right) \quad (3.30)$$

where, $B_2(\cdot)$ is a continuous function. Thus,

$$y_2 \dot{y}_2 + \frac{1}{\tau_2} y_2^2 \leq B_2(\cdot) |y_2| \quad (3.31)$$

By using Young's inequality, it gives:

$$y_2 \dot{y}_2 \leq -\frac{1}{\tau_2} y_2^2 + \frac{y_2^2}{2} + \frac{B_2^2(\cdot)}{2} \quad (3.32)$$

as similarly for, $i = 3, \dots, n$, we obtain:

$$y_n \dot{y}_n \leq -\frac{1}{\tau_n} y_n^2 + \frac{y_n^2}{2} + \frac{B_n^2(\cdot)}{2} \quad (3.33)$$

where, $B_n(\cdot) = B_n(S_1 \cdots S_n, y_2 \cdots y_n, \hat{\theta}_1 \cdots \hat{\theta}_n, x_{1d}, \dot{x}_{1d}, \ddot{x}_{1d})$ is a continuous function. From (3.32) and (3.33), we can write:

$$\dot{V}_{iy} \leq -\frac{1}{\tau_i} y_i^2 + \frac{y_i^2}{2} + \frac{B_i^2(\cdot)}{2}, i = 2, \dots, n \quad (3.34)$$

one has,

$$\dot{V}_{i\theta} = \tilde{\theta}_i^T \Gamma_i^{-1} \dot{\tilde{\theta}}_i = -\tilde{\theta}_i^T \Gamma_i^{-1} \dot{\tilde{\theta}}_i = -\tilde{\theta}_i^T S_i \varphi_i \quad (3.35)$$

Therefore, the derivative of the Lyapunov function \dot{V} becomes:

$$\begin{aligned} \dot{V} &= \sum_{i=1}^n \dot{V}_{is} + \sum_{i=2}^n \dot{V}_{iy} + \sum_{i=1}^n \dot{V}_{i\theta} \\ &\leq \sum_{i=1}^{n-1} \left(-K_i S_i^2 + \frac{1}{2} S_{i+1}^2 + \frac{1}{2} y_{i+1}^2 + S_i \varphi_i^T \tilde{\theta}_i \right) - K_n S_n^2 + S_n \varphi_n^T \tilde{\theta}_n + \sum_{i=2}^n \left(-\frac{1}{\tau_i} y_i^2 + \frac{y_i^2}{2} + \frac{B_i^2(\cdot)}{2} \right) - \sum_{i=1}^n \tilde{\theta}_i^T S_i \varphi_i \\ &\leq -K_1 S_1^2 - \sum_{i=2}^{n-1} \left(K_i - \frac{1}{2} \right) S_i^2 - \left(K_n - \frac{1}{2} \right) S_n^2 - \sum_{i=2}^n \left(\frac{1}{\tau_i} - 1 \right) y_i^2 + \sum_{i=2}^n \frac{B_i^2(\cdot)}{2} \\ &\leq -K_1 S_1^2 - \sum_{i=2}^{n-1} \left(K_i - \frac{1}{2} \right) S_i^2 - \left(K_n - \frac{1}{2} \right) S_n^2 - \sum_{i=2}^n \left(\frac{1}{\tau_i} - 1 \right) y_i^2 + \varphi \end{aligned} \quad (3.36)$$

where, $\varphi = \sum_{i=2}^n \frac{M_i}{2}$ and M_i are the maximums of $B_i(\cdot)$. Based on (3.36), by choosing the

design parameters such that, $K_1 > 0$, $K_i > \frac{1}{2}$, $K_n > \frac{1}{2}$ and $\tau_i < 1$, we can conclude that, S_i

and y_i are bounded.

3.3 Indirect adaptive control

The main procedures for designing the indirect adaptive control with stability analysis are described as follows.

3.3.1 Identification based x-swapping filters

To illustrate the identification based x-swapping filters design procedures, we consider the SISO uncertain nonlinear system (3.1), which can be rewritten under the following nonlinear system in parametric x-model form as [Sou18]:

$$\dot{x}_i = f_i(x, u) + \varphi_i^T(\bar{x}_i)\theta_i \quad (3.37)$$

where,

$$f_i(x, u) = \begin{bmatrix} g_1 x_2 + \psi_1 \\ \vdots \\ g_{n-1} x_n + \psi_{n-1} \\ g_n u + \psi_n \end{bmatrix} \quad (3.38)$$

We introduce the x-swapping filters as follows:

$$\dot{\Omega}_{0i} = a_i(\Omega_{0i} + x_i) - f_i(x, u), \Omega_{0i} \in \mathbb{R} \quad (3.39)$$

$$\dot{\Omega}_i^T = a_i \Omega_i^T + \varphi_i^T(\bar{x}_i), \Omega_i \in \mathbb{R}^{p_i} \quad (3.40)$$

where, $i = 1, \dots, n$ and $a_i < 0$ is a negative definite scalar function for each x continuous in t . We define the estimation errors as:

$$\epsilon_i = x_i + \Omega_{0i} - \Omega_i^T \hat{\theta}_i, \epsilon_i \in \mathbb{R} \quad (3.41)$$

with, $\hat{\theta}_i$ the estimate of θ_i and let:

$$\tilde{\epsilon}_i = x_i + \Omega_{0i} - \Omega_i^T \theta_i, \tilde{\epsilon}_i \in \mathbb{R} \quad (3.42)$$

Then, we obtain:

$$\epsilon_i = \Omega_i^T \tilde{\theta}_i + \tilde{\epsilon}_i \quad (3.43)$$

The error signal $\tilde{\epsilon}_i$ satisfies:

$$\dot{\tilde{\epsilon}}_i = \dot{x}_i + \dot{\Omega}_{0i} - \dot{\Omega}_i^T \theta_i = a_i \tilde{\epsilon}_i \quad (3.44)$$

To guarantee the boundedness of Ω_i when $\varphi_i(\bar{x}_i)$ grows unbounded, a particular choice of a_i is made:

$$a_i = a_{0i} - \lambda_i \varphi_i^T(\bar{x}_i) \varphi_i(\bar{x}_i) P_i \quad (3.45)$$

where, $\lambda_i > 0$ and a_{0i} is an arbitrary negative constant satisfying [Sou18]:

$$2P_i a_{0i} = -1, P_i > 0 \quad (3.46)$$

3.3.2 Choice of adaptive laws

The gradient adaptive laws are defined as:

$$\dot{\hat{\theta}}_i = \Gamma_i \frac{\Omega_i \epsilon_i}{1 + \nu_i \text{tr}\{\Omega_i^T \Omega_i\}}, \Gamma_i > 0, \nu_i \geq 0 \quad (3.47)$$

The least squares adaptive laws are defined as:

$$\dot{\hat{\theta}}_i = \Gamma_i \frac{\Omega_i \epsilon_i}{1 + \nu_i \text{tr}\{\Omega_i^T \Gamma_i \Omega_i\}} \quad (3.48)$$

where, Γ_i is given by:

$$\dot{\Gamma}_i = -\Gamma_i \frac{\Omega_i \Omega_i^T}{1 + \nu_i \text{tr}\{\Omega_i^T \Gamma_i \Omega_i\}} \Gamma_i, \Gamma_i(0) > 0, \nu_i \geq 0 \quad (3.49)$$

3.3.3 Proof of stability

Lemma 3.3.1: To establish the identifier properties, let $[0, t_f)$, the maximal interval of existence of solutions of (3.37), the x-swapping filters (3.39) and (3.40), and the gradient adaptive laws (3.47) or the least squares adaptive laws (3.48) and (3.49). Then for $\nu_i \geq 0$, the following properties hold:

$$\tilde{\theta}_i \in L_\infty \quad (3.50)$$

$$\epsilon_i \in L_2 \cap L_\infty \quad (3.51)$$

$$\dot{\hat{\theta}}_i \in L_2 \cap L_\infty \quad (3.52)$$

3.3.3.1 Gradient adaptive laws

We consider the following Lyapunov function as:

$$V_i = \frac{1}{2} \tilde{\theta}_i^T \Gamma_i^{-1} \tilde{\theta}_i + P_i \tilde{\epsilon}_i^2 \quad (3.53)$$

Along with dynamic equations (3.44) and (3.47), the derivative of the Lyapunov function \dot{V}_i becomes:

$$\begin{aligned} \dot{V}_i &= \tilde{\theta}_i^T \Gamma_i^{-1} \dot{\tilde{\theta}}_i + 2P_i \tilde{\epsilon}_i \dot{\tilde{\epsilon}}_i \\ &= \tilde{\theta}_i^T \Gamma_i^{-1} \dot{\tilde{\theta}}_i + 2P_i a_i \tilde{\epsilon}_i^2 \\ &= \tilde{\theta}_i^T \Gamma_i^{-1} \dot{\tilde{\theta}}_i + 2P_i (a_{0i} - \lambda_i \varphi_i^T(\bar{x}_i) \varphi_i(\bar{x}_i) P_i) \tilde{\epsilon}_i^2 \\ &= \tilde{\theta}_i^T \Gamma_i^{-1} \dot{\tilde{\theta}}_i + (-1 - 2\lambda_i P_i \varphi_i^T(\bar{x}_i) \varphi_i(\bar{x}_i) P_i) \tilde{\epsilon}_i^2 \end{aligned} \quad (3.54)$$

Applying of the following inequality [Sou18]:

$$-1 - 2\lambda_i P_i \varphi_i^T(\bar{x}_i) \varphi_i(\bar{x}_i) P_i \leq -1 \quad (3.55)$$

We obtain:

$$\begin{aligned}
\dot{V}_i &\leq -\tilde{\theta}_i^T \Gamma_i^{-1} \dot{\tilde{\theta}}_i - \tilde{\epsilon}_i^2 = -\frac{\tilde{\theta}_i^T \Omega_i \epsilon_i}{1 + \nu_i \text{tr}\{\Omega_i^T \Omega_i\}} - \tilde{\epsilon}_i^2 \\
&= -\frac{\epsilon_i^2}{1 + \nu_i \text{tr}\{\Omega_i^T \Omega_i\}} + \frac{\epsilon_i}{1 + \nu_i \text{tr}\{\Omega_i^T \Omega_i\}} \tilde{\epsilon}_i - \tilde{\epsilon}_i^2 \\
&\leq -\frac{3}{4} \frac{\epsilon_i^2}{1 + \nu_i \text{tr}\{\Omega_i^T \Omega_i\}} - \frac{1}{4} \frac{\epsilon_i^2}{\left(1 + \nu_i \text{tr}\{\Omega_i^T \Omega_i\}\right)^2} + \frac{\epsilon_i}{1 + \nu_i \text{tr}\{\Omega_i^T \Omega_i\}} \tilde{\epsilon}_i - \tilde{\epsilon}_i^2 \quad (3.56) \\
&= -\frac{3}{4} \frac{\epsilon_i^2}{1 + \nu_i \text{tr}\{\Omega_i^T \Omega_i\}} - \left(\frac{\epsilon_i}{2\left(1 + \nu_i \text{tr}\{\Omega_i^T \Omega_i\}\right)} - \tilde{\epsilon}_i \right)^2 \\
&\leq -\frac{3}{4} \frac{\epsilon_i^2}{1 + \nu_i \text{tr}\{\Omega_i^T \Omega_i\}}
\end{aligned}$$

The nonpositivity of \dot{V}_i proves that, $\tilde{\theta}_i \in L_\infty$ (bounded). Due to $\epsilon_i = \Omega_i^T \tilde{\theta}_i + \tilde{\epsilon}_i$ and the boundedness of Ω_i , it follows that $\epsilon_i \in L_\infty$, which, in turn proves that $\dot{\tilde{\theta}}_i \in L_\infty$.

By integrating of inequality (3.56) over $[0, \infty]$, we obtain:

$$\int_0^\infty \frac{\epsilon_i^2}{1 + \nu_i \text{tr}\{\Omega_i^T \Omega_i\}} d\tau \leq \frac{4}{3} (V_i(0) - V_i(\infty)) < \infty \quad (3.57)$$

This means that, $\frac{\epsilon_i}{\sqrt{1 + \nu_i \text{tr}\{\Omega_i^T \Omega_i\}}} \in L_2$. Since Ω_i is bounded, then $\epsilon_i \in L_2$. The

boundedness of Ω_i and the square integrability of ϵ_i prove that $\dot{\tilde{\theta}}_i \in L_2$.

3.3.3.2 Least squares adaptive laws

From (3.48) and (3.49), we have the following identity:

$$\frac{d}{dt} (\Gamma_i^{-1}) = -\Gamma_i^{-1} \dot{\Gamma}_i \Gamma_i^{-1} = \frac{\Omega_i \Omega_i^T}{1 + \nu_i \text{tr}\{\Omega_i^T \Gamma_i \Omega_i\}} \geq 0 \quad (3.58)$$

We consider the following Lyapunov function as:

$$V_i = \tilde{\theta}_i^T \Gamma_i^{-1}(t) \tilde{\theta}_i + P_i \tilde{\epsilon}_i^2 \quad (3.59)$$

Along with dynamic equations (3.44), (3.48) and (3.49), the derivative of the Lyapunov function \dot{V}_i becomes:

$$\begin{aligned}
\dot{V}_i &= \dot{\tilde{\theta}}_i^T \Gamma_i^{-1} \tilde{\theta}_i + \tilde{\theta}_i^T \frac{d}{dt} (\Gamma_i^{-1} \tilde{\theta}_i) + 2P_i \tilde{\epsilon}_i \dot{\tilde{\epsilon}}_i \\
&= \dot{\tilde{\theta}}_i^T \Gamma_i^{-1} \tilde{\theta}_i - \tilde{\theta}_i^T \Gamma_i^{-1} \dot{\Gamma}_i \Gamma_i^{-1} \tilde{\theta}_i - \tilde{\theta}_i^T \Gamma_i^{-1} \dot{\hat{\theta}}_i + 2P_i a_i \tilde{\epsilon}_i^2 \\
&= \dot{\tilde{\theta}}_i^T \Gamma_i^{-1} \tilde{\theta}_i - \tilde{\theta}_i^T \Gamma_i^{-1} \dot{\Gamma}_i \Gamma_i^{-1} \tilde{\theta}_i - \tilde{\theta}_i^T \Gamma_i^{-1} \dot{\hat{\theta}}_i + 2P_i (a_{0i} - \lambda_i \varphi_i^T(\bar{x}_i) \varphi_i(\bar{x}_i) P_i) \tilde{\epsilon}_i^2 \\
&= \dot{\tilde{\theta}}_i^T \Gamma_i^{-1} \tilde{\theta}_i - \tilde{\theta}_i^T \Gamma_i^{-1} \dot{\Gamma}_i \Gamma_i^{-1} \tilde{\theta}_i - \tilde{\theta}_i^T \Gamma_i^{-1} \dot{\hat{\theta}}_i + (-1 - 2\lambda_i P_i \varphi_i^T(\bar{x}_i) \varphi_i(\bar{x}_i) P_i) \tilde{\epsilon}_i^2
\end{aligned} \tag{3.60}$$

Applying of inequality (3.55), we obtain:

$$\begin{aligned}
\dot{V}_i &\leq -\dot{\tilde{\theta}}_i^T \Gamma_i^{-1} \tilde{\theta}_i - \tilde{\theta}_i^T \Gamma_i^{-1} \dot{\Gamma}_i \Gamma_i^{-1} \tilde{\theta}_i - \tilde{\theta}_i^T \Gamma_i^{-1} \dot{\hat{\theta}}_i - \tilde{\epsilon}_i^2 \\
&= -\frac{\Omega_i^T \tilde{\theta}_i \epsilon_i}{1 + \nu_i \text{tr} \{ \Omega_i^T \Gamma_i \Omega_i \}} + \frac{\tilde{\theta}_i^T \Omega_i \Omega_i^T \tilde{\theta}_i}{1 + \nu_i \text{tr} \{ \Omega_i^T \Gamma_i \Omega_i \}} - \frac{\tilde{\theta}_i^T \Omega_i \epsilon_i}{1 + \nu_i \text{tr} \{ \Omega_i^T \Gamma_i \Omega_i \}} - \tilde{\epsilon}_i^2 \\
&\leq -\frac{\Omega_i^T \tilde{\theta}_i \epsilon_i}{1 + \nu_i \text{tr} \{ \Omega_i^T \Gamma_i \Omega_i \}} - \frac{\tilde{\theta}_i^T \Omega_i \tilde{\epsilon}_i}{1 + \nu_i \text{tr} \{ \Omega_i^T \Gamma_i \Omega_i \}} - \tilde{\epsilon}_i^2 \\
&= -\frac{\epsilon_i^2}{1 + \nu_i \text{tr} \{ \Omega_i^T \Gamma_i \Omega_i \}} + \frac{\tilde{\epsilon}_i^2}{1 + \nu_i \text{tr} \{ \Omega_i^T \Gamma_i \Omega_i \}} - \tilde{\epsilon}_i^2 \\
&\leq -\frac{\epsilon_i^2}{1 + \nu_i \text{tr} \{ \Omega_i^T \Gamma_i \Omega_i \}}
\end{aligned} \tag{3.61}$$

Which, due to the positive definiteness of $\Gamma_i^{-1}(t)$, proves that, $\tilde{\theta}_i \in L_\infty$ (bounded).

By integrating of inequality (3.61) over $[0, \infty]$, we obtain:

$$\int_0^\infty \frac{\epsilon_i^2}{1 + \nu_i \text{tr} \{ \Omega_i^T \Gamma_i \Omega_i \}} d\tau \leq V_i(0) - V_i(\infty) < \infty \tag{3.62}$$

This means that, $\frac{\epsilon_i}{\sqrt{1 + \nu_i \text{tr} \{ \Omega_i^T \Gamma_i \Omega_i \}}} \in L_2$. Using the boundedness of Γ_i and Ω_i , following

the same line of argument as for the gradient adaptive laws, we prove that $\epsilon_i \in L_2 \cap L_\infty$ and

$\dot{\hat{\theta}}_i \in L_2 \cap L_\infty$.

3.4 Composite adaptive dynamic surface control

The composite adaptive dynamic surface control proposed in this section is driven by the combination of both surface error based parameter adaptive laws of the direct adaptive dynamic surface control described by (3.12) with the estimation error based parameter adaptive laws of the indirect adaptive control described by (3.47) and (3.48). The control objective of this approach is to construct a composite adaptive dynamic surface controller

u such that the system output x_1 tracks the desired trajectory x_{1d} and to guarantee that all signals in the closed-loop system are bounded. The detailed procedures for the composite adaptive dynamic surface control approach for system (3.1) with stability analysis are summarized as follows.

3.4.1 Composite projection based gradient adaptive laws

Projection properties: We assume that θ_i is estimated by $\hat{\theta}_i$, where, $\hat{\theta}_i$ are the estimates of θ_i . The estimation errors are given by:

$$\tilde{\theta}_i = \theta_i - \hat{\theta}_i \quad (3.63)$$

The projection operators are defined as [Far06, Ioa07, Ioa96, Sou18]:

$$\text{Proj}_{\hat{\theta}_i}(\bullet_i) = \begin{cases} \bullet_i & \text{if } \hat{\theta}_i^T \hat{\theta}_i < \bar{M}_i^2 \text{ or if } \left(\hat{\theta}_i^T \hat{\theta}_i = \bar{M}_i^2 \text{ and } \bullet_i \hat{\theta}_i \leq 0 \right), \\ 0 & \text{otherwise.} \end{cases} \quad (3.64)$$

where, ' \bullet_i ' represents any reasonable adaptation function. The projection algorithm guarantees that the parameter estimates $\hat{\theta}_i$ of θ_i remain bounded and satisfy the inequality, $\|\hat{\theta}_i\| \leq \bar{M}_i$.

Moreover, the projection mapping used in (3.64) guarantees that:

$$-\tilde{\theta}_i^T \text{Proj}_{\hat{\theta}_i}(\bullet_i) \leq -\tilde{\theta}_i^T \bullet_i \quad (3.65)$$

Therefore, the composite projection based gradient adaptive laws are defined as:

$$\dot{\hat{\theta}}_i = \text{Proj}_{\hat{\theta}_i} \left(\Gamma_i \left(S_i \varphi_i + \frac{\Omega_i \epsilon_i}{1 + \nu_i \text{tr} \{ \Omega_i^T \Omega_i \}} \right) \right), \Gamma_i > 0, \nu_i \geq 0 \quad (3.66)$$

The dynamics of estimation errors are given by:

$$\dot{\tilde{\theta}}_i = -\dot{\hat{\theta}}_i = \text{Proj}_{\hat{\theta}_i} \left(-\Gamma_i \left(S_i \varphi_i + \frac{\Omega_i \epsilon_i}{1 + \nu_i \text{tr} \{ \Omega_i^T \Omega_i \}} \right) \right), \Gamma_i > 0, \nu_i \geq 0 \quad (3.67)$$

where, $\epsilon_i = x_i + \Omega_{0i} - \Omega_i^T \hat{\theta}_i$.

Theorem 3.4.1: Consider the SISO uncertain nonlinear system in lower triangular form composed of the plant described by (3.1). Suppose that assumptions 3.2.1 and 3.2.2 are satisfied. Then, the virtual controllers (3.3) and (3.7), the actual control input (3.11) and the composite projection based gradient adaptive laws (3.66) guarantee that all signals in the closed-loop system are bounded.

Proof: We consider the following Lyapunov function as:

$$V = \sum_{i=1}^n V_{is} + \sum_{i=2}^n V_{iy} + \sum_{i=1}^n V_i \quad (3.68)$$

and,

$$V_{is} = \frac{1}{2} S_i^2, V_{iy} = \frac{1}{2} y_i^2, V_i = \frac{1}{2} \tilde{\theta}_i^T \Gamma_i^{-1} \tilde{\theta}_i + P_i \tilde{\epsilon}_i^2 \quad (3.69)$$

where, \dot{V}_{is} , \dot{V}_{ns} and \dot{V}_{iy} are expressed in (3.25), (3.26), (3.34), and,

$$\begin{aligned} \dot{V}_i &= -\tilde{\theta}_i^T \Gamma_i^{-1} \dot{\tilde{\theta}}_i - \tilde{\epsilon}_i^2 \\ &= -\tilde{\theta}_i^T \Gamma_i^{-1} \text{Proj}_{\tilde{\theta}_i} \left(\Gamma_i \left(S_i \varphi_i + \frac{\Omega_i \epsilon_i}{1 + \nu_i \text{tr} \{ \Omega_i^T \Omega_i \}} \right) \right) - \tilde{\epsilon}_i^2 \\ &\leq -\tilde{\theta}_i^T S_i \varphi_i - \frac{\tilde{\theta}_i^T \Omega_i \epsilon_i}{1 + \nu_i \text{tr} \{ \Omega_i^T \Omega_i \}} - \tilde{\epsilon}_i^2 \end{aligned} \quad (3.70)$$

Therefore, the derivative of the Lyapunov function \dot{V} becomes:

$$\begin{aligned} \dot{V} &= \sum_{i=1}^n \dot{V}_{is} + \sum_{i=2}^n \dot{V}_{iy} + \sum_{i=1}^n \dot{V}_i \\ &\leq \sum_{i=1}^{n-1} \left(-K_i S_i^2 + \frac{1}{2} S_{i+1}^2 + \frac{1}{2} y_{i+1}^2 + S_i \varphi_i^T \tilde{\theta}_i \right) - K_n S_n^2 + S_n \varphi_n^T \tilde{\theta}_n + \sum_{i=2}^n \left(-\frac{1}{\tau_i} y_i^2 + \frac{y_i^2}{2} + \frac{B_i^2(\cdot)}{2} \right) \\ &\quad - \sum_{i=1}^n \tilde{\theta}_i^T S_i \varphi_i - \sum_{i=1}^n \frac{\tilde{\theta}_i^T \Omega_i \epsilon_i}{1 + \nu_i \text{tr} \{ \Omega_i^T \Omega_i \}} - \sum_{i=1}^n \tilde{\epsilon}_i^2 \\ &\leq -K_1 S_1^2 - \sum_{i=2}^{n-1} \left(K_i - \frac{1}{2} \right) S_i^2 - \left(K_n - \frac{1}{2} \right) S_n^2 - \sum_{i=2}^n \left(\frac{1}{\tau_i} - 1 \right) y_i^2 + \sum_{i=2}^n \frac{B_i^2(\cdot)}{2} - \frac{3}{4} \sum_{i=1}^n \frac{\epsilon_i^2}{1 + \nu_i \text{tr} \{ \Omega_i^T \Omega_i \}} \\ &\leq -K_1 S_1^2 - \sum_{i=2}^{n-1} \left(K_i - \frac{1}{2} \right) S_i^2 - \left(K_n - \frac{1}{2} \right) S_n^2 - \sum_{i=2}^n \left(\frac{1}{\tau_i} - 1 \right) y_i^2 + \varphi - \frac{3}{4} \sum_{i=1}^n \frac{\epsilon_i^2}{1 + \nu_i \text{tr} \{ \Omega_i^T \Omega_i \}} \end{aligned} \quad (3.71)$$

where, $\varphi = \sum_{i=2}^n \frac{M_i}{2}$ and M_i are the maximums of $B_i(\cdot)$. Therefore, based on (3.71), by

choosing the design parameters such that, $K_1 > 0$, $K_i > \frac{1}{2}$, $K_n > \frac{1}{2}$ and $\tau_i < 1$, we can

conclude that, V , S_i , y_i , $\tilde{\theta}_i$ and ϵ_i are bounded. Furthermore, all signals in the closed-loop system, i.e., x_i , x_{id} , \dot{x}_{id} , $\bar{x}_2, \dots, \bar{x}_{i+1}$, u and $\hat{\theta}_i$ are also bounded.

3.4.2 Composite projection based least squares adaptive laws

The composite projection based least squares adaptive laws are defined as:

$$\dot{\hat{\theta}}_i = \text{Proj}_{\hat{\theta}_i} \left(\Gamma_i \left(S_i \varphi_i + \frac{\Omega_i \epsilon_i}{1 + \nu_i \text{tr} \{ \Omega_i^T \Gamma_i \Omega_i \}} \right) \right) \quad (3.72)$$

The dynamics of estimation errors are given by:

$$\dot{\tilde{\theta}}_i = -\dot{\hat{\theta}}_i = \text{Proj}_{\tilde{\theta}_i} \left(-\Gamma_i \left(S_i \varphi_i + \frac{\Omega_i \epsilon_i}{1 + \nu_i \text{tr} \{ \Omega_i^T \Gamma_i \Omega_i \}} \right) \right) \quad (3.73)$$

where, Γ_i are given by:

$$\dot{\Gamma}_i = -\Gamma_i \frac{\Omega_i \Omega_i^T}{1 + \nu_i \text{tr} \{ \Omega_i^T \Gamma_i \Omega_i \}} \Gamma_i, \Gamma_i(0) > 0, \nu_i \geq 0 \quad (3.74)$$

with, $\epsilon_i = x_i + \Omega_{0i} - \Omega_i^T \hat{\theta}_i$.

Theorem 3.4.2: Consider the SISO uncertain nonlinear system in lower triangular form composed of the plant described by (3.1). Suppose that assumptions 3.2.1 and 3.2.2 are satisfied. Then, the virtual controllers (3.3) and (3.7), the actual control input (3.11) and the composite projection based least squares adaptive laws (3.72) guarantee that all signals in the closed-loop system are bounded.

Proof: We consider the following Lyapunov function as:

$$V = \sum_{i=1}^n V_{is} + \sum_{i=2}^n V_{iy} + \frac{1}{2} \sum_{i=1}^n V_i \quad (3.75)$$

and,

$$V_{is} = \frac{1}{2} S_i^2, V_{iy} = \frac{1}{2} y_i^2, V_i = \tilde{\theta}_i^T \Gamma_i^{-1}(t) \tilde{\theta}_i + P_i \tilde{\epsilon}_i^2 \quad (3.76)$$

where, \dot{V}_{is} , \dot{V}_{ns} and \dot{V}_{iy} are expressed in (3.25), (3.26), (3.34), and,

$$\begin{aligned} \dot{V}_i &= -\dot{\tilde{\theta}}_i^T \Gamma_i^{-1} \tilde{\theta}_i - \tilde{\theta}_i^T \Gamma_i^{-1} \dot{\Gamma}_i \Gamma_i^{-1} \tilde{\theta}_i - \tilde{\theta}_i^T \Gamma_i^{-1} \dot{\tilde{\theta}}_i - \tilde{\epsilon}_i^2 \\ &= -\text{Proj}_{\tilde{\theta}_i} \left(\Gamma_i \left(S_i \varphi_i + \frac{\Omega_i \epsilon_i}{1 + \nu_i \text{tr} \{ \Omega_i^T \Gamma_i \Omega_i \}} \right) \right)^T \Gamma_i^{-1} \tilde{\theta}_i - \tilde{\theta}_i^T \Gamma_i^{-1} \dot{\Gamma}_i \Gamma_i^{-1} \tilde{\theta}_i \\ &\quad - \tilde{\theta}_i^T \Gamma_i^{-1} \text{Proj}_{\tilde{\theta}_i} \left(\Gamma_i \left(S_i \varphi_i + \frac{\Omega_i \epsilon_i}{1 + \nu_i \text{tr} \{ \Omega_i^T \Gamma_i \Omega_i \}} \right) \right) - \tilde{\epsilon}_i^2 \\ &\leq -\varphi_i^T S_i \tilde{\theta}_i - \frac{\epsilon_i \Omega_i^T \tilde{\theta}_i}{1 + \nu_i \text{tr} \{ \Omega_i^T \Gamma_i \Omega_i \}} + \frac{\tilde{\theta}_i^T \Omega_i \Omega_i^T \tilde{\theta}_i}{1 + \nu_i \text{tr} \{ \Omega_i^T \Gamma_i \Omega_i \}} - \tilde{\theta}_i^T S_i \varphi_i - \frac{\tilde{\theta}_i^T \Omega_i \epsilon_i}{1 + \nu_i \text{tr} \{ \Omega_i^T \Gamma_i \Omega_i \}} - \tilde{\epsilon}_i^2 \\ &\leq -2S_i \varphi_i^T \tilde{\theta}_i - \frac{\epsilon_i \Omega_i^T \tilde{\theta}_i}{1 + \nu_i \text{tr} \{ \Omega_i^T \Gamma_i \Omega_i \}} + \frac{\tilde{\theta}_i^T \Omega_i \Omega_i^T \tilde{\theta}_i}{1 + \nu_i \text{tr} \{ \Omega_i^T \Gamma_i \Omega_i \}} - \frac{\tilde{\theta}_i^T \Omega_i \epsilon_i}{1 + \nu_i \text{tr} \{ \Omega_i^T \Gamma_i \Omega_i \}} - \tilde{\epsilon}_i^2 \end{aligned} \quad (3.77)$$

Therefore, the derivative of the Lyapunov function \dot{V} becomes:

$$\begin{aligned}
\dot{V} &= \sum_{i=1}^n \dot{V}_{is} + \sum_{i=2}^n \dot{V}_{iy} + \frac{1}{2} \sum_{i=1}^n \dot{V}_i \\
&\leq \sum_{i=1}^{n-1} \left(-K_i S_i^2 + \frac{1}{2} S_{i+1}^2 + \frac{1}{2} y_{i+1}^2 + S_i \varphi_i^T \tilde{\theta}_i \right) - K_n S_n^2 + S_n \varphi_n^T \tilde{\theta}_n \\
&\quad + \sum_{i=2}^n \left(-\frac{1}{\tau_i} y_i^2 + \frac{y_i^2}{2} + \frac{B_i^2(\cdot)}{2} \right) - \sum_{i=1}^n S_i \varphi_i^T \tilde{\theta}_i - \frac{1}{2} \sum_{i=1}^n \frac{\epsilon_i \Omega_i^T \tilde{\theta}_i}{1 + \nu_i \text{tr}\{\Omega_i^T \Gamma_i \Omega_i\}} + \frac{1}{2} \sum_{i=1}^n \frac{\tilde{\theta}_i^T \Omega_i \Omega_i^T \tilde{\theta}_i}{1 + \nu_i \text{tr}\{\Omega_i^T \Gamma_i \Omega_i\}} \\
&\quad - \frac{1}{2} \sum_{i=1}^n \frac{\tilde{\theta}_i^T \Omega_i \epsilon_i}{1 + \nu_i \text{tr}\{\Omega_i^T \Gamma_i \Omega_i\}} - \frac{1}{2} \sum_{i=1}^n \tilde{\epsilon}_i^2 \\
&\leq -K_1 S_1^2 - \sum_{i=2}^{n-1} \left(K_i - \frac{1}{2} \right) S_i^2 - \left(K_n - \frac{1}{2} \right) S_n^2 - \sum_{i=2}^n \left(\frac{1}{\tau_i} - 1 \right) y_i^2 + \sum_{i=2}^n \frac{B_i^2(\cdot)}{2} - \frac{1}{2} \sum_{i=1}^n \frac{\epsilon_i^2}{1 + \nu_i \text{tr}\{\Omega_i^T \Gamma_i \Omega_i\}} \\
&\leq -K_1 S_1^2 - \sum_{i=2}^{n-1} \left(K_i - \frac{1}{2} \right) S_i^2 - \left(K_n - \frac{1}{2} \right) S_n^2 - \sum_{i=2}^n \left(\frac{1}{\tau_i} - 1 \right) y_i^2 + \varphi - \frac{1}{2} \sum_{i=1}^n \frac{\epsilon_i^2}{1 + \nu_i \text{tr}\{\Omega_i^T \Gamma_i \Omega_i\}}
\end{aligned} \tag{3.78}$$

where, $\varphi = \sum_{i=2}^n \frac{M_i}{2}$ and M_i are the maximums of $B_i(\cdot)$. Based on (3.78), by choosing the

design parameters such that, $K_1 > 0$, $K_i > \frac{1}{2}$, $K_n > \frac{1}{2}$ and $\tau_i < 1$, we can conclude that, V ,

S_i , y_i , $\tilde{\theta}_i$ and ϵ_i are bounded. Furthermore, all signals in the closed-loop system, i.e., x_i , x_{id} , \dot{x}_{id} , $\bar{x}_2, \dots, \bar{x}_{i+1}$, u and $\hat{\theta}_i$ are also bounded.

3.4.3 Composite σ -modification based gradient and least squares adaptive laws

The composite σ -modification based gradient and least squares adaptive laws are defined as:

$$\dot{\hat{\theta}}_i = \Gamma_i \left(S_i \varphi_i - \sigma_{\theta_i} (\hat{\theta}_i - \bar{\theta}_i) \right), \Gamma_i > 0, \sigma_{\theta_i} > 0 \tag{3.79}$$

where, σ_{θ_i} are small design constants to introduce the σ -modification for the closed-loop system and $\bar{\theta}_i$ are computed with the gradient method as follows:

$$\dot{\bar{\theta}}_i = \bar{\Gamma}_i \frac{\Omega_i \epsilon_i}{1 + \nu_i \text{tr}\{\Omega_i^T \Omega_i\}}, \bar{\Gamma}_i > 0, \nu_i \geq 0 \tag{3.80}$$

or with the least squares method as follows:

$$\dot{\bar{\theta}}_i = \bar{\Gamma}_i \frac{\Omega_i \epsilon_i}{1 + \nu_i \text{tr}\{\Omega_i^T \bar{\Gamma}_i \Omega_i\}} \tag{3.81}$$

where, $\bar{\Gamma}_i$ are given by:

$$\dot{\bar{\Gamma}}_i = -\bar{\Gamma}_i \frac{\Omega_i \Omega_i^T}{1 + \nu_i \text{tr}\{\Omega_i^T \bar{\Gamma}_i \Omega_i\}} \bar{\Gamma}_i, \bar{\Gamma}_i(0) > 0, \nu_i \geq 0 \quad (3.82)$$

with, $\epsilon_i = x_i + \Omega_{0i} - \Omega_i^T \bar{\theta}_i$.

Theorem 3.4.3: Consider the SISO uncertain nonlinear system in lower triangular form composed of the plant described by (3.1). Suppose that assumptions 3.2.1 and 3.2.2 are satisfied. Then, the virtual controllers (3.3) and (3.7), the actual control input (3.11) and the composite σ -modification based gradient and least squares adaptive laws (3.79) guarantee that all signals in the closed-loop system are UUB and the surface errors converge to a sufficiently small neighborhood of the origin by appropriately adjusting design parameters.

Proof: We consider the following Lyapunov function as:

$$V = \sum_{i=1}^n V_{is} + \sum_{i=2}^n V_{iy} + \sum_{i=1}^n V_{i\theta} \quad (3.83)$$

and,

$$V_{is} = \frac{1}{2} S_i^2, V_{iy} = \frac{1}{2} y_i^2, V_{i\theta} = \frac{1}{2} \tilde{\theta}_i^T \Gamma_i^{-1} \tilde{\theta}_i \quad (3.84)$$

where, \dot{V}_{is} , \dot{V}_{ns} and \dot{V}_{iy} are expressed in (3.25), (3.26), (3.34), and,

$$\begin{aligned} \dot{V}_{i\theta} &= \tilde{\theta}_i^T \Gamma_i^{-1} \dot{\tilde{\theta}}_i = -\tilde{\theta}_i^T \Gamma_i^{-1} \hat{\theta}_i \\ &= -\tilde{\theta}_i^T \Gamma_i^{-1} \left(\Gamma_i S_i \varphi_i - \Gamma_i \sigma_{\theta_i} (\hat{\theta}_i - \bar{\theta}_i) \right) \\ &= -\tilde{\theta}_i^T S_i \varphi_i + \sigma_{\theta_i} \tilde{\theta}_i^T (\hat{\theta}_i - \bar{\theta}_i) \end{aligned} \quad (3.85)$$

We assume that, $\theta_i - \bar{\theta}_i$ is bounded, thus, $e_{\theta_i} = \theta_i - \bar{\theta}_i$ is bounded, $\bar{\theta}_i = \theta_i - e_{\theta_i}$ and $\tilde{\theta}_i = \theta_i - \hat{\theta}_i$. The derivative of the Lyapunov function $\dot{V}_{i\theta}$ becomes:

$$\begin{aligned} \dot{V}_{i\theta} &= -\tilde{\theta}_i^T S_i \varphi_i + \sigma_{\theta_i} \tilde{\theta}_i^T (\hat{\theta}_i - \theta_i + e_{\theta_i}) \\ &= -\tilde{\theta}_i^T S_i \varphi_i - \sigma_{\theta_i} \tilde{\theta}_i^T \tilde{\theta}_i + \sigma_{\theta_i} \tilde{\theta}_i^T e_{\theta_i} \end{aligned} \quad (3.86)$$

Applying of the following inequality:

$$\tilde{\theta}_i^T e_{\theta_i} \leq \frac{\tilde{\theta}_i^T \tilde{\theta}_i}{2} + \frac{e_{\theta_i}^2}{2} \quad (3.87)$$

We obtain:

$$\dot{V}_{i\theta} \leq -\tilde{\theta}_i^T S_i \varphi_i - \frac{\sigma_{\theta_i}}{2} \tilde{\theta}_i^T \tilde{\theta}_i + \frac{\sigma_{\theta_i}}{2} e_{\theta_i}^2 \quad (3.88)$$

Therefore, the derivative of the Lyapunov function \dot{V} becomes:

$$\begin{aligned}
\dot{V} &= \sum_{i=1}^n \dot{V}_{is} + \sum_{i=2}^n \dot{V}_{iy} + \sum_{i=1}^n \dot{V}_{i\theta} \\
&\leq \sum_{i=1}^{n-1} \left(-K_i S_i^2 + \frac{1}{2} S_{i+1}^2 + \frac{1}{2} y_{i+1}^2 + S_i \phi_i^T \tilde{\theta}_i \right) - K_n S_n^2 + S_n \phi_n^T \tilde{\theta}_n + \sum_{i=2}^n \left(-\frac{1}{\tau_i} y_i^2 + \frac{y_i^2}{2} + \frac{B_i^2(\cdot)}{2} \right) \\
&\quad - \sum_{i=1}^n \tilde{\theta}_i^T S_i \phi_i - \sum_{i=1}^n \frac{\sigma_{\theta_i}}{2} \tilde{\theta}_i^T \tilde{\theta}_i + \sum_{i=1}^n \frac{\sigma_{\theta_i}}{2} e_{\theta_i}^2 \\
&\leq -K_1 S_1^2 - \sum_{i=2}^{n-1} \left(K_i - \frac{1}{2} \right) S_i^2 - \left(K_n - \frac{1}{2} \right) S_n^2 - \sum_{i=2}^n \left(\frac{1}{\tau_i} - 1 \right) y_i^2 + \sum_{i=2}^n \frac{B_i^2(\cdot)}{2} - \sum_{i=1}^n \frac{\sigma_{\theta_i}}{2} \tilde{\theta}_i^T \tilde{\theta}_i + \sum_{i=1}^n \frac{\sigma_{\theta_i}}{2} e_{\theta_i}^2 \\
&\leq -K_1 S_1^2 - \sum_{i=2}^{n-1} \left(K_i - \frac{1}{2} \right) S_i^2 - \left(K_n - \frac{1}{2} \right) S_n^2 - \sum_{i=2}^n \left(\frac{1}{\tau_i} - 1 \right) y_i^2 + \varphi - \sum_{i=1}^n \frac{\sigma_{\theta_i}}{2} \tilde{\theta}_i^T \tilde{\theta}_i + \sum_{i=1}^n \frac{\sigma_{\theta_i}}{2} e_{\theta_i}^2 \\
&\leq -K_1 S_1^2 - \sum_{i=2}^{n-1} \left(K_i - \frac{1}{2} \right) S_i^2 - \left(K_n - \frac{1}{2} \right) S_n^2 - \sum_{i=2}^n \left(\frac{1}{\tau_i} - 1 \right) y_i^2 - \sum_{i=1}^n \frac{\sigma_{\theta_i}}{2} \tilde{\theta}_i^T \tilde{\theta}_i + \mu
\end{aligned} \tag{3.89}$$

The above inequality can be rewritten as follows:

$$\dot{V} \leq -\pi V + \mu \tag{3.90}$$

where, $\pi = \min \left\{ 2K_1, 2 \left(K_i - \frac{1}{2} \right), 2 \left(K_n - \frac{1}{2} \right), 2 \left(\frac{1}{\tau_i} - 1 \right), \Gamma_i \sigma_{\theta_i} \right\}$, $\mu = \varphi + \sum_{i=1}^n \frac{\sigma_{\theta_i}}{2} e_{\theta_i}^2$, $\varphi = \sum_{i=2}^n \frac{M_i}{2}$

and M_i are the maximums of $B_i(\cdot)$. Multiplying (3.90) by $e^{\pi t}$ yields:

$$\frac{d}{dt} (V(t) e^{\pi t}) \leq \mu e^{\pi t} \tag{3.91}$$

Integrating (3.91) over $[0, t]$, we have:

$$0 \leq V(t) \leq \frac{\mu}{\pi} + \left(V(0) - \frac{\mu}{\pi} \right) e^{-\pi t} \tag{3.92}$$

Since $\frac{\mu}{\pi} > 0$, it can be obtained that:

$$0 \leq V(t) \leq V(0) e^{-\pi t} + \frac{\mu}{\pi} \tag{3.93}$$

Therefore, based on (3.89), by choosing the design parameters such that, $K_1 > 0$, $K_i > \frac{1}{2}$,

$K_n > \frac{1}{2}$, $\tau_i < 1$ and $\sigma_{\theta_i} > 0$, we can conclude that, S_i , y_i , $\tilde{\theta}_i$ and ϵ_i are UUB.

Furthermore, all signals in the closed-loop system, i.e., x_i , x_{id} , \dot{x}_{id} , $\bar{x}_2, \dots, \bar{x}_{i+1}$, u and $\hat{\theta}_i$ are also UUB.

In addition, from (3.83) and (3.93), it follows that: $\|S\| = \sqrt{\sum_{i=1}^n S_i^2} \leq \sqrt{2V(0)}e^{-0.5\pi t} + \sqrt{2\mu/\pi}$.

Accordingly, when $t \rightarrow \infty$, it is easy to show that: $\|S\| \leq \sqrt{2\mu/\pi}$. This completes the proof.

3.5 Simulation results

This section presents the simulation results for composite adaptive dynamic surface control approach as applied to an electromechanical system mathematical model and as in previous chapter. The control objective of this simulation is to construct the composite adaptive dynamic surface controller u for the electromechanical system in such a way that the link angular position q tracks the desired trajectory x_{1d} and all signals in the closed-loop system are bounded.

The signals x_{2d} and x_{3d} are generated by the filters:

$$\dot{x}_{2d} = \frac{1}{\tau_2}(-x_{2d} + \dot{x}_{1d} - K_1 S_1 - S_1) \quad (3.94)$$

$$\dot{x}_{3d} = \frac{1}{\tau_3} \left(-x_{3d} + \frac{1}{b_2} \left(\sin(x_1) \hat{\theta}_2 + \frac{B}{D} x_2 + \dot{x}_{2d} - K_2 S_2 \right) - b_2 S_2 \right) \quad (3.95)$$

The actual control input u is chosen as:

$$u = \frac{1}{b_3} \left(x_2 \hat{\theta}_3 + \frac{H}{M} x_3 + \dot{x}_{3d} - K_3 S_3 \right) \quad (3.96)$$

For the swapping based identifier, the x-swapping filters are the same as that in the chapter 2 described by (2.92)-(2.95).

3.5.1 Composite projection based gradient adaptive laws

The composite projection based gradient adaptive laws are defined as:

$$\dot{\hat{\theta}}_2 = \text{Proj}_{\hat{\theta}_2} \left(-\Gamma_2 \left(S_1 \sin(x_1) - \left(\frac{\Omega_2 \epsilon_2}{1 + \nu_2 \text{tr}\{\Omega_2^T \Omega_2\}} \right) \right) \right) \quad (3.97)$$

and,

$$\dot{\hat{\theta}}_3 = \text{Proj}_{\hat{\theta}_3} \left(-\Gamma_3 \left(S_3 x_2 - \left(\frac{\Omega_3 \epsilon_3}{1 + \nu_3 \text{tr}\{\Omega_3^T \Omega_3\}} \right) \right) \right) \quad (3.98)$$

where, $\epsilon_i = x_i + \Omega_{0i} - \Omega_i^T \hat{\theta}_i$, $i = 2, 3$.

The initial conditions are selected as: $x(0)=[0 \ 0 \ 0]^T$, $\hat{\theta}_2(0)=0$, $\hat{\theta}_3(0)=0$, $\Omega_{02}(0)=\Omega_2^T(0)=0$, $\Omega_{03}(0)=\Omega_3^T(0)=0$ and $x_{2d}(0)=x_{3d}(0)=0$. The control parameters are chosen as: $K_1=10$, $K_2=5$, $K_3=550$, $\Gamma_2=150$, $\Gamma_3=550$, $\lambda_2=\lambda_3=0.1$, $\nu_2=\nu_3=0.1$ and $\tau_2=\tau_3=10^{-3}$.

The simulation results are shown in Figures 3.1-3.9. Figures 3.1-3.3 show the trajectories of the output variables. The trajectories of the surface errors are illustrated in Figures 3.4-3.6. Figures 3.7 and 3.8 show the trajectories of the parameter estimates. The trajectories of the control inputs are shown in Figure 3.9.

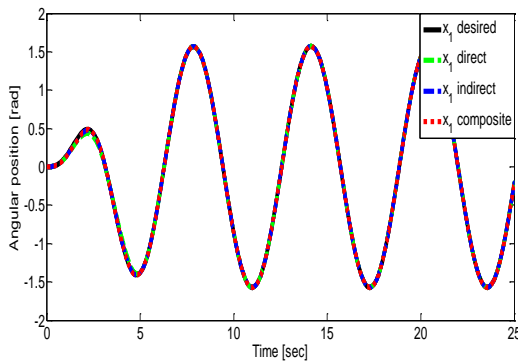


Fig. 3.1: Angular position: desired x_{1d} ("--") and actual x_1 ("--").

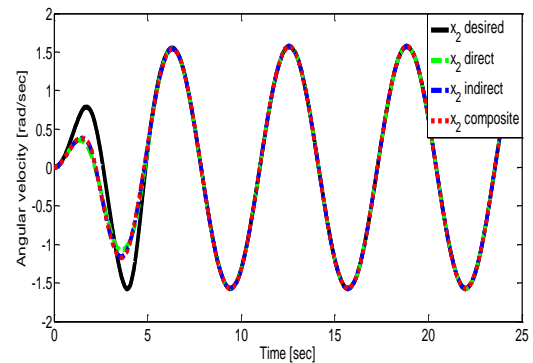


Fig. 3.2: Angular velocity: desired x_{2d} ("--") and actual x_2 ("--").

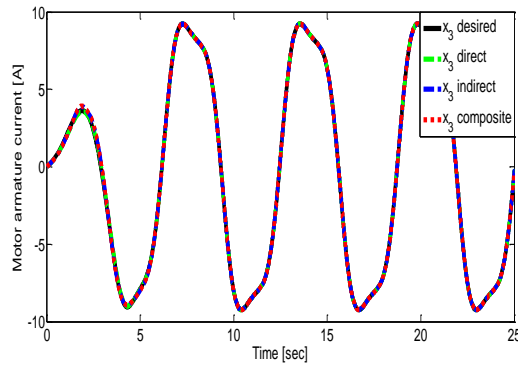


Fig. 3.3: Motor armature current: desired x_{3d} ("--") and actual x_3 ("--").

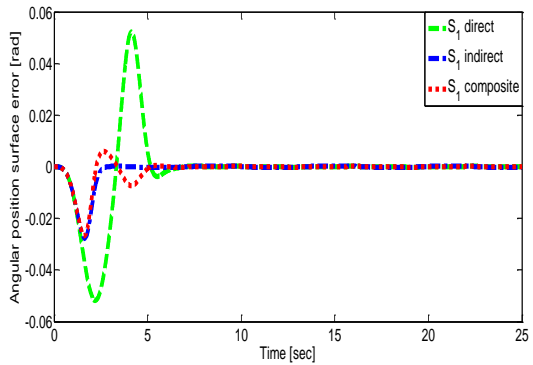


Fig. 3.4: Angular position surface error: S_1 .

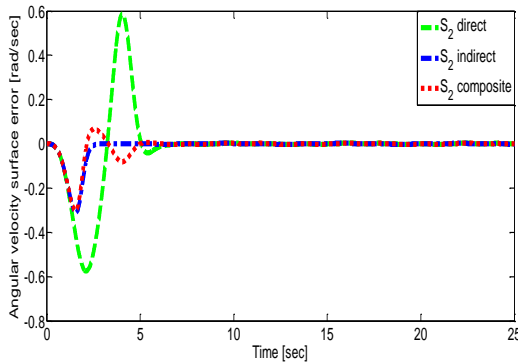


Fig. 3.5: Angular velocity surface error: S_2 .

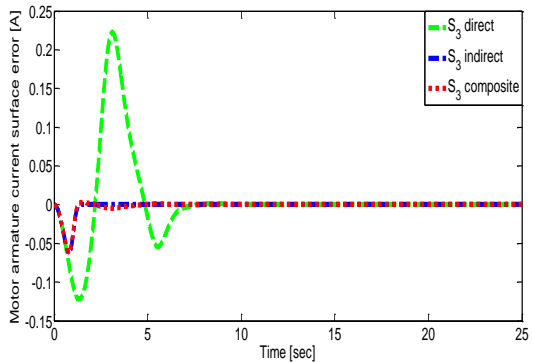


Fig. 3.6: Motor armature current surface error: S_3 .

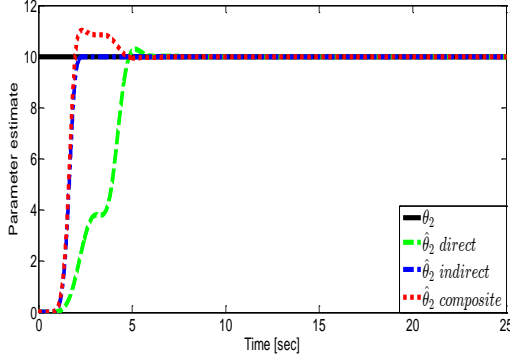


Fig. 3.7: Parameter estimate: actual θ_2 ("—") and estimate $\hat{\theta}_2$ ("--").

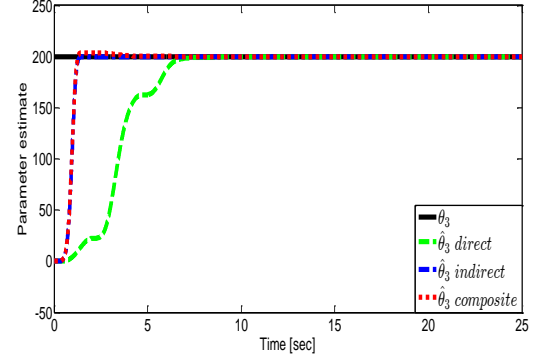


Fig. 3.8: Parameter estimate: actual θ_3 ("—") and estimate $\hat{\theta}_3$ ("--").

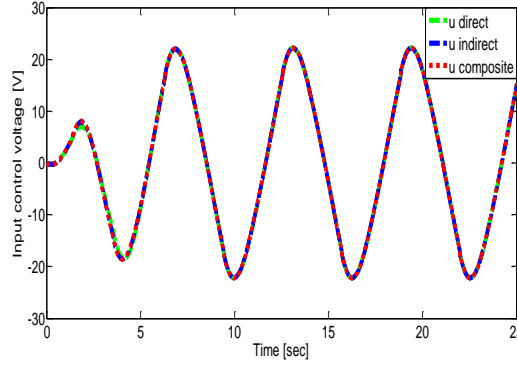


Fig. 3.9: Control input: u.

3.5.2 Composite projection based least squares adaptive laws

The composite projection based least squares adaptive laws are defined as:

$$\dot{\hat{\theta}}_2 = \text{Proj}_{\hat{\theta}_2} \left(-\Gamma_2 \left(S_1 \sin(x_1) - \left(\frac{\Omega_2 \epsilon_2}{1 + \nu_2 \text{tr}\{\Omega_2^T \Gamma_2 \Omega_2\}} \right) \right) \right) \quad (3.99)$$

and,

$$\dot{\hat{\theta}}_3 = \text{Proj}_{\hat{\theta}_3} \left(-\Gamma_3 \left(S_3 x_2 - \left(\frac{\Omega_3 \epsilon_3}{1 + \nu_3 \text{tr}\{\Omega_3^T \Gamma_3 \Omega_3\}} \right) \right) \right) \quad (3.100)$$

with, Γ_i is given by:

$$\dot{\Gamma}_i = -\Gamma_i \frac{\Omega_i \Omega_i^T}{1 + \nu_i \text{tr}\{\Omega_i^T \Gamma_i \Omega_i\}} \Gamma_i \quad (3.101)$$

where, $\epsilon_i = x_i + \Omega_{0i} - \Omega_i^T \hat{\theta}_i$, $i = 2, 3$.

The initial conditions are selected as: $x(0) = [0 \ 0 \ 0]^T$, $\hat{\theta}_2(0) = 0$, $\hat{\theta}_3(0) = 0$, $\Omega_{02}(0) = \Omega_2^T(0) = 0$, $\Omega_{03}(0) = \Omega_3^T(0) = 0$ and $x_{2d}(0) = x_{3d}(0) = 0$. The control

parameters are chosen as: $K_1 = 10$, $K_2 = 50$, $K_3 = 750$, $\Gamma_2(0) = \Gamma_3(0) = 25$, $\lambda_2 = \lambda_3 = 0.1$, $\nu_2 = \nu_3 = 0.1$ and $\tau_2 = \tau_3 = 10^{-3}$.

The simulation results are shown in Figures 3.10-3.18. Figures 3.10-3.12 show the trajectories of the output variables. The trajectories of the surface errors are illustrated in Figures 3.13-3.15. Figures 3.16 and 3.17 show the trajectories of the parameter estimates. The trajectories of the control inputs are shown in Figure 3.18.

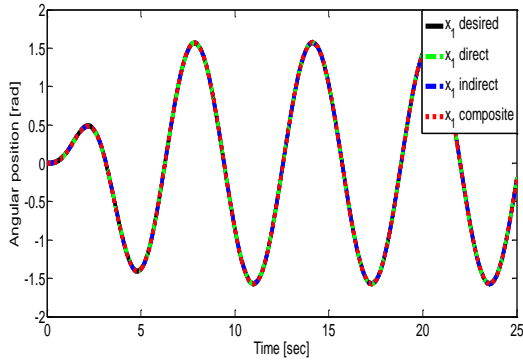


Fig. 3.10: Angular position: desired x_{1d} ("—") and actual x_1 ("--").

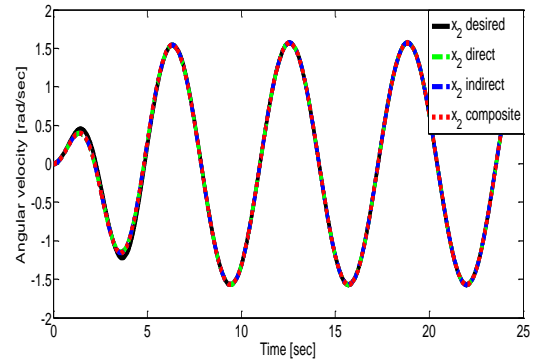


Fig. 3.11: Angular velocity: desired x_{2d} ("—") and actual x_2 ("--").

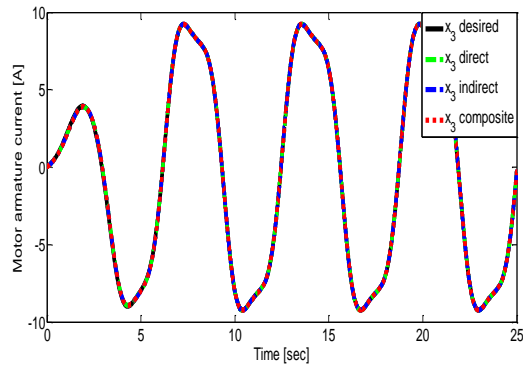


Fig. 3.12: Motor armature current: desired x_{3d} ("—") and actual x_3 ("--").

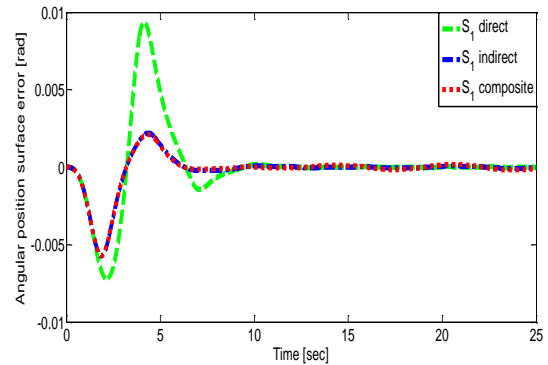


Fig. 3.13: Angular position surface error: S_1 .

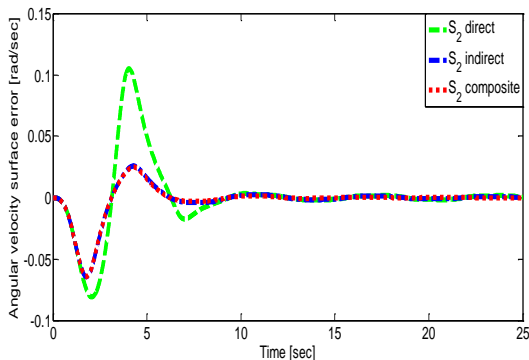


Fig. 3.14: Angular velocity surface error: S_2 .

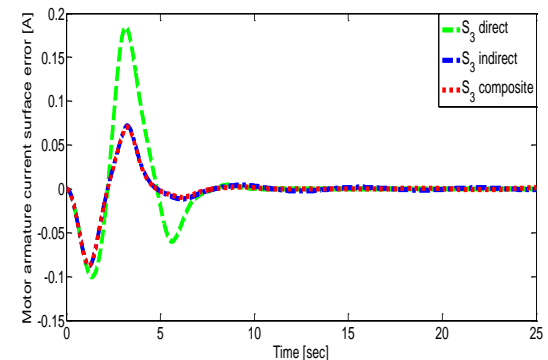


Fig. 3.15: Motor armature current surface error: S_3 .

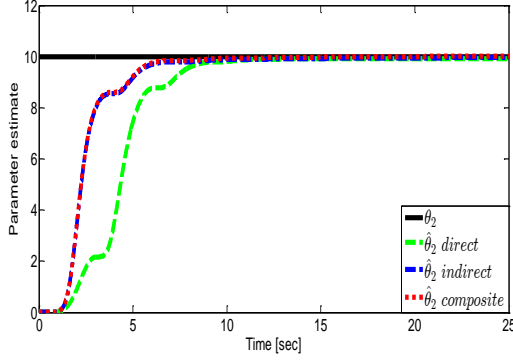


Fig. 3.16: Parameter estimate: actual θ_2 ("—") and estimate $\hat{\theta}_2$ ("--").

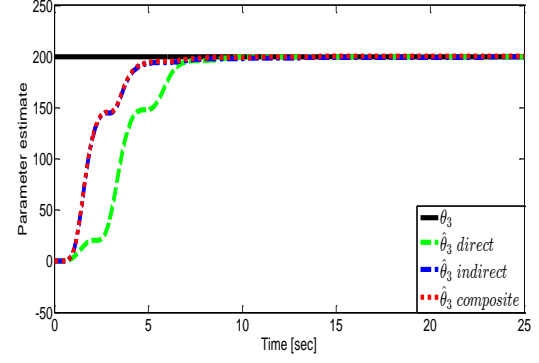


Fig. 3.17: Parameter estimate: actual θ_3 ("—") and estimate $\hat{\theta}_3$ ("--").

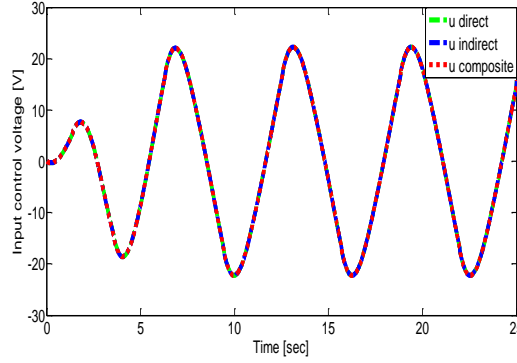


Fig. 3.18: Control input: u.

3.5.3 Composite σ -modification based gradient adaptive laws

The composite σ -modification based gradient adaptive laws are defined as:

$$\dot{\hat{\theta}}_2 = -\Gamma_2 S_1 \sin(x_1) - \Gamma_2 \sigma_{\theta_2} (\hat{\theta}_2 - \bar{\theta}_2) \quad (3.102)$$

and,

$$\dot{\hat{\theta}}_3 = -\Gamma_3 S_3 x_2 - \Gamma_3 \sigma_{\theta_3} (\hat{\theta}_3 - \bar{\theta}_3) \quad (3.103)$$

where, $\bar{\theta}_2$ and $\bar{\theta}_3$ are computed with the gradient method as follows:

$$\dot{\bar{\theta}}_i = \bar{\Gamma}_i \frac{\Omega_i \epsilon_i}{1 + \nu_i \text{tr}\{\Omega_i^T \Omega_i\}} \quad (3.104)$$

with, $\epsilon_i = x_i + \Omega_{0i} - \Omega_i^T \bar{\theta}_i$, $i = 2, 3$.

The initial conditions are selected as: $x(0) = [0 \ 0 \ 0]^T$, $\hat{\theta}_2(0) = \bar{\theta}_2(0) = 0$, $\hat{\theta}_3(0) = \bar{\theta}_3(0) = 0$, $\Omega_{02}(0) = \Omega_2^T(0) = 0$, $\Omega_{03}(0) = \Omega_3^T(0) = 0$ and $x_{2d}(0) = x_{3d}(0) = 0$. The control parameters are chosen as: $K_1 = 10$, $K_2 = 5$, $K_3 = 550$, $\Gamma_2 = 150$, $\Gamma_3 = 550$, $\bar{\Gamma}_2 = 5$, $\bar{\Gamma}_3 = 50$, $\sigma_{\theta_2} = \sigma_{\theta_3} = 0.1$, $\lambda_2 = \lambda_3 = 0.1$, $\nu_2 = \nu_3 = 0.1$ and $\tau_2 = \tau_3 = 10^{-3}$.

The simulation results are shown in Figures 3.19-3.27. Figures 3.19-3.21 show the trajectories of the output variables. The trajectories of the surface errors are illustrated in Figures 3.22-3.24. Figures 3.25 and 3.26 show the trajectories of the parameter estimates. The trajectories of the control inputs are shown in Figure 3.27.

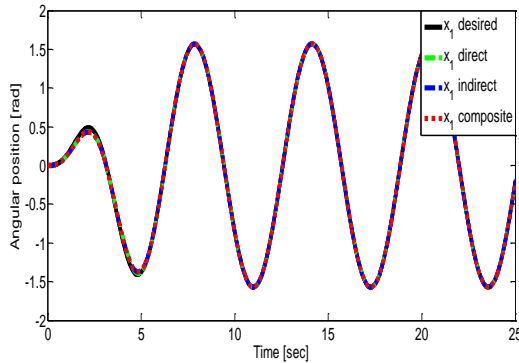


Fig. 3.19: Angular position: desired x_{1d} ("—") and actual x_1 ("--").

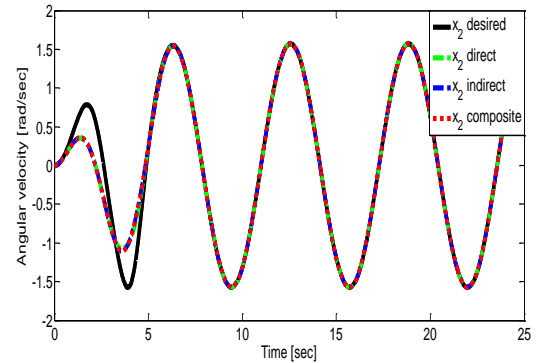


Fig. 3.20: Angular velocity: desired x_{2d} ("—") and actual x_2 ("--").

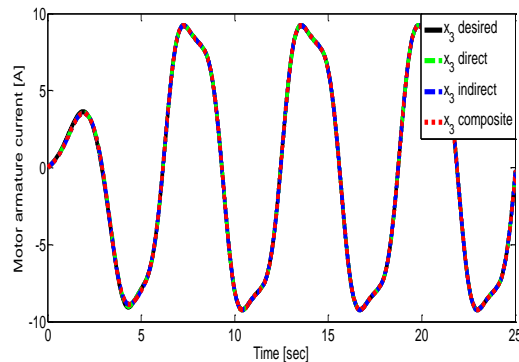


Fig. 3.21: Motor armature current: desired x_{3d} ("—") and actual x_3 ("--").

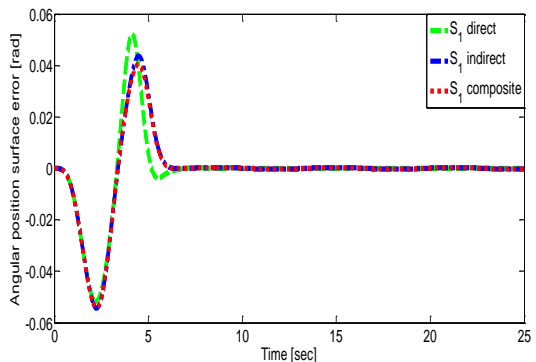


Fig. 3.22: Angular position surface error: S_1 .

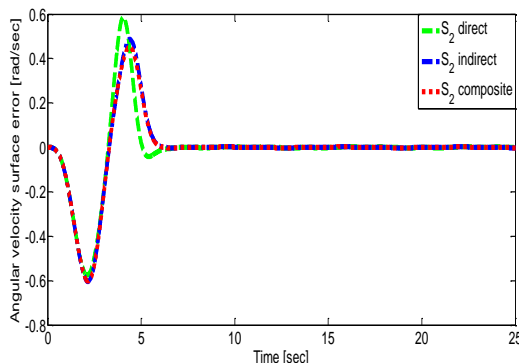


Fig. 3.23: Angular velocity surface error: S_2 .

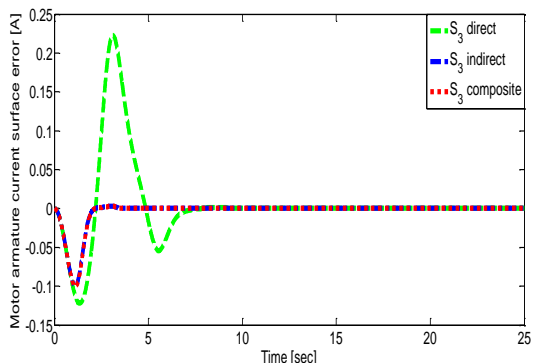


Fig. 3.24: Motor armature current surface error: S_3 .

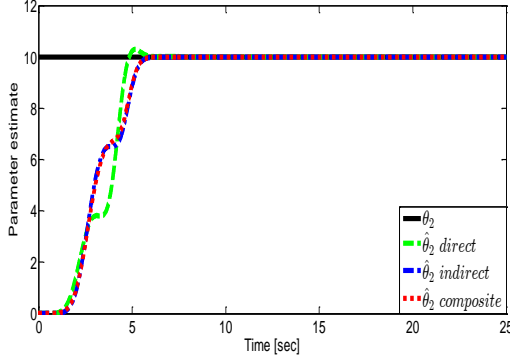


Fig. 3.25: Parameter estimate: actual θ_2 ("—") and estimate $\hat{\theta}_2$ ("--").

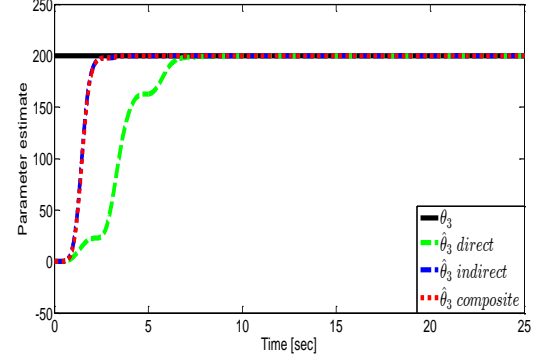


Fig. 3.26: Parameter estimate: actual θ_3 ("—") and estimate $\hat{\theta}_3$ ("--").

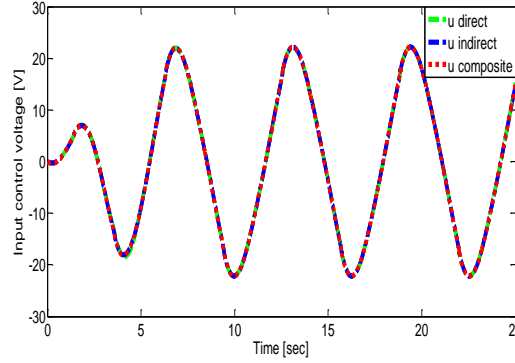


Fig. 3.27: Control input: u.

3.5.4 Composite σ -modification based least squares adaptive laws

The composite σ -modification based least squares adaptive laws are the same as that in the composite σ -modification based gradient adaptive laws described by (3.102) and (3.103).

$\bar{\theta}_2$ and $\bar{\theta}_3$ are computed with the least squares method as follows:

$$\dot{\bar{\theta}}_i = \bar{\Gamma}_i \frac{\Omega_i \epsilon_i}{1 + \nu_i \text{tr}\{\Omega_i^T \bar{\Gamma}_i \Omega_i\}} \quad (3.105)$$

with, $\bar{\Gamma}_i$ is given by:

$$\dot{\bar{\Gamma}}_i = -\bar{\Gamma}_i \frac{\Omega_i \Omega_i^T}{1 + \nu_i \text{tr}\{\Omega_i^T \bar{\Gamma}_i \Omega_i\}} \bar{\Gamma}_i \quad (3.106)$$

where, $\epsilon_i = x_i + \Omega_{0i} - \Omega_i^T \bar{\theta}_i$, $i = 2, 3$.

The initial conditions are selected as: $x(0) = [0 \ 0 \ 0]^T$, $\hat{\theta}_2(0) = \bar{\theta}_2(0) = 0$, $\hat{\theta}_3(0) = \bar{\theta}_3(0) = 0$, $\Omega_{02}(0) = \Omega_2^T(0) = 0$, $\Omega_{03}(0) = \Omega_3^T(0) = 0$ and $x_{2d}(0) = x_{3d}(0) = 0$. The control parameters are chosen as: $K_1 = 2.5$, $K_2 = 10$, $K_3 = 50$, $\Gamma_2 = 100$, $\Gamma_3 = 250$, $\bar{\Gamma}_2(0) = 55$, $\bar{\Gamma}_3(0) = 550$, $\sigma_{\theta_2} = \sigma_{\theta_3} = 0.1$, $\lambda_2 = \lambda_3 = 0.1$, $\nu_2 = \nu_3 = 0.1$ and $\tau_2 = \tau_3 = 10^{-3}$.

The simulation results are shown in Figures 3.28-3.36. Figures 3.28-3.30 show the trajectories of the output variables. The trajectories of the surface errors are illustrated in Figures 3.31-3.33. Figures 3.34 and 3.35 show the trajectories of the parameter estimates. The trajectories of the control inputs are shown in Figure 3.36.

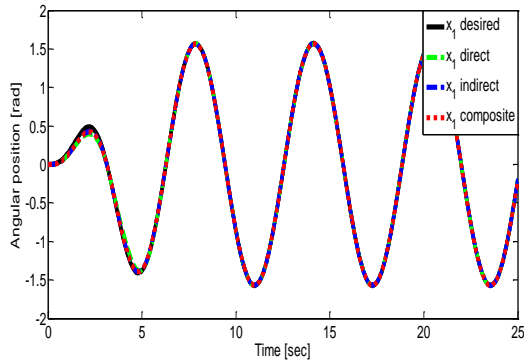


Fig. 3.28: Angular position: desired x_{1d} ("—") and actual x_1 ("--").

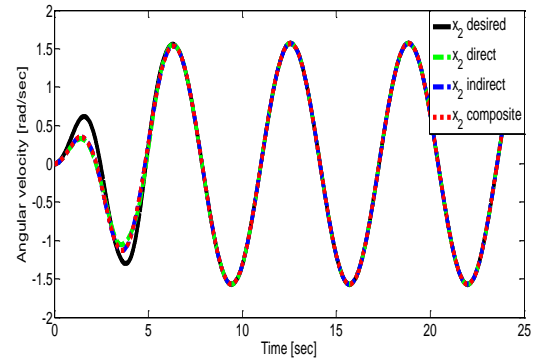


Fig. 3.29: Angular velocity: desired x_{2d} ("—") and actual x_2 ("--").

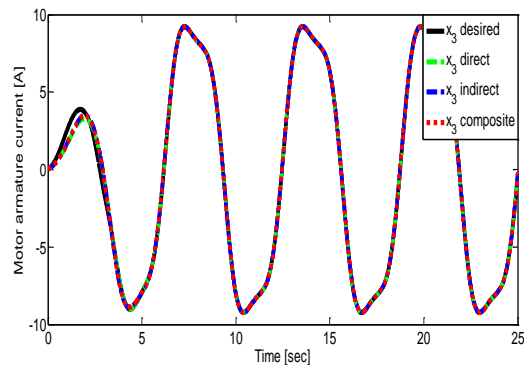


Fig. 3.30: Motor armature current: desired x_{3d} ("—") and actual x_3 ("--").

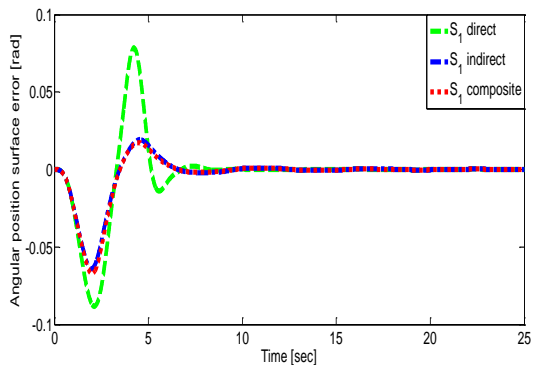


Fig. 3.31: Angular position surface error: S_1 .

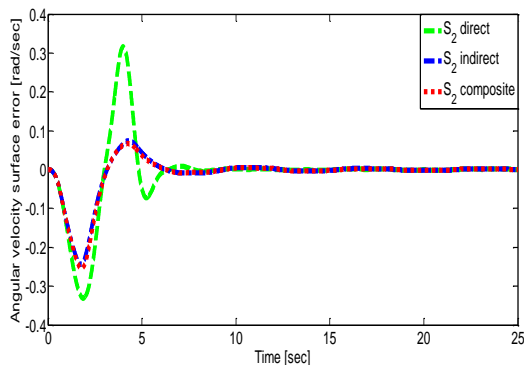


Fig. 3.32: Angular velocity surface error: S_2 .

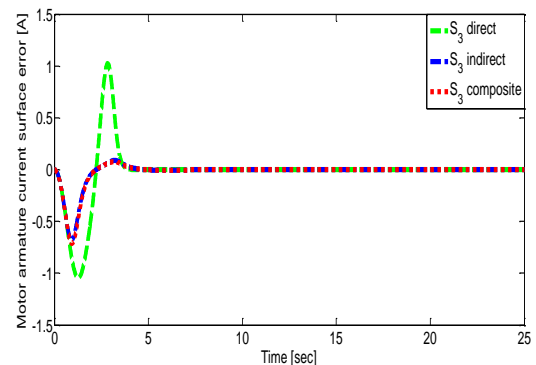


Fig. 3.33: Motor armature current surface error: S_3 .

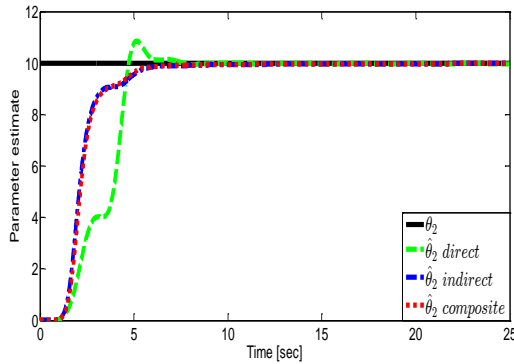


Fig. 3.34: Parameter estimate: actual θ_2 ("—") and estimate $\hat{\theta}_2$ ("--").

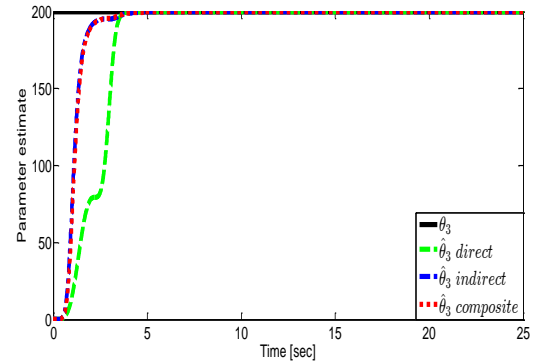


Fig. 3.35: Parameter estimate: actual θ_3 ("—") and estimate $\hat{\theta}_3$ ("--").

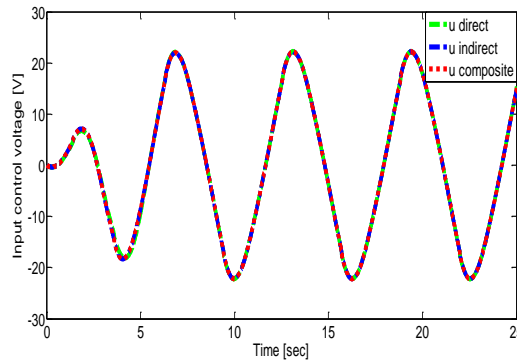


Fig. 3.36: Control input: u .

It can be clearly observed from all the results that all actual trajectories converge to their desired values, that the surface errors converge to zero, that the parameter estimates converge to its true values and that the proposed composite adaptive control approach has a reasonable control effort. The simulation results clearly show that effectiveness, higher accuracy and improved that the trajectory tracking performances can be achieved under the proposed composite adaptive control scheme compared to direct and indirect adaptive control designs.

3.6 Conclusion

This chapter presents a novel composite adaptive dynamic surface control scheme for a class of SISO uncertain nonlinear systems in lower triangular form. In order to overcome the problem of explosion of complexity inherent in the conventional adaptive backstepping control and the composite tuning functions based adaptive backstepping control designs, the proposed composite adaptive control scheme is designed. To demonstrate the effectiveness of the proposed controller, an implementation to an electromechanical system is studied. Based on the Lyapunov stability theory, the proposed composite adaptive

control scheme can guarantee that all signals in the closed-loop system are bounded. Theoretical proof improvements claimed above are proved and implemented by simulation results for an electromechanical system to show the effectiveness of the proposed composite adaptive control scheme in comparison with direct and indirect adaptive control schemes. For next work, we will focus on designing of composite robust adaptive dynamic surface control algorithm under unknown external disturbances in order to remove also the problem of explosion of complexity.

CHAPTER 4

Composite robust adaptive dynamic surface control

Chapter 4

Composite robust adaptive dynamic surface control

4.1 Introduction

During the past few years, robust adaptive control approaches that combine robust control and adaptive control methods of uncertain nonlinear systems with external disturbances have received much attention [Xi19, Yao02, Yao97, Zha15b]. Compared with the works considering the adaptive dynamic surface control, robust adaptive dynamic surface control has been also introduced to eliminate the problem of explosion of complexity inherent in the conventional adaptive backstepping control and composite tuning functions based adaptive backstepping control approaches. Recently, there are a few works regarding to the robust adaptive dynamic surface control of uncertain nonlinear systems with additive external disturbances [Elm19, Gan15, He16, Hou11, Liu18b, Li12b, Li10a, Li10b, She17c, Zha18a, Zha18b, Zha17]. In addition, composite robust adaptive dynamic surface control of uncertain nonlinear system has been also proposed [Che10].

This chapter presents a novel composite robust adaptive dynamic surface control technique for a class of SISO uncertain nonlinear systems in lower triangular form under unknown external disturbances. The proposed composite robust adaptive control scheme is utilized to achieve higher tracking accuracy and better parameter convergence. The proposed composite robust adaptive control method is introduced to avoid the problem of explosion of complexity. The boundedness of all signals in the closed-loop system is proven based on the Lyapunov stability theory. To demonstrate the effectiveness and robustness of the proposed composite robust adaptive control scheme, simulation results for an electromechanical system are provided. In addition, direct and indirect robust adaptive control designs are also studied and simulated in comparison with the proposed composite robust adaptive control scheme.

The remaining of the chapter is organized as follows. The direct robust adaptive dynamic surface control is presented in Section 4.2. Section 4.3 is devoted to the indirect robust adaptive control. The composite robust adaptive dynamic surface control is proposed in Section 4.4. Section 4.5 is concerned with the simulation results. Conclusions are given in Section 4.6.

4.2 Direct robust adaptive dynamic surface control

In this section, we will consider the following SISO uncertain nonlinear system in lower triangular form with external disturbances:

$$\begin{aligned}\dot{x}_1 &= g_1(x_1)x_2 + \varphi_1^T(x_1)\theta_1 + \psi_1(x_1) + d_1(t) \\ \dot{x}_i &= g_i(\bar{x}_i)x_{i+1} + \varphi_i^T(\bar{x}_i)\theta_i + \psi_i(\bar{x}_i) + d_i(t), i = 2, \dots, n-1 \\ \dot{x}_n &= g_n(x)u + \varphi_n^T(x)\theta_n + \psi_n(x) + d_n(t)\end{aligned}\quad (4.1)$$

where, $x = [x_1 \ x_2 \ \dots \ x_n]^T \in \mathbb{R}^n$ and $u \in \mathbb{R}$ are system states and the control input, respectively. $\theta_i \in \mathbb{R}^{p_i}$ are unknown constant parameter vectors, $\bar{x}_i = [x_1 \ x_2 \ \dots \ x_i]^T$ and $x = \bar{x}_n$. The nonlinear functions φ_i^T , ψ_i and $g_i \neq 0$ are known and continuous. The unknown functions $d_i(t) \in \mathbb{R}$, $i = 1, \dots, n$, represent the external disturbances. The control objective of this approach is to construct a direct robust adaptive dynamic surface controller u such that the system output x_1 tracks the desired trajectory x_{1d} and all signals in the closed-loop system are bounded. Throughout this chapter, the following standard assumptions and lemma of the system (4.1) are exploited to facilitate the control design and analysis.

Assumption 4.2.1: There is a positive constant g_0 where, $|g_i(\bar{x}_i)| \geq g_0$, $i = 1, \dots, n$.

Assumption 4.2.2: The desired trajectory x_{1d} and both its first and second derivatives \dot{x}_{1d} and \ddot{x}_{1d} are known, continuous and bounded.

Assumption 4.2.3: The external disturbances $d_i(t)$ are assumed to be continuous and bounded, i.e.,

$$|d_i(t)| \leq \delta_i \quad (4.2)$$

where, δ_i are an unknown positive constants.

Lemma 4.2.1 [Pol96]: The following inequality holds for any $\varepsilon > 0$ and for any $\eta \in \mathbb{R}$:

$$0 \leq |\eta| - \eta \tanh\left(\frac{\eta}{\varepsilon}\right) \leq \kappa \varepsilon \quad (4.3)$$

where, κ is a constant that satisfies $\kappa = e^{-(\kappa+1)}$, i.e., $\kappa = 0.2785$.

Remark 4.2.1: In reality, the energy of external disturbances $d_i(t)$ is always finite and hence it is reasonable to assume $d_i(t)$ is bounded by an unknown constant. For assumption 4.2.3, the external disturbances are assumed as bounded and the boundary is unknown.

Remark 4.2.2: The above assumptions and lemma are necessary and reasonable.

The main procedures for designing the direct robust adaptive dynamic surface control method for system (4.1) with stability analysis using Lyapunov stability theory are given as follows.

Step 1: Define the first surface error as $S_1 = x_1 - x_{1d}$, then, the time derivative of S_1 is obtained as:

$$\dot{S}_1 = \dot{x}_1 - \dot{x}_{1d} = g_1 x_2 + \varphi_1^T \theta_1 + \psi_1 + d_1(t) - \dot{x}_{1d} \quad (4.4)$$

We choose the virtual control \bar{x}_2 to drive S_1 towards zero with,

$$\bar{x}_2 = \frac{1}{g_1} \left(-\varphi_1^T \hat{\theta}_1 - \psi_1 - \hat{\delta}_1 \tanh\left(\frac{S_1}{\varepsilon_1}\right) + \dot{x}_{1d} - K_1 S_1 \right) - g_1 S_1 \quad (4.5)$$

where, K_1 is a positive design parameter, ε_1 is a small positive constant and $\tanh\left(\frac{S_1}{\varepsilon_1}\right)$ is an hyperbolic tangent function. To avoid the problem of explosion of complexity in the conventional adaptive backstepping control and composite tuning functions based adaptive backstepping control designs, we introduce a new variable x_{2d} and let \bar{x}_2 pass through a first order filter, with time constant τ_2 to obtain x_{2d} as:

$$\tau_2 \dot{x}_{2d} + x_{2d} = \bar{x}_2, x_{2d}(0) = \bar{x}_2(0) \quad (4.6)$$

$$\dot{x}_{2d} = \frac{1}{\tau_2} \left(-x_{2d} + \frac{1}{g_1} \left(-\varphi_1^T \hat{\theta}_1 - \psi_1 - \hat{\delta}_1 \tanh\left(\frac{S_1}{\varepsilon_1}\right) + \dot{x}_{1d} - K_1 S_1 \right) - g_1 S_1 \right) \quad (4.7)$$

Step i ($i = 2, \dots, n-1$): Define the i^{th} surface error as $S_i = x_i - x_{id}$, then, the time derivative of S_i is obtained as:

$$\dot{S}_i = \dot{x}_i - \dot{x}_{id} = g_i x_{i+1} + \varphi_i^T \theta_i + \psi_i + d_i(t) - \dot{x}_{id} \quad (4.8)$$

We choose the virtual controllers \bar{x}_{i+1} to drive S_i towards zero with,

$$\bar{x}_{i+1} = \frac{1}{g_i} \left(-\varphi_i^T \hat{\theta}_i - \psi_i - \hat{\delta}_i \tanh\left(\frac{S_i}{\varepsilon_i}\right) + \dot{x}_{id} - K_i S_i \right) - g_i S_i \quad (4.9)$$

where, K_i is the positive design parameters, ε_i are a small positive constants and $\tanh\left(\frac{S_i}{\varepsilon_i}\right)$ are an hyperbolic tangent functions. We introduce a new variable $x_{(i+1)d}$ and let

\bar{x}_{i+1} pass through a first order filter, with time constant τ_{i+1} to obtain $x_{(i+1)d}$ as:

$$\tau_{i+1} \dot{x}_{(i+1)d} + x_{(i+1)d} = \bar{x}_{i+1}, x_{(i+1)d}(0) = \bar{x}_{i+1}(0) \quad (4.10)$$

$$\dot{x}_{(i+1)d} = \frac{1}{\tau_{i+1}} \left(-x_{(i+1)d} + \frac{1}{g_i} \left(-\varphi_i^T \hat{\theta}_i - \psi_i - \hat{\delta}_i \tanh\left(\frac{S_i}{\varepsilon_i}\right) + \dot{x}_{id} - K_i S_i \right) - g_i S_i \right) \quad (4.11)$$

Step n : Define the n^{th} surface error as $S_n = x_n - x_{nd}$, then, the time derivative of S_n is obtained as:

$$\dot{S}_n = \dot{x}_n - \dot{x}_{nd} = g_n u + \varphi_n^T \theta_n + \psi_n + d_n(t) - \dot{x}_{nd} \quad (4.12)$$

We choose the actual control input u to drive S_n towards zero with,

$$u = \frac{1}{g_n} \left(-\varphi_n^T \hat{\theta}_n - \psi_n - \hat{\delta}_n \tanh\left(\frac{S_n}{\varepsilon_n}\right) + \dot{x}_{nd} - K_n S_n \right) \quad (4.13)$$

where, K_n is a positive design parameter, ε_n is a small positive constant and $\tanh\left(\frac{S_n}{\varepsilon_n}\right)$ is an hyperbolic tangent function. The direct adaptive laws for $\hat{\theta}_i$ are given by [Yip98]:

$$\begin{aligned} \dot{\hat{\theta}}_1 &= \Gamma_1 S_1 \varphi_1 \\ \dot{\hat{\theta}}_i &= \Gamma_i S_i \varphi_i, i = 2, \dots, n-1 \\ \dot{\hat{\theta}}_n &= \Gamma_n S_n \varphi_n \end{aligned} \quad (4.14)$$

The direct adaptive laws for $\hat{\delta}_i$ are given by:

$$\dot{\hat{\delta}}_i = \gamma_i S_i \tanh\left(\frac{S_i}{\varepsilon_i}\right) \quad (4.15)$$

where, $\Gamma_i > 0$, $\gamma_i > 0$, $i = 1, \dots, n$ are design parameters that can be adjusted for the rate of convergence of the parameter estimates and $\varepsilon_i > 0$ are a small constants.

4.2.1 Stability analysis

Define the boundary layer errors as [Yip98]:

$$y_i = x_{id} - \bar{x}_i, i = 2, \dots, n \quad (4.16)$$

and the parameter estimation errors as:

$$\tilde{\theta}_i = \theta_i - \hat{\theta}_i, i = 1, 2, \dots, n \quad (4.17)$$

and,

$$\tilde{\delta}_i = \delta_i - \hat{\delta}_i, i = 1, 2, \dots, n \quad (4.18)$$

Then, the closed-loop dynamics can be expressed in terms of the surface errors S_i , the boundary layer errors y_i , and the parameter estimation errors $\tilde{\theta}_i$ and $\tilde{\delta}_i$.

The dynamics of the surface errors are expressed, for $i=1$, as:

$$\begin{aligned} \dot{S}_1 &= \dot{x}_1 - \dot{x}_{1d} = g_1 x_2 + \varphi_1^T \theta_1 + \psi_1 + d_1(t) - \dot{x}_{1d} \\ &= g_1 S_2 + g_1 x_{2d} + \varphi_1^T \theta_1 + \psi_1 + d_1(t) - \dot{x}_{1d} \\ &= g_1 S_2 + g_1 y_2 + g_1 \bar{x}_2 + \varphi_1^T \theta_1 + \psi_1 + d_1(t) - \dot{x}_{1d} \\ &= g_1 S_2 + g_1 y_2 - K_1 S_1 + \varphi_1^T \tilde{\theta}_1 + d_1(t) - \hat{\delta}_1 \tanh\left(\frac{S_1}{\varepsilon_1}\right) - g_1^2 S_1 \end{aligned} \quad (4.19)$$

For $i = 2, \dots, n-1$:

$$\begin{aligned} \dot{S}_i &= \dot{x}_i - \dot{x}_{id} = g_i x_{i+1} + \varphi_i^T \theta_i + \psi_i + d_i(t) - \dot{x}_{id} \\ &= g_i S_{i+1} + g_i x_{(i+1)d} + \varphi_i^T \theta_i + \psi_i + d_i(t) - \dot{x}_{id} \\ &= g_i S_{i+1} + g_i y_{i+1} + g_i \bar{x}_{i+1} + \varphi_i^T \theta_i + \psi_i + d_i(t) - \dot{x}_{id} \\ &= g_i S_{i+1} + g_i y_{i+1} - K_i S_i + \varphi_i^T \tilde{\theta}_i + d_i(t) - \hat{\delta}_i \tanh\left(\frac{S_i}{\varepsilon_i}\right) - g_i^2 S_i \end{aligned} \quad (4.20)$$

For $i = n$:

$$\begin{aligned} \dot{S}_n &= \dot{x}_n - \dot{x}_{nd} = g_n u + \varphi_n^T \theta_n + \psi_n + d_n(t) - \dot{x}_{nd} \\ &= -K_n S_n + \varphi_n^T \tilde{\theta}_n + d_n(t) - \hat{\delta}_n \tanh\left(\frac{S_n}{\varepsilon_n}\right) \end{aligned} \quad (4.21)$$

The dynamics of the boundary layer errors y_i are expressed, for $i = 2$, as:

$$\begin{aligned} \dot{y}_2 &= \dot{x}_{2d} - \dot{\bar{x}}_2 = \frac{1}{\tau_2} \left(-x_{2d} + \frac{1}{g_1} \left(-\varphi_1^T \hat{\theta}_1 - \psi_1 - \hat{\delta}_1 \tanh\left(\frac{S_1}{\varepsilon_1}\right) + \dot{x}_{1d} - K_1 S_1 \right) - g_1 S_1 \right) - \dot{\bar{x}}_2 \\ &= \frac{1}{\tau_2} (-x_{2d} + \bar{x}_2) - \dot{\bar{x}}_2 = \frac{1}{\tau_2} (-y_2 - \bar{x}_2 + \bar{x}_2) - \dot{\bar{x}}_2 = -\frac{1}{\tau_2} y_2 - \dot{\bar{x}}_2 \end{aligned} \quad (4.22)$$

For $i = 3, \dots, n$:

$$\begin{aligned}\dot{y}_i &= \dot{x}_{id} - \dot{\bar{x}}_i = \frac{1}{\tau_i} \left(-x_{id} + \frac{1}{g_{i-1}} \left(-\varphi_{i-1}^T \hat{\theta}_{i-1} - \psi_{i-1} - \hat{\delta}_{i-1} \tanh \left(\frac{S_{i-1}}{\varepsilon_{i-1}} \right) + \dot{x}_{(i-1)d} - K_{i-1} S_{i-1} \right) - g_{i-1} S_{i-1} \right) - \dot{\bar{x}}_i \\ &= \frac{1}{\tau_i} (-x_{id} + \bar{x}_i) - \dot{\bar{x}}_i = \frac{1}{\tau_i} (-y_i - \bar{x}_i + \bar{x}_i) - \dot{\bar{x}}_i = -\frac{1}{\tau_i} y_i - \dot{\bar{x}}_i\end{aligned}\quad (4.23)$$

We consider the following Lyapunov function as:

$$V = \sum_{i=1}^n V_{is} + \sum_{i=2}^n V_{iy} + \sum_{i=1}^n V_{i\theta} + \sum_{i=1}^n V_{i\delta} \quad (4.24)$$

where,

$$V_{is} = \frac{1}{2} S_i^2, V_{iy} = \frac{1}{2} y_i^2, V_{i\theta} = \frac{1}{2} \tilde{\theta}_i^T \Gamma_i^{-1} \tilde{\theta}_i, V_{i\delta} = \frac{1}{2\gamma_i} \tilde{\delta}_i^2 \quad (4.25)$$

Then, for $i=1, \dots, n-1$, by some simple computations, one has,

$$\dot{V}_{is} = S_i \dot{S}_i = g_i S_i S_{i+1} + g_i S_i y_{i+1} - K_i S_i^2 + S_i \varphi_i^T \tilde{\theta}_i + S_i d_i(t) - S_i \hat{\delta}_i \tanh \left(\frac{S_i}{\varepsilon_i} \right) - g_i^2 S_i^2 \quad (4.26)$$

Applying of Young's inequalities (3.23) and (3.24), and, applying the following inequality:

$$S_i d_i(t) \leq |S_i| \delta_i \quad (4.27)$$

We obtain:

$$\dot{V}_{is} \leq -K_i S_i^2 + \frac{1}{2} S_{i+1}^2 + \frac{1}{2} y_{i+1}^2 + S_i \varphi_i^T \tilde{\theta}_i + |S_i| \delta_i - S_i \hat{\delta}_i \tanh \left(\frac{S_i}{\varepsilon_i} \right) \quad (4.28)$$

and, for $i=n$:

$$\dot{V}_{ns} = S_n \dot{S}_n = -K_n S_n^2 + S_n \varphi_n^T \tilde{\theta}_n + S_n d_n(t) - S_n \hat{\delta}_n \tanh \left(\frac{S_n}{\varepsilon_n} \right) \quad (4.29)$$

Applying of the following inequality:

$$S_n d_n(t) \leq |S_n| \delta_n \quad (4.30)$$

We obtain:

$$\dot{V}_{ns} \leq -K_n S_n^2 + S_n \varphi_n^T(x) \tilde{\theta}_n + |S_n| \delta_n - S_n \hat{\delta}_n \tanh \left(\frac{S_n}{\varepsilon_n} \right) \quad (4.31)$$

one has, $\dot{x}_1 = \dot{S}_1 + \dot{x}_{1d}$ and $\dot{x}_i = \dot{S}_i + y_i + \dot{\bar{x}}_i$, then from,

$$\begin{aligned}\dot{\bar{x}}_2 &= \frac{1}{g_1} \left(- \left(\frac{\partial \varphi_1^T}{\partial x_1} \dot{x}_1 \right) \hat{\theta}_1 - \varphi_1^T \dot{\hat{\theta}}_1 - \frac{\partial \psi_1}{\partial x_1} \dot{x}_1 - \dot{\hat{\delta}}_1 \tanh \left(\frac{S_1}{\varepsilon_1} \right) \right. \\ &\quad \left. - \left\{ \hat{\delta}_1 \left(\frac{\partial \left[\tanh \left(\frac{S_1}{\varepsilon_1} \right) \right]}{\partial S_1} \right) + K_1 \right\} \dot{S}_1 + \ddot{x}_{1d} \right) - g_1 \dot{S}_1 - \left(\frac{\partial g_1}{\partial x_1} \dot{x}_1 \right) S_1\end{aligned}\quad (4.32)$$

and, by induction, it is easy from:

$$\begin{aligned} \dot{\hat{x}}_i &= \frac{1}{g_{i-1}} \left(- \left(\sum_{j=1}^{i-1} \frac{\partial \varphi_{i-1}^T}{\partial x_j} \dot{x}_j \right) \hat{\theta}_{i-1} - \varphi_{i-1}^T \dot{\hat{\theta}}_{i-1} - \sum_{j=1}^{i-1} \frac{\partial \psi_{i-1}}{\partial x_j} \dot{x}_j - \hat{\delta}_{i-1} \tanh \left(\frac{S_{i-1}}{\varepsilon_{i-1}} \right) \right. \\ &\quad \left. - \left\{ \hat{\delta}_{i-1} \left(\frac{\partial \left[\tanh \left(\frac{S_{i-1}}{\varepsilon_{i-1}} \right) \right]}{\partial S_{i-1}} \right) + K_{i-1} \right\} \dot{S}_{i-1} + \ddot{x}_{(i-1)d} \right) - g_{i-1} \dot{S}_{i-1} - \left(\sum_{j=1}^{i-1} \frac{\partial g_{i-1}}{\partial x_j} \dot{x}_j \right) S_{i-1} \end{aligned} \quad (4.33)$$

one has,

$$\begin{aligned} \dot{y}_2 &= -\frac{1}{\tau_2} y_2 + \frac{1}{g_1} \left(\left(\frac{\partial \varphi_1^T}{\partial x_1} \dot{x}_1 \right) \hat{\theta}_1 + \varphi_1^T \dot{\hat{\theta}}_1 + \frac{\partial \psi_1}{\partial x_1} \dot{x}_1 + \hat{\delta}_1 \tanh \left(\frac{S_1}{\varepsilon_1} \right) \right. \\ &\quad \left. + \left\{ \hat{\delta}_1 \left(\frac{\partial \left[\tanh \left(\frac{S_1}{\varepsilon_1} \right) \right]}{\partial S_1} \right) + K_1 \right\} \dot{S}_1 - \ddot{x}_{1d} \right) + g_1 \dot{S}_1 + \left(\frac{\partial g_1}{\partial x_1} \dot{x}_1 \right) S_1 \end{aligned} \quad (4.34)$$

Since all terms in (4.34) can be dominated by some continuous functions, it follows that:

$$\dot{y}_2 + \frac{1}{\tau_2} y_2 \leq \left| \dot{y}_2 + \frac{1}{\tau_2} y_2 \right| \leq B_2 \left(S_1, S_2, y_2, \hat{\theta}_1, \hat{\delta}_1, x_{1d}, \dot{x}_{1d}, \ddot{x}_{1d} \right) \quad (4.35)$$

where, $B_2(\cdot)$ is a continuous function. Thus,

$$y_2 \dot{y}_2 + \frac{1}{\tau_2} y_2^2 \leq B_2(\cdot) |y_2| \quad (4.36)$$

By using Young's inequality, it gives:

$$y_2 \dot{y}_2 \leq -\frac{1}{\tau_2} y_2^2 + \frac{y_2^2}{2} + \frac{B_2^2(\cdot)}{2} \quad (4.37)$$

as similarly for, $i = 3, \dots, n$, we obtain:

$$y_n \dot{y}_n \leq -\frac{1}{\tau_n} y_n^2 + \frac{y_n^2}{2} + \frac{B_n^2(\cdot)}{2} \quad (4.38)$$

where, $B_n(\cdot) = B_n(S_1 \cdots S_n, y_2 \cdots y_n, \hat{\theta}_1 \cdots \hat{\theta}_n, x_{1d}, \dot{x}_{1d}, \ddot{x}_{1d})$ is a continuous function. From

(4.37) and (4.38), we can write:

$$\dot{V}_{iy} \leq -\frac{1}{\tau_i} y_i^2 + \frac{y_i^2}{2} + \frac{B_i^2(\cdot)}{2}, i = 2, \dots, n \quad (4.39)$$

one has,

$$\dot{V}_{i\theta} = \tilde{\theta}_i^T \Gamma_i^{-1} \dot{\tilde{\theta}}_i = -\tilde{\theta}_i^T \Gamma_i^{-1} \dot{\tilde{\theta}}_i = -\tilde{\theta}_i^T S_i \varphi_i \quad (4.40)$$

and, we have:

$$\dot{V}_{i\delta} = \frac{1}{\gamma_i} \tilde{\delta}_i \dot{\tilde{\delta}}_i = -\frac{1}{\gamma_i} \tilde{\delta}_i \dot{\tilde{\delta}}_i = -\tilde{\delta}_i S_i \tanh\left(\frac{S_i}{\varepsilon_i}\right) \quad (4.41)$$

Therefore, the derivative of the Lyapunov function \dot{V} becomes:

$$\begin{aligned} \dot{V} &= \sum_{i=1}^n \dot{V}_{is} + \sum_{i=2}^n \dot{V}_{iy} + \sum_{i=1}^n \dot{V}_{i\theta} + \sum_{i=1}^n \dot{V}_{i\delta} \\ &\leq \sum_{i=1}^{n-1} \left(-K_i S_i^2 + \frac{1}{2} S_{i+1}^2 + \frac{1}{2} y_{i+1}^2 + S_i \varphi_i^T \tilde{\theta}_i + |S_i| \delta_i - S_i \hat{\delta}_i \tanh\left(\frac{S_i}{\varepsilon_i}\right) \right) - K_n S_n^2 + S_n \varphi_n^T \tilde{\theta}_n + \delta_n |S_n| \\ &\quad - S_n \hat{\delta}_n \tanh\left(\frac{S_n}{\varepsilon_n}\right) + \sum_{i=2}^n \left(-\frac{1}{\tau_i} y_i^2 + \frac{y_i^2}{2} + \frac{B_i^2(\cdot)}{2} \right) - \sum_{i=1}^n \tilde{\theta}_i^T S_i \varphi_i - \sum_{i=1}^n \left(\tilde{\delta}_i S_i \tanh\left(\frac{S_i}{\varepsilon_i}\right) \right) \\ &\leq -K_1 S_1^2 - \sum_{i=2}^{n-1} \left(K_i - \frac{1}{2} \right) S_i^2 - \left(K_n - \frac{1}{2} \right) S_n^2 + \sum_{i=1}^n \left(|S_i| \delta_i - S_i \hat{\delta}_i \tanh\left(\frac{S_i}{\varepsilon_i}\right) \right) \\ &\quad - \sum_{i=2}^n \left(\frac{1}{\tau_i} - 1 \right) y_i^2 + \sum_{i=2}^n \frac{B_i^2(\cdot)}{2} - \sum_{i=1}^n \left(\tilde{\delta}_i S_i \tanh\left(\frac{S_i}{\varepsilon_i}\right) \right) \\ &\leq -K_1 S_1^2 - \sum_{i=2}^{n-1} \left(K_i - \frac{1}{2} \right) S_i^2 - \left(K_n - \frac{1}{2} \right) S_n^2 - \sum_{i=2}^n \left(\frac{1}{\tau_i} - 1 \right) y_i^2 + \varphi + \sum_{i=1}^n \left(|S_i| \delta_i - S_i \hat{\delta}_i \tanh\left(\frac{S_i}{\varepsilon_i}\right) \right) \end{aligned} \quad (4.42)$$

From lemma 4.2.1, it is easy to show that:

$$|S_i| \delta_i - S_i \hat{\delta}_i \tanh\left(\frac{S_i}{\varepsilon_i}\right) \leq \delta_i \kappa \varepsilon_i = \delta_i \bar{\varepsilon}_i \quad (4.43)$$

Substituting (4.43) into (4.42) yields to:

$$\begin{aligned} \dot{V} &\leq -K_1 S_1^2 - \sum_{i=2}^{n-1} \left(K_i - \frac{1}{2} \right) S_i^2 - \left(K_n - \frac{1}{2} \right) S_n^2 - \sum_{i=2}^n \left(\frac{1}{\tau_i} - 1 \right) y_i^2 + \varphi + \sum_{i=1}^n \delta_i \bar{\varepsilon}_i \\ &\leq -K_1 S_1^2 - \sum_{i=2}^{n-1} \left(K_i - \frac{1}{2} \right) S_i^2 - \left(K_n - \frac{1}{2} \right) S_n^2 - \sum_{i=2}^n \left(\frac{1}{\tau_i} - 1 \right) y_i^2 + \mu \end{aligned} \quad (4.44)$$

where, $\varphi = \sum_{i=2}^n \frac{M_i}{2}$, M_i are the maximums of $B_i(\cdot)$, $\mu = \varphi + \sum_{i=1}^n \delta_i \bar{\varepsilon}_i$, $\bar{\varepsilon}_i = \kappa \varepsilon_i$ and

$\kappa = 0.2785$. Therefore, based on (4.44), by choosing the design parameters such that,

$K_1 > 0$, $K_i > \frac{1}{2}$, $K_n > \frac{1}{2}$ and $\tau_i < 1$, we can conclude that, S_i and y_i are bounded.

4.3 Indirect robust adaptive control

In the following, the main procedures for designing the indirect robust adaptive control with stability analysis are introduced.

4.3.1 Identification based modified x-swapping filters

In order to demonstrate the identification based modified x-swapping filters design procedures, we consider the SISO uncertain nonlinear system with external disturbances (4.1), which can be rewritten under the following nonlinear system in parametric x-model form as:

$$\dot{x}_i = f_i(x, u) + \varphi_i^T(\bar{x}_i)\theta_i + d_i(t) \quad (4.45)$$

where,

$$f_i(x, u) = \begin{bmatrix} g_1 x_2 + \psi_1 \\ \vdots \\ g_{n-1} x_n + \psi_{n-1} \\ g_n u + \psi_n \end{bmatrix} \quad (4.46)$$

We introduce the following modified x-swapping filters as:

$$\dot{\Omega}_{0i} = a_i(\Omega_{0i} + x_i) - f_i(x, u) - \hat{\delta}_i \text{sign}(\tilde{\epsilon}_i), \Omega_{0i} \in \mathbb{R} \quad (4.47)$$

$$\dot{\Omega}_i^T = a_i \Omega_i^T + \varphi_i^T(\bar{x}_i), \Omega_i \in \mathbb{R}^{p_i} \quad (4.48)$$

where, $i=1, \dots, n$, $\hat{\delta}_i$ denote the estimates of δ_i , $\tilde{\epsilon}_i$ is given in (4.50) and $a_i < 0$ is a negative definite scalar function for each x continuous in t . We define the estimation errors as:

$$\epsilon_i = x_i + \Omega_{0i} - \Omega_i^T \hat{\theta}_i, \epsilon_i \in \mathbb{R} \quad (4.49)$$

with, $\hat{\theta}_i$ the estimate of θ_i and let:

$$\tilde{\epsilon}_i = x_i + \Omega_{0i} - \Omega_i^T \theta_i, \tilde{\epsilon}_i \in \mathbb{R} \quad (4.50)$$

We obtain:

$$\epsilon_i = \Omega_i^T \tilde{\theta}_i + \tilde{\epsilon}_i \quad (4.51)$$

The dynamics of $\tilde{\epsilon}_i$ are governed by:

$$\dot{\tilde{\epsilon}}_i = \dot{x}_i + \dot{\Omega}_{0i} - \dot{\Omega}_i^T \theta_i = a_i \tilde{\epsilon}_i + d_i(t) - \hat{\delta}_i \text{sign}(\tilde{\epsilon}_i) \quad (4.52)$$

To guarantee the boundedness of Ω_i when $\varphi_i(\bar{x}_i)$ grows unbounded, a particular choice of a_i is made:

$$a_i = a_{0i} - \lambda_i \varphi_i^T(\bar{x}_i) \varphi_i(\bar{x}_i) P_i \quad (4.53)$$

where, $\lambda_i > 0$ and a_{0i} is an arbitrary negative constant satisfying [Sou18]:

$$2P_i a_{0i} = -1, P_i > 0 \quad (4.54)$$

4.3.2 Choice of adaptive laws

The gradient adaptive laws are given by:

$$\dot{\hat{\theta}}_i = \Gamma_i \frac{\Omega_i \epsilon_i}{1 + \nu_i \text{tr}\{\Omega_i^T \Omega_i\}}, \Gamma_i > 0, \nu_i \geq 0 \quad (4.55)$$

The least squares adaptive laws are given by:

$$\dot{\hat{\theta}}_i = \Gamma_i \frac{\Omega_i \epsilon_i}{1 + \nu_i \text{tr}\{\Omega_i^T \Gamma_i \Omega_i\}} \quad (4.56)$$

where, Γ_i is defined as:

$$\dot{\Gamma}_i = -\Gamma_i \frac{\Omega_i \Omega_i^T}{1 + \nu_i \text{tr}\{\Omega_i^T \Gamma_i \Omega_i\}} \Gamma_i, \Gamma(0) > 0, \nu_i \geq 0 \quad (4.57)$$

4.3.3 Proof of stability

Lemma 4.3.1: To establish the identifier properties, let $[0, t_f)$, the maximal interval of existence of solutions of (4.45), the modified x-swapping filters (4.47) and (4.48), and the gradient adaptive laws (4.55) or the least squares adaptive laws (4.56) and (4.57). Then for $\nu_i \geq 0$, the following properties hold:

$$\tilde{\theta}_i, \tilde{\delta}_i \in L_\infty \quad (4.58)$$

$$\epsilon_i \in L_2 \cap L_\infty \quad (4.59)$$

$$\dot{\hat{\theta}}_i, \dot{\hat{\delta}}_i \in L_2 \cap L_\infty \quad (4.60)$$

4.3.3.1 Gradient adaptive laws

The Lyapunov function is chosen as follows:

$$V_i = \frac{1}{2} \tilde{\theta}_i^T \Gamma_i^{-1} \tilde{\theta}_i + P_i \tilde{\epsilon}_i^2 + \frac{1}{2\gamma_i} \tilde{\delta}_i^2 \quad (4.61)$$

where, $\tilde{\theta}_i = \theta_i - \hat{\theta}_i$ and $\tilde{\delta}_i = \delta_i - \hat{\delta}_i$ are the parameter estimation errors, and $\gamma_i > 0$ is an adaptive gain.

Then, along the dynamic equations (4.52) and (4.55), the derivative of the Lyapunov function \dot{V}_i becomes:

$$\begin{aligned}
\dot{V}_i &= \tilde{\theta}_i^T \Gamma_i^{-1} \dot{\tilde{\theta}}_i + 2P_i \tilde{\epsilon}_i \dot{\tilde{\epsilon}}_i - \frac{1}{\gamma_i} \tilde{\delta}_i \dot{\hat{\delta}}_i \\
&= \tilde{\theta}_i^T \Gamma_i^{-1} \dot{\tilde{\theta}}_i + 2P_i a_i \tilde{\epsilon}_i^2 + 2P_i \tilde{\epsilon}_i d_i(t) - 2P_i \tilde{\epsilon}_i \hat{\delta}_i \text{sign}(\tilde{\epsilon}_i) - \frac{1}{\gamma_i} \tilde{\delta}_i \dot{\hat{\delta}}_i \\
&= \tilde{\theta}_i^T \Gamma_i^{-1} \dot{\tilde{\theta}}_i + 2P_i (a_{0i} - \lambda_i \varphi_i^T(\bar{x}_i) \varphi_i(\bar{x}_i) P_i) \tilde{\epsilon}_i^2 + 2P_i \tilde{\epsilon}_i d_i(t) - 2P_i \tilde{\epsilon}_i \hat{\delta}_i \text{sign}(\tilde{\epsilon}_i) - \frac{1}{\gamma_i} \tilde{\delta}_i \dot{\hat{\delta}}_i \\
&= \tilde{\theta}_i^T \Gamma_i^{-1} \dot{\tilde{\theta}}_i + (-1 - 2\lambda_i P_i \varphi_i^T(\bar{x}_i) \varphi_i(\bar{x}_i) P_i) \tilde{\epsilon}_i^2 + 2P_i \tilde{\epsilon}_i d_i(t) - 2P_i \tilde{\epsilon}_i \hat{\delta}_i \text{sign}(\tilde{\epsilon}_i) - \frac{1}{\gamma_i} \tilde{\delta}_i \dot{\hat{\delta}}_i
\end{aligned} \tag{4.62}$$

Applying of inequality (3.55) and the following inequality:

$$\tilde{\epsilon}_i d_i(t) \leq |\tilde{\epsilon}_i| \delta_i \tag{4.63}$$

We obtain:

$$\dot{V}_i \leq -\tilde{\theta}_i^T \Gamma_i^{-1} \dot{\tilde{\theta}}_i - \tilde{\epsilon}_i^2 + 2P_i |\tilde{\epsilon}_i| \delta_i - 2P_i \tilde{\epsilon}_i \hat{\delta}_i \text{sign}(\tilde{\epsilon}_i) - \frac{1}{\gamma_i} \tilde{\delta}_i \dot{\hat{\delta}}_i \tag{4.64}$$

We choose the adaptive laws for $\hat{\delta}_i$ as:

$$\dot{\hat{\delta}}_i = 2\gamma_i P_i \tilde{\epsilon}_i \text{sign}(\tilde{\epsilon}_i) \tag{4.65}$$

Substituting (4.65) into (4.64), we obtain:

$$\begin{aligned}
\dot{V}_i &\leq -\tilde{\theta}_i^T \Gamma_i^{-1} \dot{\tilde{\theta}}_i - \tilde{\epsilon}_i^2 + 2P_i |\tilde{\epsilon}_i| \delta_i - 2P_i \tilde{\epsilon}_i \hat{\delta}_i \text{sign}(\tilde{\epsilon}_i) - 2P_i \tilde{\delta}_i \tilde{\epsilon}_i \text{sign}(\tilde{\epsilon}_i) \\
&= -\frac{\tilde{\theta}_i^T \Omega_i \epsilon_i}{1 + \nu_i \text{tr}\{\Omega_i^T \Omega_i\}} - \tilde{\epsilon}_i^2 + 2P_i |\tilde{\epsilon}_i| \delta_i - 2P_i \tilde{\delta}_i \tilde{\epsilon}_i \text{sign}(\tilde{\epsilon}_i) \\
&= -\frac{\epsilon_i^2}{1 + \nu_i \text{tr}\{\Omega_i^T \Omega_i\}} + \frac{\epsilon_i}{1 + \nu_i \text{tr}\{\Omega_i^T \Omega_i\}} \tilde{\epsilon}_i - \tilde{\epsilon}_i^2 + 2P_i |\tilde{\epsilon}_i| \delta_i - 2P_i \tilde{\delta}_i |\tilde{\epsilon}_i| \\
&\leq -\frac{3}{4} \frac{\epsilon_i^2}{1 + \nu_i \text{tr}\{\Omega_i^T \Omega_i\}} - \frac{1}{4} \frac{\epsilon_i^2}{(1 + \nu_i \text{tr}\{\Omega_i^T \Omega_i\})^2} + \frac{\epsilon_i}{1 + \nu_i \text{tr}\{\Omega_i^T \Omega_i\}} \tilde{\epsilon}_i - \tilde{\epsilon}_i^2 \\
&= -\frac{3}{4} \frac{\epsilon_i^2}{1 + \nu_i \text{tr}\{\Omega_i^T \Omega_i\}} - \left(\frac{\epsilon_i}{2(1 + \nu_i \text{tr}\{\Omega_i^T \Omega_i\})} - \tilde{\epsilon}_i \right)^2 \\
&\leq -\frac{3}{4} \frac{\epsilon_i^2}{1 + \nu_i \text{tr}\{\Omega_i^T \Omega_i\}}
\end{aligned} \tag{4.66}$$

The nonpositivity of \dot{V}_i proves that, $\tilde{\theta}_i \in L_\infty$ and $\tilde{\delta}_i \in L_\infty$ (bounded). Due to $\epsilon_i = \Omega_i^T \tilde{\theta}_i + \tilde{\epsilon}_i$ and the boundedness of Ω_i , it follows that $\epsilon_i \in L_\infty$, which, in turn proves that $\hat{\theta}_i \in L_\infty$ and $\hat{\delta}_i \in L_\infty$.

By integrating of inequality (4.66) over $[0, \infty]$, we obtain:

$$\int_0^{\infty} \frac{\epsilon_i^2}{1 + \nu_i \text{tr}\{\Omega_i^T \Omega_i\}} d\tau \leq \frac{4}{3} (V_i(0) - V_i(\infty)) < \infty \quad (4.67)$$

This means that, $\frac{\epsilon_i}{\sqrt{1 + \nu_i \text{tr}\{\Omega_i^T \Omega_i\}}} \in L_2$. Since Ω_i is bounded, then $\epsilon_i \in L_2$. The

boundedness of Ω_i and the square integrability of ϵ_i prove that $\dot{\hat{\theta}}_i \in L_2$ and $\dot{\hat{\delta}}_i \in L_2$.

4.3.3.2 Least squares adaptive laws

From (4.56) and (4.57), we have the following identity:

$$\frac{d}{dt}(\Gamma_i^{-1}) = -\Gamma_i^{-1} \dot{\Gamma}_i \Gamma_i^{-1} = \frac{\Omega_i \Omega_i^T}{1 + \nu_i \text{tr}\{\Omega_i^T \Gamma_i \Omega_i\}} \geq 0 \quad (4.68)$$

We consider the following Lyapunov function as:

$$V_i = \tilde{\theta}_i^T \Gamma_i^{-1}(t) \tilde{\theta}_i + P_i \tilde{\epsilon}_i^2 + \frac{1}{2\gamma_i} \tilde{\delta}_i^2 \quad (4.69)$$

Along the dynamic equations (4.52), (4.56) and (4.57), the derivative of the Lyapunov function \dot{V}_i becomes:

$$\begin{aligned} \dot{V}_i &= \dot{\tilde{\theta}}_i^T \Gamma_i^{-1} \tilde{\theta}_i + \tilde{\theta}_i^T \frac{d}{dt}(\Gamma_i^{-1} \tilde{\theta}_i) + 2P_i \tilde{\epsilon}_i \dot{\tilde{\epsilon}}_i - \frac{1}{\gamma_i} \tilde{\delta}_i \dot{\tilde{\delta}}_i \\ &= \dot{\tilde{\theta}}_i^T \Gamma_i^{-1} \tilde{\theta}_i - \tilde{\theta}_i^T \Gamma_i^{-1} \dot{\Gamma}_i \Gamma_i^{-1} \tilde{\theta}_i - \tilde{\theta}_i^T \Gamma_i^{-1} \dot{\tilde{\theta}}_i + 2P_i a_i \tilde{\epsilon}_i^2 + 2P_i \tilde{\epsilon}_i d_i(t) - 2P_i \tilde{\epsilon}_i \hat{\delta}_i \text{sign}(\tilde{\epsilon}_i) - \frac{1}{\gamma_i} \tilde{\delta}_i \dot{\tilde{\delta}}_i \\ &= \dot{\tilde{\theta}}_i^T \Gamma_i^{-1} \tilde{\theta}_i - \tilde{\theta}_i^T \Gamma_i^{-1} \dot{\Gamma}_i \Gamma_i^{-1} \tilde{\theta}_i - \tilde{\theta}_i^T \Gamma_i^{-1} \dot{\tilde{\theta}}_i + 2P_i (a_{0i} - \lambda_i \phi_i^T(\bar{x}_i) \phi_i(\bar{x}_i) P_i) \tilde{\epsilon}_i^2 + 2P_i \tilde{\epsilon}_i d_i(t) - 2P_i \tilde{\epsilon}_i \hat{\delta}_i \text{sign}(\tilde{\epsilon}_i) - \frac{1}{\gamma_i} \tilde{\delta}_i \dot{\tilde{\delta}}_i \\ &= \dot{\tilde{\theta}}_i^T \Gamma_i^{-1} \tilde{\theta}_i - \tilde{\theta}_i^T \Gamma_i^{-1} \dot{\Gamma}_i \Gamma_i^{-1} \tilde{\theta}_i - \tilde{\theta}_i^T \Gamma_i^{-1} \dot{\tilde{\theta}}_i + (-1 - 2\lambda_i P_i \phi_i^T(\bar{x}_i) \phi_i(\bar{x}_i) P_i) \tilde{\epsilon}_i^2 + 2P_i \tilde{\epsilon}_i d_i(t) - 2P_i \tilde{\epsilon}_i \hat{\delta}_i \text{sign}(\tilde{\epsilon}_i) - \frac{1}{\gamma_i} \tilde{\delta}_i \dot{\tilde{\delta}}_i \end{aligned} \quad (4.70)$$

Applying of inequalities (3.55) and (4.63), we obtain:

$$\dot{V}_i \leq -\dot{\tilde{\theta}}_i^T \Gamma_i^{-1} \tilde{\theta}_i - \tilde{\theta}_i^T \Gamma_i^{-1} \dot{\Gamma}_i \Gamma_i^{-1} \tilde{\theta}_i - \tilde{\theta}_i^T \Gamma_i^{-1} \dot{\tilde{\theta}}_i - \tilde{\epsilon}_i^2 + 2P_i |\tilde{\epsilon}_i| \delta_i - 2P_i \tilde{\epsilon}_i \hat{\delta}_i \text{sign}(\tilde{\epsilon}_i) - \frac{1}{\gamma_i} \tilde{\delta}_i \dot{\tilde{\delta}}_i \quad (4.71)$$

We choose the adaptive laws for $\hat{\delta}_i$ described by (4.65) and substituting (4.71) into (4.70), we obtain:

$$\begin{aligned}
\dot{V}_i &\leq -\dot{\hat{\theta}}_i^T \Gamma_i^{-1} \tilde{\theta}_i - \tilde{\theta}_i^T \Gamma_i^{-1} \dot{\Gamma}_i \Gamma_i^{-1} \tilde{\theta}_i - \tilde{\theta}_i^T \Gamma_i^{-1} \dot{\hat{\theta}}_i - \tilde{\zeta}_i^2 + 2P_i |\tilde{\zeta}_i| \delta_i - 2P_i \tilde{\zeta}_i \hat{\delta}_i \text{sign}(\tilde{\zeta}_i) - 2P_i \tilde{\zeta}_i \tilde{\zeta}_i \text{sign}(\tilde{\zeta}_i) \\
&= -\dot{\hat{\theta}}_i^T \Gamma_i^{-1} \tilde{\theta}_i - \tilde{\theta}_i^T \Gamma_i^{-1} \dot{\Gamma}_i \Gamma_i^{-1} \tilde{\theta}_i - \tilde{\theta}_i^T \Gamma_i^{-1} \dot{\hat{\theta}}_i - \tilde{\zeta}_i^2 + 2P_i |\tilde{\zeta}_i| \delta_i - 2P_i \tilde{\zeta}_i \tilde{\zeta}_i \text{sign}(\tilde{\zeta}_i) \\
&= -\frac{\Omega_i^T \tilde{\theta}_i \epsilon_i}{1 + \nu_i \text{tr}\{\Omega_i^T \Gamma_i \Omega_i\}} + \frac{\tilde{\theta}_i^T \Omega_i \Omega_i^T \tilde{\theta}_i}{1 + \nu_i \text{tr}\{\Omega_i^T \Gamma_i \Omega_i\}} - \frac{\tilde{\theta}_i^T \Omega_i \epsilon_i}{1 + \nu_i \text{tr}\{\Omega_i^T \Gamma_i \Omega_i\}} - \tilde{\zeta}_i^2 + 2P_i |\tilde{\zeta}_i| \delta_i - 2P_i \tilde{\zeta}_i |\tilde{\zeta}_i| \\
&\leq -\frac{\Omega_i^T \tilde{\theta}_i \epsilon_i}{1 + \nu_i \text{tr}\{\Omega_i^T \Gamma_i \Omega_i\}} - \frac{\tilde{\theta}_i^T \Omega_i \tilde{\zeta}_i}{1 + \nu_i \text{tr}\{\Omega_i^T \Gamma_i \Omega_i\}} - \tilde{\zeta}_i^2 \\
&= -\frac{\epsilon_i^2}{1 + \nu_i \text{tr}\{\Omega_i^T \Gamma_i \Omega_i\}} + \frac{\tilde{\zeta}_i^2}{1 + \nu_i \text{tr}\{\Omega_i^T \Gamma_i \Omega_i\}} - \tilde{\zeta}_i^2 \\
&\leq -\frac{\epsilon_i^2}{1 + \nu_i \text{tr}\{\Omega_i^T \Gamma_i \Omega_i\}}
\end{aligned} \tag{4.72}$$

Which, due to the positive definiteness of $\Gamma_i^{-1}(t)$, proves that, $\tilde{\theta}_i \in L_\infty$ and $\tilde{\delta}_i \in L_\infty$ (bounded).

By integrating of inequality (4.72) over $[0, \infty]$, we obtain:

$$\int_0^\infty \frac{\epsilon_i^2}{1 + \nu_i \text{tr}\{\Omega_i^T \Gamma_i \Omega_i\}} d\tau \leq V_i(0) - V_i(\infty) < \infty \tag{4.73}$$

This means that, $\frac{\epsilon_i}{\sqrt{1 + \nu_i \text{tr}\{\Omega_i^T \Gamma_i \Omega_i\}}} \in L_2$. Using the boundedness of Γ_i and Ω_i , following

the same line of argument as for the gradient adaptive laws, we prove that $\epsilon_i \in L_2 \cap L_\infty$,

$\dot{\hat{\theta}}_i \in L_2 \cap L_\infty$ and $\dot{\hat{\delta}}_i \in L_2 \cap L_\infty$.

4.4 Composite robust adaptive dynamic surface control

In this section, the composite robust adaptive dynamic surface control is proposed, which utilizes both surface error based parameter adaptive laws of the direct robust adaptive dynamic surface control described by (4.14) and (4.15) with the estimation error based parameter adaptive laws of the indirect robust adaptive control described by (4.55), (4.56) and (4.65). The control objective of this approach is to construct a composite robust adaptive dynamic surface controller u such that the system output x_1 tracks the desired trajectory x_{1d} and to guarantee the boundedness of all signals in the closed-loop system. In the following, the main procedures for designing the composite robust adaptive dynamic surface control technique for system (4.1) with stability analysis are described.

4.4.1 Composite projection based gradient adaptive laws

Projection properties: The projection operators and the projection mapping for the adaptive laws $\hat{\theta}_i$ are similar as that in the chapter 3 described by (3.64) and (3.65).

As similarly, we assume that δ_i is estimated by $\hat{\delta}_i$, where, $\hat{\delta}_i$ are the estimates of δ_i . The estimation errors are given by:

$$\tilde{\delta}_i = \delta_i - \hat{\delta}_i \quad (4.74)$$

Therefore, the projection mapping for the adaptive laws $\hat{\delta}_i$ is similar as that in the chapter 3 described by (3.65), i.e.,

$$-\tilde{\delta}_i \text{Proj}_{\hat{\delta}_i}(\bullet_i) \leq -\tilde{\delta}_i \bullet_i \quad (4.75)$$

The composite projection based gradient adaptive laws are defined as:

$$\dot{\hat{\theta}}_i = \text{Proj}_{\hat{\theta}_i} \left(\Gamma_i \left(S_i \varphi_i + \frac{\Omega_i \epsilon_i}{1 + \nu_i \text{tr} \{ \Omega_i^T \Omega_i \}} \right) \right), \Gamma_i > 0, \nu_i \geq 0 \quad (4.76)$$

and,

$$\dot{\hat{\delta}}_i = \text{Proj}_{\hat{\delta}_i} \left(\gamma_i \left(S_i \tanh \left(\frac{S_i}{\epsilon_i} \right) + 2P_i \tilde{\epsilon}_i \text{sign}(\tilde{\epsilon}_i) \right) \right), \gamma_i > 0, \epsilon_i > 0 \quad (4.77)$$

The dynamics of estimation errors are given by:

$$\dot{\tilde{\theta}}_i = -\dot{\hat{\theta}}_i = \text{Proj}_{\hat{\theta}_i} \left(-\Gamma_i \left(S_i \varphi_i + \frac{\Omega_i \epsilon_i}{1 + \nu_i \text{tr} \{ \Omega_i^T \Omega_i \}} \right) \right), \Gamma_i > 0, \nu_i \geq 0 \quad (4.78)$$

and,

$$\dot{\tilde{\delta}}_i = -\dot{\hat{\delta}}_i = \text{Proj}_{\hat{\delta}_i} \left(-\gamma_i \left(S_i \tanh \left(\frac{S_i}{\epsilon_i} \right) + 2P_i \tilde{\epsilon}_i \text{sign}(\tilde{\epsilon}_i) \right) \right), \gamma_i > 0, \epsilon_i > 0 \quad (4.79)$$

where, $\epsilon_i = x_i + \Omega_{0i} - \Omega_i^T \hat{\theta}_i$ and $\tilde{\epsilon}_i = x_i + \Omega_{0i} - \Omega_i^T \theta_i$.

Theorem 4.4.1: Consider the SISO uncertain nonlinear system in lower triangular form with external disturbances composed of the plant described by state space form (4.1). Suppose that assumptions 4.2.1-4.2.3 are satisfied. Then, the virtual controllers (4.5) and (4.9), the actual control input (4.13) and the composite projection based gradient adaptive laws (4.76) and (4.77) guarantee that all signals in the closed-loop system are bounded.

Proof: We consider the following Lyapunov function as:

$$V = \sum_{i=1}^n V_{is} + \sum_{i=2}^n V_{iy} + \sum_{i=1}^n V_i \quad (4.80)$$

and,

$$V_{is} = \frac{1}{2} S_i^2, V_{iy} = \frac{1}{2} y_i^2, V_i = \frac{1}{2} \tilde{\theta}_i^T \Gamma_i^{-1} \tilde{\theta}_i + P_i \tilde{\epsilon}_i^2 + \frac{1}{2\gamma_i} \tilde{\delta}_i^2 \quad (4.81)$$

where, \dot{V}_{is} , \dot{V}_{ns} and \dot{V}_i are expressed in (4.28), (4.31), (4.39), and,

$$\begin{aligned} \dot{V}_i &= -\tilde{\theta}_i^T \Gamma_i^{-1} \dot{\tilde{\theta}}_i - \tilde{\epsilon}_i^2 + 2P_i |\tilde{\epsilon}_i| \delta_i - 2P_i \tilde{\epsilon}_i \hat{\delta}_i \text{sign}(\tilde{\epsilon}_i) - \frac{1}{\gamma_i} \tilde{\delta}_i \dot{\tilde{\delta}}_i \\ &= -\tilde{\theta}_i^T \Gamma_i^{-1} \text{Proj}_{\tilde{\theta}_i} \left(\Gamma_i \left(S_i \varphi_i + \frac{\Omega_i \epsilon_i}{1 + \nu_i \text{tr} \{ \Omega_i^T \Omega_i \}} \right) \right) - \tilde{\epsilon}_i^2 + 2P_i |\tilde{\epsilon}_i| \delta_i \\ &\quad - 2P_i \tilde{\epsilon}_i \hat{\delta}_i \text{sign}(\tilde{\epsilon}_i) - \frac{1}{\gamma_i} \tilde{\delta}_i \text{Proj}_{\tilde{\delta}_i} \left(\gamma_i \left(S_i \tanh \left(\frac{S_i}{\epsilon_i} \right) + 2P_i \tilde{\epsilon}_i \text{sign}(\tilde{\epsilon}_i) \right) \right) \\ &\leq -\tilde{\theta}_i^T S_i \varphi_i - \frac{\tilde{\theta}_i^T \Omega_i \epsilon_i}{1 + \nu_i \text{tr} \{ \Omega_i^T \Omega_i \}} - \tilde{\epsilon}_i^2 - \tilde{\delta}_i S_i \tanh \left(\frac{S_i}{\epsilon_i} \right) \end{aligned} \quad (4.82)$$

Therefore, the derivative of the Lyapunov function \dot{V} becomes:

$$\begin{aligned} \dot{V} &= \sum_{i=1}^n \dot{V}_{is} + \sum_{i=2}^n \dot{V}_{iy} + \sum_{i=1}^n \dot{V}_i \\ &\leq \sum_{i=1}^{n-1} \left(-K_i S_i^2 + \frac{1}{2} S_{i+1}^2 + \frac{1}{2} y_{i+1}^2 + S_i \varphi_i^T \tilde{\theta}_i + |S_i| \delta_i - S_i \hat{\delta}_i \tanh \left(\frac{S_i}{\epsilon_i} \right) \right) \\ &\quad - K_n S_n^2 + S_n \varphi_n^T \tilde{\theta}_n + |S_n| \delta_n - S_n \hat{\delta}_n \tanh \left(\frac{S_n}{\epsilon_n} \right) + \sum_{i=2}^n \left(-\frac{1}{\tau_i} y_i^2 + \frac{y_i^2}{2} + \frac{B_i^2(\cdot)}{2} \right) \\ &\quad - \sum_{i=1}^n \tilde{\theta}_i^T S_i \varphi_i - \sum_{i=1}^n \frac{\tilde{\theta}_i^T \Omega_i \epsilon_i}{1 + \nu_i \text{tr} \{ \Omega_i^T \Omega_i \}} - \sum_{i=1}^n \tilde{\epsilon}_i^2 - \sum_{i=1}^n \left(\tilde{\delta}_i S_i \tanh \left(\frac{S_i}{\epsilon_i} \right) \right) \\ &\leq -K_1 S_1^2 - \sum_{i=2}^{n-1} \left(K_i - \frac{1}{2} \right) S_i^2 - \left(K_n - \frac{1}{2} \right) S_n^2 + \sum_{i=1}^n \left(|S_i| \delta_i - S_i \hat{\delta}_i \tanh \left(\frac{S_i}{\epsilon_i} \right) \right) \\ &\quad - \sum_{i=2}^n \left(\frac{1}{\tau_i} - 1 \right) y_i^2 + \sum_{i=2}^n \frac{B_i^2(\cdot)}{2} - \frac{3}{4} \sum_{i=1}^n \frac{\epsilon_i^2}{1 + \nu_i \text{tr} \{ \Omega_i^T \Omega_i \}} - \sum_{i=1}^n \left(\tilde{\delta}_i S_i \tanh \left(\frac{S_i}{\epsilon_i} \right) \right) \\ &\leq -K_1 S_1^2 - \sum_{i=2}^{n-1} \left(K_i - \frac{1}{2} \right) S_i^2 - \left(K_n - \frac{1}{2} \right) S_n^2 - \sum_{i=2}^n \left(\frac{1}{\tau_i} - 1 \right) y_i^2 \\ &\quad + \varphi - \frac{3}{4} \sum_{i=1}^n \frac{\epsilon_i^2}{1 + \nu_i \text{tr} \{ \Omega_i^T \Omega_i \}} + \sum_{i=1}^n \left(|S_i| \delta_i - S_i \hat{\delta}_i \tanh \left(\frac{S_i}{\epsilon_i} \right) \right) \end{aligned} \quad (4.83)$$

Applying of inequality (4.43), we obtain:

$$\begin{aligned}
\dot{V} &\leq -K_1 S_1^2 - \sum_{i=2}^{n-1} \left(K_i - \frac{1}{2} \right) S_i^2 - \left(K_n - \frac{1}{2} \right) S_n^2 - \sum_{i=2}^n \left(\frac{1}{\tau_i} - 1 \right) y_i^2 + \varphi - \frac{3}{4} \sum_{i=1}^n \frac{\epsilon_i^2}{1 + \nu_i \text{tr} \{ \Omega_i^T \Omega_i \}} + \sum_{i=1}^n \delta_i \bar{\epsilon}_i \\
&\leq -K_1 S_1^2 - \sum_{i=2}^{n-1} \left(K_i - \frac{1}{2} \right) S_i^2 - \left(K_n - \frac{1}{2} \right) S_n^2 - \sum_{i=2}^n \left(\frac{1}{\tau_i} - 1 \right) y_i^2 - \frac{3}{4} \sum_{i=1}^n \frac{\epsilon_i^2}{1 + \nu_i \text{tr} \{ \Omega_i^T \Omega_i \}} + \mu
\end{aligned} \tag{4.84}$$

where, $\varphi = \sum_{i=2}^n \frac{M_i}{2}$, M_i are the maximums of $B_i(\cdot)$, $\mu = \varphi + \sum_{i=1}^n \delta_i \bar{\epsilon}_i$, $\bar{\epsilon}_i = \kappa \epsilon_i$ and

$\kappa = 0.2785$. Based on (4.84), by choosing the design parameters such that, $K_1 > 0$, $K_i > \frac{1}{2}$,

$K_n > \frac{1}{2}$ and $\tau_i < 1$, we can conclude that, V , S_i , y_i , $\tilde{\theta}_i$, $\tilde{\delta}_i$ and ϵ_i are bounded.

Furthermore, all signals in the closed-loop system, i.e., x_i , x_{id} , \dot{x}_{id} , $\bar{x}_2, \dots, \bar{x}_{i+1}$, u , $\hat{\theta}_i$ and $\hat{\delta}_i$ are also bounded.

4.4.2 Composite projection based least squares adaptive laws

The composite projection based least squares adaptive laws are defined as:

$$\dot{\hat{\theta}}_i = \text{Proj}_{\hat{\theta}_i} \left(\Gamma_i \left(S_i \varphi_i + \frac{\Omega_i \epsilon_i}{1 + \nu_i \text{tr} \{ \Omega_i^T \Gamma_i \Omega_i \}} \right) \right) \tag{4.85}$$

and,

$$\dot{\hat{\delta}}_i = \text{Proj}_{\hat{\delta}_i} \left(\gamma_i \left(S_i \tanh \left(\frac{S_i}{\epsilon_i} \right) + P_i \tilde{\epsilon}_i \text{sign}(\tilde{\epsilon}_i) \right) \right), \gamma_i > 0, \epsilon_i > 0 \tag{4.86}$$

The dynamics of estimation errors are given by:

$$\dot{\tilde{\theta}}_i = -\dot{\hat{\theta}}_i = \text{Proj}_{\tilde{\theta}_i} \left(-\Gamma_i \left(S_i \varphi_i + \frac{\Omega_i \epsilon_i}{1 + \nu_i \text{tr} \{ \Omega_i^T \Gamma_i \Omega_i \}} \right) \right) \tag{4.87}$$

and,

$$\dot{\tilde{\delta}}_i = -\dot{\hat{\delta}}_i = \text{Proj}_{\tilde{\delta}_i} \left(-\gamma_i \left(S_i \tanh \left(\frac{S_i}{\epsilon_i} \right) + P_i \tilde{\epsilon}_i \text{sign}(\tilde{\epsilon}_i) \right) \right), \gamma_i > 0, \epsilon_i > 0 \tag{4.88}$$

where, Γ_i are given by:

$$\dot{\Gamma}_i = -\Gamma_i \frac{\Omega_i \Omega_i^T}{1 + \nu_i \text{tr} \{ \Omega_i^T \Gamma_i \Omega_i \}} \Gamma_i, \Gamma_i(0) > 0, \nu_i \geq 0 \tag{4.89}$$

with, $\epsilon_i = x_i + \Omega_{0i} - \Omega_i^T \hat{\theta}_i$ and $\tilde{\epsilon}_i = x_i + \Omega_{0i} - \Omega_i^T \theta_i$.

Theorem 4.4.2: Consider the SISO uncertain nonlinear system in lower triangular form with external disturbances composed of the plant described by state space form (4.1). Suppose that assumptions 4.2.1-4.2.3 are satisfied. Then, the virtual controllers (4.5) and (4.9), the actual control input (4.13) and the composite projection based least squares adaptive laws (4.85) and (4.86) guarantee that all signals in the closed-loop system are bounded.

Proof: We consider the following Lyapunov function as:

$$V = \sum_{i=1}^n V_{is} + \sum_{i=2}^n V_{iy} + \frac{1}{2} \sum_{i=1}^n V_i \quad (4.90)$$

and,

$$V_{is} = \frac{1}{2} S_i^2, V_{iy} = \frac{1}{2} y_i^2, V_i = \tilde{\theta}_i^T \Gamma_i^{-1}(t) \tilde{\theta}_i + P_i \tilde{\epsilon}_i^2 + \frac{1}{\gamma_i} \tilde{\delta}_i^2 \quad (4.91)$$

where, \dot{V}_{is} , \dot{V}_{ns} and \dot{V}_{iy} are expressed in (4.28), (4.31), (4.39), and,

$$\begin{aligned} \dot{V}_i &= -\dot{\tilde{\theta}}_i^T \Gamma_i^{-1} \tilde{\theta}_i - \tilde{\theta}_i^T \Gamma_i^{-1} \dot{\Gamma}_i \Gamma_i^{-1} \tilde{\theta}_i - \tilde{\theta}_i^T \Gamma_i^{-1} \dot{\tilde{\theta}}_i - \tilde{\epsilon}_i^2 + 2P_i |\tilde{\epsilon}_i| \delta_i - 2P_i \tilde{\epsilon}_i \hat{\delta}_i \text{sign}(\tilde{\epsilon}_i) - \frac{2}{\gamma_i} \tilde{\delta}_i \dot{\tilde{\delta}}_i \\ &= -\text{Proj}_{\tilde{\theta}_i} \left(\Gamma_i \left(S_i \varphi_i + \frac{\Omega_i \epsilon_i}{1 + \nu_i \text{tr} \{ \Omega_i^T \Gamma_i \Omega_i \}} \right) \right)^T \Gamma_i^{-1} \tilde{\theta}_i - \tilde{\theta}_i^T \Gamma_i^{-1} \dot{\Gamma}_i \Gamma_i^{-1} \tilde{\theta}_i \\ &\quad - \tilde{\theta}_i^T \Gamma_i^{-1} \text{Proj}_{\tilde{\theta}_i} \left(\Gamma_i \left(S_i \varphi_i + \frac{\Omega_i \epsilon_i}{1 + \nu_i \text{tr} \{ \Omega_i^T \Gamma_i \Omega_i \}} \right) \right) - \tilde{\epsilon}_i^2 + 2P_i |\tilde{\epsilon}_i| \delta_i \\ &\quad - 2P_i \tilde{\epsilon}_i \hat{\delta}_i \text{sign}(\tilde{\epsilon}_i) - \frac{2}{\gamma_i} \tilde{\delta}_i \text{Proj}_{\tilde{\delta}_i} \left(\gamma_i \left(S_i \tanh \left(\frac{S_i}{\epsilon_i} \right) + P_i \tilde{\epsilon}_i \text{sign}(\tilde{\epsilon}_i) \right) \right) \\ &\leq -\varphi_i^T S_i \tilde{\theta}_i - \frac{\epsilon_i \Omega_i^T \tilde{\theta}_i}{1 + \nu_i \text{tr} \{ \Omega_i^T \Gamma_i \Omega_i \}} + \frac{\tilde{\theta}_i^T \Omega_i \Omega_i^T \tilde{\theta}_i}{1 + \nu_i \text{tr} \{ \Omega_i^T \Gamma_i \Omega_i \}} - \tilde{\theta}_i^T S_i \varphi_i \\ &\quad - \frac{\tilde{\theta}_i^T \Omega_i \epsilon_i}{1 + \nu_i \text{tr} \{ \Omega_i^T \Gamma_i \Omega_i \}} - \tilde{\epsilon}_i^2 - 2\tilde{\delta}_i S_i \tanh \left(\frac{S_i}{\epsilon_i} \right) \\ &\leq -2S_i \varphi_i^T \tilde{\theta}_i - \frac{\epsilon_i \Omega_i^T \tilde{\theta}_i}{1 + \nu_i \text{tr} \{ \Omega_i^T \Gamma_i \Omega_i \}} + \frac{\tilde{\theta}_i^T \Omega_i \Omega_i^T \tilde{\theta}_i}{1 + \nu_i \text{tr} \{ \Omega_i^T \Gamma_i \Omega_i \}} - \frac{\tilde{\theta}_i^T \Omega_i \epsilon_i}{1 + \nu_i \text{tr} \{ \Omega_i^T \Gamma_i \Omega_i \}} - \tilde{\epsilon}_i^2 - 2\tilde{\delta}_i S_i \tanh \left(\frac{S_i}{\epsilon_i} \right) \end{aligned} \quad (4.92)$$

Therefore, the derivative of the Lyapunov function \dot{V} becomes:

$$\begin{aligned}
\dot{V} &= \sum_{i=1}^n \dot{V}_{is} + \sum_{i=2}^n \dot{V}_{iy} + \frac{1}{2} \sum_{i=1}^n \dot{V}_i \\
&\leq \sum_{i=1}^{n-1} \left(-K_i S_i^2 + \frac{1}{2} S_{i+1}^2 + \frac{1}{2} y_{i+1}^2 + S_i \varphi_i^T \tilde{\theta}_i + |S_i| \delta_i - S_i \hat{\delta}_i \tanh \left(\frac{S_i}{\varepsilon_i} \right) \right) \\
&\quad - K_n S_n^2 + S_n \varphi_n^T \tilde{\theta}_n + |S_n| \delta_n - S_n \hat{\delta}_n \tanh \left(\frac{S_n}{\varepsilon_n} \right) + \sum_{i=2}^n \left(-\frac{1}{\tau_i} y_i^2 + \frac{y_i^2}{2} + \frac{B_i^2(\cdot)}{2} \right) \\
&\quad - \sum_{i=1}^n S_i \varphi_i^T \tilde{\theta}_i - \frac{1}{2} \sum_{i=1}^n \frac{\epsilon_i \Omega_i^T \tilde{\theta}_i}{1 + \nu_i \text{tr} \{ \Omega_i^T \Gamma_i \Omega_i \}} + \frac{1}{2} \sum_{i=1}^n \frac{\tilde{\theta}_i^T \Omega_i \Omega_i^T \tilde{\theta}_i}{1 + \nu_i \text{tr} \{ \Omega_i^T \Gamma_i \Omega_i \}} \\
&\quad - \frac{1}{2} \sum_{i=1}^n \frac{\tilde{\theta}_i^T \Omega_i \epsilon_i}{1 + \nu_i \text{tr} \{ \Omega_i^T \Gamma_i \Omega_i \}} - \frac{1}{2} \sum_{i=1}^n \tilde{\epsilon}_i^2 - \sum_{i=1}^n \left(\tilde{\delta}_i S_i \tanh \left(\frac{S_i}{\varepsilon_i} \right) \right) \\
&\leq -K_1 S_1^2 - \sum_{i=2}^{n-1} \left(K_i - \frac{1}{2} \right) S_i^2 - \left(K_n - \frac{1}{2} \right) S_n^2 + \sum_{i=1}^n \left(|S_i| \delta_i - S_i \hat{\delta}_i \tanh \left(\frac{S_i}{\varepsilon_i} \right) \right) \\
&\quad - \sum_{i=2}^n \left(\frac{1}{\tau_i} - 1 \right) y_i^2 + \sum_{i=2}^n \frac{B_i^2(\cdot)}{2} - \frac{1}{2} \sum_{i=1}^n \frac{\epsilon_i^2}{1 + \nu_i \text{tr} \{ \Omega_i^T \Gamma_i \Omega_i \}} - \sum_{i=1}^n \left(\tilde{\delta}_i S_i \tanh \left(\frac{S_i}{\varepsilon_i} \right) \right) \\
&\leq -K_1 S_1^2 - \sum_{i=2}^{n-1} \left(K_i - \frac{1}{2} \right) S_i^2 - \left(K_n - \frac{1}{2} \right) S_n^2 - \sum_{i=2}^n \left(\frac{1}{\tau_i} - 1 \right) y_i^2 + \varphi - \frac{1}{2} \sum_{i=1}^n \frac{\epsilon_i^2}{1 + \nu_i \text{tr} \{ \Omega_i^T \Gamma_i \Omega_i \}} \quad (4.93) \\
&\quad + \sum_{i=1}^n \left(|S_i| \delta_i - S_i \hat{\delta}_i \tanh \left(\frac{S_i}{\varepsilon_i} \right) \right)
\end{aligned}$$

Applying of inequality (4.43), we obtain:

$$\begin{aligned}
\dot{V} &\leq -K_1 S_1^2 - \sum_{i=2}^{n-1} \left(K_i - \frac{1}{2} \right) S_i^2 - \left(K_n - \frac{1}{2} \right) S_n^2 - \sum_{i=2}^n \left(\frac{1}{\tau_i} - 1 \right) y_i^2 + \varphi - \frac{1}{2} \sum_{i=1}^n \frac{\epsilon_i^2}{1 + \nu_i \text{tr} \{ \Omega_i^T \Gamma_i \Omega_i \}} + \sum_{i=1}^n \delta_i \bar{\varepsilon}_i \\
&\leq -K_1 S_1^2 - \sum_{i=2}^{n-1} \left(K_i - \frac{1}{2} \right) S_i^2 - \left(K_n - \frac{1}{2} \right) S_n^2 - \sum_{i=2}^n \left(\frac{1}{\tau_i} - 1 \right) y_i^2 - \frac{1}{2} \sum_{i=1}^n \frac{\epsilon_i^2}{1 + \nu_i \text{tr} \{ \Omega_i^T \Gamma_i \Omega_i \}} + \mu \quad (4.94)
\end{aligned}$$

where, $\varphi = \sum_{i=2}^n \frac{M_i}{2}$, M_i are the maximums of $B_i(\cdot)$, $\mu = \varphi + \sum_{i=1}^n \delta_i \bar{\varepsilon}_i$, $\bar{\varepsilon}_i = \kappa \varepsilon_i$ and

$\kappa = 0.2785$. Based on (4.94), by choosing the design parameters such that, $K_1 > 0$, $K_i > \frac{1}{2}$,

$K_n > \frac{1}{2}$ and $\tau_i < 1$, we can concluded that, V , S_i , y_i , $\tilde{\theta}_i$, $\tilde{\delta}_i$ and ϵ_i are bounded.

Furthermore, all signals in the closed-loop system, i.e., x_i , x_{id} , \dot{x}_{id} , $\bar{x}_2, \dots, \bar{x}_{i+1}$, u , $\hat{\theta}_i$ and $\hat{\delta}_i$ are also bounded.

4.4.3 Composite σ -modification based gradient and least squares adaptive laws

The composite σ -modification based gradient and least squares adaptive laws are defined as:

$$\dot{\hat{\theta}}_i = \Gamma_i \left(S_i \varphi_i - \sigma_{\theta_i} (\hat{\theta}_i - \bar{\theta}_i) \right), \Gamma_i > 0, \sigma_{\theta_i} > 0 \quad (4.95)$$

and,

$$\dot{\hat{\delta}}_i = \gamma_i \left(S_i \tanh \left(\frac{S_i}{\varepsilon_i} \right) - \sigma_{\delta_i} (\hat{\delta}_i - \bar{\delta}_i) \right), \gamma_i > 0, \varepsilon_i > 0, \sigma_{\delta_i} > 0 \quad (4.96)$$

where, σ_{θ_i} and σ_{δ_i} are small design constants to introduce the σ -modification for the closed-loop system and $\bar{\theta}_i$ are computed with the gradient method as follows:

$$\dot{\bar{\theta}}_i = \bar{\Gamma}_i \frac{\Omega_i \epsilon_i}{1 + \nu_i \text{tr} \{ \Omega_i^T \Omega_i \}}, \bar{\Gamma}_i > 0 \quad (4.97)$$

or with the least squares method as follows:

$$\dot{\bar{\theta}}_i = \bar{\Gamma}_i \frac{\Omega_i \epsilon_i}{1 + \nu_i \text{tr} \{ \Omega_i^T \bar{\Gamma}_i \Omega_i \}} \quad (4.98)$$

where, $\bar{\Gamma}_i$ are given by:

$$\dot{\bar{\Gamma}}_i = -\bar{\Gamma}_i \frac{\Omega_i \Omega_i^T}{1 + \nu_i \text{tr} \{ \Omega_i^T \bar{\Gamma}_i \Omega_i \}} \bar{\Gamma}_i, \bar{\Gamma}_i(0) > 0, \nu_i \geq 0 \quad (4.99)$$

$\bar{\delta}_i$ are computed as follows:

$$\dot{\bar{\delta}}_i = 2\bar{\gamma}_i P_i \tilde{\epsilon}_i \text{sign}(\tilde{\epsilon}_i), \bar{\gamma}_i > 0 \quad (4.100)$$

with, $\epsilon_i = x_i + \Omega_{0i} - \Omega_i^T \bar{\theta}_i$ and $\tilde{\epsilon}_i = x_i + \Omega_{0i} - \Omega_i^T \theta_i$.

Theorem 4.4.3: Consider the SISO uncertain nonlinear system in lower triangular form with external disturbances composed of the plant described by state space form (4.1). Suppose that assumptions 4.2.1-4.2.3 are satisfied. Then, the virtual controllers (4.5) and (4.9), the actual control input (4.13) and the composite σ -modification based gradient and least squares adaptive laws (4.95) et (4.96) guarantee that all signals in the closed-loop system are UUB and the surface errors converge to a sufficiently small neighborhood of the origin by appropriately adjusting the design parameters.

Proof: We consider the following Lyapunov function as:

$$V = \sum_{i=1}^n V_{is} + \sum_{i=2}^n V_{iy} + \sum_{i=1}^n V_{i\theta} + \sum_{i=1}^n V_{i\delta} \quad (4.101)$$

and,

$$V_{is} = \frac{1}{2} S_i^2, V_{iy} = \frac{1}{2} y_i^2, V_{i\theta} = \frac{1}{2} \tilde{\theta}_i^T \Gamma_i^{-1} \tilde{\theta}_i, V_{i\delta} = \frac{1}{2\gamma_i} \tilde{\delta}_i^2 \quad (4.102)$$

where, \dot{V}_{is} , \dot{V}_{ns} and \dot{V}_{iy} are expressed in (4.28), (4.31), (4.39), and,

$$\begin{aligned} \dot{V}_{i\theta} &= \tilde{\theta}_i^T \Gamma_i^{-1} \dot{\tilde{\theta}}_i = -\tilde{\theta}_i^T \Gamma_i^{-1} \hat{\dot{\theta}}_i \\ &= -\tilde{\theta}_i^T \left(S_i \varphi_i - \sigma_{\theta_i} (\hat{\theta}_i - \bar{\theta}_i) \right) \\ &= -\tilde{\theta}_i^T S_i \varphi_i + \sigma_{\theta_i} \tilde{\theta}_i^T (\hat{\theta}_i - \bar{\theta}_i) \end{aligned} \quad (4.103)$$

We assume that, $\theta_i - \bar{\theta}_i$ is bounded, thus, $e_{\theta_i} = \theta_i - \bar{\theta}_i$ is bounded, $\bar{\theta}_i = \theta_i - e_{\theta_i}$ and $\tilde{\theta}_i = \theta_i - \hat{\theta}_i$, and, applying of inequality (3.87), the derivative of the Lyapunov function $\dot{V}_{i\theta}$ becomes:

$$\begin{aligned} \dot{V}_{i\theta} &= -\tilde{\theta}_i^T S_i \varphi_i + \sigma_{\theta_i} \tilde{\theta}_i^T (\hat{\theta}_i - \theta_i + e_{\theta_i}) \\ &= -\tilde{\theta}_i^T S_i \varphi_i - \sigma_{\theta_i} \tilde{\theta}_i^T \tilde{\theta}_i + \sigma_{\theta_i} \tilde{\theta}_i^T e_{\theta_i} \\ &\leq -\tilde{\theta}_i^T S_i \varphi_i - \frac{\sigma_{\theta_i}}{2} \tilde{\theta}_i^T \tilde{\theta}_i + \frac{\sigma_{\theta_i}}{2} e_{\theta_i}^2 \end{aligned} \quad (4.104)$$

and, we have,

$$\begin{aligned} \dot{V}_{i\delta} &= -\frac{1}{\gamma_i} \tilde{\delta}_i \dot{\tilde{\delta}}_i = -\tilde{\delta}_i \left(S_i \tanh \left(\frac{S_i}{\varepsilon_i} \right) - \sigma_{\delta_i} (\hat{\delta}_i - \bar{\delta}_i) \right) \\ &= -\tilde{\delta}_i S_i \tanh \left(\frac{S_i}{\varepsilon_i} \right) + \tilde{\delta}_i \sigma_{\delta_i} (\hat{\delta}_i - \bar{\delta}_i) \end{aligned} \quad (4.105)$$

We assume that, $\delta_i - \bar{\delta}_i$ is bounded, thus, $e_{\delta_i} = \delta_i - \bar{\delta}_i$ is bounded, $\bar{\delta}_i = \delta_i - e_{\delta_i}$ and $\tilde{\delta}_i = \delta_i - \hat{\delta}_i$, and, applying of the following inequality:

$$\tilde{\delta}_i e_{\delta_i} \leq \frac{\tilde{\delta}_i^2}{2} + \frac{e_{\delta_i}^2}{2} \quad (4.106)$$

The derivative of the Lyapunov function $\dot{V}_{i\delta}$ becomes:

$$\begin{aligned} \dot{V}_{i\delta} &= -\tilde{\delta}_i S_i \tanh \left(\frac{S_i}{\varepsilon_i} \right) + \tilde{\delta}_i \sigma_{\delta_i} (\hat{\delta}_i - \delta_i + e_{\delta_i}) \\ &= -\tilde{\delta}_i S_i \tanh \left(\frac{S_i}{\varepsilon_i} \right) - \sigma_{\delta_i} \tilde{\delta}_i^2 + \sigma_{\delta_i} \tilde{\delta}_i e_{\delta_i} \\ &\leq -\tilde{\delta}_i S_i \tanh \left(\frac{S_i}{\varepsilon_i} \right) - \frac{\sigma_{\delta_i}}{2} \tilde{\delta}_i^2 + \frac{\sigma_{\delta_i}}{2} e_{\delta_i}^2 \end{aligned} \quad (4.107)$$

Therefore, the derivative of the Lyapunov function \dot{V} becomes:

$$\begin{aligned}
\dot{V} &= \sum_{i=1}^n \dot{V}_{is} + \sum_{i=2}^n \dot{V}_{iy} + \sum_{i=1}^n \dot{V}_{i\theta} + \sum_{i=1}^n \dot{V}_{i\delta} \\
&\leq \sum_{i=1}^{n-1} \left(-K_i S_i^2 + \frac{1}{2} S_{i+1}^2 + \frac{1}{2} y_{i+1}^2 + S_i \varphi_i^T \tilde{\theta}_i + |S_i| \delta_i - S_i \hat{\delta}_i \tanh \left(\frac{S_i}{\varepsilon_i} \right) \right) - K_n S_n^2 \\
&\quad + S_n \varphi_n^T \tilde{\theta}_n + |S_n| \delta_n - S_n \hat{\delta}_n \tanh \left(\frac{S_n}{\varepsilon_n} \right) + \sum_{i=2}^n \left(-\frac{1}{\tau_i} y_i^2 + \frac{y_i^2}{2} + \frac{B_i^2(\cdot)}{2} \right) - \sum_{i=1}^n \tilde{\theta}_i^T S_i \varphi_i \\
&\quad - \sum_{i=1}^n \frac{\sigma_{\theta_i}}{2} \tilde{\theta}_i^T \tilde{\theta}_i + \sum_{i=1}^n \frac{\sigma_{\theta_i}}{2} e_{\theta_i}^2 - \sum_{i=1}^n \left(\tilde{\delta}_i S_i \tanh \left(\frac{S_i}{\varepsilon_i} \right) \right) - \sum_{i=1}^n \frac{\sigma_{\delta_i}}{2} \tilde{\delta}_i^2 + \sum_{i=1}^n \frac{\sigma_{\delta_i}}{2} e_{\delta_i}^2 \\
&\leq -K_1 S_1^2 - \sum_{i=2}^{n-1} \left(K_i - \frac{1}{2} \right) S_i^2 - \left(K_n - \frac{1}{2} \right) S_n^2 + \sum_{i=1}^n \left(|S_i| \delta_i - S_i \hat{\delta}_i \tanh \left(\frac{S_i}{\varepsilon_i} \right) \right) - \sum_{i=2}^n \left(\frac{1}{\tau_i} - 1 \right) y_i^2 \\
&\quad + \sum_{i=2}^n \frac{B_i^2(\cdot)}{2} - \sum_{i=1}^n \frac{\sigma_{\theta_i}}{2} \tilde{\theta}_i^T \tilde{\theta}_i + \sum_{i=1}^n \frac{\sigma_{\theta_i}}{2} e_{\theta_i}^2 - \sum_{i=1}^n \left(\tilde{\delta}_i S_i \tanh \left(\frac{S_i}{\varepsilon_i} \right) \right) - \sum_{i=1}^n \frac{\sigma_{\delta_i}}{2} \tilde{\delta}_i^2 + \sum_{i=1}^n \frac{\sigma_{\delta_i}}{2} e_{\delta_i}^2 \\
&\leq -K_1 S_1^2 - \sum_{i=2}^{n-1} \left(K_i - \frac{1}{2} \right) S_i^2 - \left(K_n - \frac{1}{2} \right) S_n^2 - \sum_{i=2}^n \left(\frac{1}{\tau_i} - 1 \right) y_i^2 + \varphi - \sum_{i=1}^n \frac{\sigma_{\theta_i}}{2} \tilde{\theta}_i^T \tilde{\theta}_i \\
&\quad + \sum_{i=1}^n \frac{\sigma_{\theta_i}}{2} e_{\theta_i}^2 + \sum_{i=1}^n \left(|S_i| \delta_i - S_i \hat{\delta}_i \tanh \left(\frac{S_i}{\varepsilon_i} \right) \right) - \sum_{i=1}^n \frac{\sigma_{\delta_i}}{2} \tilde{\delta}_i^2 + \sum_{i=1}^n \frac{\sigma_{\delta_i}}{2} e_{\delta_i}^2
\end{aligned} \tag{4.108}$$

Applying of inequality (4.43), we obtain:

$$\begin{aligned}
\dot{V} &\leq -K_1 S_1^2 - \sum_{i=2}^{n-1} \left(K_i - \frac{1}{2} \right) S_i^2 - \left(K_n - \frac{1}{2} \right) S_n^2 - \sum_{i=2}^n \left(\frac{1}{\tau_i} - 1 \right) y_i^2 + \varphi - \sum_{i=1}^n \frac{\sigma_{\theta_i}}{2} \tilde{\theta}_i^T \tilde{\theta}_i \\
&\quad + \sum_{i=1}^n \frac{\sigma_{\theta_i}}{2} e_{\theta_i}^2 + \sum_{i=1}^n \delta_i \bar{\varepsilon}_i - \sum_{i=1}^n \frac{\sigma_{\delta_i}}{2} \tilde{\delta}_i^2 + \sum_{i=1}^n \frac{\sigma_{\delta_i}}{2} e_{\delta_i}^2 \\
&\leq -K_1 S_1^2 - \sum_{i=2}^{n-1} \left(K_i - \frac{1}{2} \right) S_i^2 - \left(K_n - \frac{1}{2} \right) S_n^2 - \sum_{i=2}^n \left(\frac{1}{\tau_i} - 1 \right) y_i^2 - \sum_{i=1}^n \frac{\sigma_{\theta_i}}{2} \tilde{\theta}_i^T \tilde{\theta}_i - \sum_{i=1}^n \frac{\sigma_{\delta_i}}{2} \tilde{\delta}_i^2 + \mu
\end{aligned} \tag{4.109}$$

Based on the above discussions, we can get the following inequality:

$$\dot{V} \leq -\pi V + \mu \tag{4.110}$$

where, $\varphi = \sum_{i=2}^n \frac{M_i}{2}$, M_i are the maximums of $B_i(\cdot)$, $\mu = \varphi + \sum_{i=1}^n \delta_i \bar{\varepsilon}_i + \sum_{i=1}^n \frac{\sigma_{\theta_i}}{2} e_{\theta_i}^2 + \sum_{i=1}^n \frac{\sigma_{\delta_i}}{2} e_{\delta_i}^2$,

$$\bar{\varepsilon}_i = \kappa \varepsilon_i, \quad \kappa = 0.2785 \quad \text{and} \quad \pi = \min \left\{ 2K_1, 2 \left(K_i - \frac{1}{2} \right), 2 \left(K_n - \frac{1}{2} \right), 2 \left(\frac{1}{\tau_i} - 1 \right), \Gamma_i \sigma_{\theta_i}, \gamma_i \sigma_{\delta_i} \right\}.$$

Multiplying both sides in (4.110) by $e^{\pi t}$ yields:

$$\frac{d}{dt}(V(t)e^{\pi t}) \leq \mu e^{\pi t} \quad (4.111)$$

Moreover, by integrating (4.111) over $[0, t]$, we obtain:

$$0 \leq V(t) \leq \frac{\mu}{\pi} + \left(V(0) - \frac{\mu}{\pi} \right) e^{-\pi t} \quad (4.112)$$

Since $\frac{\mu}{\pi} > 0$, it can be obtained that:

$$0 \leq V(t) \leq V(0) e^{-\pi t} + \frac{\mu}{\pi} \quad (4.113)$$

Therefore, based on (4.109), by choosing the design parameters such that, $K_1 > 0$, $K_i > \frac{1}{2}$,

$K_n > \frac{1}{2}$, $\tau_i < 1$, $\sigma_{\theta_i} > 0$ and $\sigma_{\delta_i} > 0$, we can conclude that, S_i , y_i , $\tilde{\theta}_i$, $\tilde{\delta}_i$ and ϵ_i are UUB.

Furthermore, all signals in the closed-loop system, i.e., x_i , x_{id} , \dot{x}_{id} , $\bar{x}_2, \dots, \bar{x}_{i+1}$, u , $\hat{\theta}_i$ and $\hat{\delta}_i$ are also UUB. In addition, from (4.101) and (4.113), it follows that:

$\|S\| = \sqrt{\sum_{i=1}^n S_i^2} \leq \sqrt{2V(0)} e^{-0.5\pi t} + \sqrt{2\mu/\pi}$. Accordingly, when $t \rightarrow \infty$, it is easy to show that:

$\|S\| \leq \sqrt{2\mu/\pi}$. This completes the proof.

4.5 Simulation results

This section presents the simulation results for composite robust adaptive dynamic surface control technique as applied to an electromechanical system mathematical model and as in previous chapters. The time-varying external disturbance is chosen as [Bec13, Li10a,

Zha18a, Zha18b, Zha17]: $d_2(t) = \frac{\Delta_l(t)}{D} = \frac{4 \sin(t)}{D}$ to test the performance robustness of

the proposed composite scheme. The control objective of this simulation is to design the composite robust adaptive dynamic surface controller u for the electromechanical system in such a way that the link angular position q tracks the desired trajectory x_{1d} and to ensure the boundedness of all signals in the closed-loop system. The signals x_{2d} and x_{3d} are generated by the filters:

$$\dot{x}_{2d} = \frac{1}{\tau_2} (-x_{2d} + \dot{x}_{1d} - K_1 S_1 - S_1) \quad (4.114)$$

$$\dot{x}_{3d} = \frac{1}{\tau_3} \left(-x_{3d} + \frac{1}{b_2} \left(\sin(x_1) \hat{\theta}_2 + \frac{B}{D} x_2 - \hat{\delta}_2 \tanh\left(\frac{S_2}{\varepsilon_2}\right) + \dot{x}_{2d} - K_2 S_2 \right) - b_2 S_2 \right) \quad (4.115)$$

The actual control input u is chosen as:

$$u = \frac{1}{b_3} \left(x_2 \hat{\theta}_3 + \frac{H}{M} x_3 + \dot{x}_{3d} - K_3 S_3 \right) \quad (4.116)$$

For the swapping based identifier, we use the following modified x-swapping filters:

$$\dot{\Omega}_{02} = \left(-0.5 - \lambda_2 (\sin(x_1))^2 \right) (\Omega_{02} + x_2) + \frac{B}{D} x_2 - b_2 x_3 - \hat{\delta}_2 \text{sign}(\tilde{\varepsilon}_2) \quad (4.117)$$

$$\dot{\Omega}_2^T = \left(-0.5 - \lambda_2 (\sin(x_1))^2 \right) \Omega_2^T - \sin(x_1) \quad (4.118)$$

$$\dot{\Omega}_{03} = \left(-0.5 - \lambda_3 x_2^2 \right) (\Omega_{03} + x_3) + \frac{H}{M} x_3 - b_3 u \quad (4.119)$$

$$\dot{\Omega}_3^T = \left(-0.5 - \lambda_3 x_2^2 \right) \Omega_3^T - x_2 \quad (4.120)$$

4.5.1 Composite projection based gradient adaptive laws

The composite projection based gradient adaptive laws are defined as:

$$\dot{\hat{\theta}}_2 = \text{Proj}_{\hat{\theta}_2} \left(-\Gamma_2 \left(S_1 \sin(x_1) - \left(\frac{\Omega_2 \varepsilon_2}{1 + \nu_2 \text{tr}\{\Omega_2^T \Omega_2\}} \right) \right) \right) \quad (4.121)$$

$$\dot{\hat{\theta}}_3 = \text{Proj}_{\hat{\theta}_3} \left(-\Gamma_3 \left(S_3 x_2 - \left(\frac{\Omega_3 \varepsilon_3}{1 + \nu_3 \text{tr}\{\Omega_3^T \Omega_3\}} \right) \right) \right) \quad (4.122)$$

$$\dot{\hat{\delta}}_2 = \text{Proj}_{\hat{\delta}_2} \left(\gamma_2 \left(S_2 \tanh\left(\frac{S_2}{\varepsilon_2}\right) + 2\tilde{\varepsilon}_2 \text{sign}(\tilde{\varepsilon}_2) \right) \right) \quad (4.123)$$

where, $\varepsilon_i = x_i + \Omega_{0i} - \Omega_i^T \hat{\theta}_i$, $i = 2, 3$ and $\tilde{\varepsilon}_2 = x_2 + \Omega_{02} - \Omega_2^T \hat{\theta}_2$. The selected initial conditions are set as: $x(0) = [0 \ 0 \ 0]^T$, $\hat{\theta}_2(0) = 0$, $\hat{\theta}_3(0) = 0$, $\hat{\delta}_2(0) = 0$, $\Omega_{02}(0) = \Omega_2^T(0) = 0$, $\Omega_{03}(0) = \Omega_3^T(0) = 0$ and $x_{2d}(0) = x_{3d}(0) = 0$. The design parameters are selected as follows: $K_1 = 200$, $K_2 = 5$, $K_3 = 550$, $\Gamma_2 = 40$, $\Gamma_3 = 550$, $\gamma_2 = 4.5$, $\varepsilon_2 = 0.01$, $\lambda_2 = \lambda_3 = 0.1$, $\nu_2 = \nu_3 = 0.1$ and $\tau_2 = \tau_3 = 10^{-3}$. The simulation results are shown in Figures 4.1-4.10. Figures 4.1-4.3 show the trajectories of the output variables. The trajectories of the surface errors are illustrated in Figures 4.4-4.6. Figures 4.7-4.9 show the trajectories of the parameter estimates. The trajectories of the control inputs are shown in Figure 4.10.

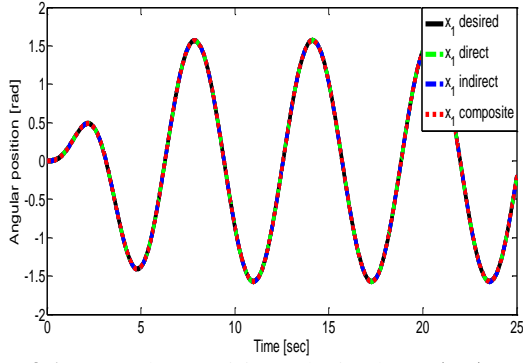


Fig. 4.1: Angular position: desired x_{1d} ("--") and actual x_1 ("--").

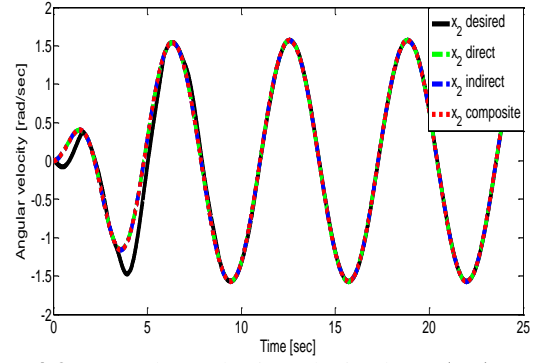


Fig. 4.2: Angular velocity: desired x_{2d} ("--") and actual x_2 ("--").

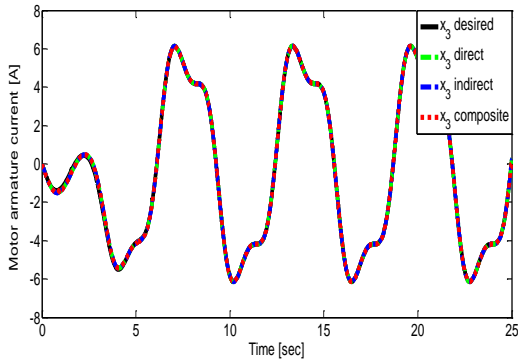


Fig. 4.3: Motor armature current: desired x_{3d} ("--") and actual x_3 ("--").

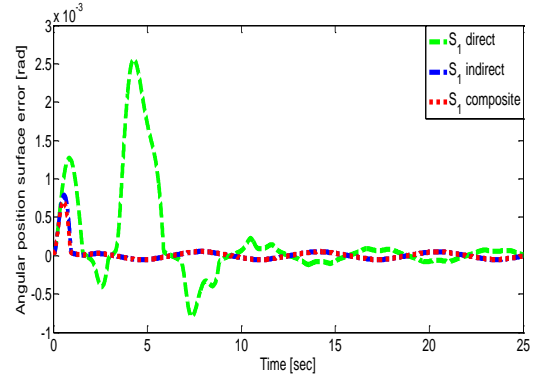


Fig. 4.4: Angular position surface error: S_1 .

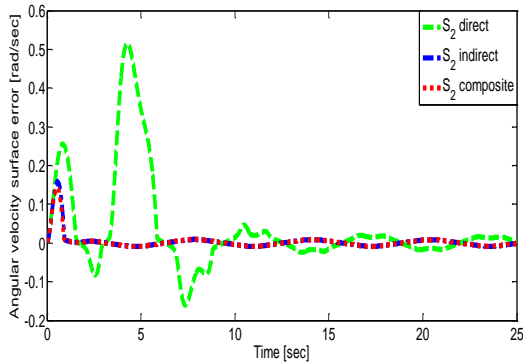


Fig. 4.5: Angular velocity surface error: S_2 .

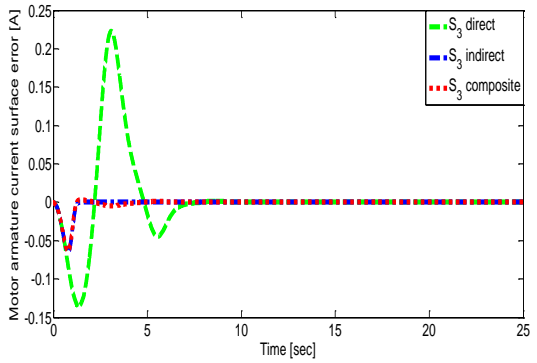


Fig. 4.6: Motor armature current surface error: S_3 .

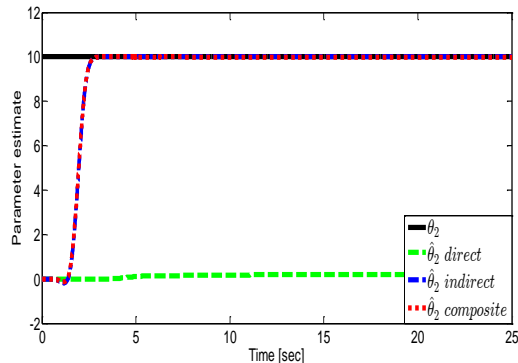


Fig. 4.7: Parameter estimate: actual θ_2 ("--") and estimate $\hat{\theta}_2$ ("--").

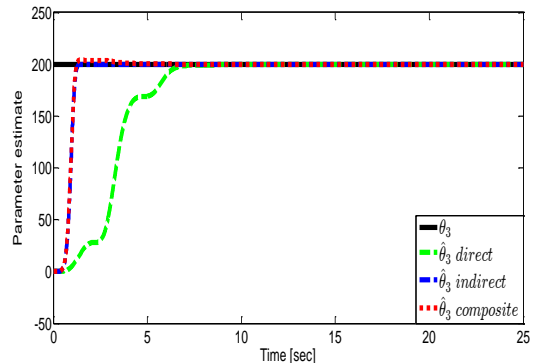


Fig. 4.8: Parameter estimate: actual θ_3 ("--") and estimate $\hat{\theta}_3$ ("--").

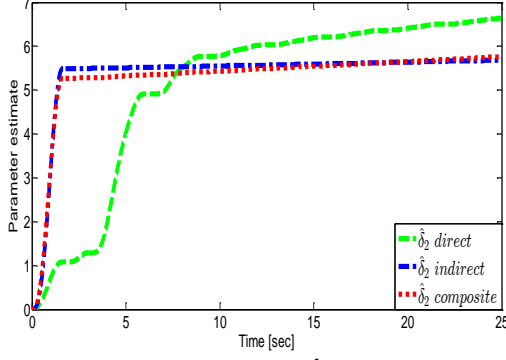


Fig. 4.9: Parameter estimate: $\hat{\delta}_2$.

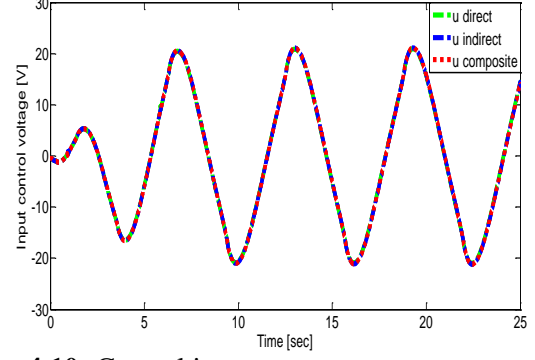


Fig. 4.10: Control input: u .

4.5.2 Composite projection based least squares adaptive laws

The composite projection based least squares adaptive laws are defined as:

$$\dot{\hat{\theta}}_2 = \text{Proj}_{\hat{\theta}_2} \left(-\Gamma_2 \left(S_1 \sin(x_1) - \left(\frac{\Omega_2 \epsilon_2}{1 + \nu_2 \text{tr}\{\Omega_2^T \Gamma_2 \Omega_2\}} \right) \right) \right) \quad (4.124)$$

$$\dot{\hat{\theta}}_3 = \text{Proj}_{\hat{\theta}_3} \left(-\Gamma_3 \left(S_3 x_2 - \left(\frac{\Omega_3 \epsilon_3}{1 + \nu_3 \text{tr}\{\Omega_3^T \Gamma_3 \Omega_3\}} \right) \right) \right) \quad (4.125)$$

and,

$$\dot{\hat{\delta}}_2 = \text{Proj}_{\hat{\delta}_2} \left(\gamma_2 \left(S_2 \tanh\left(\frac{S_2}{\epsilon_2}\right) + \tilde{\epsilon}_2 \text{sign}(\tilde{\epsilon}_2) \right) \right) \quad (4.126)$$

with, Γ_i is given by:

$$\dot{\Gamma}_i = -\Gamma_i \frac{\Omega_i \Omega_i^T}{1 + \nu_i \text{tr}\{\Omega_i^T \Gamma_i \Omega_i\}} \Gamma_i \quad (4.127)$$

where, $\epsilon_i = x_i + \Omega_{0i} - \Omega_i^T \hat{\theta}_i$, $i = 2, 3$ and $\tilde{\epsilon}_2 = x_2 + \Omega_{02} - \Omega_2^T \hat{\theta}_2$. The selected initial conditions are set as: $x(0) = [0 \ 0 \ 0]^T$, $\hat{\theta}_2(0) = 0$, $\hat{\theta}_3(0) = 0$, $\hat{\delta}_2(0) = 0$, $\Omega_{02}(0) = \Omega_2^T(0) = 0$, $\Omega_{03}(0) = \Omega_3^T(0) = 0$ and $x_{2d}(0) = x_{3d}(0) = 0$. The design parameters are selected as follows: $K_1 = 25$, $K_2 = 5$, $K_3 = 1050$, $\Gamma_2(0) = 50$, $\Gamma_3(0) = 500$, $\gamma_2 = 4.5$, $\epsilon_2 = 0.01$, $\lambda_2 = \lambda_3 = 0.1$, $\nu_2 = \nu_3 = 0.1$ and $\tau_2 = \tau_3 = 10^{-3}$. The simulation results are shown in Figures 4.11-4.20. Figures 4.11-4.13 show the trajectories of the output variables. The trajectories of the surface errors are illustrated in Figures 4.14-4.16. Figures 4.17-4.19 show the trajectories of the parameter estimates. The trajectories of the control inputs are shown in Figure 4.20.

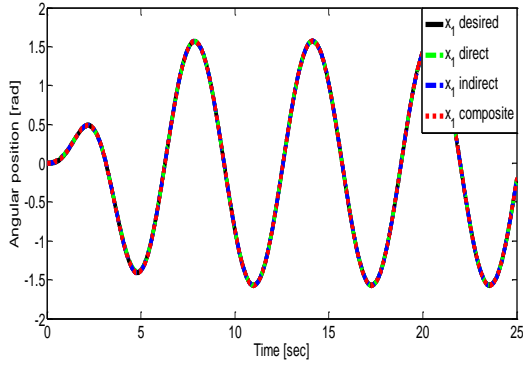


Fig. 4.11: Angular position: desired x_{1d} ("--") and actual x_1 ("--").

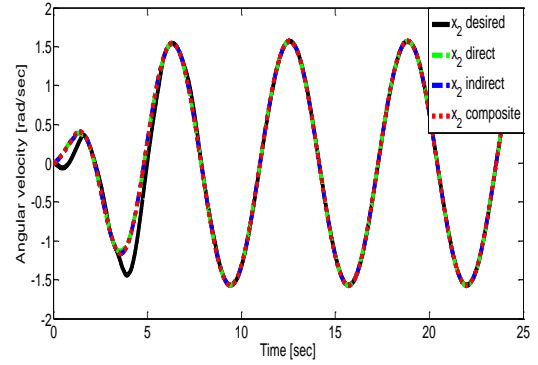


Fig. 4.12: Angular velocity: desired x_{2d} ("--") and actual x_2 ("--").

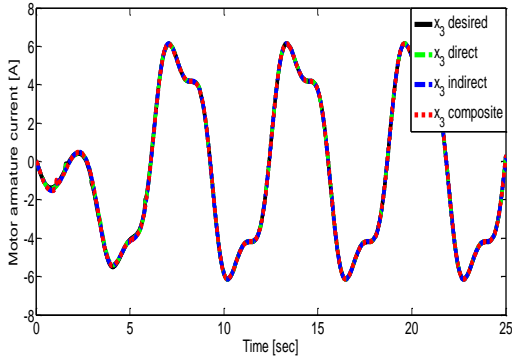


Fig. 4.13: Motor armature current: desired x_{3d} ("--") and actual x_3 ("--").

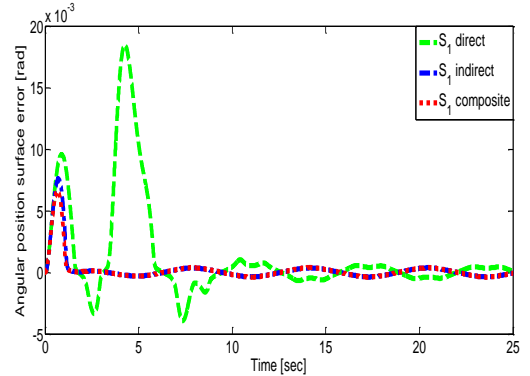


Fig. 4.14: Angular position surface error: S_1 .

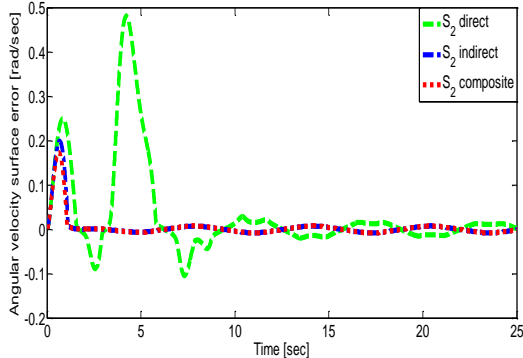


Fig. 4.15: Angular velocity surface error: S_2 .

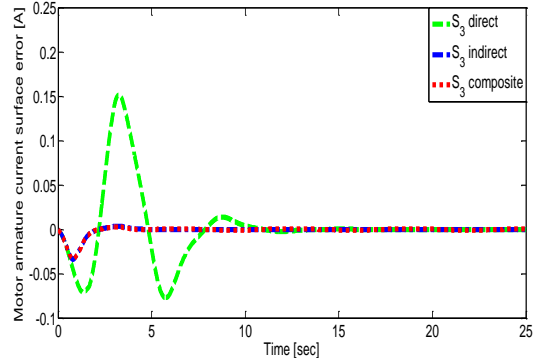


Fig. 4.16: Motor armature current surface error: S_3 .

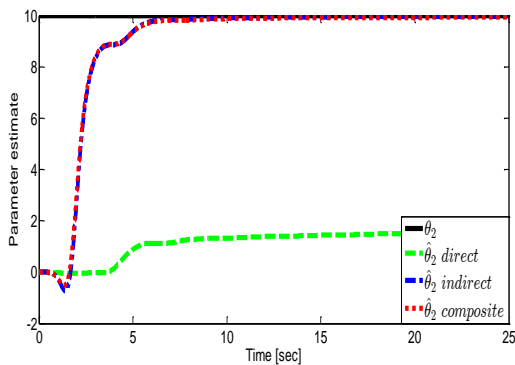


Fig. 4.17: Parameter estimate: actual θ_2 ("--") and estimate $\hat{\theta}_2$ ("--").

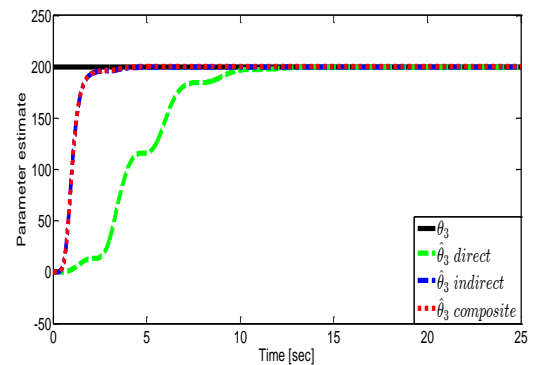


Fig. 4.18: Parameter estimate: actual θ_3 ("--") and estimate $\hat{\theta}_3$ ("--").

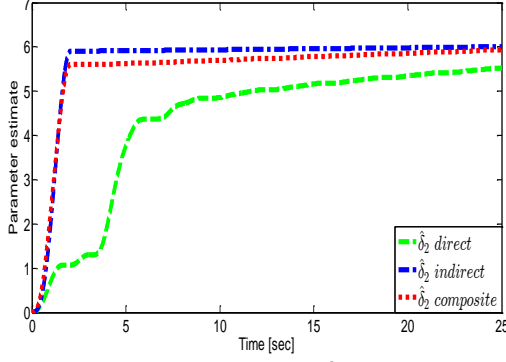


Fig. 4.19: Parameter estimate: $\hat{\delta}_2$.

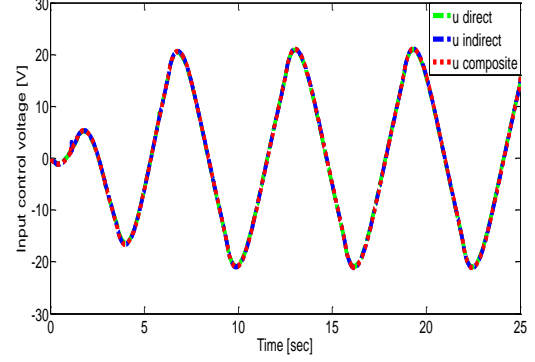


Fig. 4.20: Control input: u .

4.5.3 Composite σ -modification based gradient adaptive laws

The composite σ -modification based gradient adaptive laws are defined as:

$$\dot{\hat{\theta}}_2 = -\Gamma_2 S_1 \sin(x_1) - \Gamma_2 \sigma_{\theta_2} (\hat{\theta}_2 - \bar{\theta}_2) \quad (4.128)$$

$$\dot{\hat{\theta}}_3 = -\Gamma_3 S_3 x_2 - \Gamma_3 \sigma_{\theta_3} (\hat{\theta}_3 - \bar{\theta}_3) \quad (4.129)$$

and,

$$\dot{\hat{\delta}}_2 = \gamma_2 \left(S_2 \tanh\left(\frac{S_2}{\varepsilon_2}\right) - \sigma_{\delta_2} (\hat{\delta}_2 - \bar{\delta}_2) \right) \quad (4.130)$$

where, $\bar{\theta}_2$ and $\bar{\theta}_3$ are computed with the gradient method as follows:

$$\dot{\bar{\theta}}_i = \bar{\Gamma}_i \frac{\Omega_i \epsilon_i}{1 + \nu_i \text{tr}\{\Omega_i^T \Omega_i\}} \quad (4.131)$$

and, $\bar{\delta}_2$ is computed as follows:

$$\dot{\bar{\delta}}_2 = 2\bar{\gamma}_2 \tilde{\epsilon}_2 \text{sign}(\tilde{\epsilon}_2) \quad (4.132)$$

with, $\epsilon_i = x_i + \Omega_{0i} - \Omega_i^T \bar{\theta}_i$, $i = 2, 3$ and $\tilde{\epsilon}_2 = x_2 + \Omega_{02} - \Omega_2^T \bar{\theta}_2$. The selected initial conditions are set as: $x(0) = [0 \ 0 \ 0]^T$, $\hat{\theta}_2(0) = \bar{\theta}_2(0) = 0$, $\hat{\theta}_3(0) = \bar{\theta}_3(0) = 0$, $\hat{\delta}_2(0) = \bar{\delta}_2(0) = 0$, $\Omega_{02}(0) = \Omega_2^T(0) = 0$, $\Omega_{03}(0) = \Omega_3^T(0) = 0$ and $x_{2d}(0) = x_{3d}(0) = 0$. The design parameters are selected as follows: $K_1 = 2.5$, $K_2 = 10$, $K_3 = 50$, $\Gamma_2 = 10$, $\Gamma_3 = 250$, $\bar{\Gamma}_2 = 5$, $\bar{\Gamma}_3 = 50$, $\sigma_{\theta_2} = \sigma_{\theta_3} = 0.1$, $\sigma_{\delta_2} = 0.5$, $\gamma_2 = \bar{\gamma}_2 = 4.5$, $\varepsilon_2 = 0.01$, $\lambda_2 = \lambda_3 = 0.1$, $\nu_2 = \nu_3 = 0.1$ and $\tau_2 = \tau_3 = 10^{-3}$. The simulation results are shown in Figures 4.21-4.30. Figures 4.21-4.23 show the trajectories of the output variables. The trajectories of the surface errors are illustrated in Figures 4.24-4.26. Figures 4.27-4.29 show the trajectories of the parameter estimates. The trajectories of the control inputs are shown in Figure 4.30.

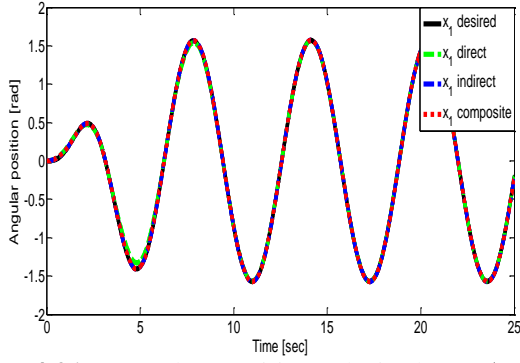


Fig. 4.21: Angular position: desired x_{1d} ("--") and actual x_1 ("--").

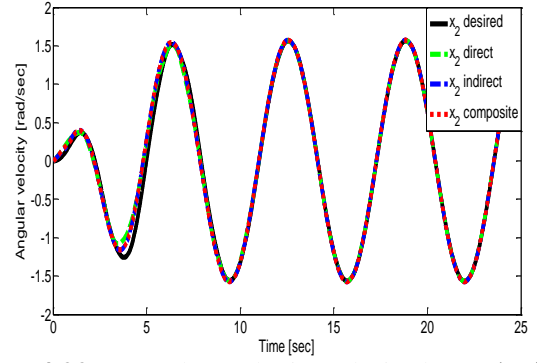


Fig. 4.22: Angular velocity: desired x_{2d} ("--") and actual x_2 ("--").

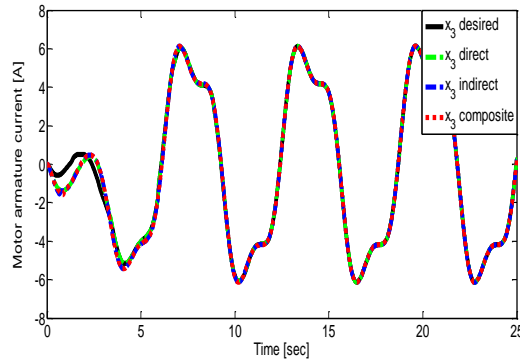


Fig. 4.23: Motor armature current: desired x_{3d} ("--") and actual x_3 ("--").

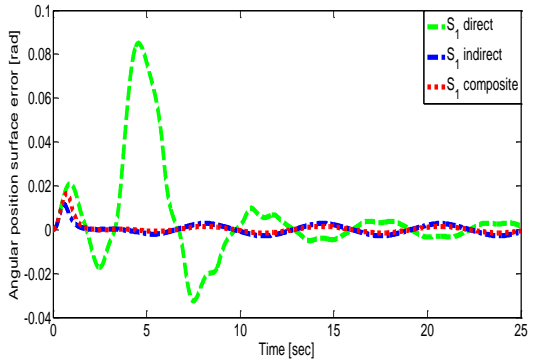


Fig. 4.24: Angular position surface error: S_1 .

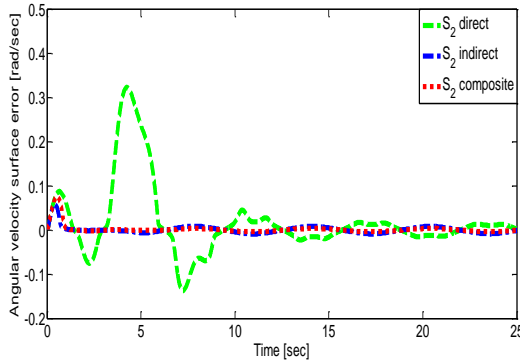


Fig. 4.25: Angular velocity surface error: S_2 .

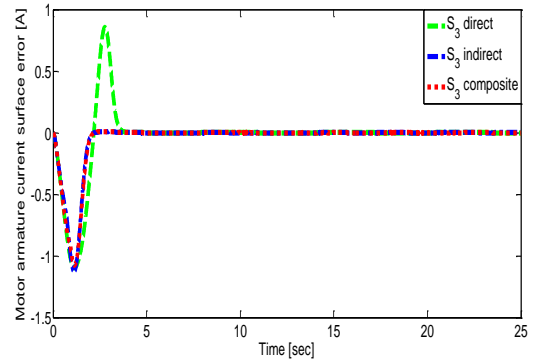


Fig. 4.26: Motor armature current surface error: S_3 .

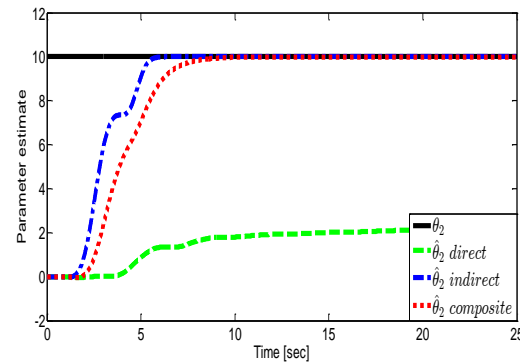


Fig. 4.27: Parameter estimate: actual θ_2 ("—") and estimate $\hat{\theta}_2$ ("--").

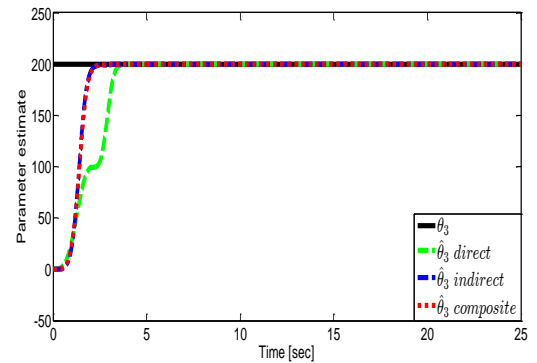


Fig. 4.28: Parameter estimate: actual θ_3 ("—") and estimate $\hat{\theta}_3$ ("--").

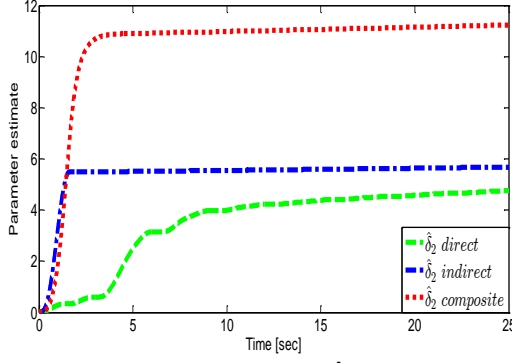


Fig. 4.29: Parameter estimate: $\hat{\delta}_2$.

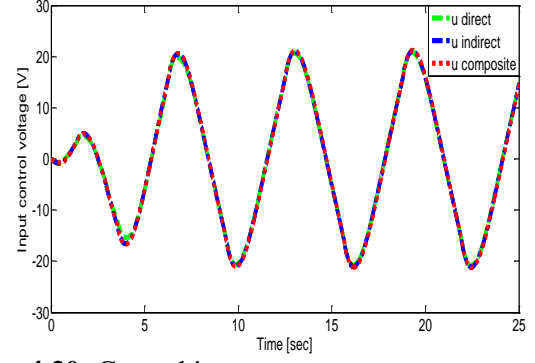


Fig. 4.30: Control input: u .

4.5.4 Composite σ -modification based least squares adaptive laws

The composite σ -modification based least squares adaptive laws are the same as that in the composite σ -modification based gradient adaptive laws described by (4.128)-(4.130). $\bar{\theta}_2$ and $\bar{\theta}_3$ are computed with the least squares method as follows:

$$\dot{\bar{\theta}}_i = \bar{\Gamma}_i \frac{\Omega_i \epsilon_i}{1 + \nu_i \text{tr}\{\Omega_i^T \bar{\Gamma}_i \Omega_i\}} \quad (4.133)$$

with, $\bar{\Gamma}_i$ is given by:

$$\dot{\bar{\Gamma}}_i = -\bar{\Gamma}_i \frac{\Omega_i \Omega_i^T}{1 + \nu_i \text{tr}\{\Omega_i^T \bar{\Gamma}_i \Omega_i\}} \bar{\Gamma}_i \quad (4.134)$$

and, $\bar{\delta}_2$ is computed as follows:

$$\dot{\bar{\delta}}_2 = \bar{\gamma}_2 \tilde{\epsilon}_2 \text{sign}(\tilde{\epsilon}_2) \quad (4.135)$$

where, $\epsilon_i = x_i + \Omega_{0i} - \Omega_i^T \bar{\theta}_i$, $i = 2, 3$ and $\tilde{\epsilon}_2 = x_2 + \Omega_{02} - \Omega_2^T \bar{\theta}_2$. The selected initial conditions are set as: $x(0) = [0 \ 0 \ 0]^T$, $\hat{\theta}_2(0) = \bar{\theta}_2(0) = 0$, $\hat{\theta}_3(0) = \bar{\theta}_3(0) = 0$, $\hat{\delta}_2(0) = \bar{\delta}_2(0) = 0$, $\Omega_{02}(0) = \Omega_2^T(0) = 0$, $\Omega_{03}(0) = \Omega_3^T(0) = 0$ and $x_{2d}(0) = x_{3d}(0) = 0$. The design parameters are selected as follows: $K_1 = 2.5$, $K_2 = 10$, $K_3 = 50$, $\Gamma_2 = 10$, $\Gamma_3 = 250$, $\bar{\Gamma}_2(0) = 550$, $\bar{\Gamma}_3(0) = 5500$, $\sigma_{\theta_2} = \sigma_{\theta_3} = 0.1$, $\sigma_{\delta_2} = 0.5$, $\gamma_2 = \bar{\gamma}_2 = 4.5$, $\varepsilon_2 = 0.01$, $\lambda_2 = \lambda_3 = 0.1$, $\nu_2 = \nu_3 = 0.1$ and $\tau_2 = \tau_3 = 10^{-3}$. The simulation results are shown in Figures 4.31-4.40. Figures 4.31-4.33 show the trajectories of the output variables. The trajectories of the surface errors are illustrated in Figures 4.34-4.36. Figures 4.37-4.39 show the trajectories of the parameter estimates. The trajectories of the control inputs are shown in Figure 4.40.

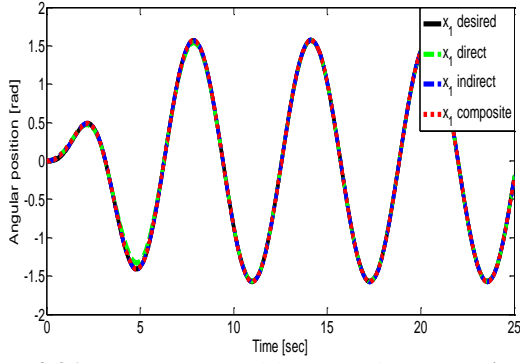


Fig. 4.31: Angular position: desired x_{1d} ("--") and actual x_1 ("--").

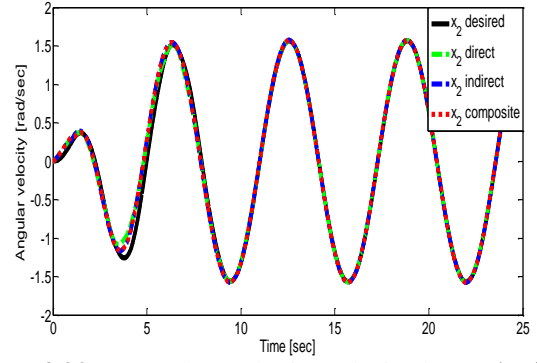


Fig. 4.32: Angular velocity: desired x_{2d} ("--") and actual x_2 ("--").

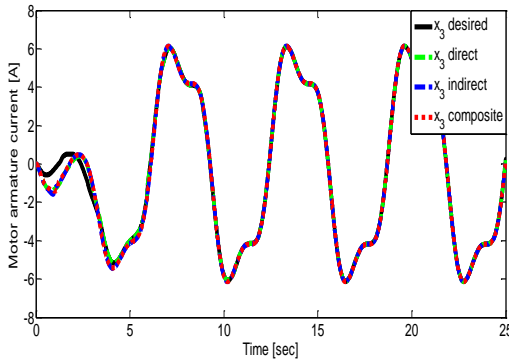


Fig. 4.33: Motor armature current: desired x_{3d} ("--") and actual x_3 ("--").

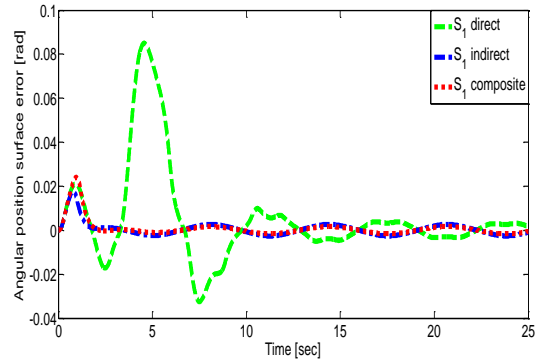


Fig. 4.34: Angular position surface error: S_1 .

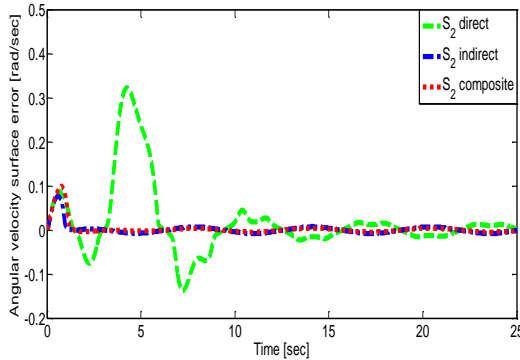


Fig. 4.35: Angular velocity surface error: S_2 .

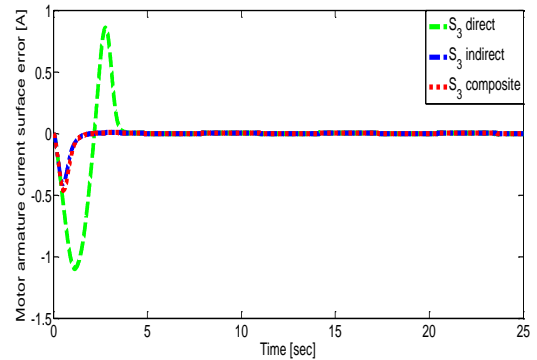


Fig. 4.36: Motor armature current surface error: S_3 .

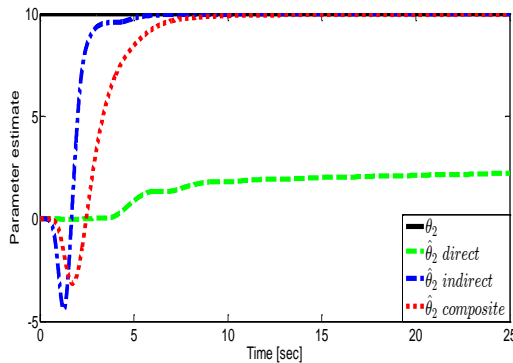


Fig. 4.37: Parameter estimate: actual θ_2 ("—") and estimate $\hat{\theta}_2$ ("--").

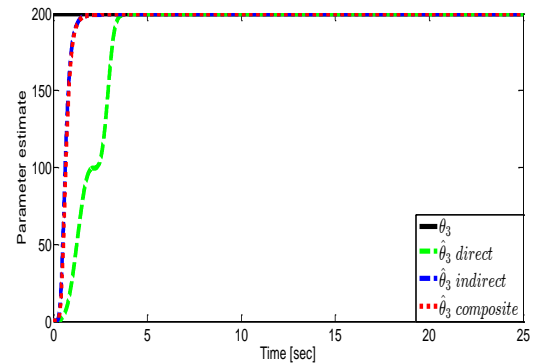


Fig. 4.38: Parameter estimate: actual θ_3 ("—") and estimate $\hat{\theta}_3$ ("--").

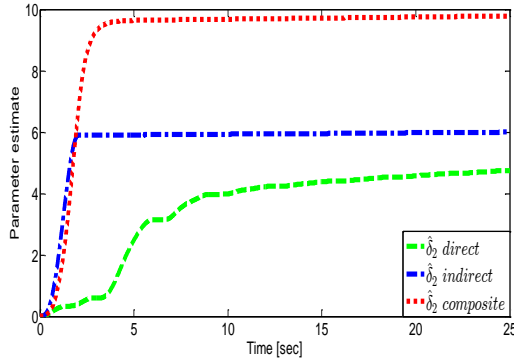


Fig. 4.39: Parameter estimate: $\hat{\delta}_2$.

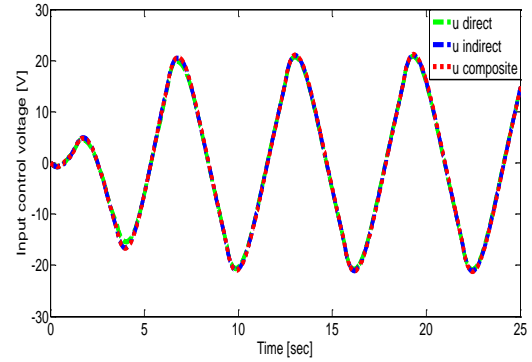


Fig. 4.40: Control input: u .

It can be seen from the results that all system states converge to their desired values, the surface errors converge to zero and the parameter estimates converge to its true values. All the results further verify that the proposed composite robust adaptive control approach is robust against the unknown external disturbances. The simulation results verify that designing of the proposed composite robust adaptive control scheme compared to direct and indirect robust adaptive control approaches is effective and useful to improve the performance of control and parameter estimation.

4.6 Conclusion

In this chapter, a new composite robust adaptive dynamic surface control approach for a class of SISO uncertain nonlinear systems in lower triangular form under unknown external disturbances is proposed. The proposed composite robust adaptive control scheme is designed also to avoid the problem of explosion of complexity inherent in the conventional adaptive backstepping control and the composite tuning functions based adaptive backstepping control designs. The proposed composite robust adaptive control scheme is applied to an electromechanical system. The proposed composite robust adaptive control method can guarantee the boundedness of all signals in the closed loop system by using the Lyapunov stability theory. In order to verify the effectiveness and robustness of the proposed composite robust adaptive control method, a comparative study between the proposed composite robust adaptive control approach over the direct and indirect robust adaptive control designs is performed. Next work will focus on developing of composite immersion and invariance based adaptive command filtered backstepping control technique to avoid also the problem of explosion of complexity.

CHAPTER 5

Composite immersion and invariance based adaptive command filtered backstepping control

Chapter 5

Composite immersion and invariance based adaptive command filtered backstepping control

5.1 Introduction

A drawback in the adaptive backstepping control and composite tuning functions based adaptive backstepping control designs is the problem of explosion of complexity caused by the repeated derivations of virtual control inputs. Command filtered backstepping control design has been proposed to solve this problem of explosion of complexity for the non-adaptive case [Far09, Far08]. In [Don12, Don10], the command filtered backstepping control method has been extended to adaptive control and has been extensively used to control a large class of uncertain nonlinear systems in lower triangular form [Pan18, Sou19, Yu18b, Yu15a, Zou20]. Composite adaptive command filtered backstepping control has been also introduced of uncertain nonlinear systems [Pan16a, Pan16b, Pan16c].

In recent years, immersion and invariance based adaptive control of nonlinear systems has been proposed by Astolfi and Ortega [Ast03]. It has been established for controlling of uncertain nonlinear systems in lower triangular form [Ast08a, Ast08b, Kar08, Kar07, Kar04, Sou21]. It has been also a great attention in the few recent years, which has been widely used to the control of uncertain nonlinear systems [Han19, Han18, Han17, Han16, Liu14, Lou18, Mon13, Son10a, Zha12b, Zha11]. The design procedure of immersion and invariance based adaptive control consists of a general two-step. While the first step deals with the design of an estimator, the second step consists in designing a control law. Over the past few years, many different types of nonlinear control methodologies have been proposed including adaptive command filtered backstepping control [Son10a, Son10b],

adaptive backstepping control [Mon13, Kar08, Kar07, Zha12b, Zha11], adaptive sliding mode control [Han15] and adaptive dynamic surface control [Fuj12, Sou21].

In this chapter, a new composite immersion and invariance based adaptive command filtered backstepping control approach is proposed for a class of SISO uncertain nonlinear systems in lower triangular form. The proposed composite adaptive control method is designed in order to improve parameter adaptation. The proposed composite adaptive control technique is introduced to avoid the problem of explosion of complexity inherent in the conventional adaptive backstepping control and composite tuning functions based adaptive backstepping control schemes. Based on the Lyapunov stability theory, it is proved that all signals in the closed-loop system are bounded. Simulation results for an electromechanical system are provided to verify the effectiveness of the proposed composite adaptive control methodology compared to immersion and invariance based adaptive control and indirect adaptive control approaches.

The rest of this chapter is arranged as follows. The immersion and invariance based adaptive command filtered backstepping control is presented in Section 5.2. Section 5.3 is dedicated to the indirect adaptive control is constructed. The composite immersion and invariance based adaptive command filtered backstepping control is proposed in Section 5.4. The simulation results are demonstrated in Section 5.5. Finally, some conclusions are given in Section 5.6.

5.2 Immersion and invariance based adaptive command filtered backstepping control

In this section, we will consider the following SISO uncertain nonlinear system in lower triangular form:

$$\begin{aligned}\dot{x}_1 &= g_1(x_1)x_2 + \varphi_1^T(x_1)\theta + \psi_1(x_1) \\ \dot{x}_i &= g_i(\bar{x}_i)x_{i+1} + \varphi_i^T(\bar{x}_i)\theta + \psi_i(\bar{x}_i), i = 2, \dots, n-1 \\ \dot{x}_n &= g_n(x)u + \varphi_n^T(x)\theta + \psi_n(x)\end{aligned}\tag{5.1}$$

where, $x = [x_1 \ x_2 \ \dots \ x_n]^T \in \mathbb{R}^n$ and $u \in \mathbb{R}$ are system states and the control input, respectively. $\theta \in \mathbb{R}^P$ is unknown constant parameter vector, $\bar{x}_i = [x_1 \ x_2 \ \dots \ x_i]^T$ and $x = \bar{x}_n$. The nonlinear functions φ_i^T , ψ_i and $g_i \neq 0$ are known and continuous. The control objective of this approach is to construct an immersion and invariance based adaptive command filtered backstepping controller u such that the system output x_1 tracks the

desired trajectory x_{1d} and all signals in the closed-loop system are bounded. Throughout this chapter, to facilitate the control design and synthesis, the following standard assumptions of the system (5.1) are necessary.

Assumption 5.2.1: There is a positive constant g_0 where, $|g_i(\bar{x}_i)| \geq g_0$, $i = 1, \dots, n$.

Assumption 5.2.2: The desired trajectory x_{1d} and its first derivative \dot{x}_{1d} are known, smooth and bounded.

Remark 5.2.1: For the composite tuning functions based adaptive backstepping control design, the information of $x_{1d}^{(i)}$ ($i = 0, \dots, n$) are required, and the composite adaptive and robust adaptive dynamic surface control designs require x_{1d} and both its first and second derivatives \dot{x}_{1d} and \ddot{x}_{1d} , whereas our proposed composite adaptive control approach only requires x_{1d} and its first derivative \dot{x}_{1d} , which is less stringent. Therefore, it is more appropriate for some practical applications.

5.2.1 Estimator design

Define the estimation errors as:

$$\tilde{\theta}_i = \hat{\theta}_i - \theta + \beta_i(\bar{x}_i) \quad (5.2)$$

where, $\hat{\theta}_i$ are the estimator states and $\beta_i: \mathbb{R}^i \rightarrow \mathbb{R}^p$ are function yet to be specified. Then, the dynamics of $\tilde{\theta}_i$ are given by [Kar08]:

$$\begin{aligned} \dot{\tilde{\theta}}_i &= \dot{\hat{\theta}}_i + \dot{\beta}_i = \dot{\hat{\theta}}_i + \sum_{k=1}^i \frac{\partial \beta_i}{\partial x_k} \dot{x}_k \\ &= \dot{\hat{\theta}}_i + \sum_{k=1}^i \frac{\partial \beta_i}{\partial x_k} \left(g_k x_{k+1} + \varphi_k^T (\hat{\theta}_i + \beta_i) + \psi_k \right) \end{aligned} \quad (5.3)$$

where, $x_{n+1} = u$. Selecting the adaptive laws $\dot{\hat{\theta}}_i$ to cancel the known quantities in the dynamics of $\tilde{\theta}_i$, i.e.,

$$\dot{\hat{\theta}}_i = - \sum_{k=1}^i \frac{\partial \beta_i}{\partial x_k} \left(g_k x_{k+1} + \varphi_k^T (\hat{\theta}_i + \beta_i) + \psi_k \right) \quad (5.4)$$

Substituting (5.4) into (5.3), we obtain the error dynamics as:

$$\dot{\tilde{\theta}}_i = - \left[\sum_{k=1}^i \frac{\partial \beta_i}{\partial x_k} \varphi_k^T \right] \tilde{\theta}_i \quad (5.5)$$

We select the functions β_i as [Kar08]:

$$\beta_i = \Gamma_i \int_0^{x_i} \varphi_i d\chi + \varepsilon_i \quad (5.6)$$

where, $\Gamma_i > 0$ are constants and ε_i are functions with $\varepsilon_1 = 0$. Now, we consider the following assumption.

Assumption 5.2.3: There exist functions ε_i satisfying the partial differential (matrix) inequality [Kar08]:

$$F_i + F_i^T \geq 0 \quad (5.7)$$

for, $i = 2, \dots, n-1$, where,

$$F_i = \Gamma_i \sum_{k=1}^{i-1} \frac{\partial}{\partial x_k} \left(\int_0^{x_i} \varphi_i d\chi \right) \varphi_k^T + \frac{\partial \varepsilon_i}{\partial x_i} \varphi_i^T \quad (5.8)$$

Remark 5.2.2: In the special case when $\varphi_i(\bullet)$ is a function of x_i only, the partial differential (matrix) inequality (5.7) admits the trivial solution $\varepsilon_i = 0$ for, $i = 2, \dots, n$. The same simplification occurs when only one of the functions $\varphi_i(\bullet)$ in (5.1) is nonzero. In general, the solvability of (5.7) relies strongly on the structure of the regressor $\varphi_i(\bullet)$ [Kar08].

Lemma 5.2.1: Consider the system (5.1), where the functions β_i are given by (5.6) and functions ε_i exist which satisfy (5.7). Then, the system (5.1) has a uniformly globally stable equilibrium at the origin, $\tilde{\theta}_i \in L_\infty$ and $\varphi_i^T \tilde{\theta}_i \in L_2$. In addition, φ_i and its time derivative $\dot{\varphi}_i$ are bounded, then $\varphi_i^T \tilde{\theta}_i$ converges to zero.

Proof: We consider the Lyapunov function W as:

$$W = \frac{1}{2} \sum_{i=1}^n \tilde{\theta}_i^T \Gamma_i^{-1} \tilde{\theta}_i \quad (5.9)$$

The derivative of the Lyapunov function \dot{W} becomes:

$$\begin{aligned} \dot{W} &= \frac{1}{2} \sum_{i=1}^n \left(\dot{\tilde{\theta}}_i^T \Gamma_i^{-1} \tilde{\theta}_i + \tilde{\theta}_i^T \Gamma_i^{-1} \dot{\tilde{\theta}}_i \right) \\ &= - \sum_{i=1}^n \tilde{\theta}_i^T \Gamma_i^{-1} \left(\Gamma_i \varphi_i \varphi_i^T + F_i + F_i^T \right) \tilde{\theta}_i \\ &\leq - \sum_{i=1}^n \tilde{\theta}_i^T \varphi_i \varphi_i^T \tilde{\theta}_i \\ &\leq - \sum_{i=1}^n \left(\varphi_i^T \tilde{\theta}_i \right)^2 \end{aligned} \quad (5.10)$$

By integrating of inequality (5.10) over $[0, \infty]$, we obtain:

$$\int_0^{\infty} \sum_{i=1}^n (\varphi_i^T \tilde{\theta}_i)^2 d\tau \leq W(0) - W(\infty) < \infty \quad (5.11)$$

As a result, $W \in L_{\infty}$, $\tilde{\theta}_i \in L_{\infty}$ and $\varphi_i^T \tilde{\theta}_i \in L_2$. Furthermore, φ_i and $\dot{\varphi}_i$ are bounded. By using Barbala's lemma [Slo91], we get $\lim_{t \rightarrow \infty} \varphi_i^T \tilde{\theta}_i = 0$. By definition (5.2), this implies that an asymptotic estimate of each term $\varphi_i^T \theta$ in (5.1) is given by $\varphi_i^T (\hat{\theta}_i + \beta_i)$.

5.2.2 Controller design

In this section, the controller design presented here includes command filters. Then, the controller design procedures for system (5.1) with stability analysis using Lyapunov stability theory are established as follows.

Step 1: Define the first tracking error as $e_1 = x_1 - x_{1d}$, then, the time derivative of e_1 is obtained as:

$$\dot{e}_1 = g_1 x_2 + \varphi_1^T \theta + \psi_1 - \dot{x}_{1d} = g_1 e_2 + g_1 x_{2c} + \varphi_1^T \theta + \psi_1 - \dot{x}_{1d} \quad (5.12)$$

We choose the virtual control α_1 as:

$$\alpha_1 = \frac{1}{g_1} \left(-k_1 e_1 - \varphi_1^T (\hat{\theta}_1 + \beta_1) - \psi_1 + \dot{x}_{1d} \right) \quad (5.13)$$

where, $k_1 > 0$ is a positive design constant. The corresponding Lyapunov function candidate V_1 is defined as:

$$V_1 = \frac{1}{2} e_1^2 \quad (5.14)$$

The time derivative of V_1 is given by:

$$\begin{aligned} \dot{V}_1 &= e_1 \left(g_1 e_2 + g_1 (x_{2c} - \alpha_1) + g_1 \alpha_1 + \varphi_1^T \theta + \psi_1 - \dot{x}_{1d} \right) \\ &= e_1 \left(-k_1 e_1 + g_1 e_2 + g_1 (x_{2c} - \alpha_1) - \varphi_1^T \tilde{\theta}_1 \right) \\ &= -k_1 e_1^2 + g_1 (x_{2c} - \alpha_1) e_1 + g_1 e_1 e_2 - e_1 \varphi_1^T \tilde{\theta}_1 \end{aligned} \quad (5.15)$$

Step i ($i = 2, \dots, n-1$): The command filter output signal x_{ic} is generated by the command filter [Don12, Don10]:

$$\dot{x}_{ic} = -\omega_i (x_{ic} - \alpha_{i-1}), x_{ic}(0) = \alpha_{i-1}(0) \quad (5.16)$$

where, $\omega_i > 0$ is a positive design constants.

Define the i^{th} tracking error as $e_i = x_i - x_{ic}$, then, the time derivative of e_i is obtained as:

$$\dot{e}_i = g_i e_{i+1} + g_i x_{(i+1)c} + \varphi_i^T \theta + \psi_i - \dot{x}_{ic} \quad (5.17)$$

We choose the virtual controllers α_i as:

$$\alpha_i = \frac{1}{g_i} \left(-k_i e_i - \varphi_i^T (\hat{\theta}_i + \beta_i) - \psi_i + \dot{x}_{ic} - g_{i-1} e_{i-1} \right) \quad (5.18)$$

where, $k_i > 0$ is a positive design constants. The corresponding Lyapunov function candidate V_i is defined as:

$$V_i = V_{i-1} + \frac{1}{2} e_i^2 \quad (5.19)$$

The time derivative of V_i is given by:

$$\dot{V}_i = -\sum_{i=1}^{n-1} k_i e_i^2 + \sum_{i=1}^{n-1} g_i (x_{(i+1)c} - \alpha_i) e_i + g_i e_i e_{i+1} - \sum_{i=1}^{n-1} e_i \varphi_i^T \tilde{\theta}_i \quad (5.20)$$

Step n : The command filter output signal x_{nc} is generated by the command filter [Don12, Don10]:

$$\dot{x}_{nc} = -\omega_n (x_{nc} - \alpha_{n-1}), x_{nc}(0) = \alpha_{n-1}(0) \quad (5.21)$$

where, $\omega_n > 0$ is a positive design constant. Define the n^{th} tracking error as $e_n = x_n - x_{nc}$, then, the time derivative of e_n is obtained as:

$$\dot{e}_n = g_n u + \varphi_n^T \theta + \psi_n - \dot{x}_{nc} \quad (5.22)$$

We choose the actual control input u as:

$$u = \frac{1}{g_n} \left(-k_n e_n - \varphi_n^T (\hat{\theta}_n + \beta_n) - \psi_n + \dot{x}_{nc} - g_{n-1} e_{n-1} \right) \quad (5.23)$$

where, $k_n > 0$ is a positive design constant. The corresponding Lyapunov function candidate $V = V_n$ is defined as:

$$V = \frac{1}{2} \sum_{i=1}^n e_i^2 \quad (5.24)$$

The time derivative of V is given by:

$$\dot{V} = -\sum_{i=1}^n k_i e_i^2 + \sum_{i=1}^{n-1} g_i (x_{(i+1)c} - \alpha_i) e_i - \sum_{i=1}^n e_i \varphi_i^T \tilde{\theta}_i \quad (5.25)$$

Applying of the following Young's inequality:

$$-e_i \varphi_i^T \tilde{\theta}_i \leq \frac{1}{2} e_i^2 + \frac{1}{2} (\varphi_i^T \tilde{\theta}_i)^2 \quad (5.26)$$

Note that, $|x_{(i+1)c} - \alpha_i| \leq \bar{\mu}$, therefore,

$$\begin{aligned} \dot{V} &\leq -\sum_{i=1}^n k_i e_i^2 + \bar{\mu} \bar{g} \sum_{i=1}^{n-1} |e_i| - \sum_{i=1}^n e_i \varphi_i^T \tilde{\theta}_i \\ &\leq -\sum_{i=1}^n \left(k_i - \frac{1}{2} \right) e_i^2 + \bar{\mu} \bar{g} \sum_{i=1}^{n-1} |e_i| + \frac{1}{2} \sum_{i=1}^n (\varphi_i^T \tilde{\theta}_i)^2 \\ &\leq -k_0 \|e\|^2 - k_0 \sum_{i=1}^{n-1} \left(e_i^2 - \frac{\bar{\mu} \bar{g}}{k_0} |e_i| \right) + \frac{1}{2} \sum_{i=1}^n (\varphi_i^T \tilde{\theta}_i)^2 \end{aligned} \quad (5.27)$$

where, $k_0 = 2 \min_{1 \leq i \leq n} \left\{ k_i - \frac{1}{2} \right\}$, $\bar{g} = \max_{1 \leq i \leq n-1} \{g_i\}$ and $\bar{\mu} > 0$. Applying of Young's

inequality, $ab \leq a^2 + \frac{1}{4} b^2$ où $a, b \in \mathbb{R}$, we obtain:

$$\dot{V} \leq -k_0 \|e\|^2 + (n-1) \frac{\bar{\mu}^2 \bar{g}^2}{4k_0} + \frac{1}{2} \sum_{i=1}^n (\varphi_i^T \tilde{\theta}_i)^2 \quad (5.28)$$

with, $\rho = (n-1) \frac{\bar{\mu}^2 \bar{g}^2}{4k_0}$, therefore,

$$\dot{V} \leq -k_0 \|e\|^2 + \rho + \frac{1}{2} \sum_{i=1}^n (\varphi_i^T \tilde{\theta}_i)^2 \quad (5.29)$$

We choose the Lyapunov function V_c as follows:

$$V_c = \frac{1}{2} \sum_{i=1}^n e_i^2 + \frac{1}{2} \sum_{i=1}^n \tilde{\theta}_i^T \Gamma_i^{-1} \tilde{\theta}_i \quad (5.30)$$

The derivative of the Lyapunov function \dot{V}_c becomes:

$$\dot{V}_c \leq -k_0 \|e\|^2 + \rho - \frac{1}{2} \sum_{i=1}^n (\varphi_i^T \tilde{\theta}_i)^2 \quad (5.31)$$

\dot{V}_c is negative for, $\|e\| > \sqrt{n-1} \frac{\bar{\mu} \bar{g}}{2k_0}$. Therefore, we can conclude that, V_c , e and $\varphi_i^T \tilde{\theta}_i$ are

bounded. Furthermore, all signals in the closed-loop system, i.e., x_1 , x_{1d} , \dot{x}_{1d} , x_i , x_{ic} , \dot{x}_{ic} ($i = 2, \dots, n$), α_i , u and $\hat{\theta}_i + \beta_i$ ($i = 1, \dots, n$) are also bounded.

5.3 Indirect adaptive control

The detailed procedures for the indirect adaptive control design with stability analysis are given as follows.

5.3.1 Identification based x-swapping filters

We consider the uncertain nonlinear system (5.1), which can be rewritten under the following nonlinear system in parametric x-model form as:

$$\dot{x}_i = f_i(x, u) + \varphi_i^T(\bar{x}_i)\theta \quad (5.32)$$

where,

$$f_i(x, u) = \begin{bmatrix} g_1 x_2 + \psi_1 \\ \vdots \\ g_{n-1} x_n + \psi_{n-1} \\ g_n u + \psi_n \end{bmatrix} \quad (5.33)$$

We introduce the following x-swapping filters as:

$$\dot{\Omega}_{0i} = a_i(\Omega_{0i} + x_i) - f_i(x, u), \Omega_{0i} \in \mathbb{R} \quad (5.34)$$

$$\dot{\Omega}_i^T = a_i \Omega_i^T + \varphi_i^T(\bar{x}_i), \Omega_i \in \mathbb{R}^{p_i} \quad (5.35)$$

where, $i = 1, \dots, n$ and $a_i < 0$ is a negative definite scalar function for each x continuous in t . We define the estimation errors as:

$$\epsilon_i = x_i + \Omega_{0i} - \Omega_i^T(\hat{\theta}_i + \beta_i), \epsilon_i \in \mathbb{R} \quad (5.36)$$

with, $\hat{\theta}_i + \beta_i$ the estimate of θ and let:

$$\tilde{\epsilon}_i = x_i + \Omega_{0i} - \Omega_i^T \theta, \tilde{\epsilon}_i \in \mathbb{R} \quad (5.37)$$

Then, we obtain:

$$\epsilon_i = -\Omega_i^T \tilde{\theta}_i + \tilde{\epsilon}_i \quad (5.38)$$

The error signal $\tilde{\epsilon}_i$ satisfies:

$$\dot{\tilde{\epsilon}}_i = \dot{x}_i + \dot{\Omega}_{0i} - \dot{\Omega}_i^T \theta = a_i \tilde{\epsilon}_i \quad (5.39)$$

To guarantee the boundedness of Ω_i when $\varphi_i(\bar{x}_i)$ grows unbounded, a particular choice of a_i is made:

$$a_i = a_{0i} - \lambda_i \varphi_i^T(\bar{x}_i) \varphi_i(\bar{x}_i) P_i \quad (5.40)$$

where, $\lambda_i > 0$ and a_{0i} is an arbitrary negative constant satisfying [Sou18]:

$$2P_i a_{0i} = -1, P_i > 0 \quad (5.41)$$

5.3.2 Choice of modified adaptive laws

The modified gradient adaptive laws are defined as:

$$\dot{\hat{\theta}}_i = \Gamma_i \frac{\Omega_i \epsilon_i}{1 + \nu_i \text{tr}\{\Omega_i^T \Omega_i\}} - \dot{\beta}_i, \Gamma_i > 0, \nu_i \geq 0 \quad (5.42)$$

The modified least squares adaptive laws are defined as:

$$\dot{\hat{\theta}}_i = \Gamma_i \frac{\Omega_i \epsilon_i}{1 + \nu_i \text{tr}\{\Omega_i^T \Gamma_i \Omega_i\}} - \dot{\beta}_i \quad (5.43)$$

where, Γ_i is given by:

$$\dot{\Gamma}_i = -\Gamma_i \frac{\Omega_i \Omega_i^T}{1 + \nu_i \text{tr}\{\Omega_i^T \Gamma_i \Omega_i\}} \Gamma_i, \Gamma_i(0) > 0, \nu_i \geq 0 \quad (5.44)$$

with, $\dot{\beta}_i = \sum_{k=1}^i \frac{\partial \beta_i}{\partial x_k} \dot{x}_k$.

5.3.3 Proof of stability

Lemma 4.3.1: To establish the identifier properties, let $[0, t_f)$, the maximal interval of existence of solutions of (5.32), the x-swapping filters (5.34) and (5.35), and the modified gradient adaptive laws (5.42) or the modified least squares adaptive laws (5.43) and (5.44).

Then for $\nu_i \geq 0$, the following properties hold:

$$\tilde{\theta}_i \in L_\infty \quad (5.45)$$

$$\epsilon_i \in L_2 \cap L_\infty \quad (5.46)$$

$$\dot{\hat{\theta}}_i \in L_2 \cap L_\infty \quad (5.47)$$

5.3.3.1 Modified gradient adaptive laws

We consider the following Lyapunov function as:

$$V_i = \frac{1}{2} \tilde{\theta}_i^T \Gamma_i^{-1} \tilde{\theta}_i + P_i \tilde{\epsilon}_i^2 \quad (5.48)$$

Along of dynamic equations (5.39) and (5.42), the derivative of the Lyapunov function \dot{V}_i becomes:

$$\begin{aligned} \dot{V}_i &= \tilde{\theta}_i^T \Gamma_i^{-1} \dot{\tilde{\theta}}_i + 2P_i \tilde{\epsilon}_i \dot{\tilde{\epsilon}}_i \\ &= \tilde{\theta}_i^T \Gamma_i^{-1} \dot{\tilde{\theta}}_i + 2P_i a_i \tilde{\epsilon}_i^2 \\ &= \tilde{\theta}_i^T \Gamma_i^{-1} \dot{\tilde{\theta}}_i + 2P_i (a_{0i} - \lambda_i \phi_i^T(\bar{x}_i) \phi_i(\bar{x}_i) P_i) \tilde{\epsilon}_i^2 \\ &= \tilde{\theta}_i^T \Gamma_i^{-1} \dot{\tilde{\theta}}_i + (-1 - 2\lambda_i P_i \phi_i^T(\bar{x}_i) \phi_i(\bar{x}_i) P_i) \tilde{\epsilon}_i^2 \end{aligned} \quad (5.49)$$

Applying of inequality (3.55), we obtain:

$$\begin{aligned}
\dot{V}_i &\leq \tilde{\theta}_i^T \Gamma_i^{-1} \left(\dot{\hat{\theta}}_i + \dot{\beta}_i \right) - \tilde{\epsilon}_i^2 = \frac{\tilde{\theta}_i^T \Omega_i \epsilon_i}{1 + \nu_i \text{tr} \{ \Omega_i^T \Omega_i \}} - \tilde{\epsilon}_i^2 \\
&= -\frac{\epsilon_i^2}{1 + \nu_i \text{tr} \{ \Omega_i^T \Omega_i \}} + \frac{\epsilon_i}{1 + \nu_i \text{tr} \{ \Omega_i^T \Omega_i \}} \tilde{\epsilon}_i - \tilde{\epsilon}_i^2 \\
&\leq -\frac{3}{4} \frac{\epsilon_i^2}{1 + \nu_i \text{tr} \{ \Omega_i^T \Omega_i \}} - \frac{1}{4} \frac{\epsilon_i^2}{\left(1 + \nu_i \text{tr} \{ \Omega_i^T \Omega_i \} \right)^2} + \frac{\epsilon_i}{1 + \nu_i \text{tr} \{ \Omega_i^T \Omega_i \}} \tilde{\epsilon}_i - \tilde{\epsilon}_i^2 \quad (5.50) \\
&= -\frac{3}{4} \frac{\epsilon_i^2}{1 + \nu_i \text{tr} \{ \Omega_i^T \Omega_i \}} - \left(\frac{\epsilon_i}{2 \left(1 + \nu_i \text{tr} \{ \Omega_i^T \Omega_i \} \right)} - \tilde{\epsilon}_i \right)^2 \\
&\leq -\frac{3}{4} \frac{\epsilon_i^2}{1 + \nu_i \text{tr} \{ \Omega_i^T \Omega_i \}}
\end{aligned}$$

The nonpositivity of \dot{V}_i proves that, $\tilde{\theta}_i \in L_\infty$ (bounded). Due to $\epsilon_i = -\Omega_i^T \tilde{\theta}_i + \tilde{\epsilon}_i$ and the boundedness of Ω_i , it follows that $\epsilon_i \in L_\infty$, which, in turn proves that $\dot{\hat{\theta}}_i \in L_\infty$.

By integrating of inequality (5.50) over $[0, \infty]$, we obtain:

$$\int_0^\infty \frac{\epsilon_i^2}{1 + \nu_i \text{tr} \{ \Omega_i^T \Omega_i \}} d\tau \leq \frac{4}{3} (V_i(0) - V_i(\infty)) < \infty \quad (5.51)$$

This means that, $\frac{\epsilon_i}{\sqrt{1 + \nu_i \text{tr} \{ \Omega_i^T \Omega_i \}}} \in L_2$. Since Ω_i is bounded, then $\epsilon_i \in L_2$. The

boundedness of Ω_i and the square integrability of ϵ_i prove that $\dot{\hat{\theta}}_i \in L_2$.

5.3.3.2 Modified least squares adaptive laws

From (5.43) and (5.44), we have the following identity:

$$\frac{d}{dt} (\Gamma_i^{-1}) = -\Gamma_i^{-1} \dot{\Gamma}_i \Gamma_i^{-1} = \frac{\Omega_i \Omega_i^T}{1 + \nu_i \text{tr} \{ \Omega_i^T \Gamma_i \Omega_i \}} \geq 0 \quad (5.52)$$

The Lyapunov function is chosen as follows:

$$V_i = \tilde{\theta}_i^T \Gamma_i^{-1}(t) \tilde{\theta}_i + P_i \tilde{\epsilon}_i^2 \quad (5.53)$$

Along of dynamic equations (5.39), (5.43) and (5.44), the derivative of the Lyapunov function \dot{V}_i becomes:

$$\begin{aligned}
\dot{V}_i &= \dot{\tilde{\theta}}_i^T \Gamma_i^{-1} \tilde{\theta}_i + \tilde{\theta}_i^T \frac{d}{dt} (\Gamma_i^{-1} \tilde{\theta}_i) + 2P_i \tilde{\epsilon}_i \dot{\tilde{\epsilon}}_i \\
&= \dot{\tilde{\theta}}_i^T \Gamma_i^{-1} \tilde{\theta}_i - \tilde{\theta}_i^T \Gamma_i^{-1} \dot{\Gamma}_i \Gamma_i^{-1} \tilde{\theta}_i + \tilde{\theta}_i^T \Gamma_i^{-1} \dot{\tilde{\theta}}_i + 2P_i a_i \tilde{\epsilon}_i^2 \\
&= \dot{\tilde{\theta}}_i^T \Gamma_i^{-1} \tilde{\theta}_i - \tilde{\theta}_i^T \Gamma_i^{-1} \dot{\Gamma}_i \Gamma_i^{-1} \tilde{\theta}_i + \tilde{\theta}_i^T \Gamma_i^{-1} \dot{\tilde{\theta}}_i + 2P_i (a_{0i} - \lambda_i \varphi_i^T(\bar{x}_i) \varphi_i(\bar{x}_i) P_i) \tilde{\epsilon}_i^2 \\
&= \dot{\tilde{\theta}}_i^T \Gamma_i^{-1} \tilde{\theta}_i - \tilde{\theta}_i^T \Gamma_i^{-1} \dot{\Gamma}_i \Gamma_i^{-1} \tilde{\theta}_i + \tilde{\theta}_i^T \Gamma_i^{-1} \dot{\tilde{\theta}}_i + (-1 - 2\lambda_i P_i \varphi_i^T(\bar{x}_i) \varphi_i(\bar{x}_i) P_i) \tilde{\epsilon}_i^2
\end{aligned} \tag{5.54}$$

Applying of inequality (3.55), we obtain:

$$\begin{aligned}
\dot{V}_i &\leq (\dot{\hat{\theta}}_i^T + \dot{\beta}_i) \Gamma_i^{-1} \tilde{\theta}_i - \tilde{\theta}_i^T \Gamma_i^{-1} \dot{\Gamma}_i \Gamma_i^{-1} \tilde{\theta}_i + \tilde{\theta}_i^T \Gamma_i^{-1} (\dot{\hat{\theta}}_i + \dot{\beta}_i) - \tilde{\epsilon}_i^2 \\
&= \frac{\Omega_i^T \tilde{\theta}_i \epsilon_i}{1 + \nu_i \text{tr}\{\Omega_i^T \Gamma_i \Omega_i\}} + \frac{\tilde{\theta}_i^T \Omega_i \Omega_i^T \tilde{\theta}_i}{1 + \nu_i \text{tr}\{\Omega_i^T \Gamma_i \Omega_i\}} + \frac{\tilde{\theta}_i^T \Omega_i \epsilon_i}{1 + \nu_i \text{tr}\{\Omega_i^T \Gamma_i \Omega_i\}} - \tilde{\epsilon}_i^2 \\
&\leq \frac{\Omega_i^T \tilde{\theta}_i \epsilon_i}{1 + \nu_i \text{tr}\{\Omega_i^T \Gamma_i \Omega_i\}} + \frac{\tilde{\theta}_i^T \Omega_i \tilde{\epsilon}_i}{1 + \nu_i \text{tr}\{\Omega_i^T \Gamma_i \Omega_i\}} - \tilde{\epsilon}_i^2 \\
&= -\frac{\epsilon_i^2}{1 + \nu_i \text{tr}\{\Omega_i^T \Gamma_i \Omega_i\}} + \frac{\tilde{\epsilon}_i^2}{1 + \nu_i \text{tr}\{\Omega_i^T \Gamma_i \Omega_i\}} - \tilde{\epsilon}_i^2 \\
&\leq -\frac{\epsilon_i^2}{1 + \nu_i \text{tr}\{\Omega_i^T \Gamma_i \Omega_i\}}
\end{aligned} \tag{5.55}$$

Which, due to the positive definiteness of $\Gamma_i^{-1}(t)$, proves that, $\tilde{\theta}_i \in L_\infty$ (bounded).

By integrating of inequality (5.55) over $[0, \infty]$, we obtain:

$$\int_0^\infty \frac{\epsilon_i^2}{1 + \nu_i \text{tr}\{\Omega_i^T \Gamma_i \Omega_i\}} d\tau \leq V_i(0) - V_i(\infty) < \infty \tag{5.56}$$

This means that, $\frac{\epsilon_i}{\sqrt{1 + \nu_i \text{tr}\{\Omega_i^T \Gamma_i \Omega_i\}}} \in L_2$. Using the boundedness of Γ_i and Ω_i , following

the same line of argument as for the modified gradient adaptive laws, we prove that

$\epsilon_i \in L_2 \cap L_\infty$ and $\dot{\tilde{\theta}}_i \in L_2 \cap L_\infty$.

5.4 Composite immersion and invariance based adaptive command filtered backstepping control

The proposed composite immersion and invariance based adaptive command filtered backstepping control in this section uses both parameter adaptive laws of the immersion and invariance based adaptive command filtered backstepping control described by (5.4) with the estimation error based parameter adaptive laws of the indirect adaptive control

described by (5.42) and (5.43). The control objective of this approach is to construct a composite immersion and invariance based adaptive command filtered backstepping controller u such that the system output x_1 tracks the desired trajectory x_{1d} and to ensure that all signals in the closed-loop system are bounded. The main procedures for designing the composite immersion and invariance based adaptive command filtered backstepping control scheme for system (5.1) with stability analysis are summarized as follows.

5.4.1 Composite projection based gradient adaptive laws

Projection properties: We assume that θ is estimated by $\bar{\Theta}_i = \hat{\theta}_i + \beta_i$, where, $\bar{\Theta}_i$ are the estimates of θ . Terms $\hat{\theta}_i$ and β_i are two parts of the estimates need to be judiciously designed. The estimation errors are given by:

$$\tilde{\theta}_i = \bar{\Theta}_i - \theta = \hat{\theta}_i + \beta_i - \theta \quad (5.57)$$

The projection operator is defined as:

$$\text{Proj}_{\bar{\Theta}_i}(\bullet_i) = \begin{cases} \bullet_i & \text{if } \bar{\Theta}_i^T \bar{\Theta}_i < \bar{M}_i^2 \text{ or if } (\bar{\Theta}_i^T \bar{\Theta}_i = \bar{M}_i^2 \text{ and } \bullet_i \bar{\Theta}_i \leq 0), \\ 0 & \text{otherwise.} \end{cases} \quad (5.58)$$

where, ' \bullet_i ' represents any reasonable adaptation function. The projection algorithm guarantees that the parameter estimates $\bar{\Theta}_i$ of θ remain bounded and satisfy the inequality, $\|\bar{\Theta}_i\| \leq \bar{M}_i$.

Moreover, the projection mapping used in (5.58) guarantees that:

$$-\tilde{\theta}_i^T \text{Proj}_{\bar{\Theta}_i}(\bullet_i) \leq -\tilde{\theta}_i^T \bullet_i \quad (5.59)$$

Therefore, the composite projection based gradient adaptive laws are defined as:

$$\dot{\hat{\theta}}_i = \text{Proj}_{\hat{\theta}_i} \left(-\sum_{k=1}^i \frac{\partial \beta_i}{\partial x_k} (g_k x_{k+1} + \varphi_k^T (\hat{\theta}_i + \beta_i) + \psi_k) + \Gamma_i \frac{\Omega_i \epsilon_i}{1 + \nu_i \text{tr} \{ \Omega_i^T \Omega_i \}} \right) \quad (5.60)$$

The dynamics of estimation errors are given by:

$$\begin{aligned} \dot{\tilde{\theta}}_i = & \text{Proj}_{\hat{\theta}_i} \left(-\sum_{k=1}^i \frac{\partial \beta_i}{\partial x_k} (g_k x_{k+1} + \varphi_k^T (\hat{\theta}_i + \beta_i) + \psi_k) + \Gamma_i \frac{\Omega_i \epsilon_i}{1 + \nu_i \text{tr} \{ \Omega_i^T \Omega_i \}} \right) \\ & + \sum_{k=1}^i \frac{\partial \beta_i}{\partial x_k} (g_k x_{k+1} + \varphi_k^T (\hat{\theta}_i + \beta_i) + \psi_k) - \left[\sum_{k=1}^i \frac{\partial \beta_i}{\partial x_k} \varphi_k^T \right] \tilde{\theta}_i \end{aligned} \quad (5.61)$$

where, $\epsilon_i = x_i + \Omega_{0i} - \Omega_i^T (\hat{\theta}_i + \beta_i)$.

Theorem 5.4.1: Consider the SISO uncertain nonlinear system in lower triangular form composed of the plant described by (5.1). Suppose that assumptions 5.2.1 and 5.2.2 are satisfied. Then, the virtual controllers (5.13) and (5.18), the actual control input (5.23) and the composite projection based gradient adaptive laws (5.60) guarantee that all signals in the closed-loop system are bounded.

Proof: We consider the following Lyapunov function as:

$$V = \frac{1}{2} \sum_{i=1}^n e_i^2 + \frac{1}{2} \sum_{i=1}^n \tilde{\theta}_i^T \Gamma_i^{-1} \tilde{\theta}_i + \sum_{i=1}^n P_i \tilde{\epsilon}_i^2 \quad (5.62)$$

The derivative of the Lyapunov function \dot{V} becomes:

$$\begin{aligned} \dot{V} &\leq -k_0 \|e\|^2 + \rho + \frac{1}{2} \sum_{i=1}^n (\varphi_i^T \tilde{\theta}_i)^2 + \sum_{i=1}^n \tilde{\theta}_i^T \Gamma_i^{-1} \dot{\tilde{\theta}}_i + 2 \sum_{i=1}^n P_i \tilde{\epsilon}_i \dot{\tilde{\epsilon}}_i \\ &\leq -k_0 \|e\|^2 + \rho + \frac{1}{2} \sum_{i=1}^n (\varphi_i^T \tilde{\theta}_i)^2 + \sum_{i=1}^n \frac{\tilde{\theta}_i^T \Omega_i \epsilon_i}{1 + \nu_i \text{tr}\{\Omega_i^T \Omega_i\}} - \sum_{i=1}^n \tilde{\theta}_i^T \Gamma_i^{-1} \left[\sum_{k=1}^i \frac{\partial \beta_i}{\partial x_k} \varphi_k^T \right] \tilde{\theta}_i - \sum_{i=1}^n \tilde{\epsilon}_i^2 \quad (5.63) \\ &\leq -k_0 \|e\|^2 + \rho - \frac{1}{2} \sum_{i=1}^n (\varphi_i^T \tilde{\theta}_i)^2 - \frac{3}{4} \sum_{i=1}^n \frac{\epsilon_i^2}{1 + \nu_i \text{tr}\{\Omega_i^T \Omega_i\}} \end{aligned}$$

\dot{V} is negative for, $\|e\| > \sqrt{n-1} \frac{\bar{\mu} \bar{g}}{2k_0}$. Therefore, we can conclude that, V , e , $\varphi_i^T \tilde{\theta}_i$, $\tilde{\theta}_i$ and

ϵ_i are bounded. Furthermore, all signals in the closed-loop system, i.e., x_1 , x_{1d} , \dot{x}_{1d} , x_i , x_{ic} , \dot{x}_{ic} ($i=2, \dots, n$), α_i , u and $\hat{\theta}_i + \beta_i$ ($i=1, \dots, n$) are also bounded.

5.4.2 Composite σ -modification based gradient and least squares adaptive laws

The composite σ -modification based gradient and least squares adaptive laws are defined as:

$$\dot{\hat{\theta}}_i = - \sum_{k=1}^i \frac{\partial \beta_i}{\partial x_k} \left(g_k x_{k+1} + \varphi_k^T (\hat{\theta}_i + \beta_i) + \psi_k \right) - \Gamma_i \sigma_{\theta_i} (\hat{\theta}_i + \beta_i - \bar{\theta}_i), \Gamma_i > 0, \sigma_{\theta_i} > 0 \quad (5.64)$$

where, σ_{θ_i} are small design constants to introduce the σ -modification for the closed-loop system and $\bar{\theta}_i$ are computed with the gradient method as follows:

$$\dot{\bar{\theta}}_i = \bar{\Gamma}_i \frac{\Omega_i \epsilon_i}{1 + \nu_i \text{tr}\{\Omega_i^T \Omega_i\}} - \dot{\beta}_i, \bar{\Gamma}_i > 0, \nu_i \geq 0 \quad (5.65)$$

or with the least squares method as follows:

$$\dot{\bar{\theta}}_i = \bar{\Gamma}_i \frac{\Omega_i \epsilon_i}{1 + \nu_i \text{tr}\{\Omega_i^T \bar{\Gamma}_i \Omega_i\}} - \dot{\beta}_i \quad (5.66)$$

where, $\bar{\Gamma}_i$ are given by:

$$\dot{\bar{\Gamma}}_i = -\bar{\Gamma}_i \frac{\Omega_i \Omega_i^T}{1 + \nu_i \text{tr}\{\Omega_i^T \bar{\Gamma}_i \Omega_i\}} \bar{\Gamma}_i, \bar{\Gamma}_i(0) > 0, \nu_i \geq 0 \quad (5.67)$$

with, $\epsilon_i = x_i + \Omega_{0i} - \Omega_i^T (\bar{\theta}_i + \beta_i)$ and $\dot{\beta}_i = \sum_{k=1}^i \frac{\partial \beta_i}{\partial x_k} \dot{x}_k$. The dynamics of estimation errors are

given by:

$$\dot{\tilde{\theta}}_i = - \left[\sum_{k=1}^i \frac{\partial \beta_i}{\partial x_k} \varphi_k^T \right] \tilde{\theta}_i - \Gamma_i \sigma_{\theta_i} (\hat{\theta}_i + \beta_i - \bar{\theta}_i) \quad (5.68)$$

Theorem 5.4.2: Consider SISO the uncertain nonlinear system in lower triangular form composed of the plant described by (5.1). Suppose that assumptions 5.2.1 and 5.2.2 are satisfied. Then, the virtual controllers (5.13) and (5.18), the actual control input (5.23) and the composite σ -modification based gradient and least squares adaptive laws (5.64) guarantee that all signals in the closed-loop system are UUB and the tracking errors converge to a sufficiently small neighborhood of the origin by appropriately adjusting the design parameters.

Proof: We consider the following Lyapunov function as:

$$V = \frac{1}{2} \sum_{i=1}^n e_i^2 + \frac{1}{2} \sum_{i=1}^n \tilde{\theta}_i^T \Gamma_i^{-1} \tilde{\theta}_i \quad (5.69)$$

The derivative of the Lyapunov function \dot{V} is given by:

$$\begin{aligned} \dot{V} &\leq -k_0 \|e\|^2 + \rho + \frac{1}{2} \sum_{i=1}^n (\varphi_i^T \tilde{\theta}_i)^2 + \sum_{i=1}^n \tilde{\theta}_i^T \Gamma_i^{-1} \dot{\tilde{\theta}}_i \\ &\leq -k_0 \|e\|^2 + \rho + \frac{1}{2} \sum_{i=1}^n (\varphi_i^T \tilde{\theta}_i)^2 - \sum_{i=1}^n \tilde{\theta}_i^T \Gamma_i^{-1} \left[\sum_{k=1}^i \frac{\partial \beta_i}{\partial x_k} \varphi_k^T \right] \tilde{\theta}_i - \sum_{i=1}^n \sigma_{\theta_i} \tilde{\theta}_i^T (\hat{\theta}_i + \beta_i - \bar{\theta}_i) \\ &\leq -k_0 \|e\|^2 + \rho - \frac{1}{2} \sum_{i=1}^n (\varphi_i^T \tilde{\theta}_i)^2 - \sum_{i=1}^n \sigma_{\theta_i} \tilde{\theta}_i^T (\hat{\theta}_i + \beta_i - \bar{\theta}_i) \end{aligned} \quad (5.70)$$

We assume that, $\theta - \bar{\theta}_i$ is bounded, thus, $e_{\theta_i} = \theta - \bar{\theta}_i$ is bounded, $\bar{\theta}_i = \theta - e_{\theta_i}$ and

$\tilde{\theta}_i = \hat{\theta}_i + \beta_i - \theta$. The derivative of the Lyapunov function \dot{V} becomes:

$$\begin{aligned} \dot{V} &\leq -k_0 \|e\|^2 + \rho - \frac{1}{2} \sum_{i=1}^n (\varphi_i^T \tilde{\theta}_i)^2 - \sum_{i=1}^n \sigma_{\theta_i} \tilde{\theta}_i^T (\tilde{\theta}_i + e_{\theta_i}) \\ &\leq -k_0 \|e\|^2 + \rho - \frac{1}{2} \sum_{i=1}^n (\varphi_i^T \tilde{\theta}_i)^2 - \sum_{i=1}^n \sigma_{\theta_i} \tilde{\theta}_i^T \tilde{\theta}_i - \sum_{i=1}^n \sigma_{\theta_i} \tilde{\theta}_i^T e_{\theta_i} \end{aligned} \quad (5.71)$$

Applying of inequality (3.87), we obtain:

$$\begin{aligned}\dot{V} &\leq -k_0 \|e\|^2 + \rho - \frac{1}{2} \sum_{i=1}^n (\varphi_i^T \tilde{\theta}_i)^2 - \sum_{i=1}^n \frac{\sigma_{\theta_i}}{2} \tilde{\theta}_i^T \tilde{\theta}_i + \sum_{i=1}^n \frac{\sigma_{\theta_i}}{2} e_{\theta_i}^2 \\ &\leq -k_0 \|e\|^2 - \frac{1}{2} \sum_{i=1}^n (\varphi_i^T \tilde{\theta}_i)^2 - \sum_{i=1}^n \frac{\sigma_{\theta_i}}{2} \tilde{\theta}_i^T \tilde{\theta}_i + \mu\end{aligned}\quad (5.72)$$

In addition, the above inequality can be rewritten as:

$$\dot{V} \leq -\pi V + \mu \quad (5.73)$$

where, $\pi = \min\{2k_0, \Gamma_i \sigma_{\theta_i}\}$ and $\mu = \rho + \sum_{i=1}^n \frac{\sigma_{\theta_i}}{2} e_{\theta_i}^2$. Multiplying both sides by $e^{\pi t}$, (5.73)

can be rewritten as:

$$\frac{d}{dt} (V(t) e^{\pi t}) \leq \mu e^{\pi t} \quad (5.74)$$

Integrating (5.74) over $[0, t]$, we have:

$$0 \leq V(t) \leq \frac{\mu}{\pi} + \left(V(0) - \frac{\mu}{\pi} \right) e^{-\pi t} \quad (5.75)$$

Since $\frac{\mu}{\pi} > 0$, it can be obtained that:

$$0 \leq V(t) \leq V(0) e^{-\pi t} + \frac{\mu}{\pi} \quad (5.76)$$

Therefore, we can conclude that, e , $\varphi_i^T \tilde{\theta}_i$, $\tilde{\theta}_i$ and ϵ_i are UUB. Furthermore, all signals in the closed-loop system, i.e., x_1 , x_{1d} , \dot{x}_{1d} , x_i , x_{ic} , \dot{x}_{ic} ($i=2, \dots, n$), α_i , u and $\hat{\theta}_i + \beta_i$ ($i=1, \dots, n$) are also UUB. In addition, from (5.69) and (5.76), it follows that:

$\|e\| = \sqrt{\sum_{i=1}^n e_i^2} \leq \sqrt{2V(0)} e^{-0.5\pi t} + \sqrt{2\mu/\pi}$. Accordingly, when $t \rightarrow \infty$, it is easy to show that:

$\|e\| \leq \sqrt{2\mu/\pi}$. This completes the proof.

Remark 5.4.1: In this chapter, we consider a first order command filter to simplify the analysis. The purpose of this command filter is to generate x_{ic} and its derivative \dot{x}_{ic} such that $|x_{ic} - \alpha_{i-1}|$ is small. A second order filter is discussed in [Far09, Far08].

Remark 5.4.2: It should be pointed that the command filters may cause the filtering errors which will add the difficulty to get a small tracking error. To deal with this problem, the compensating signals are constructed in order to remove the effect of the known filtering errors $(x_{(i+1)c} - \alpha_i)$ caused by the command filters.

The compensating signals ξ_i are defined as [Don12, Don10]:

$$\dot{\xi}_1 = -k_1 \xi_1 + g_1 \xi_2 + g_1 (x_{2c} - \alpha_1) \quad (5.77)$$

$$\dot{\xi}_i = -k_i \xi_i + g_i \xi_{i+1} - g_{i-1} \xi_{i-1} + g_i (x_{(i+1)c} - \alpha_i) \quad (5.78)$$

$$\dot{\xi}_n = -k_n \xi_n - g_{n-1} \xi_{n-1} \quad (5.79)$$

where, $k_i > 0$ are design parameters and $\xi_i(0) = 0$. We can get $\|\xi_i\|$ is bounded. Define the compensated tracking errors as $v_i = e_i - \xi_i$. The closed-loop compensated tracking error dynamics are given by:

$$\dot{v}_1 = -k_1 v_1 + g_1 v_2 - \varphi_1^T \tilde{\theta}_1 \quad (5.80)$$

$$\dot{v}_i = -k_i v_i + g_i v_{i+1} - g_{i-1} v_{i-1} - \varphi_i^T \tilde{\theta}_i \quad (5.81)$$

$$\dot{v}_n = -k_n v_n - g_{n-1} v_{n-1} - \varphi_n^T \tilde{\theta}_n \quad (5.82)$$

The command filters are also designed as follows [Far09, Far08]:

$$\begin{cases} \dot{\varphi}_{i,1} = \omega_n \varphi_{i,2} \\ \dot{\varphi}_{i,2} = -2\zeta \omega_n \varphi_{i,2} - \omega_n (\varphi_{i,1} - \alpha_i) \end{cases} \quad (5.83)$$

with, $i = 1, \dots, n-1$, $x_{(i+1)c} = \varphi_{i,1}$ and $\dot{x}_{(i+1)c} = \omega_n \varphi_{i,2}$. Assume that the initial conditions of each filter are denoted $\varphi_{i,1}(0) = \alpha_i(0)$ and $\varphi_{i,2}(0) = 0$.

Moreover, the parameters $\omega_n > 0$ and $\zeta \in (0, 1]$ may be found to satisfy $|\varphi_{i,1} - \alpha_i| \leq \mu$ for any $\mu > 0$.

5.5 Simulation results

This section presents the simulation results for composite immersion and invariance based adaptive command filtered backstepping control scheme as applied to an electromechanical system mathematical model and as in previous chapters. The control objective of this simulation is to construct the composite immersion and invariance based adaptive command filtered backstepping controller u for the electromechanical system in such a way that the link angular position q tracks the desired trajectory x_{1d} and all signals in the closed-loop system are bounded.

The virtual controllers α_1 and α_2 are defined as:

$$\alpha_1 = -k_1 e_1 + \dot{x}_{1d} \quad (5.84)$$

$$\alpha_2 = \frac{1}{b_2} \left(-k_2 e_2 - e_1 + \sin(x_1) (\hat{\theta}_2 + \beta_2) + \frac{B}{D} x_2 + \dot{x}_{2c} \right) \quad (5.85)$$

The command filter output signal x_{ic} for $i = 2, 3$, is generated by the command filter:

$$\dot{x}_{ic} = -\omega_i (x_{ic} - \alpha_{i-1}) \quad (5.86)$$

where, $\omega_i > 0$. The actual control input u is chosen as:

$$u = \frac{1}{b_3} \left(-k_3 e_3 - b_2 e_2 + x_2 (\hat{\theta}_3 + \beta_3) + \frac{H}{M} x_3 + \dot{x}_{3c} \right) \quad (5.87)$$

For the swapping based identifier, the x-swapping filters are the same as that in the chapter 2 described by (2.92)-(2.95).

5.5.1 Composite projection based gradient adaptive laws

The composite projection based gradient adaptive laws are defined as:

$$\dot{\hat{\theta}}_2 = \text{Proj}_{\hat{\theta}_2} \left(-\frac{\partial \beta_2}{\partial x_1} x_2 - \frac{\partial \beta_2}{\partial x_2} \left(b_2 x_3 - \sin(x_1) (\hat{\theta}_2 + \beta_2) - \frac{B}{D} x_2 \right) + \Gamma_2 \frac{\Omega_2 \epsilon_2}{1 + \nu_2 \text{tr} \{ \Omega_2^T \Omega_2 \}} \right) \quad (5.88)$$

and,

$$\begin{aligned} \dot{\hat{\theta}}_3 = \text{Proj}_{\hat{\theta}_3} \left(-\frac{\partial \beta_3}{\partial x_1} x_2 - \frac{\partial \beta_3}{\partial x_2} \left(b_2 x_3 - \sin(x_1) (\hat{\theta}_3 + \beta_3) - \frac{B}{D} x_2 \right) \right. \\ \left. - \frac{\partial \beta_3}{\partial x_3} \left(b_3 u - x_2 (\hat{\theta}_3 + \beta_3) - \frac{H}{M} x_3 \right) + \Gamma_3 \frac{\Omega_3 \epsilon_3}{1 + \nu_3 \text{tr} \{ \Omega_3^T \Omega_3 \}} \right) \end{aligned} \quad (5.89)$$

where, $\beta_2 = -\Gamma_2 x_2 \sin(x_1)$, $\beta_3 = -\Gamma_3 x_2 x_3$ and $\epsilon_i = x_i + \Omega_{0i} - \Omega_i^T (\hat{\theta}_i + \beta_i)$, $i = 2, 3$.

The initial conditions are selected as: $x(0) = [0 \ 0 \ 0]^T$, $\hat{\theta}_2(0) = 0$, $\hat{\theta}_3(0) = 0$, $\Omega_{02}(0) = \Omega_2^T(0) = 0$, $\Omega_{03}(0) = \Omega_3^T(0) = 0$ and $x_{2c}(0) = x_{3c}(0) = 0$. The control parameters are chosen as: $k_1 = k_2 = 50$, $k_3 = 500$, $\Gamma_2 = \Gamma_3 = 0.65$, $\lambda_2 = \lambda_3 = 0.1$, $\nu_2 = \nu_3 = 0.1$ and $\omega_2 = \omega_3 = 150$.

The simulation results are shown in Figures 5.1-5.9. Figures 5.1-5.3 show the trajectories of the output variables. The trajectories of the tracking errors are illustrated in Figures 5.4-5.6. Figures 5.7 and 5.8 show the trajectories of the parameter estimates. The trajectories of the control inputs are shown in Figure 5.9.

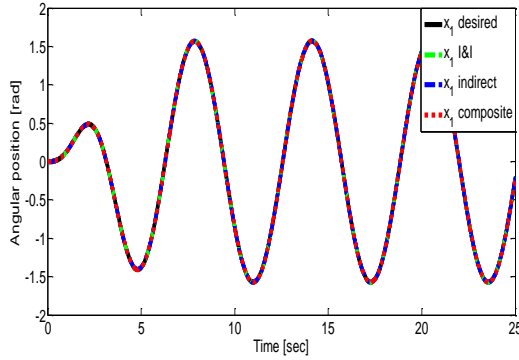


Fig. 5.1: Angular position: desired x_{1d} ("—") and actual x_1 ("--").

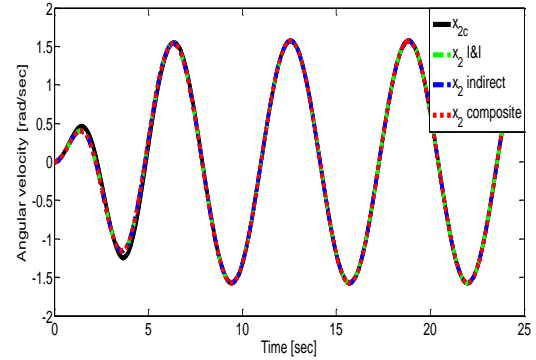


Fig. 5.2: Angular velocity: signal x_{2c} ("—") and actual x_2 ("--").

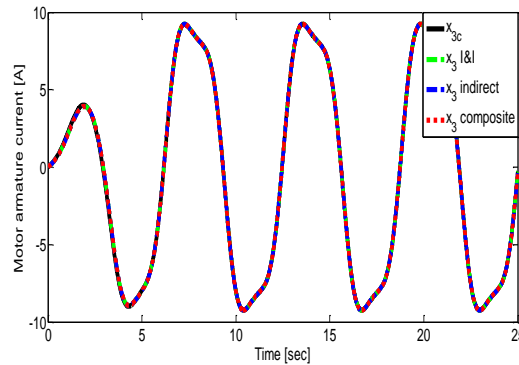


Fig. 5.3: Motor armature current: signal x_{3c} ("—") and actual x_3 ("--").

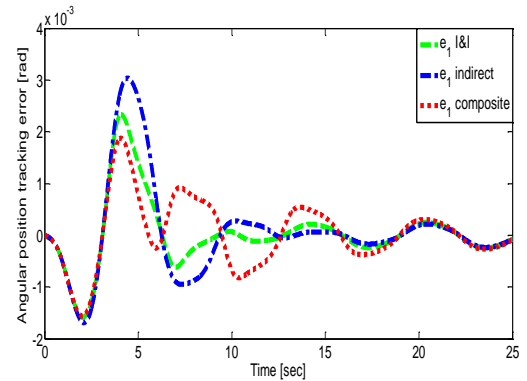


Fig. 5.4: Angular position tracking error: e_1 .

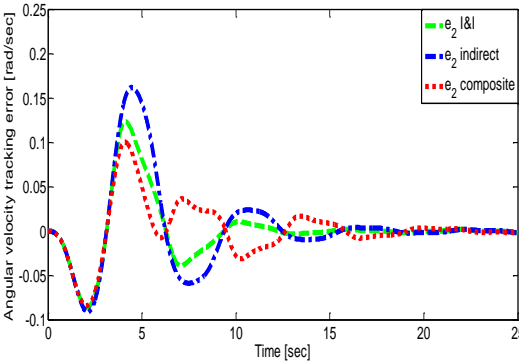


Fig. 5.5: Angular velocity tracking error: e_2 .

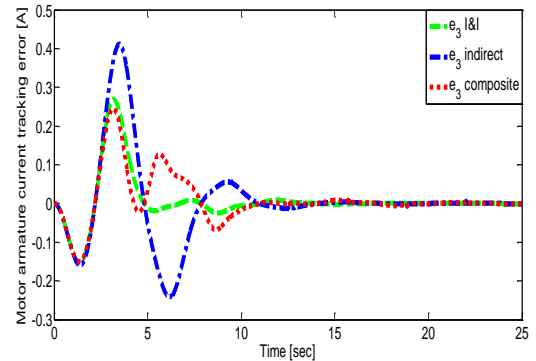


Fig. 5.6: Motor armature current tracking error: e_3 .

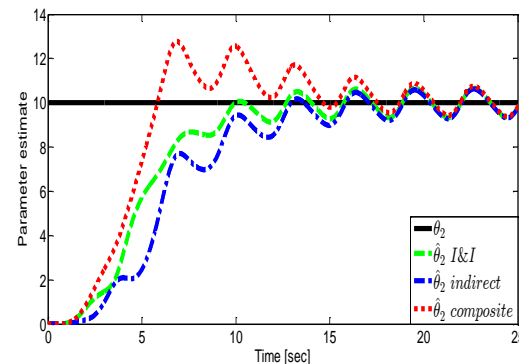


Fig. 5.7: Parameter estimate: actual θ_2 ("—") and estimate $\hat{\theta}_2$ ("--").

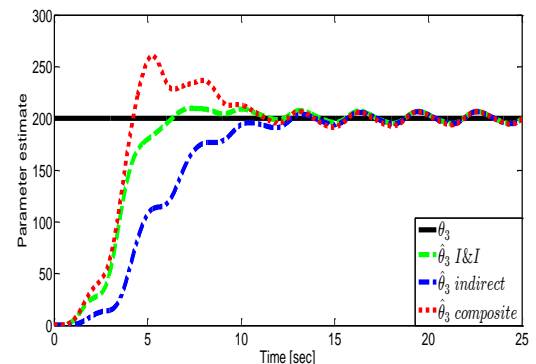


Fig. 5.8: Parameter estimate: actual θ_3 ("—") and estimate $\hat{\theta}_3$ ("--").

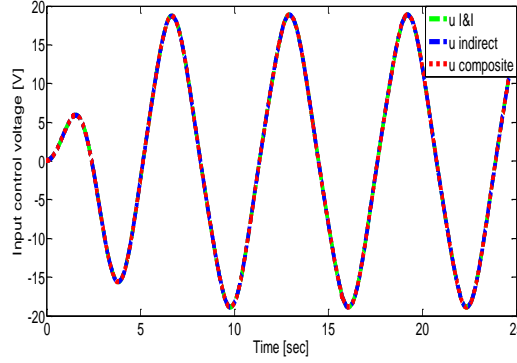


Fig. 5.9: Control input: u .

5.5.2 Composite σ -modification based gradient adaptive laws

The composite σ -modification based gradient adaptive laws are defined as:

$$\dot{\hat{\theta}}_2 = -\frac{\partial \beta_2}{\partial x_1} x_2 - \frac{\partial \beta_2}{\partial x_2} \left(b_2 x_3 - \sin(x_1) (\hat{\theta}_2 + \beta_2) - \frac{B}{D} x_2 \right) - \Gamma_2 \sigma_{\theta_2} (\hat{\theta}_2 + \beta_2 - \bar{\theta}_2) \quad (5.90)$$

and,

$$\begin{aligned} \dot{\hat{\theta}}_3 = & -\frac{\partial \beta_3}{\partial x_1} x_2 - \frac{\partial \beta_3}{\partial x_2} \left(b_2 x_3 - \sin(x_1) (\hat{\theta}_3 + \beta_3) - \frac{B}{D} x_2 \right) \\ & - \frac{\partial \beta_3}{\partial x_3} \left(b_3 u - x_2 (\hat{\theta}_3 + \beta_3) - \frac{H}{M} x_3 \right) - \Gamma_3 \sigma_{\theta_3} (\hat{\theta}_3 + \beta_3 - \bar{\theta}_3) \end{aligned} \quad (5.91)$$

where, $\bar{\theta}_2$ and $\bar{\theta}_3$ are computed with the gradient method as follows:

$$\dot{\bar{\theta}}_i = \bar{\Gamma}_i \frac{\Omega_i \epsilon_i}{1 + \nu_i \text{tr} \{ \Omega_i^T \Omega_i \}} - \dot{\beta}_i \quad (5.92)$$

with, $\beta_2 = -\Gamma_2 x_2 \sin(x_1)$, $\beta_3 = -\Gamma_3 x_2 x_3$ and $\epsilon_i = x_i + \Omega_{0i} - \Omega_i^T (\bar{\theta}_i + \beta_i)$, $i = 2, 3$.

The initial conditions are selected as: $x(0) = [0 \ 0 \ 0]^T$, $\hat{\theta}_2(0) = \bar{\theta}_2(0) = 0$, $\hat{\theta}_3(0) = \bar{\theta}_3(0) = 0$, $\Omega_{02}(0) = \Omega_2^T(0) = 0$, $\Omega_{03}(0) = \Omega_3^T(0) = 0$ and $x_{2c}(0) = x_{3c}(0) = 0$. The control parameters are chosen as: $k_1 = k_2 = 50$, $k_3 = 500$, $\Gamma_2 = \Gamma_3 = 0.65$, $\bar{\Gamma}_2 = \bar{\Gamma}_3 = 0.5$, $\sigma_{\theta_2} = \sigma_{\theta_3} = 0.01$, $\lambda_2 = \lambda_3 = 0.1$, $\nu_2 = \nu_3 = 0.1$ and $\omega_2 = \omega_3 = 150$.

The simulation results are shown in Figures 5.10-5.18. Figures 5.10-5.12 show the trajectories of the output variables. The trajectories of the tracking errors are illustrated in Figures 5.13-5.15. Figures 5.16 and 5.17 show the trajectories of the parameter estimates. The trajectories of the control inputs are shown in Figure 5.18.

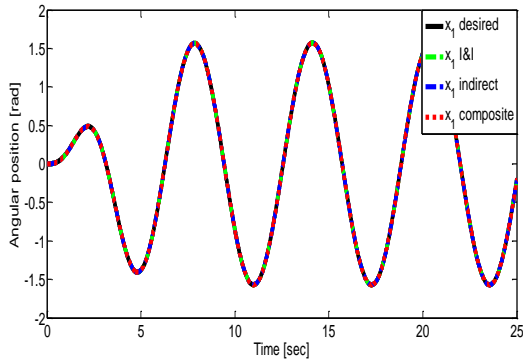


Fig. 5.10: Angular position: desired x_{1d} ("—") and actual x_1 ("--").

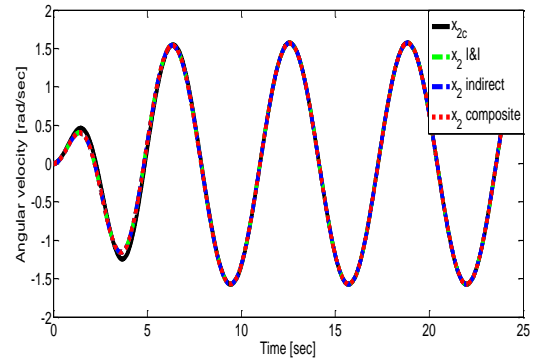


Fig. 5.11: Angular velocity: signal x_{2c} ("—") and actual x_2 ("--").

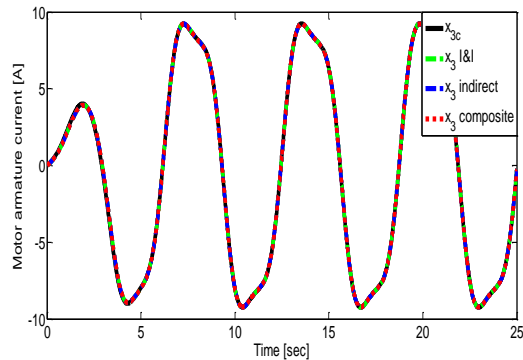


Fig. 5.12: Motor armature current: signal x_{3c} ("—") and actual x_3 ("--").

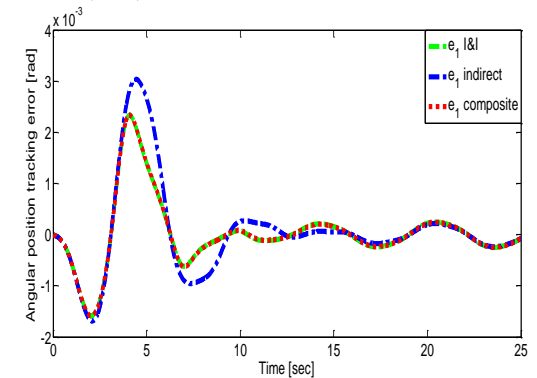


Fig. 5.13: Angular position tracking error: e_1 .

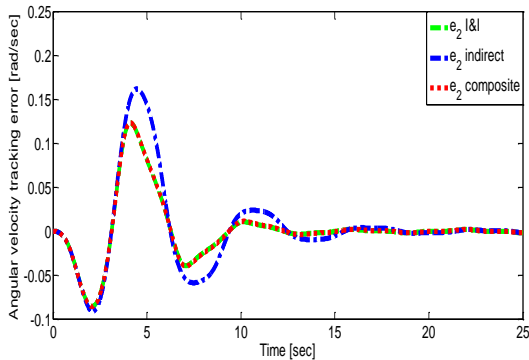


Fig. 5.14: Angular velocity tracking error: e_2 .

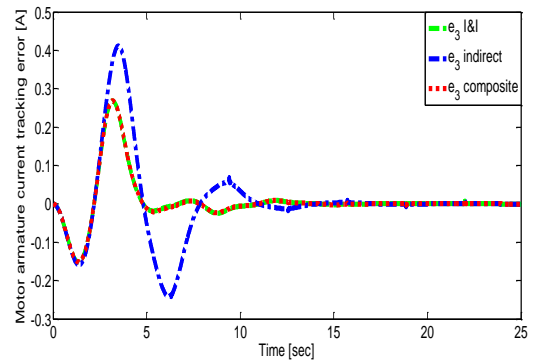


Fig. 5.15: Motor armature current tracking error: e_3 .

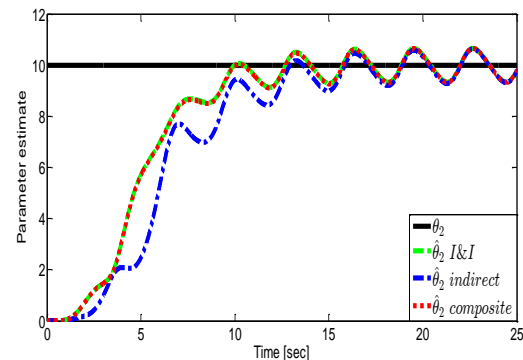


Fig. 5.16: Parameter estimate: actual θ_2 ("—") and estimate $\hat{\theta}_2$ ("--").

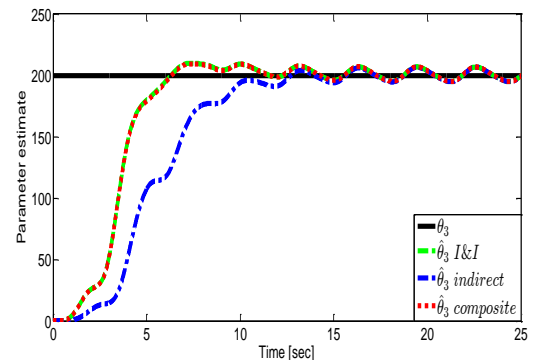


Fig. 5.17: Parameter estimate: actual θ_3 ("—") and estimate $\hat{\theta}_3$ ("--").

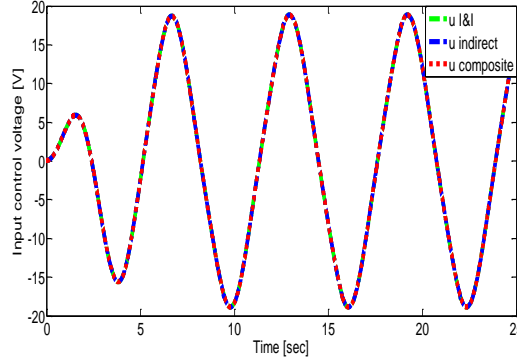


Fig. 5.18: Control input: u .

5.5.3 Composite σ -modification based least squares adaptive laws

The composite σ -modification based least squares adaptive laws are the same as that in the composite σ -modification based gradient adaptive laws described by (5.90) and (5.91). $\bar{\theta}_2$ and $\bar{\theta}_3$ are computed with the least squares method as follows:

$$\dot{\bar{\theta}}_i = \bar{\Gamma}_i \frac{\Omega_i \epsilon_i}{1 + \nu_i \text{tr}\{\Omega_i^T \bar{\Gamma}_i \Omega_i\}} - \dot{\beta}_i \quad (5.93)$$

with, $\bar{\Gamma}_i$ is given by:

$$\dot{\bar{\Gamma}}_i = -\bar{\Gamma}_i \frac{\Omega_i \Omega_i^T}{1 + \nu_i \text{tr}\{\Omega_i^T \bar{\Gamma}_i \Omega_i\}} \bar{\Gamma}_i \quad (5.94)$$

where, $\beta_2 = -\Gamma_2 x_2 \sin(x_1)$, $\beta_3 = -\Gamma_3 x_2 x_3$ and $\epsilon_i = x_i + \Omega_{0i} - \Omega_i^T (\bar{\theta}_i + \beta_i)$, $i = 2, 3$.

The initial conditions are selected as: $x(0) = [0 \ 0 \ 0]^T$, $\hat{\theta}_2(0) = \bar{\theta}_2(0) = 0$, $\hat{\theta}_3(0) = \bar{\theta}_3(0) = 0$, $\Omega_{02}(0) = \Omega_2^T(0) = 0$, $\Omega_{03}(0) = \Omega_3^T(0) = 0$ and $x_{2c}(0) = x_{3c}(0) = 0$. The control parameters are chosen as: $k_1 = k_2 = 50$, $k_3 = 500$, $\Gamma_2 = \Gamma_3 = 0.65$, $\bar{\Gamma}_2(0) = 5$, $\bar{\Gamma}_3(0) = 10$, $\sigma_{\theta_2} = \sigma_{\theta_3} = 0.01$, $\lambda_2 = \lambda_3 = 0.1$, $\nu_2 = \nu_3 = 0.1$ and $\omega_2 = \omega_3 = 150$.

The simulation results are shown in Figures 5.19-5.27. Figures 5.19-5.21 show the trajectories of the output variables. The trajectories of the tracking errors are illustrated in Figures 5.22-5.24. Figures 5.25 and 5.26 show the trajectories of the parameter estimates. The trajectories of the control inputs are shown in Figure 5.27.

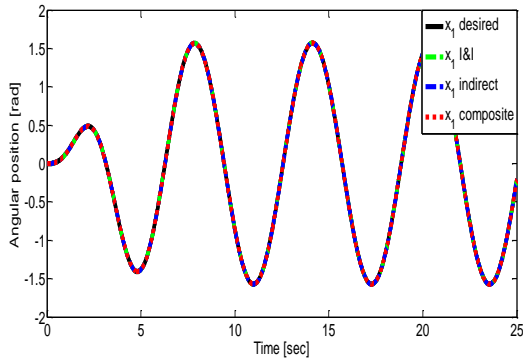


Fig. 5.19: Angular position: desired x_{1d} ("—") and actual x_1 ("--").

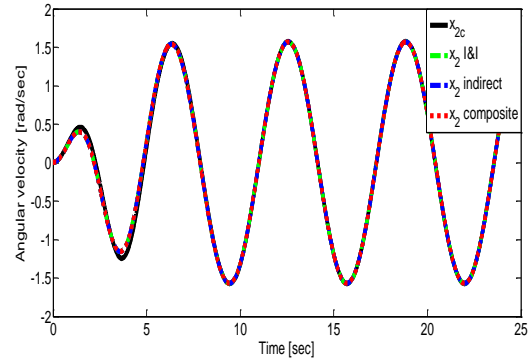


Fig. 5.20: Angular velocity: signal x_{2c} ("—") and actual x_2 ("--").

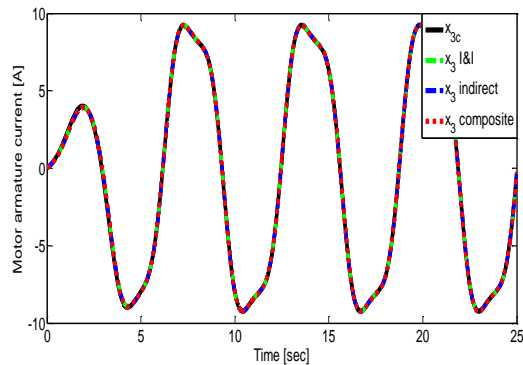


Fig. 5.21: Motor armature current: signal x_{3c} ("—") and actual x_3 ("--").

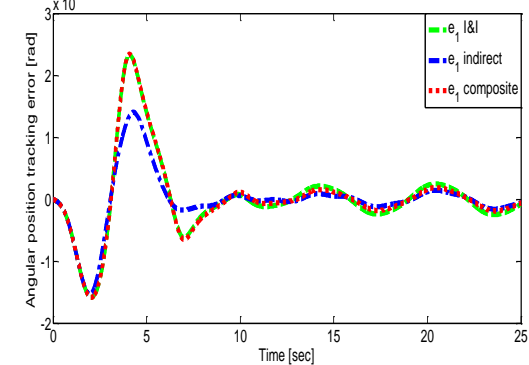


Fig. 5.22: Angular position tracking error: e_1 .

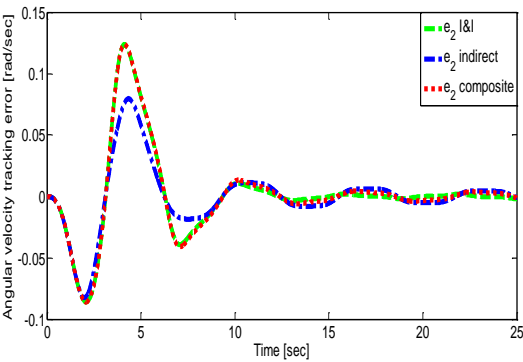


Fig. 5.23: Angular velocity tracking error: e_2 .

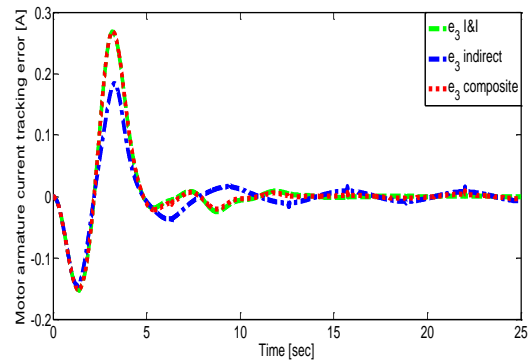


Fig. 5.24: Motor armature current tracking error: e_3 .

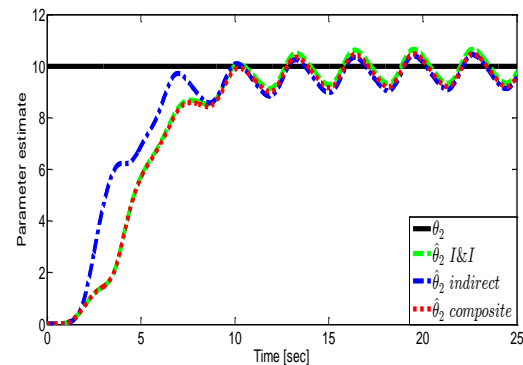


Fig. 5.25: Parameter estimate: actual θ_2 ("—") and estimate $\hat{\theta}_2$ ("--").

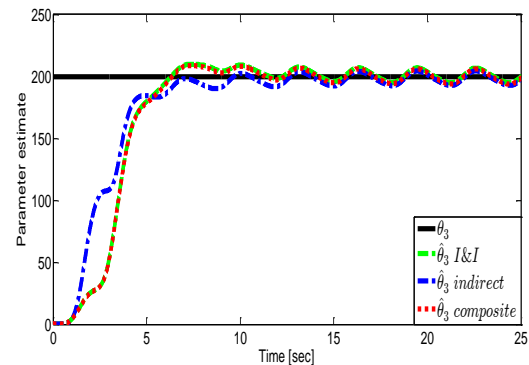


Fig. 5.26: Parameter estimate: actual θ_3 ("—") and estimate $\hat{\theta}_3$ ("--").

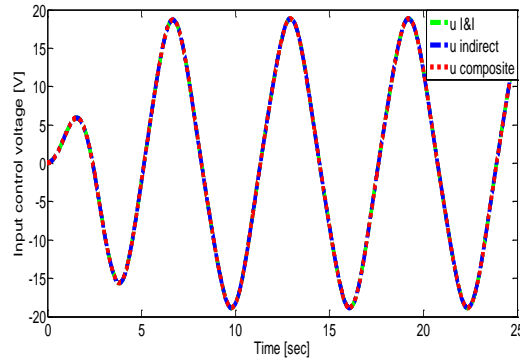


Fig. 5.27: Control input: u .

From all the results, we can obviously see that all actual trajectories asymptotically converge to their reference signals, that the ultimate tracking errors converge to zero and that the convergence of the parameter estimates to their true values is guaranteed. As seen in simulation results, we can conclude then that the proposed composite adaptive control method is effective, gives a well control effort performance and has good trajectory tracking performances in comparison with direct and indirect robust adaptive control approaches.

5.6 Conclusion

This chapter presents a novel design of composite immersion and invariance based adaptive command filtered backstepping control for a class of SISO uncertain nonlinear systems in lower triangular form. By designing of the proposed composite adaptive control method, the problem of explosion of complexity is also eliminated. By using the Lyapunov stability theory, it has been proven that the proposed composite adaptive control technique guarantees the boundedness of all signals in the closed-loop system. The simulation results for an electromechanical system clearly demonstrate the effectiveness of the proposed composite adaptive control scheme compared to immersion and invariance based adaptive command filtered backstepping control and indirect adaptive control schemes. Some future work will be mainly considered to apply the composite immersion and invariance based adaptive command filtered backstepping control method by using the compensating signals in order to remove the effect of the filtering errors caused by the command filters.

General conclusion and future works

The research work presented in this thesis deals with the study and development of new composite adaptive control schemes for a class of SISO uncertain nonlinear systems in lower triangular form. In the chapters, numerous types of composite adaptive control approaches for a class of SISO uncertain nonlinear systems in lower triangular form have been studied and developed as follows: composite tuning functions based adaptive backstepping control, composite adaptive dynamic surface control, composite robust adaptive dynamic surface control, and composite immersion and invariance based adaptive command filtered backstepping control methods. These composite adaptive control techniques require the synthesis of stable adaptive control laws with composite adaptive laws. The principle of these composite adaptive control schemes aims to combine the adaptive laws by considering sum, projection and σ -modification based adaptive laws. The main drawback in adaptive backstepping control approach is the overparametrization problem. Composite tuning functions based adaptive backstepping control has been utilized to avoid the overparametrization problem. The adaptive backstepping control and composite tuning functions based adaptive backstepping control designs suffer from the problem of explosion of complexity, which is caused by repeated differentiations of the virtual controls at each step. To overcome the problem of explosion of complexity, composite adaptive and robust adaptive dynamic surface control, and immersion and invariance based adaptive command filtered backstepping control techniques have been proposed. By utilizing the above composite adaptive control designs, a novel composite mechanisms of adaptive laws are developed. The boundedness of all signals in the closed-loop system is guaranteed by using the Lyapunov stability analysis theory. Simulation results for an electromechanical system are provided to demonstrate the effectiveness of the proposed composite adaptive control schemes.

The first chapter presents the Lyapunov stability concepts with some necessary definitions, Lyapunov's direct method, control Lyapunov function (CLF) and some useful lemmas. The backstepping control technique procedures with stability analysis have been discussed. The chapter closes with a state of the art on the adaptive control techniques.

In the second chapter, novel composite tuning functions based adaptive backstepping control for a class of SISO uncertain nonlinear systems in lower triangular form has been studied and developed to avoid the overparametrization problem inherent in the conventional adaptive backstepping control design. The principle of this composite adaptive control approach is to combine the direct and indirect adaptive laws by considering sum and σ -modification based adaptive laws. Stability analysis is performed based on the Lyapunov stability theory to guarantee the boundedness of all signals in the closed-loop system. In order to verify the effectiveness of the proposed composite adaptive control scheme compared to direct and indirect adaptive control schemes, simulation results have been tested for an electromechanical system.

In the third chapter, a new composite adaptive dynamic surface control for a class of SISO uncertain nonlinear systems in lower triangular form has been presented and developed to overcome the problem of explosion of complexity inherent in the conventional adaptive backstepping control and the composite tuning functions based adaptive backstepping control designs. By introducing the Lyapunov stability theory, it is proved that all signals in the closed-loop system are bounded. Simulation results for an electromechanical system have been tested in order to validate the effectiveness of the proposed composite adaptive control scheme compared to direct and indirect adaptive control schemes.

The fourth chapter presents a novel composite robust adaptive dynamic surface control for a class of SISO uncertain nonlinear systems in lower triangular form with unknown external disturbances. The proposed composite robust adaptive control method has been also introduced and developed to avoid the problem of explosion of complexity. By using the Lyapunov stability theory, the boundedness of all signals in the closed-loop system is guaranteed. In order to verify the effectiveness and robustness of the proposed composite robust adaptive control scheme in comparison with direct and indirect robust adaptive control schemes, simulation results have been tested for an electromechanical system.

In the last chapter, a novel design of composite immersion and invariance based adaptive command filtered backstepping control for a class of SISO uncertain nonlinear systems in lower triangular form has been also investigated and developed to avoid the problem of explosion of complexity. Stability analysis is performed by using the Lyapunov stability theory to ensure the boundedness of all signals in the closed-loop system. In order to verify the effectiveness of the proposed composite adaptive control scheme compared to immersion and invariance based adaptive control and indirect adaptive control schemes.

As a result of this research work, this thesis opens new future research works on what follows:

- Applying of the proposed composite adaptive control designs with different types of indirect adaptive control.
- Developing of composite adaptive command filtered backstepping control technique by using the compensating signals to remove the effect of the filtering errors caused by the command filters.
- Designing of composite immersion and invariance based adaptive dynamic surface control method in order to avoid the problem of explosion of complexity.
- Study of the proposed composite adaptive control designs using Nussbaum functions, barrier Lyapunov functions (BLFs), barrier Lyapunov functions based Nussbaum functions and finite-time control technique.
- Investigate the use of the proposed composite adaptive control approaches with sliding mode control methods.
- Investigate an extension of the proposed composite adaptive control approaches for a class of fractional order and chaotic systems.
- Designing of uncertain nonlinear systems with unmeasured states by using observer adaptive backstepping control with tuning functions and observer adaptive dynamic surface control schemes.
- Design of the composite adaptive neural/fuzzy control based on command filtered backstepping control and dynamic surface control strategies.
- Apply of the proposed composite adaptive control methods to other practical industrial applications.
- Validation of the proposed composite adaptive control techniques via real-time implementations.

Bibliographical references

- [Ast08a] A. Astolfi, D. Karagiannis, and R. Ortega, “Nonlinear and adaptive control with applications,” Springer-Verlag, London, 2008.
- [Ast08b] A. Astolfi, D. Karagiannis, and R. Ortega, “Towards applied nonlinear adaptive control,” *Annual Reviews in Control*, vol. 32, no. 2, pp. 136-148, 2008.
- [Ast03] A. Astolfi, and R. Ortega, “Immersion and invariance: a new tool for stabilization and adaptive control of nonlinear systems,” *IEEE Transactions on Automatic Control*, vol. 48, no. 4, pp. 590-606, 2003.
- [Bec13] C. P. Bechlioulis, and G. A. Rovithakis, “Reinforcing robustness of adaptive dynamic surface control,” *International Journal of Adaptive Control and Signal Processing*, vol. 27, no. 4, pp. 323-339, 2013.
- [Ben00] A. R. Benaskeur, “Aspects de l’application du backstepping adaptatif à la commande décentralisée des systèmes non linéaires,” PhD Thesis, Laval University, 2000.
- [Car95] J. J. Carroll, and D. M. Dawson, “Integrator backstepping techniques for the tracking control of permanent magnet brush DC motors,” *IEEE Transactions on Industry Applications*, vol. 31, no. 2, pp. 248-255, 1995.
- [Che10] J. Chen, Z. Li, G. Zhang, and M. Gan, “Adaptive robust dynamic surface control with composite adaptation laws,” *International Journal of Adaptive Control and Signal Processing*, vol. 24, no. 12, pp. 1036-1050, 2010.
- [Cil09] M. K. Ciliz, “Combined direct and indirect adaptive control for a class of nonlinear systems,” *IET Control Theory & Applications*, vol. 3, no. 1, pp. 151-159, 2009.
- [Cil07] M. K. Ciliz, “Adaptive backstepping control using combined direct and indirect adaptation,” *Circuits, Systems and Signal Processing*, vol. 26, no. 6, pp. 911-939, 2007.
- [Cob19] R. Coban, “Adaptive backstepping sliding mode control with tuning functions for nonlinear uncertain systems,” *International Journal of Systems Science*, vol. 50, no. 8, pp. 1517-1529, 2019.
- [Daw94] D. M. Dawson, J. J. Carroll, and M. Schneider, “Integrator backstepping control of a brush DC motor turning a robotic load,” *IEEE Transactions on Control Systems Technology*, vol. 2, no. 3, pp. 233-244, 1994.
- [Din15] D. Ding, D. Qi, J. Peng, and Q. Wang, “Asymptotic pseudo-state stabilization of commensurate fractional-order nonlinear systems with additive disturbance,” *Nonlinear Dynamics*, vol. 81, no. 1-2, pp. 667-677, 2015.
- [Don12] W. Dong, J. A. Farrell, M. M. Polycarpou, V. Djapic, and M. Sharma, “Command filtered adaptive backstepping,” *IEEE Transactions on Control Systems Technology*, vol. 20, no. 3, pp. 566-580, 2012.
- [Don10] W. Dong, J. A. Farrell, M. M. Polycarpou, and M. Sharma, “Command filtered adaptive backstepping,” *American Control Conference*, Baltimore, MD, pp. 105-110, 2010.
- [Elm19] M. Elmi, H. A. Talebi, and M. B. Menhaj, “Robust adaptive dynamic surface control of nonlinear time-varying systems in strict-feedback form,” *International Journal of Control, Automation and Systems*, vol. 17, no. 6, pp. 1432-1444, 2019.
- [Far09] J. A. Farrell, M. M. Polycarpou, M. Sharma, and W. Dong, “Command filtered backstepping,” *IEEE Transactions on Automatic Control*, vol. 54, no. 6, pp. 1391-1395, 2009.
- [Far08] J. A. Farrell, M. M. Polycarpou, M. Sharma, and W. Dong, “Command filtered backstepping,” *American Control Conference*, Seattle, Washington, pp. 1923-

- 1928, 2008.
- [Far06] J. A. Farrell, and M. M. Polycarpou, “Adaptive approximation based control: unifying neural, fuzzy and traditional adaptive approximation approaches,” John Wiley & Sons, New Jersey, 2006.
- [Fuj12] K. Fujimoto, and M. Yokoyama, “I&I adaptive control by DSC approach for parametric strict-feedback systems,” Proceedings of the 5th ASME Annual Dynamic Systems and Control Conference joint with the 11th JSME Motion and Vibration Conference, Fort Lauderdale, Florida, pp. 381-386, 2012.
- [Gan15] M. Gan, J. Chen, and Z. Li, “Multiple-model adaptive robust dynamic surface control with estimator resetting,” International Journal of Adaptive Control and Signal Processing, vol. 29, no.8, pp. 939-953, 2015.
- [Ge04] S. S. Ge, “Adaptive control of uncertain Lorenz system using decoupled backstepping,” International Journal of Bifurcation and Chaos, vol. 14, no. 4, pp. 1439-1445, 2004.
- [Ge00a] S. S. Ge, and C. Wang, “Adaptive control of uncertain Chua’s circuits,” IEEE Transactions on Circuits and Systems-I: Fundamental Theory and Applications, vol. 47, no.9, pp. 1397-1402, 2000.
- [Ge00b] S. S. Ge, C. Wang, and T. H. Lee, “Adaptive backstepping control of a class of chaotic systems,” International Journal of Bifurcation and Chaos, vol. 10, no. 5, pp. 1149-1156, 2000.
- [Han19] C. Han, Z. Liu, and J. Yi, “Immersion and invariance adaptive finite-time control of air-breathing hypersonic vehicles,” Proceedings of the Institution of Mechanical Engineers, Part G: Journal of Aerospace Engineering, vol. 233, no. 7, pp. 2626-2641, 2019.
- [Han18] C. Han, Z. Liu, and J. Yi, “Immersion and invariance adaptive control with σ -modification for uncertain nonlinear systems,” Journal of the Franklin Institute, vol. 355, no. 5, pp. 2091-2111, 2018.
- [Han17] C. Han, Z. Liu, and J. Yi, “Immersion and invariance adaptive control with σ -modification for air-breathing hypersonic vehicles,” IEEE International Conference on Mechatronics and Automation, Takamatsu, pp. 1138-1143, 2017.
- [Han16] C. Han, Z. Liu, X. Tan, and J. Yi, “Adaptive immersion and invariance continuous finite-time control of hypersonic vehicles,” IEEE International Conference on Robotics and Biomimetics, Qingdao, pp. 1239-1244, 2016.
- [Han15] C. Han, Z. Liu, X. Tan, and J. Yi, “Adaptive immersion and invariance sliding mode control for hypersonic vehicles with parametric uncertainty,” IEEE International Conference on Robotics and Biomimetics, Zhuhai, pp. 1536-1541, 2015.
- [He16] Y. He, J. Wang, W. Shen, and J. Zhao, “Indirect adaptive robust dynamic surface control of electro-hydraulic fatigue testing system with huge elastic load,” Proceedings of the Institution of Mechanical Engineers, Part 1: Journal of Systems and Control Engineering, vol. 230, no. 2, pp. 115-129, 2016.
- [Hed00] J. K. Hedrick, and P. P. Yip, “Multiple sliding surface control: theory and application,” Journal of Dynamic Systems, Measurement, and Control, vol. 122, no. 4, pp. 586-593, 2000.
- [Hou11] M. Z. Hou, and G. R. Duan, “Robust adaptive dynamic surface control of uncertain nonlinear systems,” International Journal of Control, Automation and Systems, vol. 9, no. 1, pp. 161-168, 2011.
- [Hu10] C. Hu, B. Yao, and Q. Wang, “Integrated direct/indirect adaptive robust contouring control of a biaxial gantry with accurate parameter estimations,” Automatica, vol. 46, no. 4, pp. 701-707, 2010.
- [Ioa07] P. A. Ioannou, and B. Fidan, “Adaptive control tutorial. Advances in Design and Control,” PA: SIAM, Philadelphia, 2007.
- [Ioa96] P. A. Ioannou, and J. Sun, “Robust adaptive control,” Prentice Hall, Englewood Cliffs, New Jersey, 1996.
- [Isi89] A. Isidori, “Nonlinear Control Systems,” Springer-Verlag, New York, 2nd edition,

- 1989.
- [Kan91] I. Kanellakopoulos, P. V. Kokotović, and A. S. Morse, "Systematic design of adaptive controllers for feedback linearizable systems," *IEEE Transactions on Automatic Control*, vol. 36, no. 11, pp. 1241-1253, 1991.
- [Kar08] D. Karagiannis, and A. Astolfi, "Nonlinear adaptive control of systems in feedback form: An alternative to adaptive backstepping," *Systems & Control Letters*, vol. 57, no. 9, pp. 733-739, 2008.
- [Kar07] D. Karagiannis, and A. Astolfi, "Adaptive state feedback design via immersion and invariance," *European Control Conference, Kos*, pp. 553-558, 2007.
- [Kar04] D. Karagiannis, and A. Astolfi, "Nonlinear adaptive control of systems in feedback form: An alternative to adaptive backstepping," *IFAC Large Scale Systems: Theory and Applications, Osaka*, pp. 67-72, 2004.
- [Kha02] H. K. Khalil, "Nonlinear systems," Prentice Hall, Upper Saddle River, New Jersey, 3rd edition, 2002.
- [Kha96] H. K. Khalil, "Nonlinear systems," Prentice Hall, Upper Saddle River, New Jersey, 2nd edition, 1996.
- [Khe15] T. Kheowree, and S. Kuntanapreeda, "Adaptive dynamic surface control of an electrohydraulic actuator with friction compensation," *Asian Journal of Control*, vol. 17, no. 3, pp. 1-13, 2015.
- [Krs95a] M. Krstić, I. Kanellakopoulos, and P. V. Kokotović, "Nonlinear and adaptive control design," John Wiley & Sons, New York, 1995.
- [Krs95b] M. Krstić, and P. V. Kokotović, "Adaptive nonlinear design with controller-identifier separation and swapping," *IEEE Transactions on Automatic Control*, vol. 40, no. 3, pp. 426-440, 1995.
- [Krs93] M. Krstić, and P. V. Kokotović, "Adaptive nonlinear control with nonlinear swapping," *Proceedings of the 32nd Conference on Decision and Control, San Antonio, Texas*, pp. 1073-1080, 1993.
- [Krs92] M. Krstić, I. Kanellakopoulos, and P. V. Kokotović, "Adaptive nonlinear control without overparameterization," *Systems & Control Letters*, vol. 19, no. 3, pp. 177-185, 1992.
- [Lee12] C. H. Lee, and B. R. Chung, "Adaptive backstepping controller design for nonlinear uncertain systems using fuzzy neural systems," *International Journal of Systems Science*, vol. 43, no. 10, pp. 1855-1869, 2012.
- [Li12a] D. J. Li, "Adaptive output feedback control of uncertain nonlinear chaotic systems based on dynamic surface control technique," *Nonlinear Dynamics*, vol. 68, no. 1-2, pp. 235-243, 2012.
- [Li12b] Z. Li, J. Chen, G. Zhang, and M. Gan, "Stabilising tracking of uncertain switched non-linear systems in semi-strict feedback form," *IET Control Theory & Applications*, vol. 6, no. 4, pp. 588-595, 2012.
- [Li10a] T. S. Li, D. Wang, G. Feng, and S. C. Tong, "A DSC approach to robust adaptive NN tracking control for strict-feedback nonlinear systems," *IEEE Transactions on Systems, Man, and Cybernetics-Part B: Cybernetics*, vol. 40, no. 3, pp. 915-927, 2010.
- [Li10b] Z. Li, J. Chen, M. Gan, H. Fang, and G. Zhang, "Adaptive robust dynamic surface control of DC torque motors with true parameter estimates," *American Control Conference, Baltimore, MD*, pp. 3524-3529, 2010.
- [Liu18a] Y. H. Liu, "Adaptive dynamic surface asymptotic tracking for a class of uncertain nonlinear systems," *International Journal of Robust and Nonlinear Control*, vol. 28, no. 4, pp. 1233-1245, 2018.
- [Liu18b] Y. H. Liu, "Dynamic surface asymptotic tracking of a class of uncertain nonlinear hysteretic systems using adaptive filters," *Journal of the Franklin Institute*, vol. 355, no. 1, pp. 123-140, 2018.
- [Liu17a] Y. H. Liu, L. Huang, and D. Xiao, "Adaptive dynamic surface control for uncertain nonaffine nonlinear systems," *International Journal of Robust and Nonlinear Control*, vol. 27, no. 4, pp. 535-546, 2017.

- [Liu17b] Y. H. Liu, "Saturated robust adaptive control for uncertain non-linear systems using a new approximate model," *IET Control Theory & Applications*, vol. 11, no. 6, pp. 870-876, 2017.
- [Liu14] Z. Liu, X. Tan, R. Yuan, G. Fan, and J. Yi, "Adaptive trajectory tracking control system design for hypersonic vehicles with parametric uncertainty," *Proceedings of the Institution of Mechanical Engineers, Part G: Journal of Aerospace Engineering*, vol. 229, no. 1, pp. 119-134, 2014.
- [Liu12] Y. J. Liu, and W. Wang, "Adaptive output feedback control of uncertain nonlinear systems based on dynamic surface control technique," *International Journal of Robust and Nonlinear Control*, vol. 22, no. 9, pp. 945-958, 2012.
- [Liu11] Y. J. Liu, C. L. P. Chen, and D. J. Li, "Observer-based adaptive control for a class of nonlinear chaotic systems," *IEEE International Conference on Systems, Man, and Cybernetics, Anchorage, AK*, pp. 2011-2014, 2011.
- [Lou18] Z. E. Lou, and G. Zhao, "Immersion- and invariance-based adaptive stabilization of switched nonlinear systems," *International Journal of Robust and Nonlinear Control*, vol. 28, no. 1, pp. 197-212, 2018.
- [Moh11] A. Mohanty, and B. Yao, "Integrated direct/indirect adaptive robust control of hydraulic manipulators with valve deadband," *IEEE-ASME Transactions on Mechatronics*, vol. 16, no. 4, pp. 707-715, 2011.
- [Mon13] O. Monfared, A. Khayatian, M. Mahzoon, and P. Karimaghaee, "Immersion and invariance adaptive control of a class of nonlinear systems with unknown control direction," *International Journal of Systems Science*, vol. 44, no. 12, pp. 2287-2294, 2013.
- [Pan18] Y. Pan, H. Wang, X. Li, and H. Yu, "Adaptive command-filtered backstepping control of robot arms with compliant actuators," *IEEE Transactions on Control Systems Technology*, vol. 26, no. 3, pp. 1149-1156, 2018.
- [Pan17] Y. Pan, T. Sun, Y. Liu and H. Yu, "Composite learning from adaptive backstepping neural network control," *Neural Networks*, vol. 95, pp. 134-142, 2017.
- [Pan16a] Y. Pan, Y. Liu, and H. Yu, "Online data-driven composite adaptive backstepping control with exact differentiators," *International Journal of Adaptive Control and Signal Processing*, vol. 30, no. 5, pp. 779-789, 2016.
- [Pan16b] Y. Pan, T. Sun, and H. Yu, "Composite adaptive dynamic surface control using online recorded data," *International Journal of Robust and Nonlinear Control*, vol. 26, no. 18, pp. 3921-3936, 2016.
- [Pan16c] Y. Pan, and H. Yu, "Composite learning from adaptive dynamic surface control," *IEEE Transactions on Automatic Control*, vol. 61, no. 9, pp. 2603-2609, 2016.
- [Pan15] Y. Pan, and H. Yu, "Dynamic surface control via singular perturbation analysis," *Automatica*, vol. 57, pp. 29-33, 2015.
- [Pan13] Y. Pan, Y. Zhou, T. Sun, and M. J. Er, "Composite adaptive fuzzy H^∞ tracking control of uncertain nonlinear systems," *Neurocomputing*, vol. 99, pp. 15-24, 2013.
- [Pat10] P. M. Patre, S. Bhasin, Z. D. Wilcox, and W. E. Dixon, "Composite adaptation for neural network-based controllers," *IEEE Transactions on Automatic Control*, vol. 55, no. 4, pp. 944-950, 2010.
- [Pol96] M. M. Polycarpou, and P. A. Ioannou, "A robust adaptive nonlinear control design," *Automatica*, vol. 32, no. 3, pp. 423-427, 1996.
- [Sas89] S. Sastry, and A. Isidori, "Adaptive control of linearizable systems," *IEEE Transactions on Automatic Control*, vol. 34, no. 11, pp. 1123-1131, 1989.
- [She17a] D. Sheng, Y. Wei, S. Cheng, and J. Shuai, "Adaptive backstepping control for fractional order systems with input saturation," *Journal of the Franklin Institute*, vol. 354, no. 5, pp. 2245-2268, 2017.
- [She17b] D. Sheng, Y. Wei, S. Cheng, and Y. Wang, "Observer-based adaptive backstepping control for fractional order systems with input saturation," *ISA Transactions*, vol. 82, pp. 18-29, 2017.

- [She17c] W. Shen, J. Z. Wang, and S. K. Wang, "The control of the electro-hydraulic shaking table based on dynamic surface adaptive robust control," *Transactions of the Institute of Measurement and Control*, vol. 39, no. 8, pp. 1271-1280, 2017.
- [Slo91] J. J. E. Slotine, and W. Li, "Applied nonlinear control," Prentice Hall, Englewood Cliffs, New Jersey, 1991.
- [Slo89] J. J. E. Slotine, and W. Li, "Composite adaptive control of robot manipulators," *Automatica*, vol. 25, no. 4, pp. 509-519, 1989.
- [Son10a] L. Sonneveldt, "Adaptive backstepping flight control for modern fighter aircraft," PhD Thesis, Delft University of Technology, 2010.
- [Son10b] L. Sonneveldt, E. R. van Oort, Q. P. Chu, and J. A. Mulder, "Immersion and invariance based nonlinear adaptive flight control," *AIAA Guidance, Navigation, and Control Conference*, Toronto, Ontario, pp. 1-18, 2010.
- [Son09] L. Sonneveldt, E. R. van Oort, Q. P. Chu, C. C. de Visser, and J. A. Mulder, "Lyapunov-based fault tolerant flight control designs for a modern fighter aircraft model," *AIAA Guidance, Navigation, and Control Conference*, Chicago, Illinois, pp. 1-23, 2009.
- [Sou21] **Y. Soukkou**, S. Labiod, M. Tadjine, Q. M. Zhu, and M. Nibouche, "Immersion and invariance based adaptive dynamic surface control for parametric strict-feedback nonlinear systems," *Lecture Notes in Electrical Engineering*, Springer, Singapore, vol. 682, pp. 247-261, 2021.
- [Sou19] **Y. Soukkou**, S. Labiod, M. Tadjine, Q. M. Zhu, and M. Nibouche, "Adaptive command filtered backstepping control and its application to permanent magnet synchronous generator based wind energy conversion system," *Proceedings of the 1st International Conference on Sustainable Renewable Energy Systems and Applications*, Tebessa, 2019.
- [Sou18] **Y. Soukkou**, S. Labiod, and M. Tadjine, "Composite adaptive dynamic surface control of nonlinear systems in parametric strict-feedback form," *Transactions of the Institute of Measurement and Control*, vol. 40, no. 4, pp. 1127-1135, 2018.
- [Sou17] **Y. Soukkou**, and S. Labiod, "Adaptive backstepping control using combined direct and indirect σ -modification adaptation," *Lecture Notes in Electrical Engineering*, Springer, Cham, vol. 411, pp. 17-30, 2017.
- [Sou15] **Y. Soukkou**, and S. Labiod, "Adaptive backstepping control using combined direct and indirect adaptation for a single-link flexible-joint robot," *International Journal of Industrial Electronics and Drives*, vol. 2, no. 1, pp. 11-19, 2015.
- [Sun13] G. Sun, D. Wang, X. Li, and Z. Peng, "A DSC approach to adaptive neural network tracking control for pure-feedback nonlinear systems," *Applied Mathematics and Computation*, vol. 219, no. 11, pp. 6224-6235, 2013.
- [Swa00] D. Swaroop, J. K. Hedrick, P. P. Yip, and J. C. Gerdes, "Dynamic surface control for a class of nonlinear systems," *IEEE Transactions on Automatic Control*, vol. 45, no. 10, pp. 1893-1899, 2000.
- [Swa97] D. Swaroop, J. C. Gerdes, P. P. Yip, and J. K. Hedrick, "Dynamic surface control of nonlinear systems," *Proceedings of the American Control Conference*, Albuquerque, New Mexico, pp. 3028-3034, 1997.
- [Utk92] V. I. Utkin, "Sliding Modes in Control and Optimization," Springer-Verlag, New York, 1992.
- [van11] E. R. van Oort, "Adaptive backstepping control and safety analysis for modern fighter aircraft," PhD Thesis, Delft University of Technology, 2011.
- [van10] E. R. van Oort, L. Sonneveldt, Q. P. Chu, and J. A. Mulder, "Full-envelope modular adaptive control of a fighter aircraft using orthogonal least squares," *Journal of Guidance, Control, and Dynamics*, vol. 33, no. 5, pp. 1461-1472, 2010.
- [Wan17] F. Wang, Q. Zou, and Q. Zong, "Robust adaptive backstepping control for an uncertain nonlinear system with input constraint based on Lyapunov redesign," *International Journal of Control, Automation and Systems*, vol. 15, no. 1, pp. 212-225, 2017.
- [Wan16] M. Wang, Z. Zhang, and Y. Liu, "Adaptive backstepping control that is equivalent

- to tuning functions design,” *International Journal of Control, Automation and Systems*, vol. 14, no. 1, pp. 90-98, 2016.
- [Wan12] C. Wang, and Y. Lin, “Decentralised adaptive dynamic surface control for a class of interconnected non-linear systems,” *IET Control Theory & Applications*, vol. 6, no. 9, pp. 1172-1181, 2012.
- [Wan05] D. Wang, and J. Huang, “Neural network-based adaptive dynamic surface control for a class of uncertain nonlinear systems in strict-feedback form,” *IEEE Transactions on Neural Networks*, 2005, vol. 16, no. 1, pp. 195-202, 2005.
- [Wan01] C. Wang, and S. S. Ge, “Adaptive backstepping control of uncertain Lorenz system,” *International Journal of Bifurcation and Chaos*, vol. 11, no. 4, pp. 1115-1119, 2001.
- [Wei16] Y. Wei, P. W. Tse, Z. Yao, and Y. Wang, “Adaptive backstepping output feedback control for a class of nonlinear fractional order systems,” *Nonlinear Dynamics*, vol. 86, no. 2, pp. 1047-1056, 2016.
- [Wei15] Y. Wei, Y. Chen, S. Liang, and Y. Wang, “A novel algorithm on adaptive backstepping control of fractional order systems,” *Neurocomputing*, vol. 165, pp. 395-402, 2015.
- [Wei13] X. J. Wei, N. Chen, and W. Q. Li, “Composite adaptive disturbance observer-based control for a class of nonlinear systems with multisource disturbance,” *International Journal of Adaptive Control and Signal Processing*, vol. 27, no. 3, pp. 199-208, 2013.
- [Wu18] J. Wu, J. Zhao, and D. Wu, “Indirect adaptive robust control of nonlinear systems with time-varying parameters in a strict feedback form,” *International Journal of Robust and Nonlinear Control*, vol. 28, no. 13, pp. 3835-3851, 2018.
- [Xi19] C. Xi, and J. Dong, “Adaptive reliable guaranteed performance control of uncertain nonlinear systems by using exponent-dependent barrier Lyapunov function,” *International Journal of Robust and Nonlinear Control*, vol. 29, no. 4, pp. 1051-1062, 2019.
- [Yao03] B. Yao, “Integrated direct/indirect adaptive robust control of SISO nonlinear systems in semi-strict feedback form,” *Proceedings of the American Control Conference*, Denver, Colorado, pp. 3020-3025, 2003.
- [Yao02] B. Yao, and A. Palmer, “Indirect adaptive robust control of SISO nonlinear systems in semi-strict feedback forms,” *Proceedings of the 15th IFAC Triennial World Congress*, Barcelona, 2002.
- [Yao97] B. Yao, and M. Tomizuka, “Adaptive robust control of SISO nonlinear systems in semi-strict feedback form,” *Automatica*, vol. 33, no. 5, pp. 893-900, 1997.
- [Yip98] P. P. Yip, and J. K. Hedrick, “Adaptive dynamic surface control: a simplified algorithm for adaptive backstepping control of nonlinear systems,” *International Journal of Control*, vol. 71, no. 5, pp. 959-979, 1998.
- [Yoo07] S. J. Yoo, J. B. Park, and Y. H. Choi, “Adaptive dynamic surface control for stabilization of parametric strict-feedback nonlinear systems with unknown time delays,” *IEEE Transactions on Automatic Control*, vol. 52, no. 12, pp. 2360-2365, 2007.
- [Yu18a] J. Yu, P. Shi, and L. Zhao, “Finite-time command filtered backstepping control for a class of nonlinear systems,” *Automatica*, vol. 92, pp. 173-180, 2018.
- [Yu18b] J. Yu, B. Chen, H. Yu, C. Lin, and L. Zhao, “Neural networks-based command filtering control of nonlinear systems with uncertain disturbance,” *Information Sciences*, vol. 426, pp. 50-60, 2018.
- [Yu15a] J. Yu, P. Shi, W. Dong, and H. Yu, “Observer and command filter-based adaptive fuzzy output feedback control of uncertain nonlinear systems,” *IEEE Transactions on Industrial Electronics*, vol. 62, no. 9, pp. 5962-5970, 2015.
- [Yu15b] J. Yu, P. Shi, W. Dong, B. Chen, and C. Lin, “Neural network-based adaptive dynamic surface control for permanent magnet synchronous motors,” *IEEE Transactions on Neural Network and Learning Systems*, vol. 26, no. 3, pp. 640-645, 2015.

- [Zha18a] Z. Zhang, G. Duan, and M. Hou, "An improved adaptive dynamic surface control approach for uncertain nonlinear systems," *International Journal of Adaptive Control and Signal Processing*, vol. 32, no. 5, pp. 713-728, 2018.
- [Zha18b] Z. Zhang, G. Duan, and Y. Hu, "Robust adaptive control for a class of semi-strict feedback systems with state and input constraints," *International Journal of Robust and Nonlinear Control*, vol. 28, no. 9, pp. 3189-3211, 2018.
- [Zha17] Z. Zhang, G. Duan, and M. Hou, "Robust adaptive dynamic surface control of uncertain non-linear systems with output constraints," *IET Control Theory & Applications*, vol. 11, no. 1, pp. 110-121, 2017.
- [Zha16] D. Zhai, L. An, J. Li, and Q. Zhang, "Simplified filtering-based adaptive fuzzy dynamic surface control approach for non-linear strict-feedback systems," *IET Control Theory & Applications*, vol. 10, no. 5, pp. 493-503, 2016.
- [Zha15a] T. Zhang, and X. Xia, "Adaptive output feedback tracking control of stochastic nonlinear systems with dynamic uncertainties," *International Journal of Robust and Nonlinear Control*, vol. 25, no. 9, pp. 1282-1300, 2015.
- [Zha15b] Z. Zhang, J. H. Park, H. Shao, and Z. Qi, "Exact tracking control of uncertain non-linear systems with additive disturbance," *IET Control Theory & Applications*, vol. 9, no. 5, pp. 736-744, 2015.
- [Zha13] Q. Zhao, Y. Li, and Y. Lin, "Adaptive nonlinear output-feedback dynamic surface control with unknown high-frequency gain sign," *International Journal of Control*, vol. 86, no. 12, pp. 2203-2214, 2013.
- [Zha12a] X. Zhang, and Y. Lin, "Adaptive output feedback tracking for a class of nonlinear systems," *Automatica*, vol. 48, no. 9, pp. 2372-2376, 2012.
- [Zha12b] J. Zhang, Q. Li, N. Cheng, and B. Liang, "Non-linear flight control for unmanned aerial vehicles using adaptive backstepping based on invariant manifolds," *Proceedings of the Institution of Mechanical Engineers, Part G: Journal of Aerospace Engineering*, vol. 227, no. 1, pp. 33-44, 2012.
- [Zha11] J. Zhang, Q. Li, N. Cheng, and B. Liang, "Immersion and invariance based nonlinear adaptive longitudinal control for autonomous aircraft," *Proceedings of the 8th World Congress on Intelligent Control and Automation*, Taipei, pp. 985-989, 2011.
- [Zha08] T. P. Zhang, and S. S. Ge, "Adaptive dynamic surface control of nonlinear systems with unknown dead zone in pure feedback form," *Automatica*, vol. 44, no. 7, pp. 1895-1903, 2008.
- [Zho08] J. Zhou, and C. Y. Wen, "Adaptive Backstepping Control of Uncertain Systems," Berlin/Heidelberg: Springer-Verlag, 2008.
- [Zho07] J. Zhou, and M. J. Er, "Adaptive output control of a class of uncertain chaotic systems," *Systems & Control Letters*, vol. 19, no. 6, pp. 452-460, 2007.
- [Zou20] M. Zou, J. Yu, Y. Ma, L. Zhao, and C. Lin, "Command filtering-based adaptive fuzzy control for permanent magnet synchronous motors with full-state constraints," *Information Sciences*, vol. 518, pp. 1-12, 2020.